European Journal of Taxonomy 1054: 1–126
https://doi.org/10.5852/ejt.2026.1054.3276
europeanjournaloftaxonomy.eu
ISSN 2118-9773
2026 · Huber B.A. *et al.*

Received: 27 October 2025 • *Accepted: 12 March 2026* • *Published: 14 May 2026*

Topic editor: Magalie Castelin • *Section editor: Arnaud Henrard* • *Desk editor: Pepe Fernández*

Monograph

urn:lsid:zoobank.org:pub:5A57B885-FEC8-4563-8245-AA9CFDF31577

Ninetine spiders in Brazilian Caatinga and Cerrado: revision of *Kambiwa* and description of *Sertana* gen. nov. (Araneae, Pholcidae), with analyses of predicted range shifts due to climate change

Bernhard A. HUBER [1,*], Guanliang MENG [2], Jiří KRÁL [3], Ivalú M. ÁVILA HERRERA [4] & Leonardo S. CARVALHO [5]

[1,2] Zoological Research Museum Alexander Koenig, LIB, Bonn, Germany.
[2] Present address: State Key Laboratory of Animal Biodiversity Conservation and Integrated Pest Management, Institute of Zoology, Chinese Academy of Sciences, Beijing, China.
[3,4] Department of Genetics and Microbiology, Faculty of Science, Charles University, Prague, Czech Republic.
[5] Campus Amílcar Ferreira Sobral, Universidade Federal do Piauí, Floriano, Piauí, Brazil.

[*] Corresponding author: b.huber@leibniz-lib.de
[2] Email: guanliang.meng@ioz.ac.cn
[3] Email: spider@natur.cuni.cz
[4] Email: avilai@natur.cuni.cz
[5] Email: carvalho@ufpi.edu.br

Abstract. Among daddy long-legs spiders (Pholcidae), Ninetinae is a distinctive subfamily that comprises short-legged, fast-running spiders. Most species are small or tiny, lead reclusive lives, and are largely restricted to semiarid regions, which together has made them poorly collected and poorly known. Here, we build on focused recent collections in the Brazilian Cerrado and Caatinga biomes, two of the World's richest tropical savanna, xeric shrubland and thorn forest regions. Our focus is on the taxonomy of the genus *Kambiwa* Huber, 2000 that previously contained only two nominal species, each known from a single locality. Combining morphological and molecular (*CO1* barcode) data, we describe six new species in *Kambiwa* (*K. brumado* Huber sp. nov.; *K. coribe* Huber sp. nov.; *K. ibo* Huber sp. nov.; *K. itacarambi* Huber sp. nov.; *K. maracas* Huber sp. nov.; *K. mucuge* Huber sp. nov.), redescribe the type species *K. neotropica* (Kraus, 1957), and synonymize the monotypic genus *Pemona* Huber, 2019 with *Kambiwa*, resulting in the new combination *K. sapo* (Huber, 2019) comb. nov. In addition, we describe a new genus of superficially *Kambiwa*-like spiders from the same geographic region: *Sertana* Huber gen. nov., with five new species (*S. bumba* Huber gen. et sp. nov.; *S. capivara* Huber gen. et sp. nov.; *S. igapora* Huber gen. et sp. nov.; *S. lapa* Huber gen. et sp. nov.; *S. sagarana* Huber gen. et sp. nov.). In line with previous efforts to explore the processes underlying the geographical distribution of Ninetinae, we also evaluate the potential effects of future climate change on the environmental niche occupied by three selected species of *Kambiwa*. Our results corroborate previous findings that demonstrate an altitude-mediated response to climate change. For a highland species, areas of high habitat suitability almost disappear under more severe climate change scenarios. For two species with lowland records,

the areas with high habitat suitability increase significantly. Finally, we analyze the male karyotype of *K. ibo* which consists of 28 chromosomes including a $X_1X_2X_3Y$ system. All chromosomes are biarmed except for the Y chromosome. This contribution concludes a series of publications on the subfamily Ninetinae. We use this opportunity to summarize current knowledge about the subfamily, to discuss open questions and knowledge gaps, and to suggest further research topics focusing on these tiny but exceptional pholcids.

Keywords. *CO1* barcodes, climate change, karyotype, niche modeling, taxonomy.

Huber B.A., Meng G., Král J., Ávila Herrera I.M. & Carvalho L.S. 2026. Ninetine spiders in Brazilian Caatinga and Cerrado: revision of *Kambiwa* and description of *Sertana* gen. nov. (Araneae, Pholcidae), with analyses of predicted range shifts due to climate change. *European Journal of Taxonomny* 1054: 1–126.
https://doi.org/10.5852/ejt.2026.1054.3276

Table of contents

Introduction

Pholcidae C.L. Koch, 1850, or daddy long-legs spiders, are among the most species rich spider families (World Spider Catalog 2025) but most of this diversity (>80% of the currently known species) are contained within only two of the currently seven subfamilies: in Pholcinae C.L. Koch, 1850 and Modisiminae Simon, 1893. Representatives of these two subfamilies occupy a wide range of microhabitats in tropical forests around the world, with a corresponding diversity of body shapes, sizes, colors, and behaviors (Huber *et al.* 2015, 2019; Eberle *et al.* 2018; Huber 2018a). Other groups within the family are largely restricted to semiarid environments that offer a more limited number of microhabitats with different ecological parameters, which is probably the reason for their generally more conservative morphology and behavior (Aharon *et al.* 2017; Huber 2001, 2012, 2022). This is particularly true for Ninetinae Simon, 1890, which is among the smallest subfamilies in terms of described species. Its 91 nominal species (including the species newly described herein) occupy small sheltered spaces at ground level in semiarid environments, and they are all small to tiny, short-legged, fast-running spiders (Huber *et al.* 2023a, 2023b, 2023c, 2024a, 2024b, 2024c; Huber & Meng 2025) that do not fit the popular image of a daddy long-legs spider.

Geographically, Ninetinae diversity is concentrated in the New World, where the subfamily ranges from Argentina to Canada and from sea level to over 4500 m in the Andes (e.g., Huber *et al.* 2023a, 2023b). In the Old World, Ninetinae is restricted to Africa, Madagascar, and the Arabian Peninsula, with currently only ten described species (Huber & Meng 2025). In previous studies, we provided evidence that ninetines are associated with dry and arid environments (Huber *et al.* 2023a, 2024a), occupy a conserved environmental niche (Huber *et al.* 2023a), tend to live at relatively low elevation areas (Huber *et al.* 2024a) and suffer from a strong sampling bias (Huber *et al.* 2023a, 2024c). With respect to New World Ninetinae, the Brazilian Cerrado and Caatinga biomes appear particularly diverse. These biomes cover approximately 20% of the Brazilian territory; they are exceptionally rich for a specific biota that is absent or rare in the neighboring megadiverse Amazon and Atlantic Forest biomes (Myers *et al.* 2000; Oliveira *et al.* 2017; Strassburg *et al.* 2017); and they are subject to massive land cover changes and biodiversity loss (Beuchle *et al.* 2015; Colli *et al.* 2020; Araujo *et al.* 2023). However, for many taxa they are also among the least studied Neotropical biomes, and this Wallacean shortfall has resulted in biased views of taxonomic and geographic diversity and species richness (e.g., Oliveira *et al.* 2016, 2017). For example, the ninetine genus *Ibotyporanga* Mello-Leitão, 1944 is largely restricted to the Brazilian Caatinga and Cerrado biomes and it has until recently been thought to be species-poor. Focused collecting showed that these spiders are in fact abundant and species-rich, and a recent revision elevated the number of nominal species from five to 24, with only a few isolated records from outside of these biomes (Huber *et al.* 2024c).

Here, we deal with a similar case of taxonomic neglect of a group that turns out to be abundant and diverse in semiarid Brazilian environments. The genus *Kambiwa* Huber, 2000 previously contained only two nominal species, each known from a single locality. During a focused field campaign in 2022, limited to four weeks and to the states of Bahia, Pernambuco, and Minas Gerais, '*Kambiwa*-like' spiders were found at 38 of the 64 visited localities, often in high abundances. Molecular analyses (Meng *et al.* 2025) showed that two genera were actually involved: *Kambiwa* (including the monotypic genus *Pemona* Huber, 2019 that we newly synonymize with *Kambiwa*) and a new genus more closely related to *Galapa* Huber, 2000 than to *Kambiwa*. Here, we describe the new taxa, present first scanning electron microscopy (SEM) data for *Kambiwa* and the new genus and present karyological data for a second species of *Kambiwa* (complementing the data on *Kambiwa neotropica* (Kraus, 1957) in Ávila Herrera *et al.* 2021). In addition, we evaluate the effects of future climate change on the environmental niche of selected species of *Kambiwa*; this is the first time that this tool is applied to understand the potential future geographic distribution and conservation outlook for pholcid spiders. Finally, we summarize

current knowledge about Ninetinae, discuss open questions and knowledge gaps, and suggest further research topics focusing on this subfamily.

Material and methods

Material examined

The taxonomic part of this study is based on the examination of more than 1100 adult specimens mostly deposited in the following two collections: Coleção de História Natural da Universidade Federal do Piauí, Floriano, Brazil (CHNUFPI); and Zoologisches Forschungsmuseum Alexander Koenig, Bonn, Germany (ZFMK). A few additional specimens studied are deposited in Museo Argentino de Ciencias Naturales "Bernardino Rivadavia", Buenos Aires, Argentina (MACN); and Senckenberg Museum, Frankfurt, Germany (SMF). Preliminary observations (by LSC) on specimens deposited in Instituto Butantan, São Paulo, Brazil (IBSP), Museu Paraense Emílio Goeldi, Belém, Brazil (MPEG), and Universidade Federal de Minas Gerais, Brazil (UFMG) are briefly mentioned but the material is largely excluded because loan requests by BAH (the coauthor responsible for the alpha taxonomic aspects) for detailed study were unsuccessful.

Taxonomy and morphology

Taxonomic descriptions follow the style of recent publications on Ninetinae (e.g., Huber *et al.* 2023c, 2024a; based on Huber 2000). Species delimitation is based mainly on the morphology of genitalia (cf. Huber 2004); *CO1* barcodes (see below) are only used to support morphological differences and to point out problematic cases. Species descriptions are sorted by morphological similarity, starting with the type species. Measurements were done on a dissecting microscope with an ocular grid and are in mm unless otherwise noted; eye measurements are ± 5 µm. Photos were made with a Nikon Coolpix 995 digital camera (2048 × 1536 pixels) mounted on a Nikon SMZ 18 stereo microscope or a Leitz Dialux 20 compound microscope. CombineZP (https://combinezp.software.informer.com/) was used for stacking photos. Drawings are partly based on photos that were traced on a light table and finalized under a dissecting microscope, or they were directly drawn with a Leitz Dialux 20 compound microscope using a drawing tube. Cleared epigyna were stained with chlorazol black. For scanning electron microscope (SEM) photos, specimens were dried in hexamethyldisilazane (HMDS) (Brown 1993) and photographed with a Zeiss Sigma 300 VP scanning electron microscope. SEM data that are presented within species descriptions are not based on the specific specimen described; scanned specimens are specified in the respective material examined sections. The number of decimals in coordinates gives a rough indication about the accuracy of the locality data: four decimals means that the collecting site is within about 10 m of the indicated spot; three decimals: within ~100 m; two decimals: within ~1 km; one decimal: within ~10 km. Distribution maps were generated with ArcMap ver. 10.0 (Environmental Systems Research Institute, Redlands, CA).

Abbreviations

ALE = anterior lateral eye(s)
ALS = anterior lateral spinneret(s)
AME = anterior median eye(s)
a.s.l. = above sea level
L/d = length/diameter
PME = posterior median eye(s)
PMS = posterior median spinneret(s)

Abbreviations used in figures only are explained in the figure legends.

Molecular data and analyses

Of the 35 cytochrome c oxidase subunit I (*CO1*) barcodes of *Kambiwa* (27) and *Sertana* Huber gen. nov. (8) used in this study (Table 1), 25 were newly generated using Sanger sequencing as described in Huber & Meng (2024) (UH codes in Table 1), seven were extracted from the target capture sequencing data of Meng *et al.* (2025) (G and E codes), and three were taken from the literature (JA and S codes; from Astrin *et al.* 2006 and Eberle *et al.* 2018). We further included *CO1* barcodes of four species of *Galapa* (from Huber *et al.* 2024a) because this genus has been shown to be the sister of *Sertana* (Meng *et al.* 2025). As a more distant ninetine outgroup we used *Ibotyporanga ziruma* Huber, 2024 (from Huber *et al.* 2024c), and as a root we used *Artema bahla* Huber, 2019 (from Eberle *et al.* 2018). The codon-based alignment of *CO1* barcodes was constructed with MAFFT (ver. 7.490; Katoh & Standley 2013) and PAL2NAL (Suyama *et al.* 2006). The Kimura 2-parameter (K2P) genetic distances (Kimura 1980) among specimens were calculated with MEGA (ver. 11.0.13; Tamura *et al.* 2021). An initial attempt to calculate a NJ tree failed because of too little overlap between specimens E074 and E078. Therefore, we created a maximum likelihood tree with IQ-TREE (-pers 0.2 -nstop 500) (ver. 2.2.0; Minh *et al.* 2020) (Fig. 1), without implying that the resulting tree reliably reflects phylogenetic relationships. The best-fitting model was automatically determined by ModelFinder (Kalyaanamoorthy *et al.* 2017). To avoid being trapped in local optima, 10 different runs were performed. The robustness of the tree was evaluated with ultrafast bootstrap (-B 2000 -bnni) (Minh *et al.* 2013; Hoang *et al.* 2018) and SH-aLRT test (-alrt 2000) (Guindon *et al.* 2010).

Data preparation for environmental niche modeling

Initially, the number of available records was quantified for each species belonging to the studied genera, establishing a minimum threshold of 12 occurrence points per species (i.e., distinct sites with unique latitude and longitude coordinates, all listed in the material examined sections of the present study). Occurrence records of the target taxa were consolidated into a single database containing taxonomic identifications and geographic coordinates. To ensure comparability and spatial accuracy, only records with valid longitude and latitude values were retained. Additional cleaning steps were carried out using the 'CoordinateCleaner' package (Zizka *et al.* 2019), which facilitated the systematic detection and removal of occurrence records with invalid or zero coordinates, degree conversion errors, duplicates, and localities erroneously positioned over the ocean (following the workflow from Moura *et al.* 2023a). Only species represented by at least 12 reliable occurrence records after cleaning were included in subsequent analyses, ensuring a minimum sample size for modeling and statistical inference. All data processing steps followed established protocols to maximize data quality and minimize geographic and taxonomic bias. The final, filtered dataset was exported for downstream analyses.

Environmental predictor variables were selected to represent both climatic and edaphic dimensions relevant to the distribution of the target taxa (as in Moura *et al.* 2023a). Climatic predictors consisted of the 19 bioclimatic variables available from WorldClim ver. 2.1 (Fick & Hijmans 2017), at a spatial resolution of 2.5 arc-minutes. Current climatic conditions and multiple future scenarios were incorporated, the latter based on projections from the Coupled Model Intercomparison Project Phase 6 – CMIP6 (Eyring *et al.* 2015), comprising alternative Shared Socioeconomic Pathways (SSP245 and SSP585) and two time periods (2041–2060 and 2081–2100).

The selection of climate models and emission scenarios followed established recommendations for ecological modeling in Brazil (e.g., Moura *et al.* 2023a; Neves *et al.* 2025). Two contrasting SSPs were selected to capture a range of plausible climate futures: SSP2-4.5 (SSP245), representing an intermediate, 'business-as-usual' scenario, and SSP5-8.5 (SSP585), describing a high-emissions, non-mitigation pathway. For each scenario and period, projections were obtained from five global climate models (GCMs) recognized for their performance in simulating regional climate in Brazil and South America: CMCC-ESM2, MRI-ESM2-0, IPSL-CM6A-LR, EC-Earth3-Veg, and MIROC6. This selection was based

Table 1 (continued on next page). Geographic origins and GenBank accession numbers of sequenced specimens of *Kambiwa* Huber, 2000 and *Sertana* Huber gen. nov. Specimens are sorted by Code. The three previously published sequences are included for the sake of completeness: JA83 (from Astrin *et al.* 2006), S328 and S358 (from Eberle *et al.* 2018).

Code	Genus	Species	Vial	Country	Admin	Locality	Lat	Long	*CO1*
E072	*Kambiwa*	*itacarambi*	Carv56	Brazil	Minas Gerais	NW of Itacarambi	-15.0500	-44.1820	PV605729
E074	*Sertana*	*capivara*	Carv64	Brazil	Piauí	PN Serra da Capivara, near Boqueirao do Ferrerira	-8.7476	-42.4870	PV605730
E076	*Kambiwa*	*neotropica*	Carv65	Brazil	Ceará	Solonópole, at BR 122	-5.5735	-38.9704	PV605731
E078	*Kambiwa*	aff. *neotropica*	Carv69	Brazil	Pernambuco	PN do Catimbau, Trilha da Igreja	-8.3343	-35.9609	PV605732
G50	*Kambiwa*	*itacarambi*	Br22-170	Brazil	Minas Gerais	SW of Manga, Parque Estadual da Mata Seca	-14.8438	-44.0592	PV605733
G52	*Sertana*	*sagarana*	Br22-179	Brazil	Bahia	SW of São Felix do Coribe	-13.4329	-44.2168	PV605734
G62	*Kambiwa*	aff. *neotropica*	Br22-256	Brazil	Bahia	between Ibó and Curaçá, Serra do Furtuoso	-8.6420	-39.5266	PV605735
JA83	*Kambiwa*	*sapo*	Ven02/100-1	Venezuela	Bolívar	Canaima, at Salto El Sapo	6.2417	-62.8500	DQ667903
S328	*Kambiwa*	*neotropica*	Br15-267	Brazil	Rio Grande do Norte	Lajedo do Arapuá	-5.5292	-37.6143	MG268617
S358	*Kambiwa*	*coribe*	MACN280	Bolivia	Santa Cruz	Yabaré	-17.4417	-62.1725	MG268618
UH045	*Kambiwa*	*brumado*	Br22-149	Brazil	Bahia	E of Milagres, Morro do São Cristóvão	-12.8711	-39.8548	PV605708
UH046	*Kambiwa*	*maracas*	Br22-150	Brazil	Bahia	SW of Maracas	-13.5858	-40.7226	PV605705
UH050	*Sertana*	*igapora*	Br22-156	Brazil	Bahia	SW of Caetité, Caetité Wind Farm	-14.1155	-42.6087	PV605724
UH059	*Kambiwa*	*coribe*	Br22-173	Brazil	Bahia	SW of Correntina, margins of BR-349	-13.4998	-44.9795	PV605706
UH066	*Sertana*	*lapa*	Br22-188	Brazil	Bahia	SE of Bom Jesus da Lapa	-13.4398	-43.1643	PV605723
UH067	*Sertana*	*lapa*	Br22-191	Brazil	Bahia	SE of Bom Jesus da Lapa	-13.4398	-43.1643	PV605725
UH070	*Sertana*	*igapora*	Br22-194	Brazil	Bahia	SE of Igaporã	-13.7977	-42.6578	PV605726
UH075	*Kambiwa*	*mucuge*	Br22-200	Brazil	Bahia	W of Mucugê, PN Chapada Diamantina	-13.0097	-41.4084	PV605709
UH076	*Kambiwa*	*mucuge*	Br22-201	Brazil	Bahia	NE of Mucugê, Parque “Sempre Viva”	-12.9980	-41.3630	PV605704
UH087	*Kambiwa*	*ibo*?	Br22-217	Brazil	Bahia	S of Xique-Xique	-11.1196	-42.7376	PV605707
UH103	*Kambiwa*	*ibo*	Br22-244	Brazil	Pernambuco	NE of Petrolina	-9.1957	-40.3832	PV605711
UH110	*Kambiwa*	*ibo*	Br22-260	Brazil	Bahia	N of Poço de Fora	-9.5880	-39.7870	PV605712
UH178	*Kambiwa*	*neotropica*	Carv68	Brazil	Piauí	PN Sete Cidades, near Cachoeira do Riachao	-4.1060	-41.6764	PV605710
UH481	*Kambiwa*	*maracas*	Br22-151	Brazil	Bahia	NE of Contendas do Sincorá	-13.7474	-41.0227	PV605721
UH482	*Kambiwa*	*brumado*	Br22-155	Brazil	Bahia	NE of Brumado	-14.1601	-41.5154	PV605716

Table 1 (continued). Geographic origins and GenBank accession numbers of sequenced specimens of *Kambiwa* Huber, 2000 and *Sertana* Huber gen. nov. Specimens are sorted by Code. The three previously published sequences are included for the sake of completeness: JA83 (from Astrin *et al.* 2006), S328 and S358 (from Eberle *et al.* 2018).

Code	Genus	Species	Vial	Country	Admin	Locality	Lat	Long	*CO1*
UH490	*Sertana*	*lapa*	Br22-187	Brazil	Bahia	SE of Bom Jesus da Lapa	-13.4398	-43.1643	PV605728
UH492	*Sertana*	*igapora*	Br22-190	Brazil	Bahia	SE of Bom Jesus da Lapa	-13.4383	-43.1645	PV605727
UH494	*Kambiwa*	*brumado*	Br22-196	Brazil	Bahia	SE of Paramirim	-13.5500	-42.2020	PV605722
UH496	*Kambiwa*	*ibo*?	Br22-207	Brazil	Bahia	NW of Ibipeba	-11.5400	-42.1700	PV605715
UH502	*Kambiwa*	*ibo*	Br22-240	Brazil	Bahia	W of Andorinha	-10.3650	-39.9114	PV605720
UH503	*Kambiwa*	*ibo*	Br22-241	Brazil	Bahia	N of Senhor do Bonfim	-10.1515	-40.2297	PV605714
UH509	*Kambiwa*	*ibo*	Br22-254	Brazil	Pernambuco	NE of Cabrobó	-8.4200	-39.1760	PV605717
UH510	*Kambiwa*	*ibo*	Br22-255	Brazil	Bahia	S of Ibó	-8.6906	-39.2682	PV605718
UH511	*Kambiwa*	*ibo*	Br22-256a	Brazil	Bahia	between Ibó and Curaçá, Serra do Furtuoso	-8.6420	-39.5266	PV605713
UH513	*Kambiwa*	*ibo*	Br22-258	Brazil	Bahia	S of Curaçá	-9.2571	-39.8163	PV605719

on regional assessments demonstrating the adequacy of these models in reproducing temperature and precipitation patterns (e.g., Dantas *et al.* 2022; Firpo *et al.* 2022; Monteverde *et al.* 2022), besides being widely used in studies like this in Brazil (e.g., Moura *et al.* 2023a; Neves *et al.* 2025). All raster files were obtained directly from the WorldClim repository and processed to ensure consistent spatial

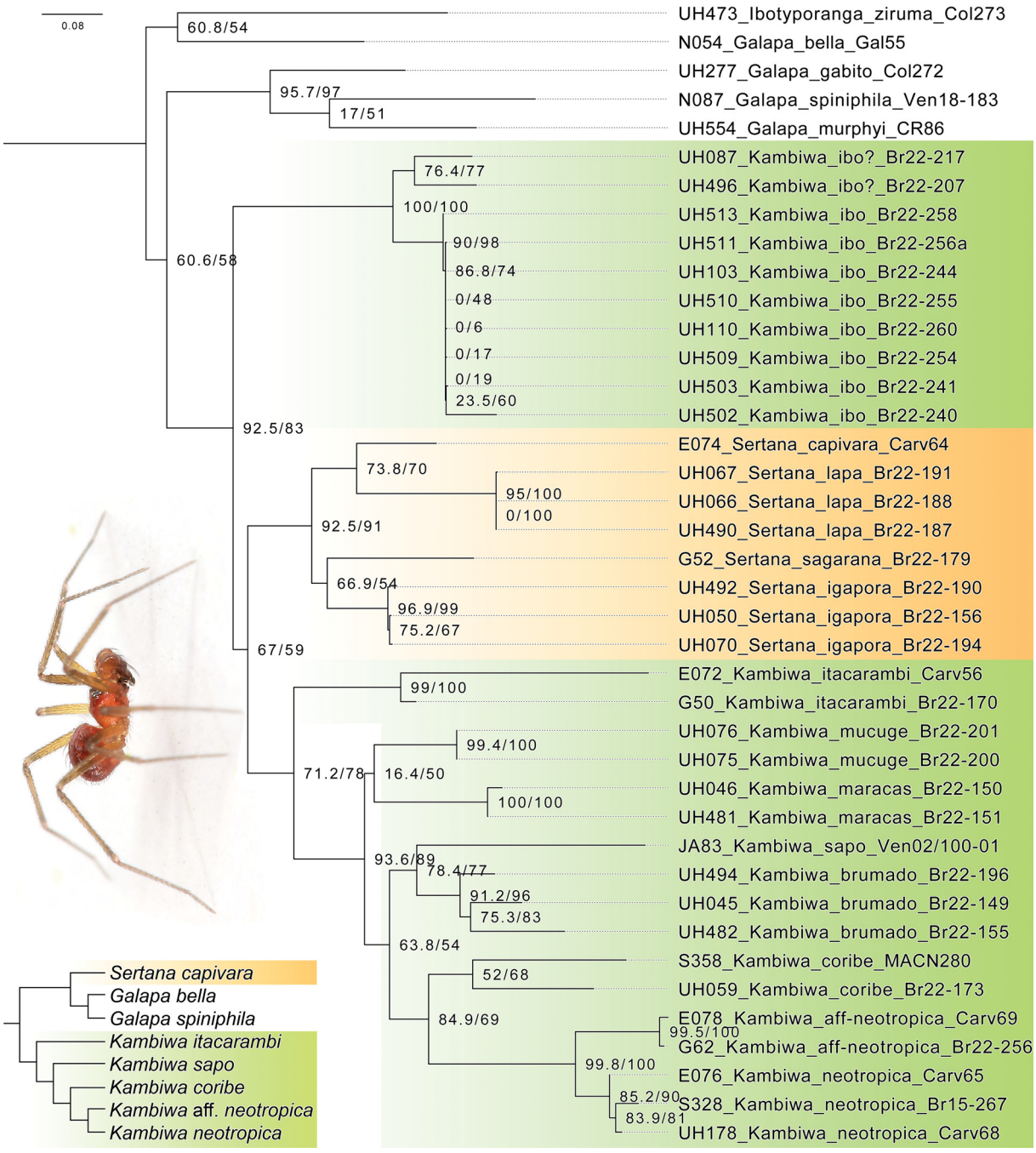

Fig. 1. Cladogram of *CO1* sequences of *Kambiwa* Huber, 2000, *Sertana* Huber gen. nov., and outgroups derived from a maximum likelihood analysis using IQ-TREE, with the best-fit model (TIM3+F+I+G4) being determined by ModelFinder. Numbers on the branches are SH-aLRT support (%) / ultrafast bootstrap support (%). Inset: relationships of *Kambiwa*, *Sertana*, and *Galapa* Huber, 2000 derived from UCE data, simplified from Meng *et al.* (2025). Photo on the left: *Kambiwa itacarambi* Huber sp. nov., male.

resolution and extent. Raster processing, including cropping, reprojection, and extraction of individual layers, was performed using functions of the 'terra', 'raster' and 'sf' packages (Pebesma 2018; Hijmans 2023a, 2023b).

Edaphic predictors were sourced from the SoilGrids ver. 2.0 database (Poggio *et al.* 2021), also at a spatial resolution of 2.5 arc-minutes, and included nine soil properties measured at 0–5 cm depth: bulk density, coarse fragment content, clay content, total nitrogen, soil organic carbon density, soil pH (H_2O), sand content, silt content, and soil organic carbon content. Soil layers were processed to guarantee alignment with the climatic predictors and the spatial boundaries of the study area.

To reduce dimensionality and avoid multicollinearity among predictors, a principal component analysis (PCA) was performed separately for the climatic and edaphic variables, employing functions of the 'flexsdm' package (Velazco *et al.* 2022). The number of principal components retained for subsequent analyses was determined by the Kaiser criterion (i.e., eigenvalue $> 1/p$, where p is the number of variables; Jackson 1993). All predictor layers, including the resulting principal component axes, were exported as georeferenced raster files for use in downstream ecological modeling. All analyses were conducted in R ver. 4.3.0 (R Core Team 2023), employing a reproducible workflow for data cleaning and preparation.

Environmental niche modeling, projection, and ensemble forecasting

Species distribution models (SDMs) were constructed using a correlative framework, employing five algorithms available in the 'biomod2' package (Thuiller *et al.* 2025), following the workflow from Neves *et al.* (2025): Generalized Linear Models (GLM), Generalized Additive Models (GAM), Maximum Entropy (MAXNET), Classification Tree Analysis (CTA), and Artificial Neural Networks (ANN). All of these algorithms are commonly used models for this type of study (Huber *et al.* 2023a, 2023c, 2024a; Moura *et al.* 2023a; Neves *et al.* 2025). Individual models were calibrated using a fourfold cross-validation strategy, with 15 replicates per algorithm, to robustly assess model performance and minimize overfitting. For each target species, presence records were complemented by pseudo-absences sampled within a biologically plausible accessible area around known occurrences (i.e., a 500 km buffer, as in Huber *et al.* 2023a, 2023c, 2024a). For *Kambiwa coribe* Huber sp. nov., the single record from Bolivia was excluded from the analysis, as it is located more than 500 km from the remaining presence sites and would thus bias the estimated species distribution area. Pseudo-absences were sampled in a ratio of two per presence, ensuring balanced calibration and minimizing sampling bias (see Barbet-Massin *et al.* 2012).

Model evaluation was based on the Boyce index (Boyce *et al.* 2002) and the area under the receiver operating characteristic curve (i.e., AUC/ROC; Fielding & Bell 1997), with models retained for projection if they achieved both BOYCE and ROC values ≥ 0.95. Evaluation metrics were summarized and exported for each algorithm and replicate for the sake of clarity (Supp. file 1). Selected models were projected onto current and future environmental scenarios, corresponding to the full factorial combination of the five GCMs, two emission scenarios (SSP245 and SSP585), and two future time periods (2041–2060, 2081–2100), using functions of the 'terra', 'raster', 'sd' and 'biomod2' packages (Pebesma 2018; Hijmans 2023a, 2023b; Thuiller *et al.* 2025). For each scenario, ensemble forecasts were generated using both weighted mean and coefficient of variation approaches. Ensemble models were constructed only from the subset of "good" models passing evaluation thresholds, and all outputs were exported as georeferenced raster layers. To facilitate comparison between scenarios and time periods, ensemble projections from all GCMs within a scenario-period combination were further aggregated to produce global scenario ensembles, representing the consensus prediction (i.e., mean) across climate models. Ensemble rasters were subsequently binarized at a 70% threshold to estimate suitable area, and

the spatial intersection between present and future ensembles was computed to assess potential range stability or turnover.

To quantify modeled range size and representation within protected areas, the area of suitable habitat was calculated for each scenario and time period, both in total and within the network of official conservation units, using functions of the 'sf' and 'terra' packages (Pebesma 2018; Hijmans 2023b). All summary statistics, binary area estimates, and intersection results were exported for reproducibility and further interpretation. For clarity, ensemble models were exported for each GCM, time period and carbon emission scenarios (see Supp. file 2). The full modeling workflow, including function definitions, data handling, model calibration, projection, model ensemble construction, and post-processing, was adapted from Neves *et al.* (2025), with modifications tailored to the present study.

Additional statistical comparisons were carried out using generalized linear models, using negative binomial distribution of errors, implemented using the 'MASS' package (Venables & Ripley 2002). Model quality was assessed by checking the dispersion parameters using base R functions. When necessary, a contrast analysis was carried out using the function 'coms' of the 'RT4Bio' package (Reis Júnior *et al.* 2015).

Preparation of chromosome slides and their evaluation

Chromosome slides were prepared from the testes of three adult males of *Kambiwa ibo* Huber sp. nov. from Bahia, 9 km W of Andorinha, collected on 28 Nov. 2022. Several mitotic and a larger number of meiotic plates were analyzed. Dissected tissues were hypotonized in 0.075M KCl solution for 25 min and fixed three times (6, 10, and 20 min) in a fresh fixative consisting of three parts of ethanol and one part of acetic acid. The preparations were made from a piece of fixed tissue that was suspended on a glass slide in a drop of dissociative (60% acetic acid) using a pair of tungsten needles. The drop was subsequently spread over the glass using tungsten needles, and this was done on a histological plate (40°C), with the chromosomes adhering to the glass surface (Dolejš *et al.* 2011). The chromosome plates were stained with a 5% solution of Giemsa dye (28 min, pH 6.8) in modified Sörensen phosphate buffer (see Huber *et al.* 2024c for its composition), studied under an Olympus BX 50 microscope, and photographed with a DP71 CCD camera (Olympus). Chromosome morphology was classified according to Levan *et al.* (1964). Relative chromosome length was estimated as a percentage of the total chromosome length (TCL) of the haploid set. In the case of the Y chromosome, its absolute length was also measured. The sex chromosome system was determined based on the sex chromosome behavior in late prophase I (diplotene and diakinesis) and the pattern of sex chromosome segregation. The karyotype of males of araneomorph spiders probably contains not only sex chromosomes that pair achiasmatically during meiosis, but also a pair of morphologically undifferentiated sex chromosomes X and Y that pair via chiasmata (Král 2007; Král *et al.* 2011; Sember *et al.* 2020). In *Kambiwa*, it is not possible to distinguish this pair from autosomes. Therefore, in this paper, autosomes and the XY pair of males are referred to collectively as chromosome pairs.

Following the analysis, the slides were dipped in xylene and benzine baths (1 min each) to remove the immersion oil and then destained by dipping in methanol : acetic acid (3 : 1) for 3 min. Subsequently, preparations were used for the visualization of nucleolus organizer regions (NORs) via a variant of fluorescence in situ hybridization (FISH) described by Forman *et al.* (2013). The FISH probe used for the detection (18S rDNA region from the spider *Dysdera erythrina* (Walckenaer, 1802)) is specified in Ávila Herrera *et al.* (2021). Chromosome plates were counterstained with 4′,6-diamidino-2-phenolindole (DAPI), studied under an Olympus IX81 microscope, and photographed with an ORCA-AG CCD camera (Hamamatsu). Images were pseudocolored (red for Cy3, blue for DAPI) and superimposed using Cell^R software (Olympus Soft Imaging Solutions, Münster, Germany).

Results

Taxonomy

Class Arachnida Lamarck, 1801
Order Araneae Clerck, 1757
Family Pholcidae C.L. Koch, 1850

Genus ***Kambiwa*** Huber, 2000

Kambiwa Huber, 2000: 87. Type species: *K. neotropica* (Kraus, 1957).
Pemona Huber in Huber & Carvalho, 2019: 34. **Syn. nov.**

Justification of synonymy

When *Pemona sapo* Huber, 2019 was described in the new monotypic genus *Pemona* Huber, 2019, a close relationship with *Kambiwa* was evident ("…the new species could in theory be assigned to *Kambiwa*"; Huber & Carvalho 2019: 34). It was nevertheless described in a new genus because it appeared to differ in relevant aspects from species of *Kambiwa* known at the time. The six new species described below show that the closest relatives of the type species *Kambiwa neotropica* actually occupy a wider morphological space than previously known. In particular, some of the characters thought to be distinctive for *Pemona sapo* also occur in certain species of *Kambiwa* (e.g., small sclerotized teeth distally on procursus and small ventral apophysis on genital bulb in *K. ibo* sp. nov.). In addition, sternum humps were thought to be present in *Pemona* but absent in *Kambiwa*; instead, they are also present (even though sometimes very basic) in *Kambiwa*. Procursus length (relative to genital bulb length) is also more variable in *Kambiwa* than previously known. Finally, the basic configuration of the genital bulb is the same in *Pemona* and *Kambiwa*, including the distinctive retrolateral-dorsal sclerite that is indistinct in *Pemona sapo* and hidden by the procursus in the original illustration (Huber & Carvalho 2019: fig. 118).

Analyses of molecular (UCE) data resolve a group of species around *K. neotropica* that receives maximum support (Meng *et al.* 2025). *Pemona sapo* is nested within this group (Fig. 1, inset), and keeping *Pemona* as a separate genus would require the creation of at least one further new, poorly diagnosable genus. We thus transfer *Pemona sapo* to *Kambiwa*, and synonymize the two genera.

Diagnosis

Small short-legged pholcids with eight eyes and globular abdomen (Fig. 2), similar in size and body shape to closely related South American ninetine genera (*Guaranita* Huber, 2000; *Galapa* Huber, 2000; *Sertana* gen. nov.). Males are distinguished from these by presence of single ventral process on genital bulb (e.g., Figs 16F, 22F, 35F; *Sertana* with pair of distinctive ventral processes; pair of small ventral processes also present in *Galapa spiniphila* Huber, 2020); from *Galapa* also distinguished by unmodified cheliceral fangs, presence of pair of apophyses on main cheliceral segment (Figs 17A, 23A, 36A; absent only in *K. itacarambi* sp. nov.), and absence of retrolateral process on procursus; from *Galapa* and *Guaranita* also by absence of dorsal flap on procursus; from *Guaranita* also by absence of ventral membrane on procursus; from *Sertana* also distinguished by much shorter male cheliceral apophyses (compare Figs 17B, 23B, 36B with 60B, 64B, 68B), by presence of humps on sternum, and by wide procursus in lateral view (main branch of procursus slender and sclerotized in *Sertana*). Females are morphologically barely distinguishable from females of *Guaranita*, *Galapa*, and *Sertana*, but anterior epigynal plate with strong lateral posterior sclerites connecting to the internal transversal sclerite (Figs 17C, 23C, 28C; lateral posterior sclerites absent or very weak in *Galapa* and *Sertana*).

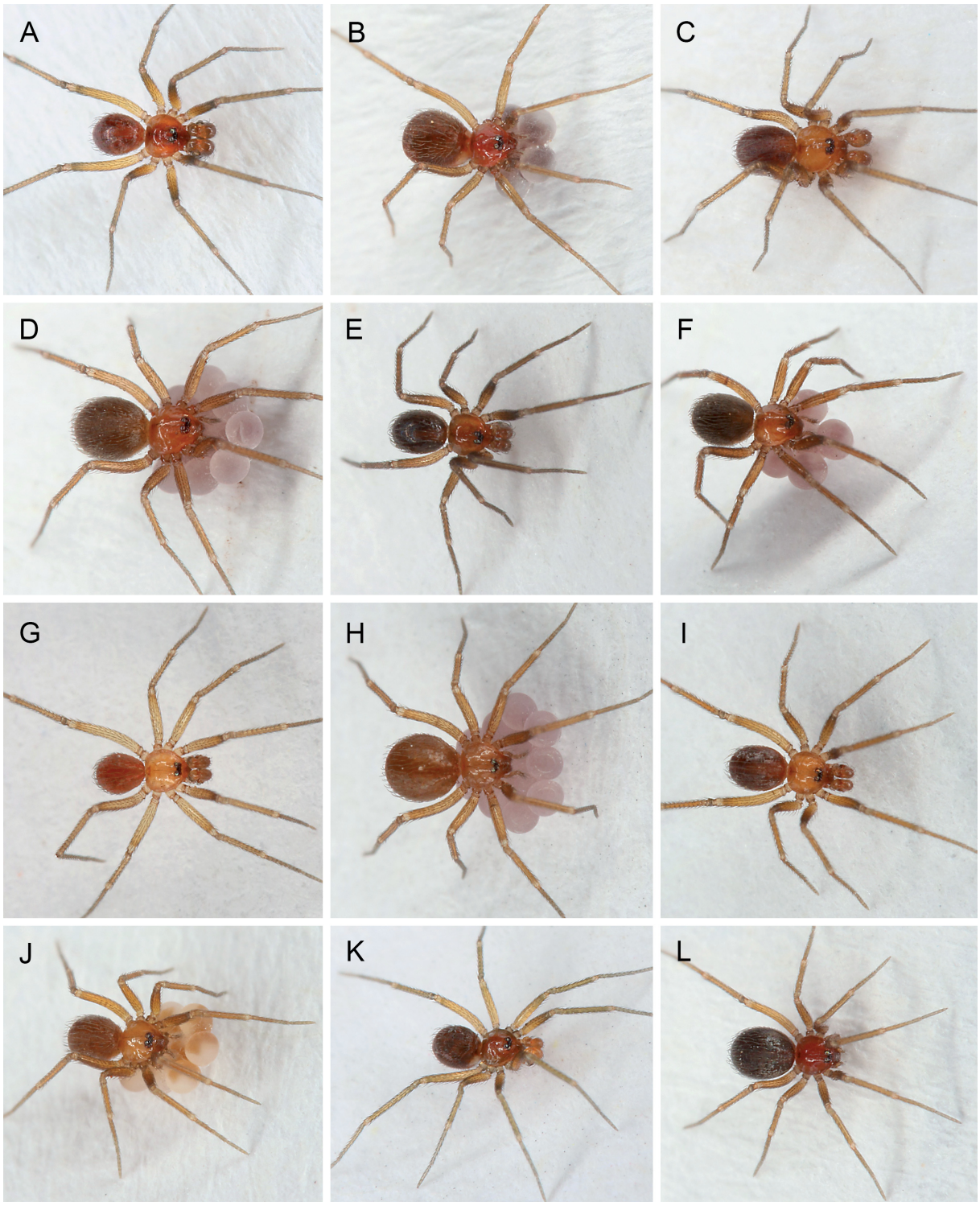

Fig. 2. *Kambiwa* Huber, 2000; live specimens from Brazil; all at same scale. **A–B**. *K. itacarambi* Huber sp. nov., ♂♀ with egg sac from NW of Itacarambi. **C–D**. *K. ibo* Huber sp. nov., ♂♀ with egg sac from NE of Lagoa Grande. **E–F**. *K. coribe* Huber sp. nov., ♂♀ with egg sac from E of São Felix do Coribe. **G–H**. *K. maracas* Huber sp. nov., ♂♀ with egg sac from S of Contendas do Sincorá. **I–J**. *K. brumado* Huber sp. nov., ♂♀ with egg sac from W of Marcolino Moura. **K–L**. *K. mucuge* Huber sp. nov., ♂♀ from NE of Mucugê.

Description

Males

Measurements. Total body length 0.9–1.3; carapace width 0.45–0.55. PME diameter 45–55 μm; AME diameter 20–35 μm. Leg 1 length 2.1–2.7; tibia 1 length 0.5–0.7; metatarsus 1 approximately same length as tibia 1 (metatarsus 1 / tibia 1 length: 0.96–1.06); tibia 4 longer than tibia 1 (tibia 4 / tibia 1 length: 1.1–1.3); leg femora diameters 110–120 μm; leg tibiae diameters 65–70 μm. Tibia 1 L/d 8–10.

Color. In ethanol mostly ochre-yellow to light brown, carapace without dark marks but sometimes medially slightly darker, legs without dark rings; abdomen sometimes pale gray, sometimes with darker

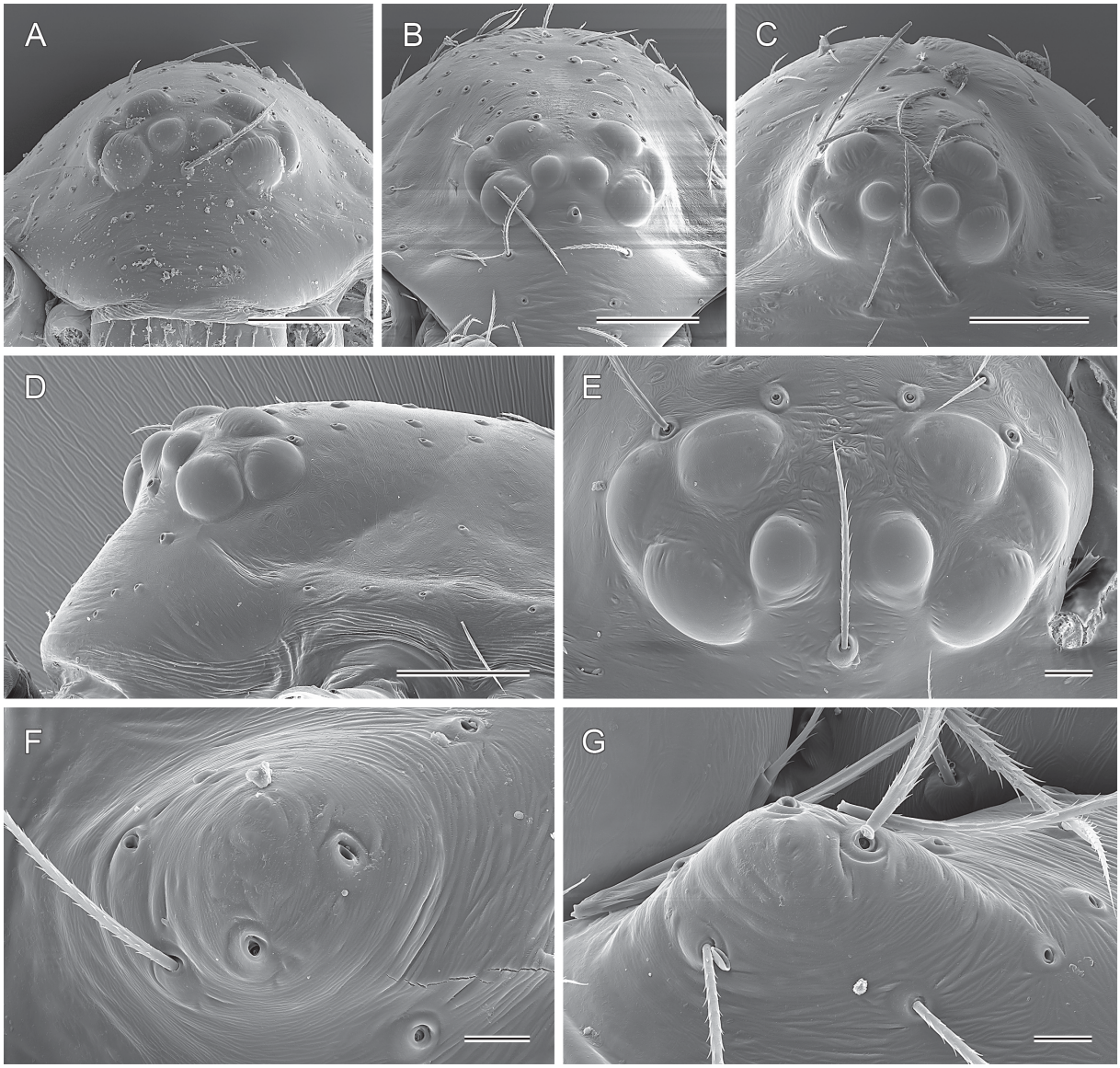

Fig. 3. *Kambiwa* Huber, 2000 spp., prosoma. **A**. *K. neotropica* (Kraus, 1957), female prosoma, frontal view. **B**. *K. brumado* Huber sp. nov., male prosoma, frontal view. **C**. *K. itacarambi* Huber sp. nov., male prosoma, frontal view. **D**. *K. maracas* Huber sp. nov., female prosoma, lateral view. **E**. *K. brumado*, male ocular area, frontal-dorsal view. **F**–**G**. *K. maracas*, male sternum humps, ventral and oblique lateral views. Scale lines: A–D = 100 μm; E = 20 μm; F–G = 10 μm.

internal marks dorsally and laterally; ventrally with light ochre to brown plate in front of gonopore. Live specimens often with slightly reddish or orange prosoma and legs (Fig. 2).

Body. Habitus as in Fig. 2. Ocular area not or barely raised. Carapace usually without thoracic groove (Fig. 3A–B), with shallow groove in *K. itacarambi* sp. nov. (Fig. 3C). Clypeus unmodified. Sternum slightly wider than long, with pair of low but distinct anterior processes near coxae 1 (Fig. 3F–G); processes without pores. Abdomen globular. Gonopore usually with four epiandrous spigots in two

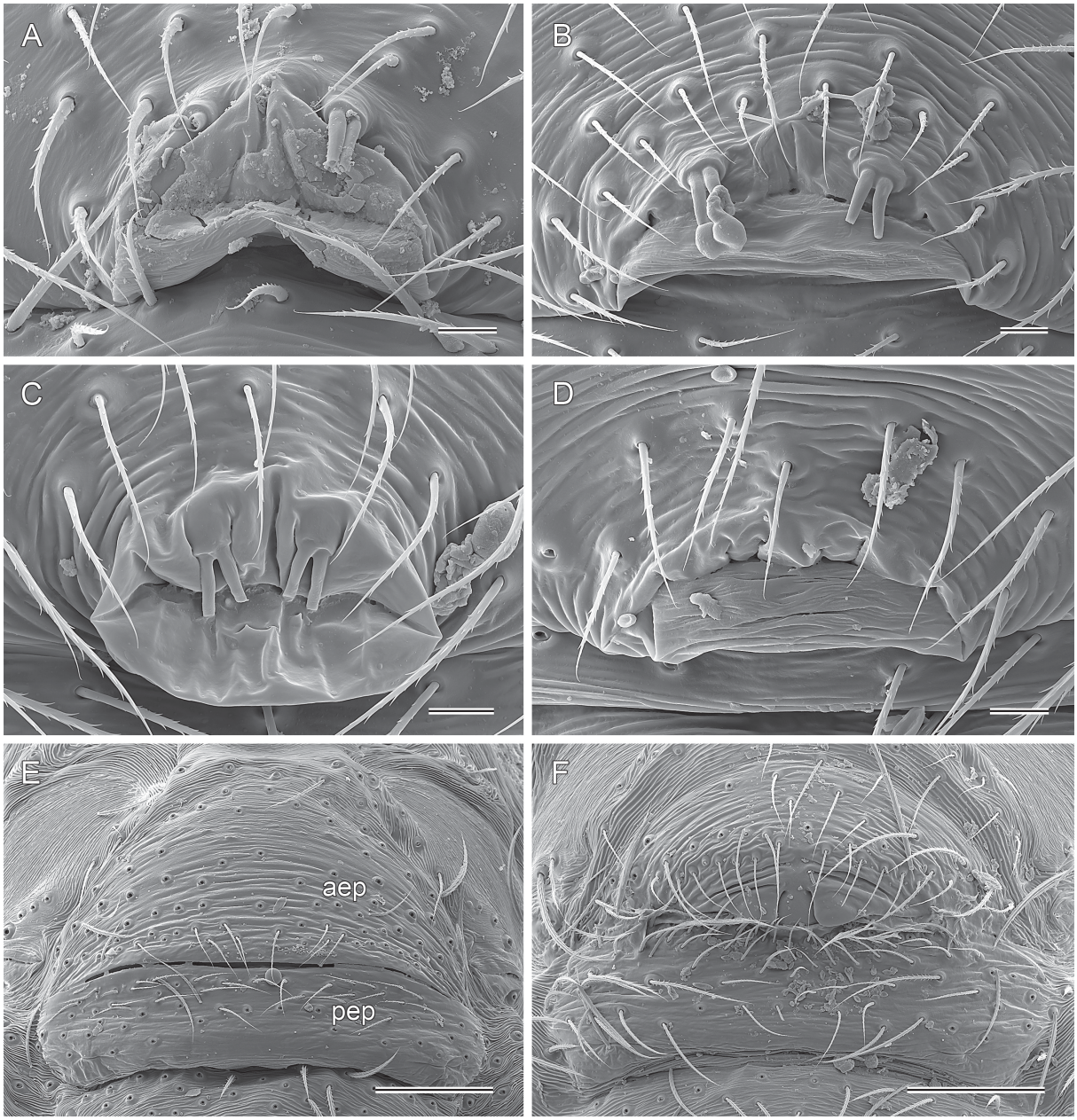

Fig. 4. *Kambiwa* Huber, 2000 spp., male gonopore and female epigynum. **A**. *K. neotropica* (Kraus, 1957), male gonopore. **B**. *K. itacarambi* Huber sp. nov., male gonopore. **C**. *K. brumado* Huber sp. nov., male gonopore. **D**. *K. maracas* Huber sp. nov., male gonopore. **E**. *K. ibo* Huber sp. nov., epigynum, ventral view. **F**. *K. itacarambi*, epigynum, ventral view. Abbreviations: aep = anterior epigynal plate; pep = posterior epigynal plate. Scale lines: A–D = 10 μm; E–F = 100 μm.

pairs (Fig. 4A–C), in *K. maracas* sp. nov. apparently without epiandrous spigots (Fig. 4D). General arrangement of spinnerets as usual in Pholcidae (cf. female, Fig. 5A); ASL with seven spigots each: one strongly widened spigot, one long and slender spigot, and five cylindrical spigots (of which one is much wider than the others) (Fig. 5); PMS with two short conical spigots (Fig. 5); PLS with strong hairs but without spigots.

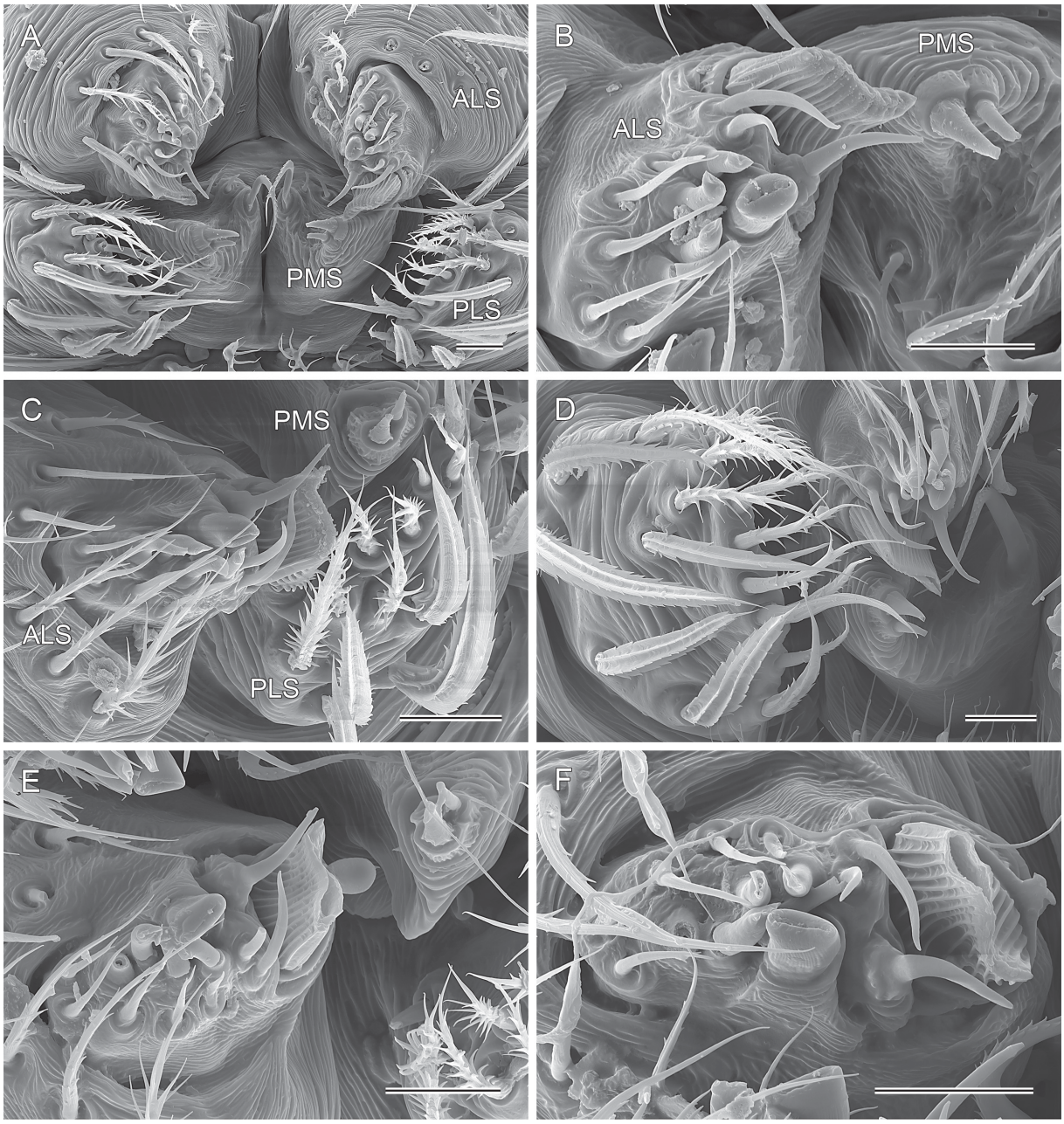

Fig. 5. *Kambiwa* Huber, 2000 spp., spinnerets. **A**. *K. brumado* Huber sp. nov., female spinnerets. **B**. *K. brumado*, female ALS and PMS. **C**. *K. itacarambi* Huber sp. nov., male spinnerets. **D**. *K. ibo* Huber sp. nov., female spinnerets. **E**. *K. maracas* Huber sp. nov., female ALS and PMS. **F**. *K. maracas*, female ALS. Scale lines = 10 μm.

Chelicerae. Usually with pair of small frontal apophyses (e.g., Fig. 17A–B), only in *K. itacarambi* sp. nov. without apophyses but with sclerotized ridge followed distally by whitish area (Fig. 40A–B). Stridulatory files (Fig. 6) usually fine but distinct, only in *K. itacarambi* very indistinct and not visible under dissecting microscope; with ~30–65 ridges, distances between ridges (in five species studied with SEM) mostly 1.3–1.8 μm, only in *K. ibo* sp. nov. wider (2.4 μm); distances between ridges very homogenous throughout file.

Palps. Coxa unmodified; trochanter with indistinct ventral protrusion; femur proximally with small ventral conical process, distally widened but otherwise unmodified; femur-patella condyles not or slightly shifted toward prolateral side; tibia almost globular, with two trichobothria; tibia-tarsus condyles not or

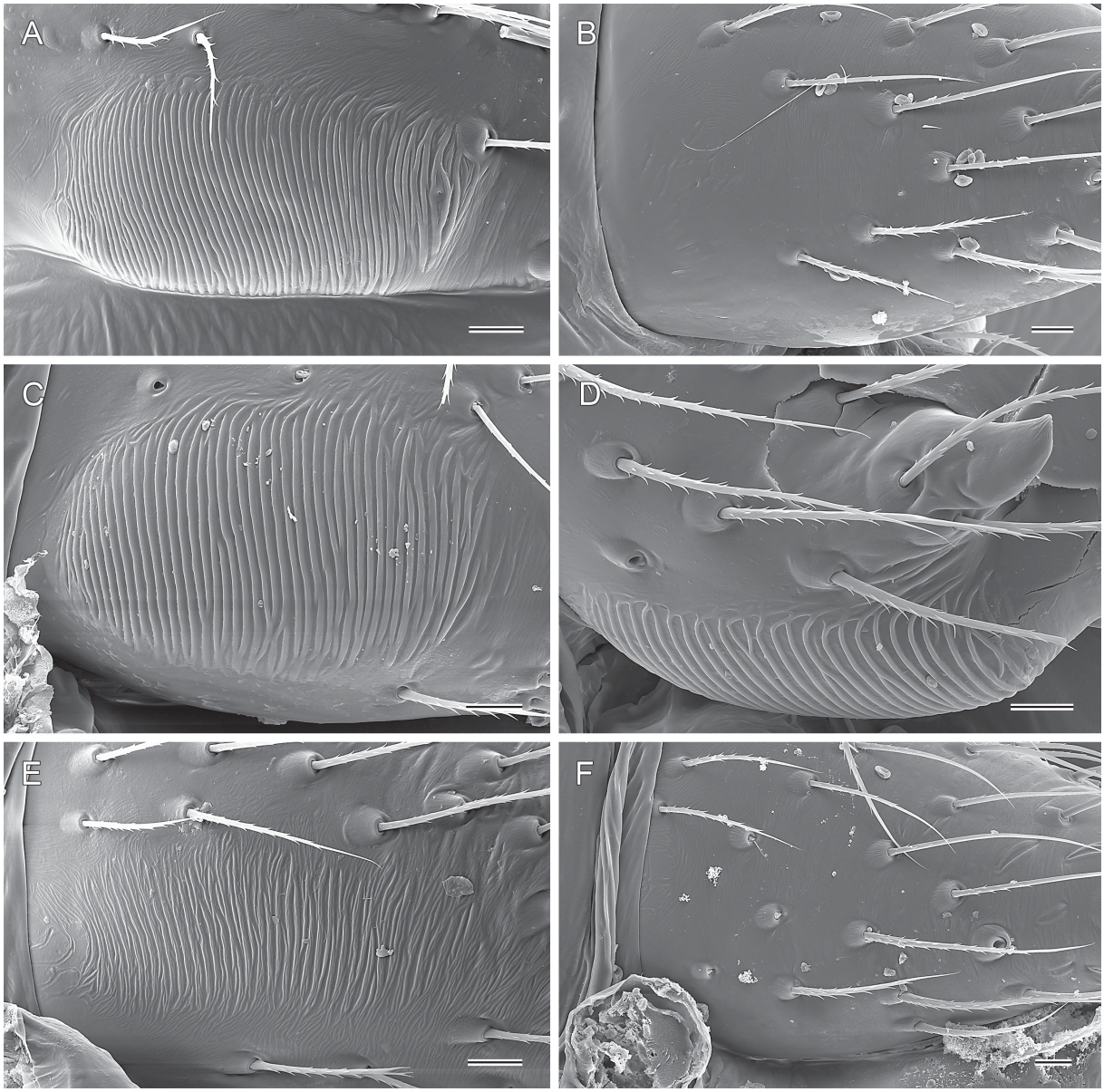

Fig. 6. *Kambiwa* Huber, 2000 spp., chelicerae. **A**–**B**. *K. maracas* Huber sp. nov., right male stridulatory file and right female chelicera. **C**. *K. brumado* Huber sp. nov., right male stridulatory file. **D**. *K. ibo* Huber sp. nov., right male stridulatory file. **E**–**F**. *K. itacarambi* Huber sp. nov., right male stridulatory file and right female chelicera. Scale lines = 10 μm.

slightly shifted toward retrolateral side; palpal tarsal organ capsulate with small opening (Fig. 7A–D), as long or slightly longer than wide, outer diameter 6–8 µm, opening diameter 0.8–1.2 µm; procursus short and simple, shape variable (e.g., Figs 16A–C, 22A–C), in *K. ibo* sp. nov. and *K. sapo* with small spikes on distal membranous flap (Figs 43A–C, 46A–C); genital bulb complex, with proximal sclerite connecting to tarsus; bulbous part of genital bulb with distinctive ventral process and variably complex dorsal processes including membranous and sclerotized elements (e.g., Figs 16D–F, 22D–F), retrolateral-dorsal sclerite in some species strongly elongated (e.g., Fig. 31D–F); sperm duct opening not located (presumably among membranous elements of dorsal bulbal process).

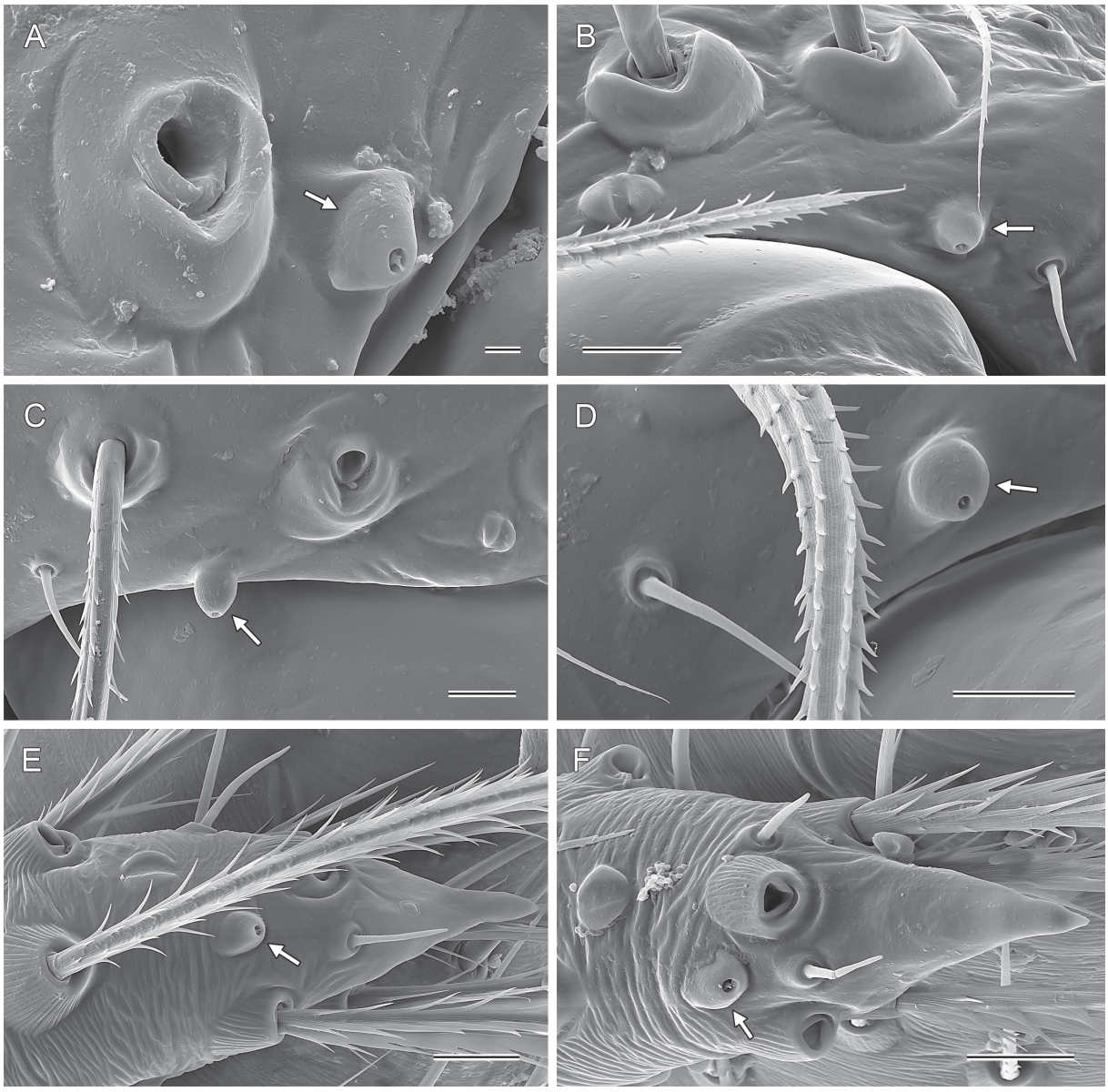

Fig. 7. *Kambiwa* Huber, 2000 spp., palpal tarsal organ (arrows) and female palp tip. **A**. *K. neotropica* (Kraus, 1957), male palpal tarsal organ. **B**. *K. maracas* Huber sp. nov., male palpal tarsal organ. **C**–**D**. *K. ibo* Huber sp. nov., male palpal tarsal organ. **E**. *K. brumado* Huber sp. nov., female palp tip. **F**. *K. maracas*, female palp tip. Scale lines: A = 2 µm; B–F = 10 µm.

Legs. Without spines; without curved hairs. Tibia 1 or tibia 1 + tibia 2 with sexually dimorphic short 'vertical' hairs (Fig. 8D–F), in several rows or bands, base diameter 4–5 µm, length 15–20 µm, diameter at half-length 0.7–0.8 µm. Distal leg segments (tarsi and metatarsi) with putative chemoreceptors (Fig. 10A–B), in light microscope similar to sexually dimorphic short vertical hairs but with one or two distal side branches, with one or two oblique furrows, and distally flattened (i.e., with oval diameter); base diameter ~4.5–5.0 µm, length 15–20 µm, diameter proximally 1.5–1.7 µm. Femora, tibiae, metatarsi, and tarsi with round or oval cuticular plates (Fig. 8A, E) at regular intervals, diameter ~5–7 µm. Rimmed

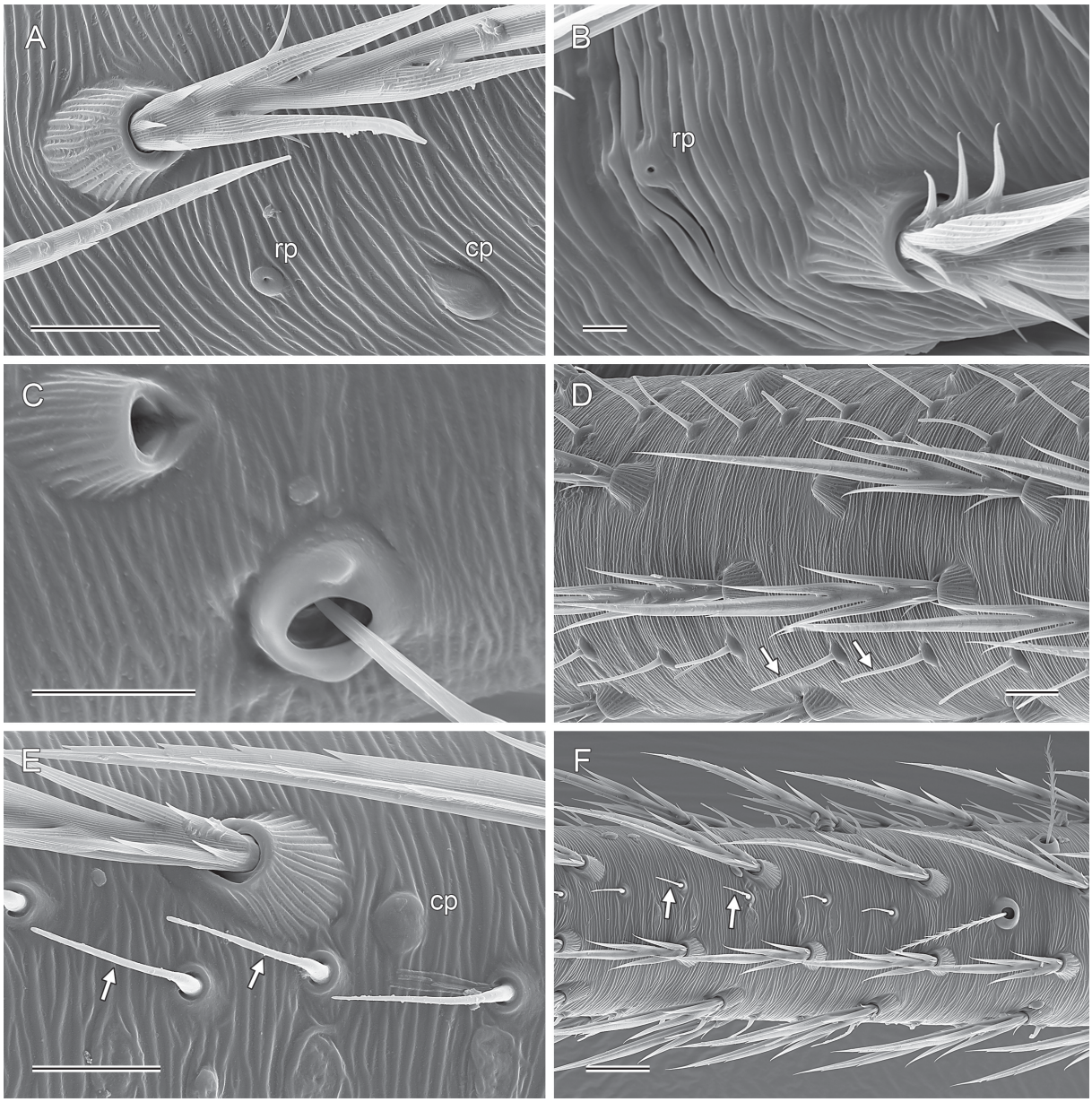

Fig. 8. *Kambiwa* Huber, 2000 spp., rimmed pores, cuticular plates, trichobothria, and sexually dimorphic short vertical hairs (arrows). **A**. *K. maracas* Huber sp. nov., left female tibia 3. **B**. *K. maracas*, left male tarsus 4. **C**. *K. maracas*, right female metatarsus 1. **D**. *K. maracas*, left male tibia 1, retrolateral-proximal view. **E**. *K. itacarambi* Huber sp. nov., left male tibia 1, prolateral view. **F**. *K. itacarambi*, left male tibia 2, retrolateral view. Abbreviations: cp = cuticular plate; rp = rimmed pore. Scale lines: A, C–E = 10 µm; B = 2 µm; F = 20 µm.

pores (Fig. 8A–B) at regular intervals, mainly dorsally on tibiae, metatarsi, and tarsi; outer diameter 2.5–2.7 μm; opening diameter: 0.3–0.4 μm. Base of trichobothria round or with pair of indistinct lateral humps (Fig. 8C); outer diameter of base: 10–14 μm; proximal diameter of seta: 1.3–1.4 μm; retrolateral trichobothrium on tibia 1 at 56–62% of tibia length; prolateral trichobothrium absent on tibia 1. Without slender metatarsal hairs (as described in Huber *et al.* 2023c, 2024d). Tarsi with 4–5 pseudosegments, only distally 2–3 distinct. Leg tarsal organs capsulate with small opening (Fig. 9), outer diameter 3–6 μm, opening diameter 0.8–1.1 μm. Tarsus 4 with two comb hairs distally on prolateral side (Fig. 10F). Tarsal claws as usual for family (Fig. 10); main claws with 8–10 teeth; teeth on tarsus 4 slightly different (shorter and directed more towards distal).

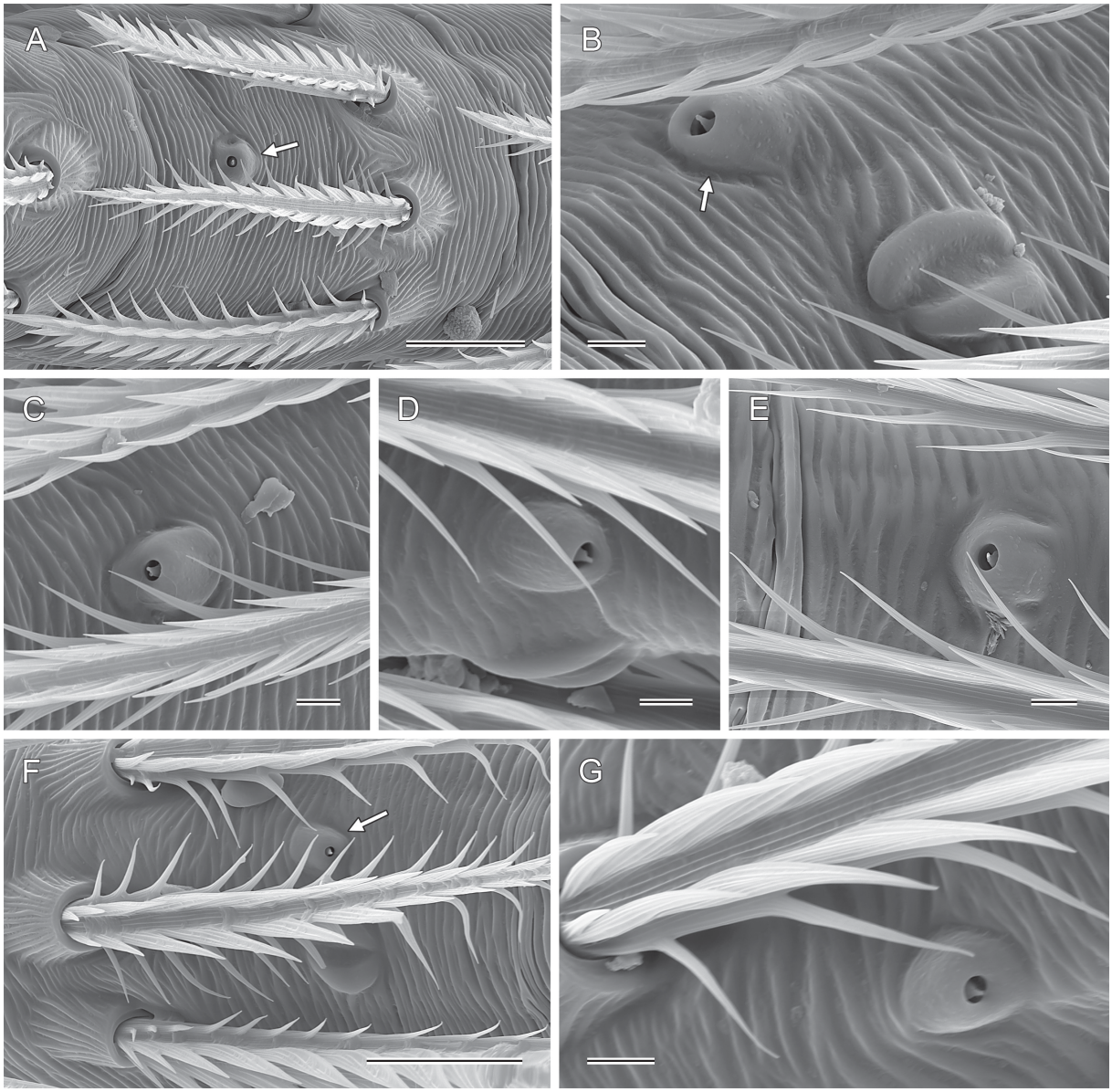

Fig. 9. *Kambiwa* Huber, 2000 spp., leg tarsal organ (arrows). **A**. *K. itacarambi* Huber sp. nov., left male tarsus 1. **B**. *K. ibo* Huber sp. nov., right male tarsus 1. **C**. *K. itacarambi*, left male tarsus 2. **D**. *K. brumado* Huber sp. nov., left male tarsus 2. **E**. *K. ibo*, left female tarsus 3. **F**. *K. maracas* Huber sp. nov., left male tarsus 4. **G**. *K. brumado*, left male tarsus 4. Scale lines: A, F = 10 μm; B–E, G = 2 μm.

Females

In general, very similar to males, but legs on average slightly shorter than in males (male / female tibia 1 length: ~1.0–1.1), without sexually dimorphic short vertical hairs on tibiae, without humps on sternum, and without stridulatory files on chelicerae (Fig. 6B, F). Palpal tarsal organ as in males but slightly less elevated (Fig. 7E–F), outer diameter 5.5–6.5 µm, opening diameter 0.8–1.0 µm. Other sensory organs and comb hairs on tarsus 4 as in males. Spinnerets as in males. Tip of palp with simple pointed process (Fig. 7E–F). Epigynum anterior plate usually trapezoidal to semicircular (e.g., Figs 18A, 24A, 33A), only in *K. itacarambi* sp. nov. rather arc-shaped (Fig. 41A), without processes or pockets. Posterior epigynal

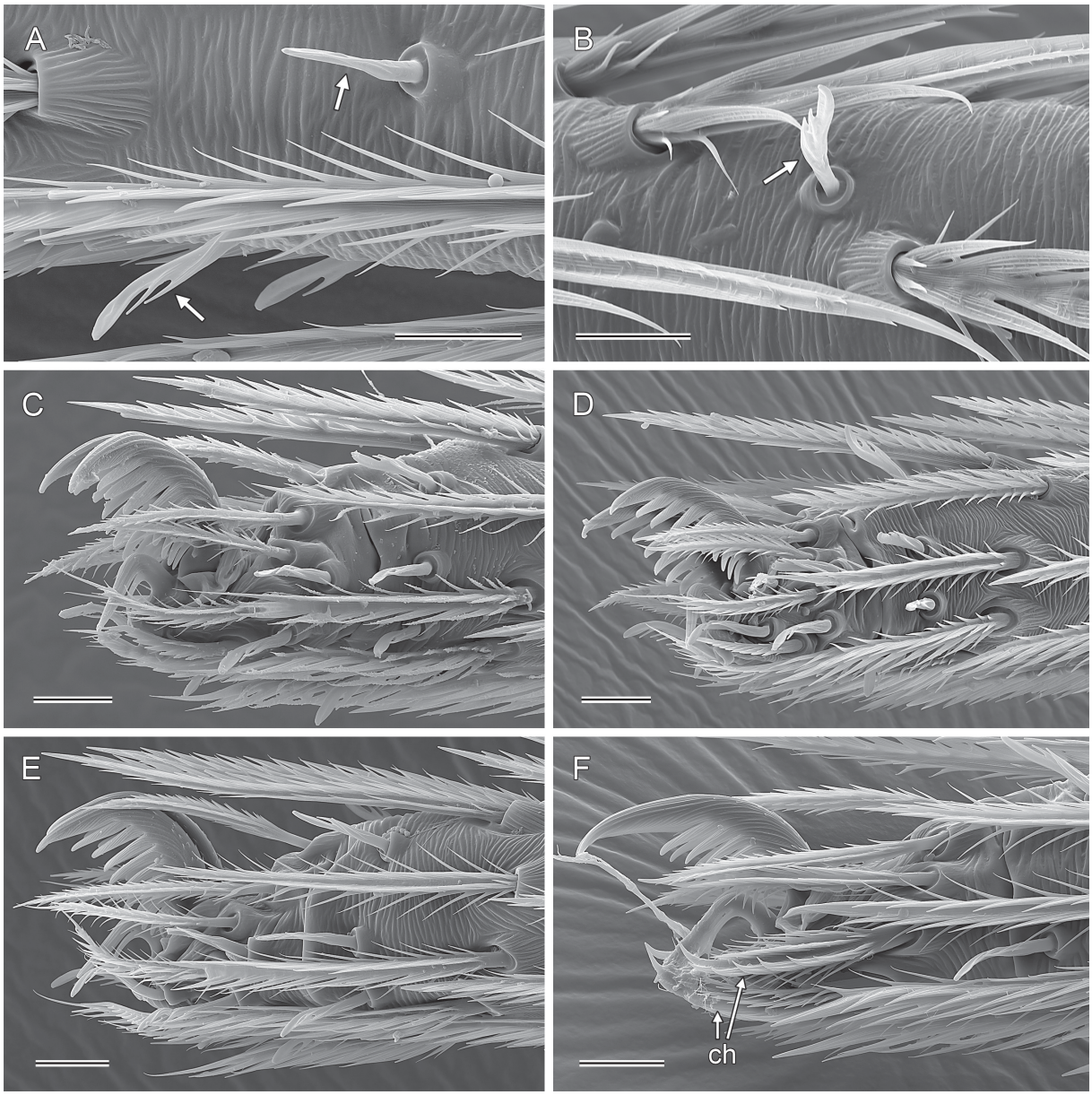

Fig. 10. *Kambiwa* Huber, 2000 spp., chemoreceptors (arrows) and leg tips. **A**. *K. ibo* Huber sp. nov., right male metatarsus 2, prolateral view. **B**. *K. maracas* Huber sp. nov., left male metatarsus 4. **C**. *K. neotropica* (Kraus, 1957), right male tarsus 2, prolateral view. **D**. *K. maracas*, right male tarsus 1, prolateral view. **E–F**. *K. itacarambi* Huber sp. nov., right male tarsi 1 and 4, prolateral views. Abbreviation: ch = comb hairs. Scale lines = 10 µm.

plate relatively large but simple, unmodified. Internal genitalia with straight or curved or bent transversal sclerite, without or with very small and indistinct pore plates (e.g., Figs 24G, 29F, 33F), in most species with median anterior modification (e.g., Figs 17C, 23C; absent in *K. itacarambi* and *K. ibo* sp. nov.); some species with median membranous sac, others with long membranous tube (Figs 28C, 32C, 36C) possibly functionally correlated with long retrolateral-dorsal sclerite of genital bulb.

Fig. 11. *Kambiwa* Huber, 2000 spp., typical habitats; all localities are in Brazil. **A**. Bahia, between Ibó and Curaçá; *K.* sp. aff. *neotropica.* **B**. Bahia, E of São Felix do Coribe; type locality of *K. coribe* Huber sp. nov. **C**. Bahia, NE of Brumado; type locality of *K. brumado* Huber sp. nov. **D**. Bahia, SW of Maracas; type locality of *K. maracas* Huber sp. nov. **E**. Bahia, NE of Mucugê; type locality of *K. mucuge* Huber sp. nov. **F**. Minas Gerais, NW of Itacarambi; type locality of *K. itacarambi* Huber sp. nov.

Relationships

The latest molecular phylogeny of Pholcidae (Meng *et al.* 2025) has a dense taxon sampling of Ninetinae, including the genera *Kambiwa*, *Galapa* and *Sertana* gen. nov. The relationships among these Neotropical genera is resolved as (*Kambiwa* (*Galapa*, *Sertana*)) (inset in Fig. 1). This is in contrast with our *CO1* tree (Fig. 1), but the tree in Meng *et al.* (2025) is based on a large number of genes and thus much more likely to reflect phylogeny. The topology in Meng *et al.* (2025) is also confirmed in an upcoming, even

Fig. 12. *Kambiwa ibo* Huber sp. nov., intraspecific habitat diversity; all localities are in Brazil. **A**. Bahia, S of Ibó; type locality. **B**. Bahia, W of Andorinha. **C**. Pernambuco, NE of Petrolina. **D**. Pernambuco, NE of Lagoa Grande. **E**. Bahia, S of Xique-Xique, 'site 1'. **F**. Bahia, S of Xique-Xique, 'site 3'.

larger dataset combining the UCA data of Meng *et al.* (2025) with results from low coverage genome sequencing (G. Meng, L. Podsiadlowski, B.A. Huber, unpubl. data). This new dataset also includes *Kambiwa ibo* sp. nov., which is resolved as sister to all other species of *Kambiwa*; the monophyly of *Kambiwa* receives maximum support. Thus, the paraphyly of *Kambiwa* shown in our *CO1* tree (Fig. 1) is very probably an artifact.

Natural history

Kambiwa spiders occupy a variety of semiarid habitats, ranging from flat areas dominated by bushes and grasses to rock outcrops, and from well preserved Caatinga to highly degraded habitats such as roadsides or Caatinga with cattle or cactus plantations (Figs 11–12). During the day, the spiders are usually hidden in ground-level microhabitats, such as under stones, in leaf litter, and in dead wood or pieces of cactus. These microhabitats were sometimes shaded by bushes and low trees, in other cases they were fully exposed to the sun. In some cases, a single species was found in a range of different microhabitats (e.g., *K. itacarambi* sp. nov.). Very few localities contained more than one species (e.g., NW of Itacarambi: *K. coribe* sp. nov. and *K. itacarambi*). Abundances were often high; several specimens sometimes shared the underside of a single rock; in one case, the careful revision of 1 m^2 of leaf litter resulted in 19 adult specimens. Upon disturbance, the spiders usually started to run rapidly, but often stopped suddenly as soon as they encountered a piece of 'dirt' or a depression for hiding. The spiders often shared localities and even microhabitats with representatives of *Ibotyporanga*; localities but not microhabitats were also

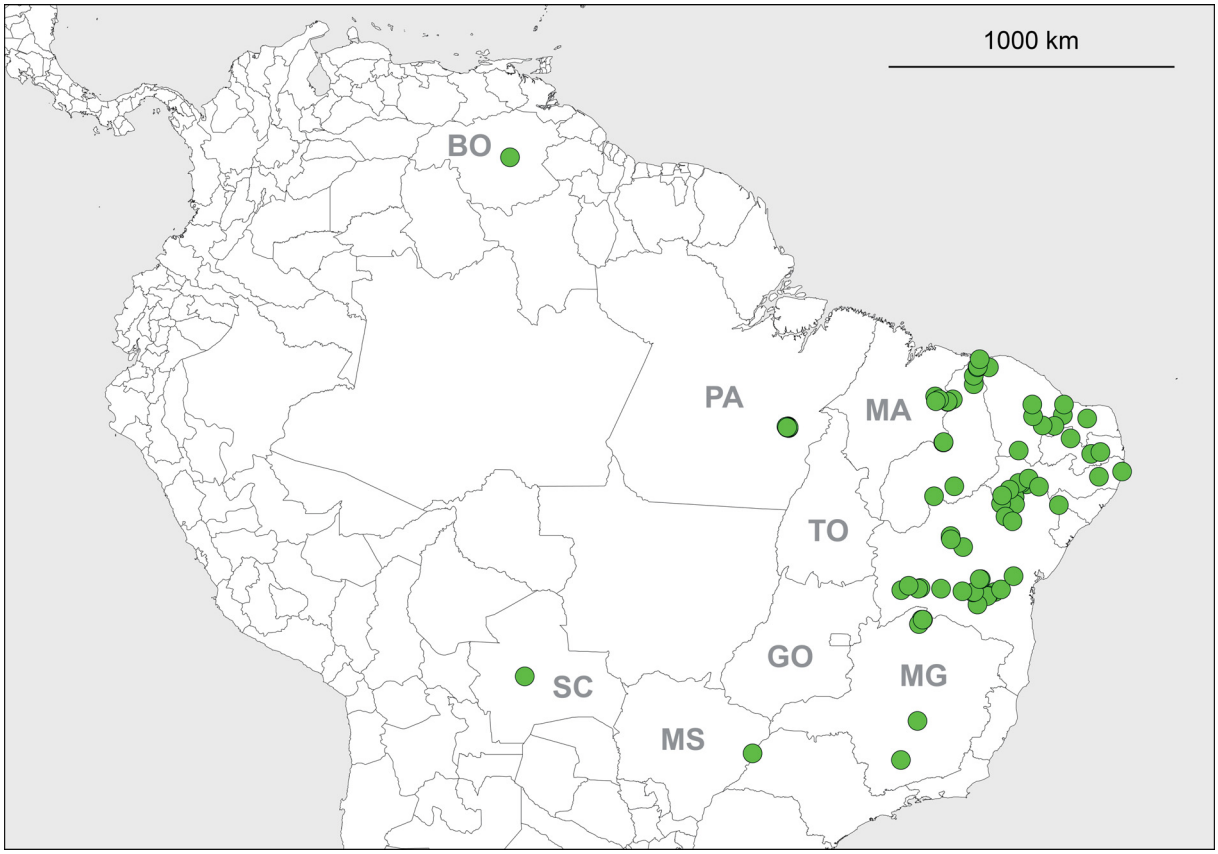

Fig. 13. Known distribution of *Kambiwa* Huber, 2000. For details on Brazilian species, see Fig. 14. The single Venezuelan dot represents *K. sapo* (Huber, 2019) comb. nov.; the single Bolivian dot represents *K. coribe* Huber sp. nov. Abbreviations: BO = Bolívar; GO = Goiás; MA = Maranhão; MG = Minas Gerais; MS = Mato Grosso do Sul; PA = Pará; SC = Santa Cruz; TO = Tocantins.

rarely shared with representatives of *Sertana* gen. nov. and certain Modisiminae (e.g., *Arenita* Huber & Carvalho, 2019). Egg sacs were carried under the prosoma (Fig. 2), and consisted of 2–14 eggs (large majority: 4–12) that were arranged in a single flat layer; eggs were covered by a few barely visible lines of silk. For further details, see individual natural history sections below.

Distribution

Kambiwa is apparently restricted to South America (Figs 13–14). The large majority of records are from the Cerrado and Caatinga biomes of northeastern Brazil. However, the isolated records from Bolivia and Venezuela suggest that the genus has in fact a much wider distribution. The large Cerrado region between Piauí/Bahia and Bolivia that has currently no record of *Kambiwa* may in fact be occupied by the genus. The same is true for semiarid environments in northern South America. However, focused collecting in northern Colombia and northern Venezuela only produced *Galapa* and *Ibotyporanga* (Huber *et al.* 2024a, 2024c), but no *Kambiwa*.

Composition and species limits

The genus now includes nine nominal species. The identity of one of them (*K. anomala* (Mello-Leitão, 1918)) remains unclear (see below). In four species (*K. brumado* sp. nov., *K. coribe* sp. nov., *K. ibo* sp. nov., *K. itacarambi* sp. nov.), we found unusually high genetic distances among putative conspecifics;

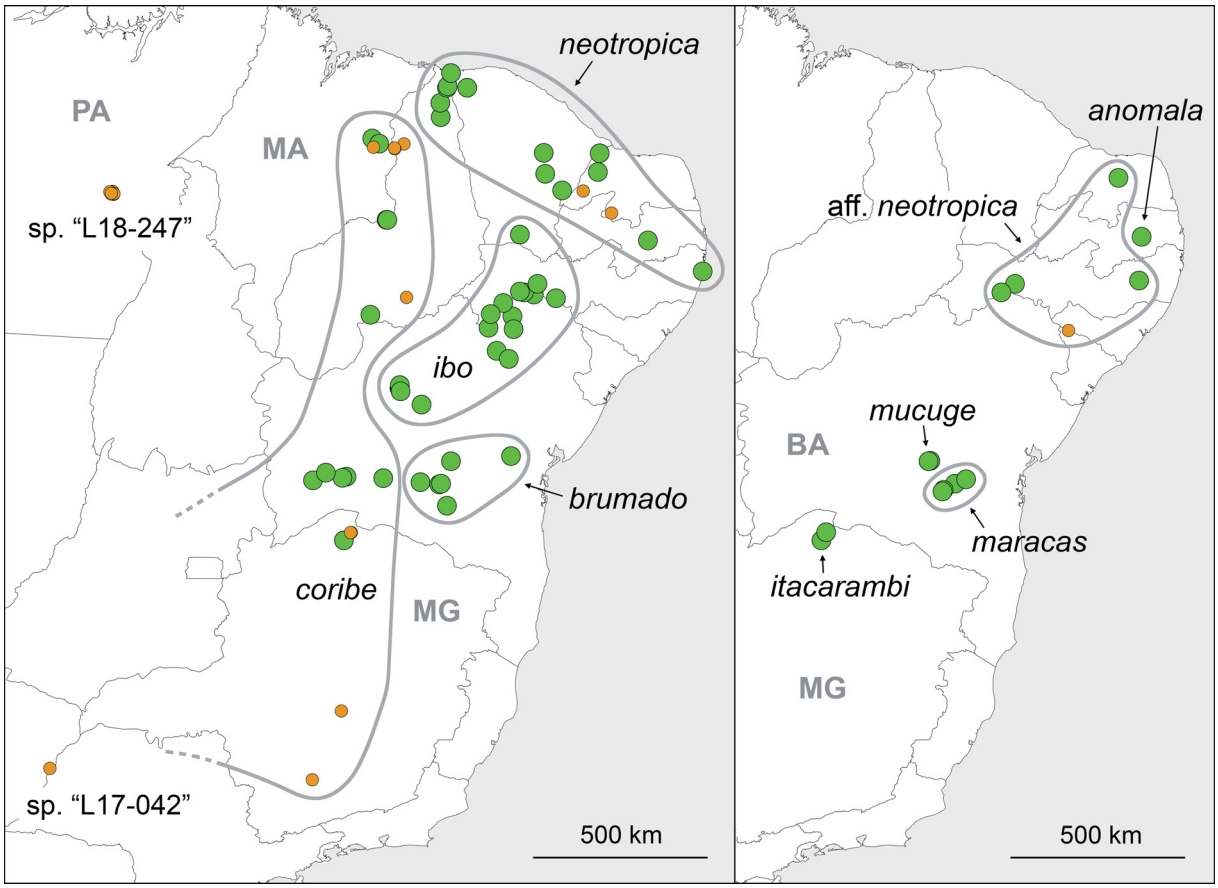

Fig. 14. Known distribution of *Kambiwa* Huber, 2000 in Brazil. The figure is split in order to avoid too much overlap. Small orange dots denote species that we do not formally describe or specimens that we could not study in detail and that may not represent the respective species. Abbreviations: BA = Bahia; MA = Maranhão; MG = Minas Gerais; PA = Pará.

some of them may eventually need to be split into two or more species each. One further probable species is available in collections but only informally described for reasons explained below (see section on *K. anomala*): *K.* sp. aff. *neotropica*. Finally, the IBSP and UFMG have specimens of two additional probable species that BAH (the coauthor responsible for the alpha taxonomic aspects) could not study in detail; one of them originates from several caves in Pará, FLONA de Carajás, (~6.03–6.11° S, 50.13–50.23° W); the other (a single male) from Mato Grosso do Sul, Três Lagoas, Horto Barra do Moeda (20.950° S, 51.783° W).

Identification key (males only, i.e., excluding *K. anomala*)

1. Chelicerae without apophyses (Fig. 40A–B) ..... ***K. itacarambi*** Huber sp. nov.
– Chelicerae with pair of frontal apophyses (e.g., Figs 17A–B, 28A–B, 44A–B) 2

2. Procursus tip is a membranous flap, i.e., without sclerotized elements (Figs 22A–C, 43A–C, 46A–C) 3
– Procursus tip with sclerotized elements (e.g., Figs 19A–C, 27A–C) 5

3. Ventral and retrolateral-dorsal processes on genital bulb long (Fig. 22D–F), prolateral-dorsal process on genital bulb distinct and hooked (Fig. 22E) ..... ***K. coribe*** Huber sp. nov.
– Ventral and retrolateral-dorsal processes on genital bulb short (Figs 43D–F, 46D–F), prolateral-dorsal process on genital bulb absent or barely visible 4

4. Tip of procursus evenly rounded (i.e., not bifid; Fig. 43C) ..... ***K. ibo*** Huber sp. nov.
– Tip of procursus bifid (Fig. 46C) ..... ***K. sapo*** (Huber, 2019) comb. nov.

5. Retrolateral-dorsal process of genital bulb very long and slender (Figs 27F, 31F, 35F), extending beyond palpal coxa (e.g., Fig. 30); ventral bulbal process short, roughly rectangular (Figs 27F, 31F, 35F) 6
– Retrolateral-dorsal process of genital bulb much shorter (Fig. 16F), barely reaching palpal trochanter (Fig. 15); ventral bulbal process longer, hooked (Figs 16F, 19F) 8

6. Procursus without prolateral process (Fig. 31B) ..... ***K. maracas*** Huber sp. nov.
– Procursus with prolateral process (Figs 27B, 35B) 7

7. Prolateral process on procursus short (Fig. 27B); retrolateral-dorsal processes on genital bulb directed ventrally ..... ***K. brumado*** Huber sp. nov.
– Prolateral process on procursus long (Fig. 35B); retrolateral-dorsal processes on genital bulb directed distally ..... ***K. mucuge*** Huber sp. nov.

8. Dorsal and ventral sclerotized elements on procursus tip wide apart (Fig. 16A, C) .... ***K. neotropica*** (Kraus, 1957)
– Dorsal and ventral sclerotized elements on procursus tip closer together (Fig. 19A, C) .... ***K***. sp. aff. ***neotropica*** CHNUFPI 9116

Kambiwa neotropica (Kraus, 1957)
Figs 3A, 4A, 7A, 10C, 15–18

Ninetis neotropica Kraus, 1957: 242, figs 73–80.

Kambiwa neotropica – Huber 2000: 89, figs 338–341.

Diagnosis

Males are easily distinguished from those of most known congeners by shape of ventral bulbal process (Fig. 16F; long, directed towards distal, and distally hooked), by retrolateral-dorsal process of genital bulb barely reaching palpal trochanter (Fig. 15C; in other species either absent or much longer), and by tip of procursus (Fig 16A–C; with dorsal and ventral sclerotized elements connected by transparent membrane); from very similar, formally undescribed *K.* sp. aff. *neotropica* by details of genital bulb (ventral bulbal process shorter and stronger, dorsal bulbal processes different, compare Figs 16E and 19E) and by dorsal and ventral sclerotized elements on procursus tip slightly wider apart (compare Figs 16A and 19A). Females appear externally indistinguishable from those of several congeners (*K.* sp. aff. *neotropica*; *K. coribe* sp. nov.; *K. maracas* sp. nov.; *K. brumado* sp. nov.; *K. mucuge* sp. nov.); they differ internally by strong median sclerotized element leading into simple membranous sac (structures '1' and '2' in Fig. 18F; very similar in *K.* sp. aff. *neotropica*; other species with smaller median sclerotized element leading into membranous tube) and by pair of lateral membranous pouches and posterior small sacs (structures '3' and '4' in Fig. 18F).

Type material

Holotype

BRAZIL – **Pernambuco** • ♂; Recife; 8.1° S, 34.9° W; date and collector unknown; SMF RII/6776a; examined by first author in 1999; reexamined.

Paratypes

BRAZIL – **Pernambuco** • 1 ♂, 4 ♀♀; same collection data as for holotype; SMF RII/6776b; examined by first author in 1999; not reexamined.

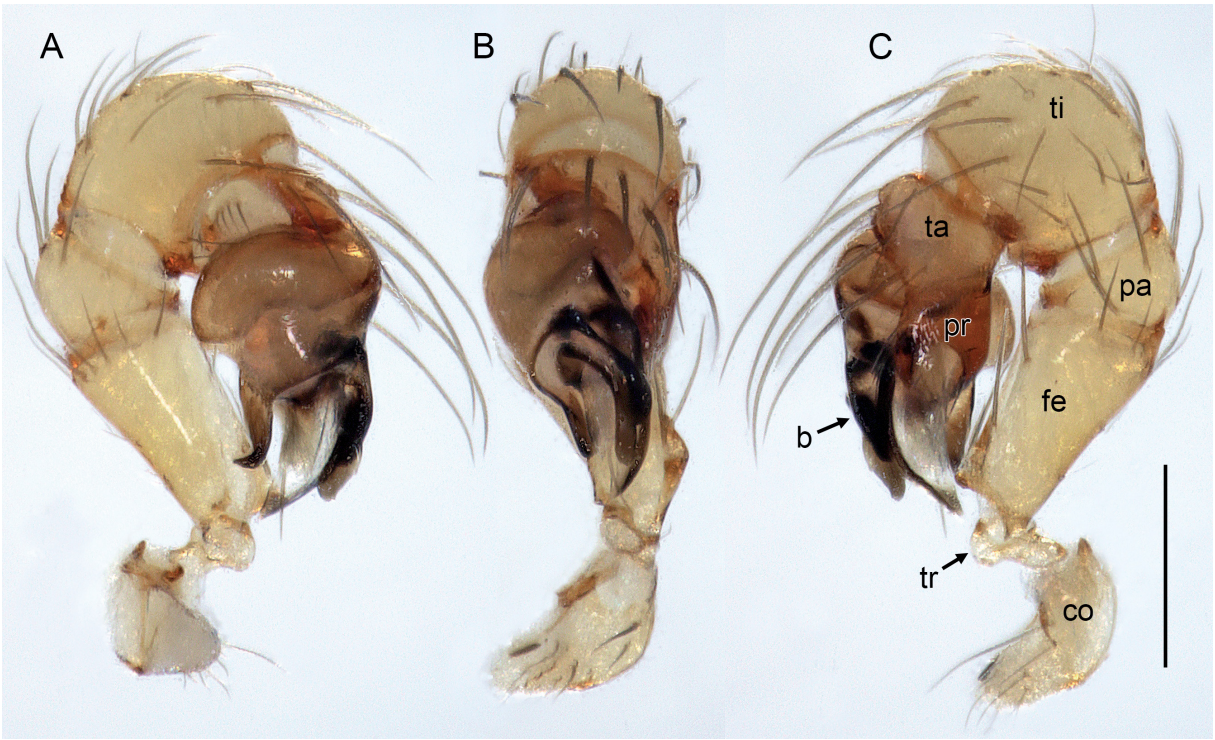

Fig. 15. *Kambiwa neotropica* (Kraus, 1957); ♂ from Brazil, Rio Grande do Norte, Lajedo do Arapuá, ZFMK Ar 24707. Left palp, prolateral, dorsal, and retrolateral views. Abbreviations: b = genital bulb; co = coxa; fe = femur; pa = patella; pr = procursus; ta = tarsus; ti = tibia; tr = trochanter. Scale line = 0.2 mm.

New records

BRAZIL – **Ceará** • 3 ♂♂; Jaguaribe, "zona rural"; 5.9992° S, 38.5366° W; 235 m a.s.l.; 2014; S.C. Sousa leg.; CHNUFPI 3773 • 2 ♂♂, 2 ♀♀, 2 juvs; Solonópole, roadside of BR 122; 5.5735° S, 38.9704° W; 185 m a.s.l.; 22 Nov. 2020; L.S. Carvalho and J.F. Lima leg.; CHNUFPI 4036 ("Carv65"; vouchers of E076) • 1 ♂, 1 ♀; same collection data as for preceding; CHNUFPI 4037 • 2 ♀♀; Quixada, Serra do Urucu, Santuário Nossa Senhora; 5.0350° S, 39.0106° W; 345 m a.s.l.; 19 Apr. 2014; M.B. Silva and N. Saraiva leg.; CHNUFPI 3665 • 3 ♂♂, 6 ♀♀, 3 juvs; Granja, Povoado Santa Teresina, roadside of CE-311; 3.3494° S, 40.9945° W; 70 m a.s.l.; 14 Feb. 2023; L.S. Carvalho and E.G. Noetzold leg.; CHNUFPI 5057 (1 ♂, 1 ♀ used for SEM) • 1 ♂, 1 ♀; same collection data as for preceding; CHNUFPI

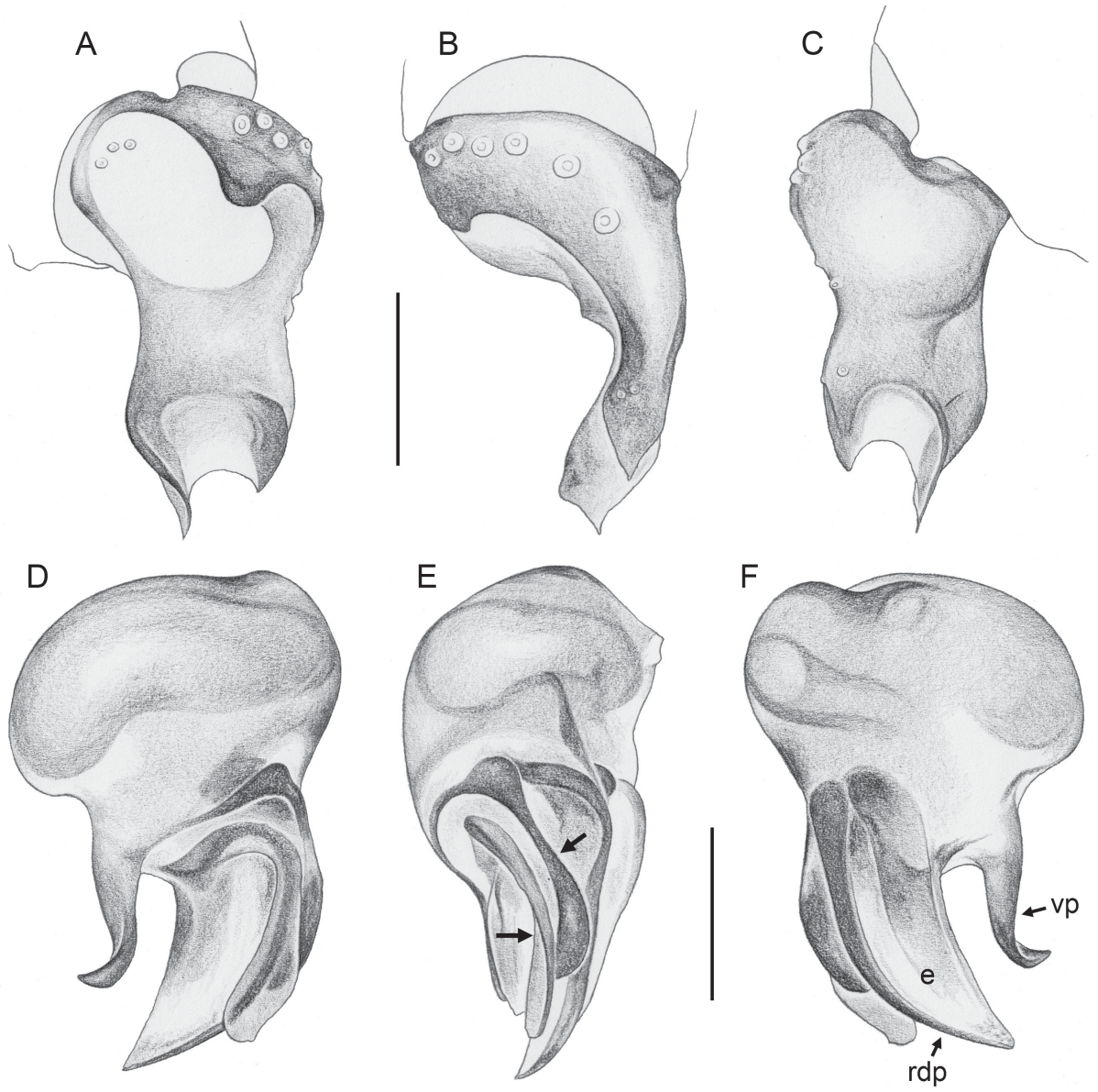

Fig. 16. *Kambiwa neotropica* (Kraus, 1957); ♂ from Brazil, Rio Grande do Norte, Lajedo do Arapuá, ZFMK Ar 24707. **A–C**. Left palpal tarsus and procursus, prolateral, dorsal, and retrolateral views. **D–F**. Left genital bulb, prolateral, dorsal, and retrolateral views; arrows: distinctive dorsal processes (compare Fig. 19E). Abbreviations: e = putative embolus; rdp = retrolateral-dorsal process; vp = ventral process. Scale lines = 0.1 mm.

5059. – **Paraíba** • 1 ♂, 7 ♀♀, 2 juvs; Boa Vista, Serrota, roadside of BR 412; 7.2968° S, 36.3161° W; 475 m a.s.l.; 19 Apr. 2023; L.S. Carvalho and E.G. Noetzold leg.; CHNUFPI 5017. – **Piauí** • 2 ♂♂, 4 ♀♀; Brasileira, Parque Nacional de Sete Cidades, near Cachoeira do Riachão; 4.1060° S, 41.6764° W; 170 m a.s.l.; 2 Dec. 2019; L.S. Carvalho and R.F. Ferreira leg.; CHNUFPI 4049 ("Carv68"; vouchers of UH 178 and E077) • 1 ♂; same collection data as for preceding; CHNUFPI 4048 • 1 ♂, 1 ♀; Piracuruca, roadside of BR 343; 3.7359° S, 41.6824° W; 60 m a.s.l.; 20 Feb. 2023; L.S. Carvalho and F.G. Noetzold leg.; CHNUFPI 5047 • 2 ♀♀; same collection data as for preceding; CHNUFPI 5053 • 2 ♂♂, 3 ♀♀, 2 juvs; Cocal, roadside of PI-301, near Ipuera village, 'site 1'; 3.3424° S, 41.5165° W; 135 m a.s.l.; 7 Jan. 2023; L.S. Carvalho and F.G. Noetzold leg.; CHNUFPI 5063 • 1 ♀; Cocal, roadside of PI-301, near Ipuera village, 'site 2'; 3.3081° S, 41.4944° W; 90 m a.s.l.; 24 Apr. 2022; L.S. Carvalho leg.; CHNUFPI 4182 • 1 ♀; same collection data as for preceding; CHNUFPI 4183 • 1 ♂, 3 ♀♀; Cajueiro de Praia, PI 302, near Praia de Barra Grande; 2.9648° S, 41.4093° W; 15 m a.s.l.; 25 Mar. 2019; L.S. Carvalho leg.; CHNUFPI 3901. – **Rio Grande do Norte** • 1 ♂, 9 ♀♀, 2 juvs; near Felipe Guerra, Lajedo do Arapuá; 5.5292° S, 37.6143° W; 80 m a.s.l.; 8 Jun. 2015; B.A. Huber and L.S. Carvalho leg.; CHNUFPI 9112 • 3 ♂♂, 3 ♀♀; same collection data as for preceding; CHNUFPI 9113 [deposited in ZFMK Ar 24707] • 3 ♀♀, in pure ethanol; same collection data as for preceding; CHNUFPI 9114 [deposited in ZFMK Br15-267] (vouchers of S328 and E019) • 6 ♀♀; same collection data as for preceding; CHNUFPI 4196 • 1 ♀; same collection data as for preceding; CHNUFPI 3698 • 1 ♀; same collection data as for preceding; CHNUFPI 3734 • 1 ♀; same collection data as for preceding; CHNUFPI 3751 • 1 ♀; same collection data as for preceding; CHNUFPI 4188 • 1 ♀; same collection data as for preceding; CHNUFPI 3768 • 1 ♂; near Baraúna, near Caverna dos Macacos; 5.0383° S, 37.5617° W; 100 m a.s.l.; 6 Jun. 2015; B.A. Huber and L.S. Carvalho leg.; CHNUFPI 9115 [deposited in ZFMK Ar 24708].

Redescription

Male (ZFMK Ar 24707)

Measurements. Total body length 1.32, carapace width 0.50. Distance PME–PME 50 µm; diameter PME 50 µm; distance PME–ALE 20 µm; distance AME–AME 10 µm; diameter AME 30 µm. Leg 1: 2.60 (0.70+0.18+0.66+0.68+0.38), tibia 2: 0.56, tibia 3: 0.51, tibia 4: 0.78; tibia 1 L/d: 10; diameters of leg femora 115 µm, of leg tibiae 65 µm.

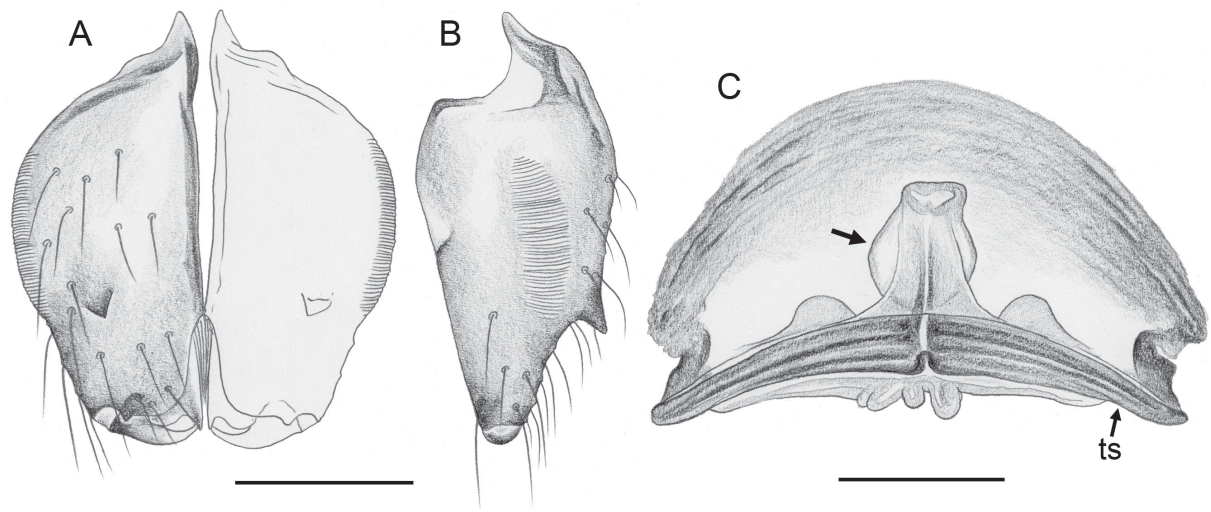

Fig. 17. *Kambiwa neotropica* (Kraus, 1957); ♂♀ from Brazil, Rio Grande do Norte, Lajedo do Arapuá, ZFMK Ar 24707. **A**–**B**. Male chelicerae, frontal and lateral views. **C**. Cleared female genitalia, dorsal view; arrow points at membranous sac. Abbreviation: ts = transversal sclerite. Scale lines = 0.1 mm.

Color (in ethanol). Prosoma and legs ochre-yellow, carapace and legs without darker marks or rings; abdomen ochre-gray, with darker internal marks and indistinct darker plate in front of gonopore.

Body. Habitus as in close relatives (e.g., Fig. 2E). Ocular area not raised. Carapace without thoracic groove. Clypeus unmodified. Sternum slightly wider than long (0.36/0.32), with small but distinct anterior humps near coxae 1 (~20 μm high, 40 μm diameter at basis; contra Huber 2000). Abdomen globular.

Chelicerae. As in Fig. 17A–B; with pair of small frontal apophyses; stridulatory files very fine and poorly visible in dissecting microscope.

Palps. As in Fig. 15; coxa unmodified; trochanter ventrally slightly protruding; femur proximally with small ventral conical process, distally widened but otherwise unmodified; femur-patella condyles slightly shifted toward prolateral side; tibia-tarsus condyles barely shifted toward retrolateral side; tarsus with small prolateral sclerotized process; procursus (Fig. 16A–C) wide in lateral view, narrower in dorsal view, with distinctive pair of distal tips connected by transparent membrane; genital bulb (Fig. 16D–F) with hooked ventral process, two distinctive prolateral-dorsal sclerites, and large membranous element (putative embolus) accompanied by retrolateral-dorsal process barely reaching palpal trochanter.

Legs. Without spines, without curved hairs; with short vertical hairs on tibia 1 (contra Huber 2000); retrolateral trichobothrium of tibia 1 at 56%; prolateral trichobothrium absent on tibia 1; tarsus 1 with ~4–5 pseudosegments, distally fairly distinct.

Variation (males)

Tibia 1 in 22 males: 0.58–0.72 (mean 0.64). Dark abdominal marks variably distinct.

Females

In general similar to males but sternum without humps and chelicerae without stridulatory files. Tibia 1 in 46 females: 0.52–0.66 (mean 0.60). Epigynum (Fig. 18A–B) anterior plate semicircular, weakly protruding, with pair of lateral posterior sclerites; posterior plate large but simple, roughly rectangular. Internal genitalia (Figs 17C, 18C–F) with weakly curved transversal sclerite connected laterally to lateral posterior sclerites of anterior epigynal plate, medially with anterior sclerotized element leading to membranous sac, and two pairs of membranous pouches/sacs (Fig. 18F); apparently without pore plates.

Barcoding

Three specimens were barcoded, from Rio Grande do Norte, Piauí, and Ceará. The K2P distances ranged from 1.6 to 3.5% (Table 2).

Distribution

Widely distributed in northeastern Brazil, ranging from eastern Pernambuco to northern Piauí (Fig. 14). However, the type locality "Pernambuco, Recife" may be incorrect. Collection date and collector are not known for the type series, and our own (LSC, BAH) efforts to find this species around Recife in 2015 failed. This species occurs at significantly lower altitudes (i.e., 145 ± 131 m, n = 14) than other congeners with broader distributions (e.g., *K. coribe* Huber sp. nov. and *K. ibo* Huber sp. nov.; see Fig. 83), as supported by likelihood ratio tests of negative binomial models ($\chi^2 = 21.66$, df = 2, p = 0.000). Specimens from further localities, deposited in CHNUFPI and IBSP, could not be studied in detail (by BAH) or include females only; they might be representatives of *K. neotropica* or of the species informally described below as *Kambiwa* sp. aff. *neotropica*. They originate from Rio Grande do Norte, Estação Ecológica do Seridó (6.5875° S, 37.2553° W); and Rio Grande do Norte, Encosta da Serra (6.0163° S, 37.9916° W).

Table 2 (continued on next page). *CO1* K2P genetic distances between sequenced specimens (ingroup only). Bold numbers are intraspecific distances (n = 62, 0–14.1%, mean 4.8%); interspecific distances within *Kambiwa* Huber, 2000 (n = 295): 8.6–35.0% (mean 18.4%); interspecific distances within *Sertana* Huber gen. nov. (n = 22): 9.3–17.5% (mean 13.4%); intergeneric distances (n = 216): 12.6–25.2% (mean 18.5%).

	UH087	UH496	UH513	UH511	UH103	UH510	UH110	UH509	UH503	UH502	E074	UH067	UH066	UH490	G52	UH492	UH050
UH087_Kambiwa_ibo?_Br22-217																	
UH496_Kambiwa_ibo?_Br22-207	**0.096**																
UH513_Kambiwa_ibo_Br22-258	**0.100**	**0.105**															
UH511_Kambiwa_ibo_Br22-256a	**0.105**	**0.107**	**0.005**														
UH103_Kambiwa_ibo_Br22-244	**0.104**	**0.109**	**0.003**	**0.002**													
UH510_Kambiwa_ibo_Br22-255	**0.104**	**0.109**	**0.003**	**0.002**	**0.000**												
UH110_Kambiwa_ibo_Br22-260	**0.102**	**0.111**	**0.005**	**0.003**	**0.002**	**0.002**											
UH509_Kambiwa_ibo_Br22-254	**0.105**	**0.111**	**0.005**	**0.003**	**0.002**	**0.002**	**0.003**										
UH503_Kambiwa_ibo_Br22-241	**0.107**	**0.113**	**0.006**	**0.005**	**0.003**	**0.003**	**0.005**	**0.005**									
UH502_Kambiwa_ibo_Br22-240	**0.129**	**0.111**	**0.056**	**0.055**	**0.053**	**0.053**	**0.055**	**0.055**	**0.053**								
E074_Sertana_capivara_Carv64	0.175	0.193	0.141	0.132	0.141	0.141	0.141	0.141	0.132	0.132							
UH067_Sertana_lapa_Br22-191	0.197	0.215	0.204	0.200	0.202	0.202	0.200	0.200	0.200	0.200	0.125						
UH066_Sertana_lapa_Br22-188	0.197	0.213	0.204	0.200	0.202	0.202	0.200	0.200	0.200	0.200	0.125	**0.002**					
UH490_Sertana_lapa_Br22-187	0.197	0.213	0.204	0.200	0.202	0.202	0.200	0.200	0.200	0.200	0.125	**0.002**	**0.000**				
G52_Sertana_sagarana_Br22-179	0.187	0.191	0.148	0.152	0.150	0.150	0.148	0.152	0.152	0.156	0.123	0.175	0.175	0.175			
UH492_Sertana_igapora_Br22-190	0.171	0.158	0.174	0.174	0.176	0.176	0.178	0.178	0.174	0.162	0.101	0.137	0.135	0.135	0.131		
UH050_Sertana_igapora_Br22-156	0.175	0.162	0.174	0.174	0.176	0.176	0.178	0.178	0.174	0.162	0.094	0.142	0.140	0.140	0.132	**0.006**	
UH070_Sertana_igapora_Br22-194	0.177	0.160	0.172	0.172	0.174	0.174	0.176	0.176	0.172	0.164	0.093	0.139	0.137	0.137	0.131	**0.008**	**0.005**
E072_Kambiwa_itacarambi_Carv56	0.262	0.243	0.242	0.247	0.245	0.245	0.247	0.247	0.240	0.247	0.149	0.238	0.236	0.236	0.242	0.223	0.221
G50_Kambiwa_itacarambi_Br22-170	0.187	0.168	0.178	0.182	0.180	0.180	0.182	0.182	0.176	0.178	0.166	0.166	0.164	0.164	0.168	0.137	0.135
UH076_Kambiwa_mucuge_Br22-201	0.195	0.180	0.174	0.176	0.178	0.178	0.180	0.176	0.178	0.172	0.128	0.186	0.183	0.183	0.156	0.162	0.165
UH075_Kambiwa_mucuge_Br22-200	0.194	0.179	0.172	0.174	0.176	0.176	0.178	0.174	0.176	0.170	0.126	0.184	0.182	0.182	0.154	0.160	0.163
UH046_Kambiwa_maracas_Br22-150	0.177	0.178	0.182	0.180	0.182	0.182	0.180	0.184	0.186	0.187	0.210	0.193	0.191	0.191	0.177	0.180	0.176
UH481_Kambiwa_maracas_Br22-151	0.167	0.172	0.178	0.176	0.178	0.178	0.176	0.180	0.182	0.187	0.209	0.182	0.180	0.180	0.176	0.176	0.181
JA83_Kambiwa_sapo_Ven02/100-01	0.210	0.204	0.175	0.178	0.178	0.178	0.178	0.178	0.175	0.188	0.175	0.183	0.183	0.183	0.198	0.194	0.202
UH494_Kambiwa_brumado_Br22-196	0.194	0.200	0.193	0.195	0.193	0.193	0.191	0.195	0.193	0.184	0.159	0.190	0.188	0.188	0.158	0.163	0.168
UH045_Kambiwa_brumado_Br22-149	0.189	0.185	0.199	0.201	0.199	0.199	0.197	0.201	0.204	0.206	0.199	0.217	0.215	0.215	0.187	0.200	0.202
UH482_Kambiwa_brumado_Br22-155	0.177	0.182	0.198	0.196	0.198	0.198	0.196	0.196	0.198	0.209	0.166	0.189	0.191	0.191	0.174	0.171	0.180
S358_Kambiwa_coribe_MACN280	0.213	0.184	0.184	0.182	0.184	0.184	0.186	0.186	0.184	0.168	0.190	0.242	0.240	0.240	0.213	0.194	0.199
UH059_Kambiwa_coribe_Br22-173	0.187	0.170	0.162	0.164	0.162	0.162	0.164	0.164	0.166	0.172	0.175	0.185	0.183	0.183	0.171	0.164	0.170
E078_Kambiwa_aff-neotropica_Carv69	0.192	0.209	0.206	0.203	0.203	0.203	0.206	0.206	0.206	0.220	?	0.214	0.212	0.212	0.205	0.188	0.192
G62_Kambiwa_aff-neotropica_Br22-256	0.179	0.197	0.192	0.192	0.190	0.190	0.192	0.192	0.194	0.205	0.240	0.211	0.209	0.209	0.198	0.192	0.194
E076_Kambiwa_neotropica_Carv65	0.203	0.189	0.192	0.192	0.190	0.190	0.192	0.192	0.194	0.194	0.240	0.209	0.207	0.207	0.191	0.180	0.190
S328_Kambiwa_neotropica_Br15-267	0.198	0.197	0.201	0.201	0.199	0.199	0.201	0.201	0.199	0.199	0.210	0.207	0.205	0.205	0.208	0.184	0.194
UH178_Kambiwa_neotropica_Carv68	0.202	0.193	0.199	0.199	0.197	0.197	0.199	0.199	0.201	0.201	0.252	0.205	0.203	0.203	0.193	0.184	0.194

Table 2 (continued). *CO1* K2P genetic distances between sequenced specimens (ingroup only). Bold numbers are intraspecific distances (n = 62, 0–14.1%, mean 4.8%); interspecific distances within *Kambiwa* Huber, 2000 (n = 295): 8.6–35.0% (mean 18.4%); interspecific distances within *Sertana* Huber gen. nov. (n = 22): 9.3–17.5% (mean 13.4%); intergeneric distances (n = 216): 12.6–25.2% (mean 18.5%).

	UH070	E072	G50	UH076	UH075	UH046	UH481	JA83	UH494	UH045	UH482	S358	UH059	E078	G62	E076	S328
E072_Kambiwa_itacarambi_Carv56	0.223																
G50_Kambiwa_itacarambi_Br22-170	0.134	**0.115**															
UH076_Kambiwa_mucuge_Br22-201	0.164	0.221	0.157														
UH075_Kambiwa_mucuge_Br22-200	0.162	0.217	0.156	**0.000**													
UH046_Kambiwa_maracas_Br22-150	0.171	0.229	0.149	0.139	0.138												
UH481_Kambiwa_maracas_Br22-151	0.176	0.228	0.146	0.128	0.126	0.018											
JA83_Kambiwa_sapo_Ven02/100-01	0.201	0.350	0.212	0.190	0.190	0.202	0.191										
UH494_Kambiwa_brumado_Br22-196	0.167	0.229	0.164	0.122	0.121	0.169	0.153	0.167									
UH045_Kambiwa_brumado_Br22-149	0.198	0.232	0.173	0.133	0.132	0.145	0.146	0.181	**0.082**								
UH482_Kambiwa_brumado_Br22-155	0.179	0.231	0.172	0.139	0.138	0.140	0.134	0.171	**0.112**	**0.112**							
S358_Kambiwa_coribe_MACN280	0.198	0.268	0.195	0.153	0.152	0.196	0.187	0.209	0.158	0.165	0.168						
UH059_Kambiwa_coribe_Br22-173	0.168	0.252	0.163	0.145	0.144	0.175	0.164	0.197	0.151	0.148	0.145	**0.141**					
E078_Kambiwa_aff-neotropica_Carv69	0.190	0.282	0.181	0.174	0.176	0.199	0.195	0.206	0.174	0.176	0.185	0.168	0.166				
G62_Kambiwa_aff-neotropica_Br22-256	0.192	0.233	0.165	0.165	0.166	0.188	0.182	0.195	0.170	0.167	0.182	0.168	0.171	**0.016**			
E076_Kambiwa_neotropica_Carv65	0.188	0.251	0.178	0.178	0.177	0.199	0.185	0.175	0.163	0.163	0.168	0.149	0.159	0.086	0.093		
S328_Kambiwa_neotropica_Br15-267	0.192	0.256	0.182	0.182	0.181	0.206	0.187	0.185	0.169	0.177	0.168	0.161	0.173	0.091	0.098	**0.035**	
UH178_Kambiwa_neotropica_Carv68	0.192	0.262	0.181	0.178	0.176	0.212	0.198	0.192	0.162	0.167	0.168	0.156	0.165	0.096	0.100	**0.016**	**0.035**

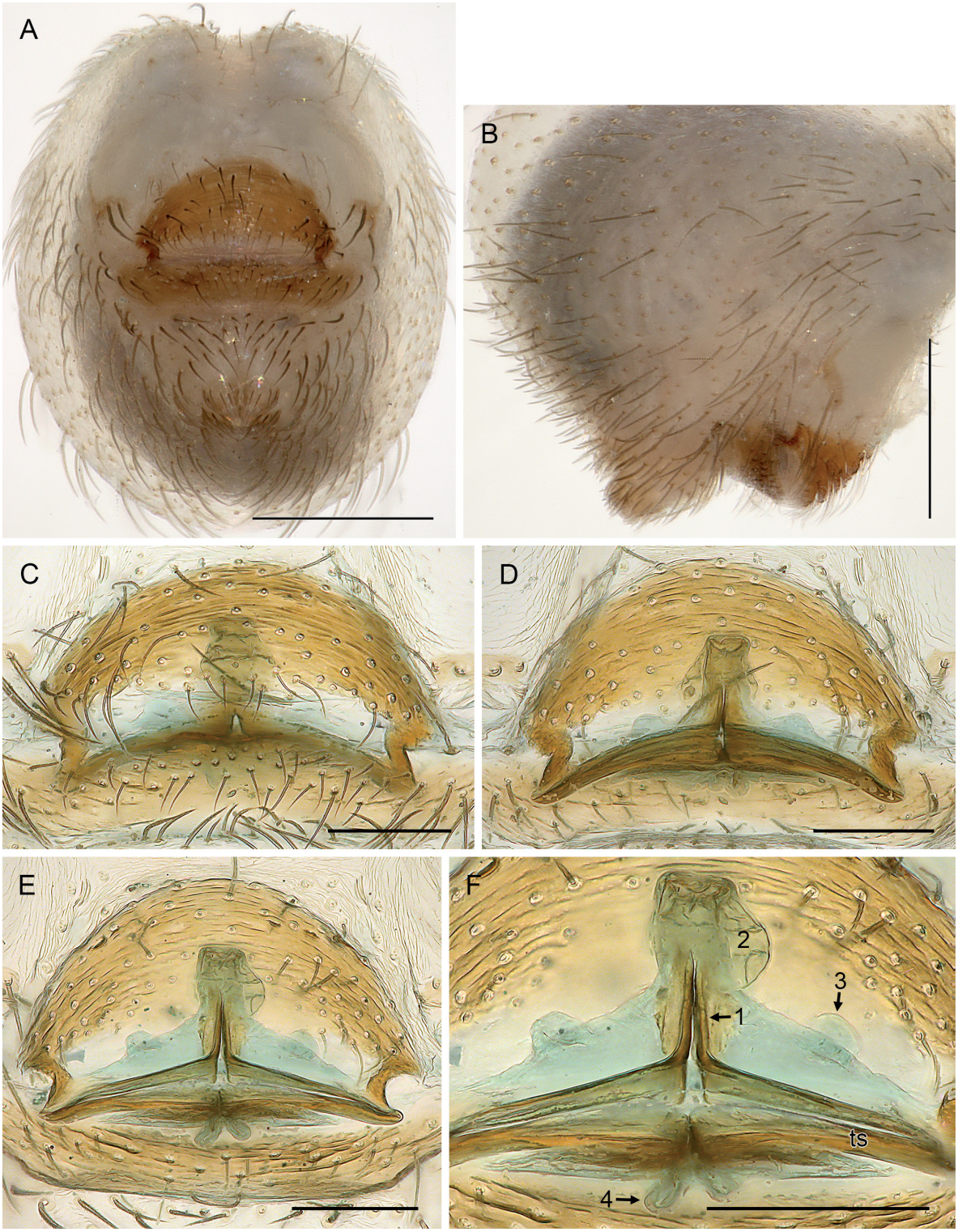

Fig. 18. *Kambiwa neotropica* (Kraus, 1957), ♀♀. **A–D**. From Brazil, Rio Grande do Norte, Lajedo do Arapuá, ZFMK Ar 24707. **E–F**. From Piauí, near Ipuera, CHNUFPI 5063. **A–B**. Abdomen, ventral and lateral views. **C–D**. Cleared genitalia, ventral and dorsal views. **E**. Cleared genitalia, dorsal view. **F**. Detail of previous figure; numbered structures: median sclerotized element (1); anterior membranous sac (2); additional anterior (3) and posterior (4) membranous pouches/sacs. Abbreviation: ts = transversal sclerite. Scale lines: A–B = 0.3 mm; C–F = 0.1 mm.

Natural history

At Lajedo do Arapuá, the spiders were collected on a semiarid slope with shrubs and low trees. They lived under small stones that were fully exposed to the sun, and started to run rapidly as soon as the stones were gently moved. Six egg sacs contained 4–8 eggs each and were flat (all eggs in a single layer); egg diameter was 0.48–0.52.

Kambiwa anomala (Mello-Leitão, 1918)

Pholcus anomalus Mello-Leitão, 1918: 118 (♀).

Myrmidonella anomala – Mello-Leitão 1946: 76.
Kambiwa anomala – Huber 2000: 87.

Remarks

As noted previously (Huber 2000: 87), the type material of this species is lost, and the rudimentary original description lacks illustrations and just reveals that this might be a representative of Ninetinae. The species was tentatively assigned to *Kambiwa*, based primarily on its geographic origin (Huber 2000). Our new data, especially the many more records of Brazilian Ninetinae available now than in 2000, are compatible with this view. However, the identity of the species, and to some degree even its generic assignment, remain uncertain.

First, *K. anomala* might be a synonym of *K. neotropica*. The geographically closest sample available of any *Kambiwa* to the type locality of *K. anomala* (Paraíba, Campina Grande) is *K. neotropica* from Serrota, just ~50 km west of Campina Grande (see above). Second, *K. anomala* could be identical to the very close relative of *K. neotropica* that we informally describe below as *Kambiwa* sp. aff. *neotropica*. The available specimens of that species originate from four localities around Paraíba (from Rio Grande do Norte, Pernambuco, northern Bahia), and they differ slightly but consistently from *K. neotropica*. Third, we cannot exclude the possibility that *K. anomala* is none of these two species. In fact, it could even be a representative of the currently monotypic genus *Pinoquio* Huber & Carvalho, 2022. That genus has been reported from Rio Grande do Norte only (~300 km NW of Campina Grande), but the ZFMK has specimens from Ceará (females only) that might also belong to *Pinoquio*.

Because of these taxonomic uncertainties and in particular because *K. anomala* might be identical with some specimens we consider slightly but consistently different from *K. neotropica*, we describe these latter specimens informally as "*Kambiwa* sp. aff. *neotropica* CHNUFPI 9116". We follow the idea that 'open nomenclature' (Bengtson 1988; Sigovini *et al*. 2016; Minelli 2019; Horton *et al*. 2021) is a valuable approach that provides all the relevant information available at the point of publication without formally naming the species. In this sense, we think that the informal description of 'problematic' species helps improve the quality of formal species lists and databases and is thus good taxonomic practice (Huber *et al.* 2024e).

In sum, the identity of *K. anomala* continues to be dubious and dense sampling around Campina Grande is necessary before a solution can be attempted or provided, both for this and for the following species.

Kambiwa sp. aff. ***neotropica*** CHNUFPI 9116
Figs 19–20

Diagnosis

Males are easily distinguished from most known congeners by shape of ventral bulbal process (Fig. 19F; long, directed towards distal, distally hooked), by retrolateral-dorsal process of genital bulb barely

reaching palpal trochanter (in other species either absent or much longer), and by tip of procursus (Fig. 19A–C; with dorsal and ventral sclerotized elements connected by transparent membrane); from very similar *K. neotropica* by details of genital bulb (ventral bulbal process longer and slenderer, dorsal bulbal processes different, compare Figs 16E and 19E) and by dorsal and ventral sclerotized elements on procursus tip slightly closer together (compare Figs 16A and 19A). Females appear externally indistinguishable from several congeners (*K. neotropica*; *K. coribe* sp. nov.; *K. maracas* sp. nov.; *K. brumado* sp. nov.; *K. mucuge* sp. nov.); they differ internally by strong median element leading into simple membranous sac (Fig. 20B, D; very similar to *K. neotropica*; other species with smaller median element leading into membranous tube).

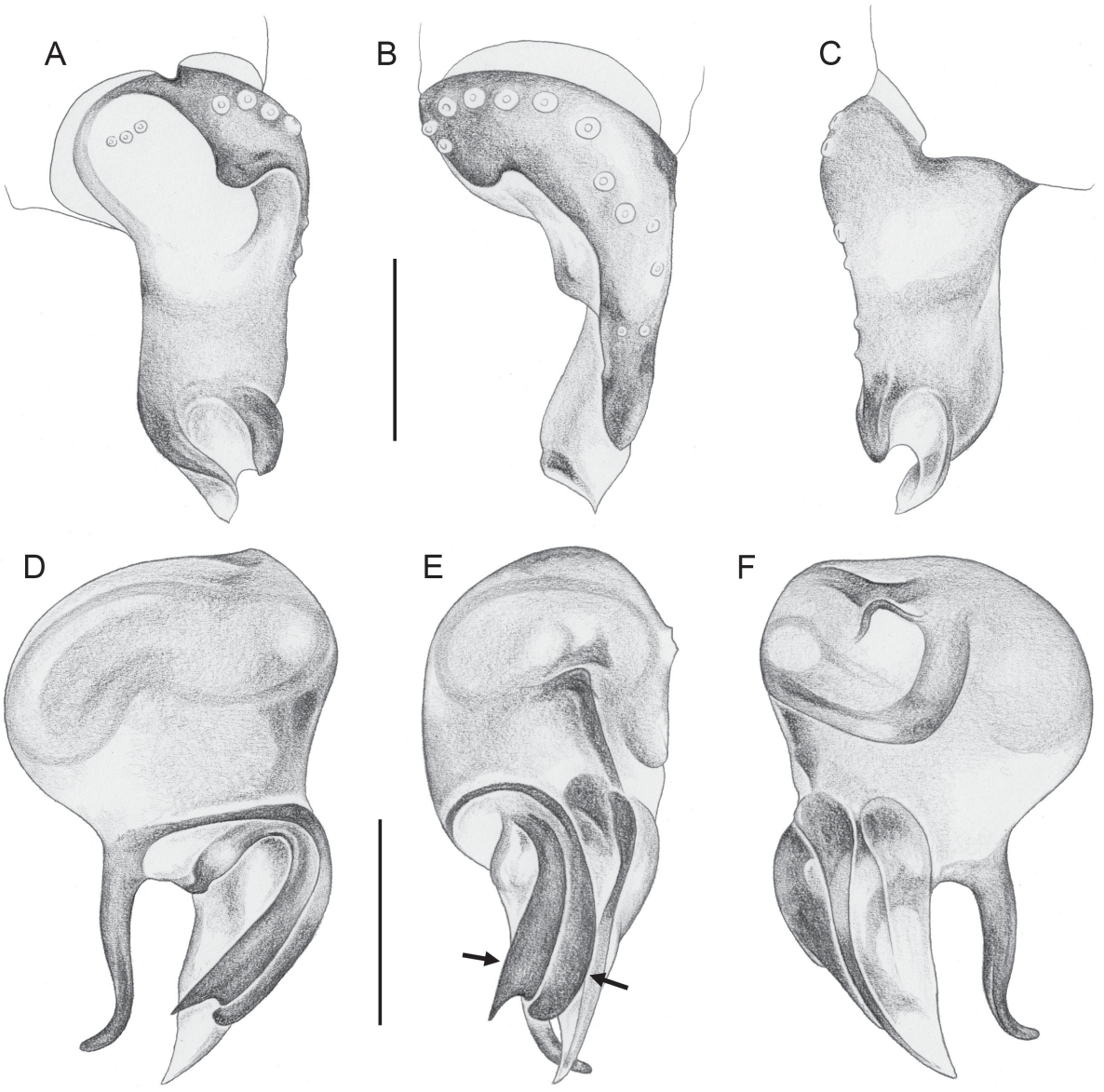

Fig. 19. *Kambiwa* sp. aff. *neotropica*; ♂ from Brazil, Pernambuco, PN do Catimbau, CHNUFPI 9116. **A–C**. Left palpal tarsus and procursus, prolateral, dorsal, and retrolateral views. **D–F**. Left genital bulb, prolateral, dorsal, and retrolateral views; arrows: distinctive dorsal processes (compare Fig. 16E). Scale lines = 0.1 mm.

Material examined

BRAZIL – **Bahia** • 2 ♂♂, 4 ♀♀; between Ibó and Curaçá, Serra do Furtuoso; 8.6420° S, 39.5266° W; 390 m a.s.l.; 2 Dec. 2022; B.A. Huber and A.S. Michelotto leg.; CHNUFPI 9118 [deposited in ZFMK Ar 24710] • 3 ♀♀; same collection data as for preceding; CHNUFPI 9119 [deposited in ZFMK Br22-256] (voucher of G62). – **Pernambuco** • 2 ♀♀; Buíque, Parque Nacional do Catimbau, Igrejinha; 8.4928° S, 37.2518° W; 940 m a.s.l.; 25 Nov. 2020; L.S. Carvalho and J.F. Lima leg.; CHNUFPI 4038 • 1 ♂, 1 ♀; same collection data as for preceding; CHNUFPI 4039 • 1 ♂, 1 ♀, 3 female abdomens (prosomata used for molecular work); same collection data as for preceding; CHNUFPI 9116 [deposited in ZFMK Carv69] (voucher of E078) • 1 ♀; NE of Cabrobó; 8.420° S, 39.176° W; 450 m a.s.l.; 2 Dec. 2022; B.A. Huber and A.S. Michelotto leg.; CHNUFPI 9117 [deposited in ZFMK Ar 24709]. – **Rio Grande do Norte** • 1 ♂; Angicos, roadside of BR 304; 5.6755° S, 36.4992° W; 145 m a.s.l.; 19 Nov. 2020; L.S. Carvalho leg.; CHNUFPI 4040.

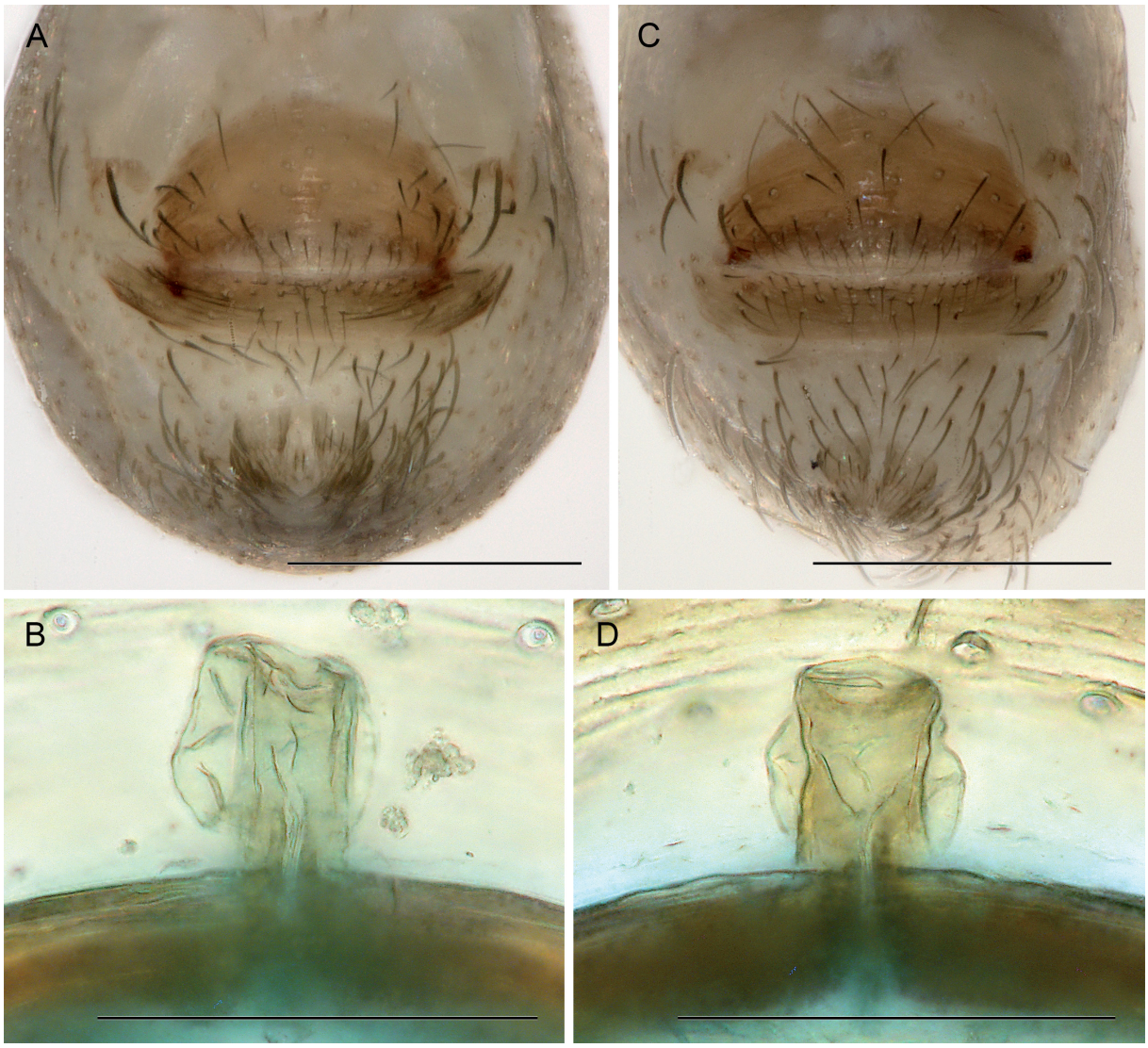

Fig. 20. *Kambiwa* sp. aff. *neotropica*; ♀♀. **A–B**. From Brazil, Pernambuco, Parque Nacional do Catimbau, CHNUFPI 9116. **C–D**. From Bahia, between Ibó and Curaçá, ZFMK Ar 24710. **A, C**. Abdomens, ventral views. **B, D**. Central elements of cleared genitalia, dorsal views. Scale lines: A, C = 0.3 mm; B, D = 0.1 mm.

Description

Male (CHNUFPI 9116)

Measurements. Total body length 1.20, carapace width 0.52. Distance PME–PME 55 μm; diameter PME 50 μm; distance PME–ALE 15 μm; distance AME–AME 10 μm; diameter AME 35 μm. Leg 1: 2.59 (0.72+0.19+0.66+0.66+0.36), tibia 2: 0.55, tibia 3: 0.50, tibia 4: 0.77; tibia 1 L/d: 9; diameters of leg femora 110 μm, of leg tibiae 70 μm.

Color (in ethanol). Prosoma and legs ochre-yellow, carapace medially slightly darker, legs without darker rings; abdomen ochre-gray, with darker internal marks and indistinct darker ochre plate in front of gonopore.

Body. Habitus as in close relatives (e.g., Fig. 2E). Ocular area not raised. Carapace without thoracic groove. Clypeus unmodified. Sternum slightly wider than long (0.37/0.33), with very small anterior humps near coxae 1 (~15 μm high, 40 μm diameter at basis). Abdomen globular.

Chelicerae. As in *K. neotropica* (cf. Fig. 17A–B); with pair of small frontal apophyses, distances between tips: 120 μm; stridulatory files very fine and poorly visible in dissecting microscope.

Palps. In general, very similar to *K. neotropica* (cf. Fig. 15); procursus (Fig. 19A–C) slightly slenderer in lateral view and distal ventral sclerotized element more strongly directed towards dorsal; genital bulb (Fig. 19D–F) ventral hooked sclerotized process slightly longer, two distinctive prolateral-dorsal sclerites of approximately same length, and prolateral process with pointed tip.

Legs. Without spines, without curved hairs; with short vertical hairs on tibia 1; retrolateral trichobothrium of tibia 1 not seen; prolateral trichobothrium absent on tibia 1; tarsus 1 with 4 pseudosegments, fairly distinct.

Variation (males)

Tibia 1 in five males: 0.61–0.66 (mean 0.63); median darker mark on carapace sometimes absent or very indistinct; cheliceral apophyses in males from Bahia slightly closer together (distance between tips 105 μm); prolateral-dorsal sclerites of genital bulb in males from Bahia minimally slenderer.

Females

In general similar to males but sternum without humps and chelicerae apparently without stridulatory files (not confirmed with SEM). Tibia 1 in nine females: 0.54–0.62 (mean 0.58). Epigynum (Fig. 20A, C) anterior plate semicircular, weakly protruding, with pair of lateral posterior sclerites; posterior plate large but simple, roughly rectangular. Internal genitalia (Fig. 20B, D) with weakly curved transversal sclerite connected laterally to lateral posterior sclerites of anterior epigynal plate, medially with anterior process leading to membranous sac; apparently without pore plates.

Barcoding

Two specimens were barcoded, from Pernambuco and Bahia. The K2P distance was 1.6%; distances to the three sequenced specimens of *K. neotropica* ranged from 8.6 to 10.0% (Table 2).

Distribution

Known from several localities in north-eastern Brazil, ranging from northern Bahia to Rio Grande do Norte (Fig. 14). Specimens from a further locality, deposited in IBSP, could not be studied in detail; they might be representatives of the present species, of *K. neotropica*, or *K. anomala*. They originate from Sergipe, Usina Hidrelétrica do Xingó (9.624° S, 37.797° W).

Natural history

Between Ibó and Curaçá, the spiders were found on a rocky hillside with thorny shrubs (Fig. 11A). They lived under stones among low bushes, together with an undescribed species of *Arenita*. They occupied the upper layer of stones, while *Arenita* sp. seemed to be restricted to a slightly deeper layer. The single female from NE of Cabrobó was found on a rock outcrop with scattered shrubs; it shared this locality with *Kambiwa ibo* sp. nov.

Kambiwa coribe Huber sp. nov.
urn:lsid:zoobank.org:act:BA851D16-51DA-4C41-882C-40C5B0C74E75
Figs 2E–F, 21–25

Ninetinae sp. 1 – Carvalho & Avelino 2010: 6.
S358 *Kambiwa* MACN273 – Eberle *et al.* 2018 (molecular data). — Huber *et al.* 2018: fig. 2.

Diagnosis

Males are distinguished from those of known congeners by distinctive shape of ventral bulbal process (Fig. 22D–F; long, gradually narrowing, on ventral side membranous, distally hooked), by distinctive prolateral-dorsal sclerite on genital bulb (Fig. 22D–E; but note variation below), by retrolateral-dorsal process of genital bulb reaching palpal coxa (Fig. 21C; longer than in *K. neotropica*; shorter than in *K. maracas* sp. nov., *K. brumado* sp. nov., and *K. mucuge* sp. nov.), and by very short but wide (in lateral view) membranous procursus without sclerotized elements (Fig. 22A–C). Females appear externally indistinguishable from those of several congeners (*K. neotropica*; *K. maracas*; *K. brumado*; *K. mucuge*); they differ from those of *K. neotropica* internally by absence of strong median element and by convoluted membranous tube rather than simple sac (Fig. 23C); other similar species may be indistinguishable even internally (*K. maracas*; *K. brumado*; *K. mucuge*).

Etymology

The species name is derived from the type locality; noun in apposition.

Type material

Holotype

BRAZIL – **Bahia** • ♂; E of São Felix do Coribe; 13.404° S, 44.110° W; 470–580 m a.s.l.; 17 Nov. 2022; B.A. Huber and L.S. Carvalho leg.; CHNUFPI 9168.

Paratypes

BRAZIL – **Bahia** • 6 ♂♂, 5 ♀♀; same collection data as for holotype; CHNUFPI 9169 • 1 ♂, 1 ♀; same collection data as for holotype; CHNUFPI 9170 • 1 ♀; same collection data as for holotype; CHNUFPI 9171 • 2 ♂♂, 2 ♀♀; same collection data as for holotype; CHNUFPI 9172 [deposited in ZFMK Ar 24720].

Other material examined

BRAZIL – **Bahia** • 1 ♂, 4 ♀♀, in pure ethanol; same collection data as for holotype; CHNUFPI 9173 [deposited in ZFMK Br22-181] • 3 ♂♂, 3 ♀♀; SW of São Felix do Coribe, 'site 1'; 13.4325° S, 44.2168° W; 470 m a.s.l.; 17 Nov. 2022; B.A. Huber and L.S. Carvalho leg.; CHNUFPI 9174 [deposited in ZFMK Ar 24721] • 2 ♀♀, in pure ethanol; same collection data as for preceding; CHNUFPI 9175 [deposited in ZFMK Br22-178] • 1 ♂, 2 ♀♀; SE of Bom Jesus da Lapa, 'site 1'; 13.4398° S, 43.1643° W; 520 m a.s.l.; 18 Nov. 2022; B.A. Huber and L.S. Carvalho leg. CHNUFPI 9176 • 2 ♂♂, 3 ♀♀, in pure ethanol; same collection data as for preceding; CHNUFPI 9177 [deposited in ZFMK Br22-189] • 1 ♂, 2 ♀♀; SW of Correntina, margins of BR-349; 13.4998° S, 44.9795° W; 770 m a.s.l.; 16 Nov. 2022; B.A. Huber and L.S. Carvalho leg.; CHNUFPI 9178 • 2 ♀♀; same collection data as for preceding;

CHNUFPI 9179 • 5 ♀♀, in pure ethanol; same collection data as for preceding; CHNUFPI 9180 [deposited in ZFMK Br22-173] (vouchers of UH059) • 1 ♂; N of Correntina, margins of BR-135; 13.3031° S, 44.6448° W; 700 m a.s.l.; 16 Nov. 2022; B.A. Huber and L.S. Carvalho leg.; CHNUFPI 9181 • 1 ♂, 1 ♀, in pure ethanol; same collection data as for preceding; CHNUFPI 9182 [deposited in ZFMK Br22-174]. – **Maranhão** • 1 ♂; Aldeias Altas, Riacho Curva, 2.5 km after bridge over Riacho Limpeza; 4.6618° S, 43.4411° W; 100 m a.s.l.; 11 Dec. 2021; G.S. Lustosa *et al*. leg.; CHNUFPI 4197 • 1 ♂; Caxias, Riacho Junco, Junco village; 4.7974° S, 43.2646° W; 95 m a.s.l.; 17 Dec. 2021; G.S. Lustosa *et al*. leg.; CHNUFPI 4202. – **Minas Gerais** • 1 ♂; NW of Itacarambi, 'site 1', near radio/TV towers; 15.0500° S, 44.1820° W; 780 m a.s.l.; 13 Nov. 2022; B.A. Huber, L.S. Carvalho and R.A. Torres leg.; CHNUFPI 9183 [deposited in ZFMK Ar 24722]. – **Piauí** • 1 ♂; Guaribas, Serra das Confusões National Park; 9.2211° S, 43.4892° W; 590 m a.s.l.; Oct. 2006; P.R.R. Silva *et al*. leg.; CHNUFPI 1131 • 1 ♂, 1 ♀; Floriano, Fazenda do Colégio Técnico de Floriano; 6.7636° S, 43.0607° W; 120 m a.s.l.; 18 Oct. 2018; L.S. Carvalho leg.; CHNUFPI 4192 • 1 ♀; same collection data as for preceding; CHNUFPI 4052 • 1 ♀; same collection data as for preceding; CHNUFPI 4191 • 2 ♀♀, 1 juv.; same collection data as for preceding; CHNUFPI 4051 • 2 ♀♀ abdomens (prosomata used for molecular work); same collection data as for preceding; CHNUFPI 9184 [deposited in ZFMK Carv70] (vouchers of E079) • 1 ♂, 2 ♀♀; Floriano, Fazenda do Colégio Técnico de Floriano, margins of Rio Parnaíba; 6.7596° S, 43.0557° W; 105 m a.s.l.; 22 Jul. 2023; L.S. Carvalho *et al*. leg.; CHNUFPI 5051 • 8 ♀♀; same collection data as for preceding; CHNUFPI 5046 • 5 ♀♀; same collection data as for preceding; CHNUFPI 5049 • 1 ♀; same locality as for preceding; 6.7636° S, 43.0750° W; 115 m a.s.l.; 12 Jun. 2023; M.S.C.S. Lima *et al*. leg.; CHNUFPI 5060 • 1 ♀; same locality as for preceding; 6.7592° S, 43.0550° W; 110 m a.s.l.; 18 Dec. 2019; M.L.S. Carvalho leg.; CHNUFPI 4043.

BOLIVIA – **Santa Cruz** • 1 ♂, 2 ♀♀; Yabaré, Estación de la Universidad A. Gabriel R. Moreno; 17.4417° S, 62.1725° W; 260 m a.s.l.; 20–24 Oct. 2010; C. Grismado, S. Ávila and M. Pérez leg.; MACN

Fig. 21. *Kambiwa coribe* Huber sp. nov., paratype, ♂, from Brazil, Bahia, E of São Felix do Coribe, ZFMK Ar 24720. Left palp, prolateral, dorsal, and retrolateral views. Scale line = 0.2 mm.

Ar29116 • 1 ♂; same collection data as for preceding; MACN Ar29117 (voucher of S358) • 1 ♀; same collection data as for preceding; MACN Ar29123.

Description

Male (holotype)

Measurements. Total body length 1.16, carapace width 0.49. Distance PME–PME 40 µm; diameter PME 45 µm; distance PME–ALE 15 µm; distance AME–AME 10 µm; diameter AME 30 µm. Leg 1: 2.18 (0.62+0.18+0.54+0.52+0.32), tibia 2: 0.44, tibia 3: 0.40, tibia 4: 0.62; tibia 1 L/d: 8; diameters of leg femora 115–120 µm, of leg tibiae 65 µm.

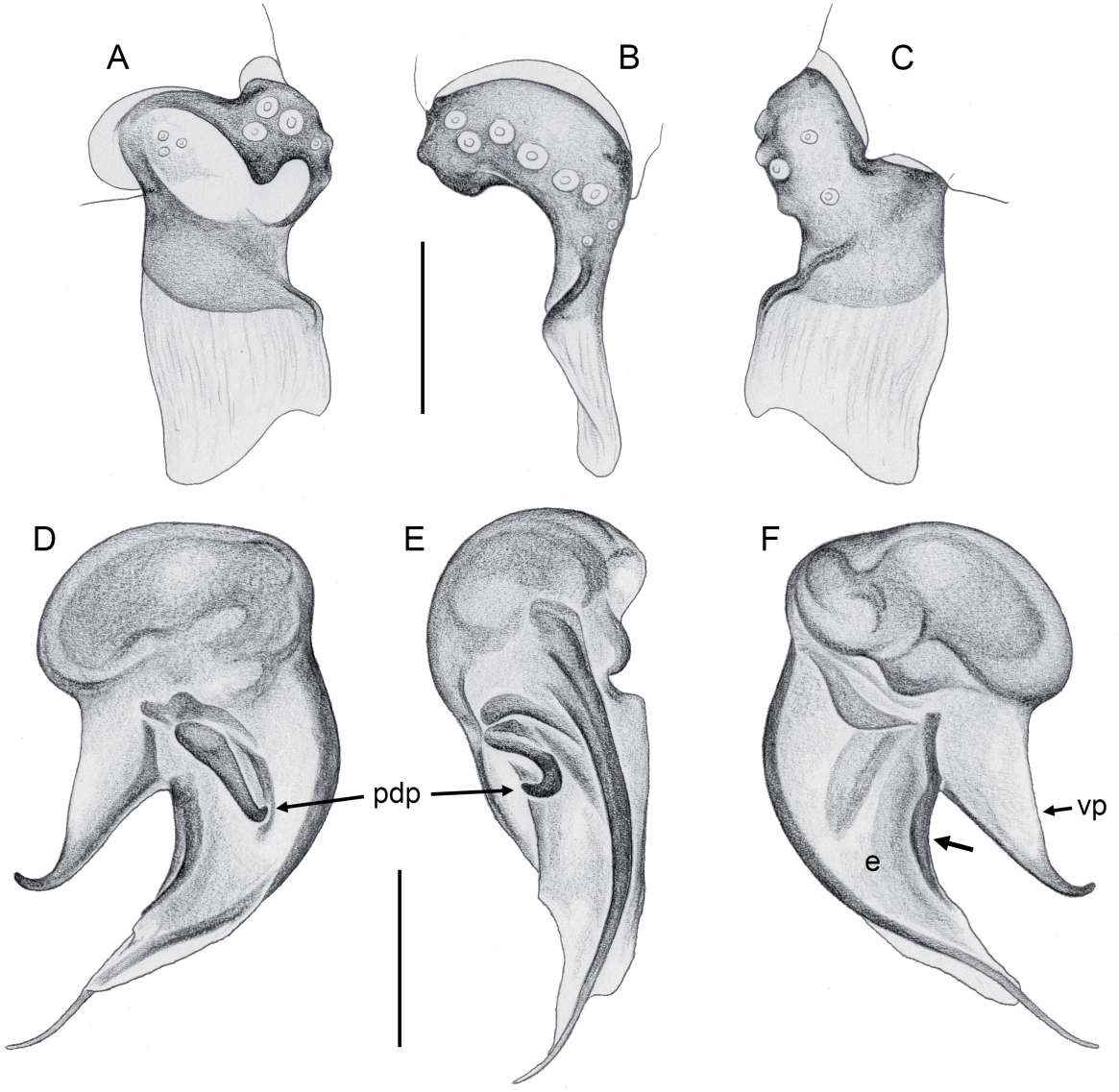

Fig. 22. *Kambiwa coribe* Huber sp. nov., paratype, ♂, from Brazil, Bahia, E of São Felix do Coribe, ZFMK Ar 24720. **A–C**. Left palpal tarsus and procursus, prolateral, dorsal, and retrolateral views. **D–F**. Left genital bulb, prolateral, dorsal, and retrolateral views; arrow in F points at sclerite that is shorter in males from Piauí. Abbreviations: e = putative embolus; pdp = prolateral-dorsal process; vp = ventral process. Scale lines = 0.1 mm.

Color (in ethanol). Prosoma and legs ochre-yellow, carapace and legs without darker marks or rings; abdomen monochromous ochre-gray except for light ochre-brown plate in front of gonopore.

Body. Habitus as in Fig. 2E. Ocular area not raised. Carapace without thoracic groove. Clypeus unmodified. Sternum slightly wider than long (0.37/0.33), with pair of very indistinct anterior humps near coxae 1 (~10 μm high, 40 μm diameter at basis, barely different from female). Abdomen globular.

Chelicerae. As in Fig. 23A–B; with pair of small frontal apophyses; stridulatory files very fine and poorly visible in dissecting microscope.

Palps. As in Fig. 21; coxa unmodified; trochanter ventrally slightly protruding; femur proximally with small ventral process, distally widened but otherwise unmodified; femur-patella condyles barely shifted toward prolateral side; tibia-tarsus condyles slightly shifted toward retrolateral side; tarsus with small prolateral sclerotized process; procursus (Fig. 22A–C) wide in lateral view, narrower in dorsal view, with large transparent distal flap; genital bulb (Fig. 22D–F) with triangular ventral process distally hooked and mostly whitish except for dorsal sclerotized margin, distinctive prolateral-dorsal sclerite slightly hooked at tip, with dorsal process (putative embolus) composed of membranous and sclerotized elements, and retrolateral-dorsal process reaching palpal coxa.

Legs. Without spines, without curved hairs; with short vertical hairs on tibia 1; retrolateral trichobothrium of tibia 1 at 58%; prolateral trichobothrium absent on tibia 1; tarsus 1 with ~4–5 pseudosegments, distally fairly distinct.

Variation (males)

Tibia 1 in 22 males: 0.50–0.66 (mean 0.57). The prolateral-dorsal process on the genital bulb varies slightly among localities: in males from near Correntina, it is lighter and lacks a distal hook; in males from Piauí, it is more evenly curved rather than hooked; in males from Maranhão, it is generally slightly stronger; in males from Bolivia, it is considerably stronger. In the latter males, also the retrolateral-dorsal process is stronger/thicker. The ventral sclerite of the putative embolus (arrow in Fig. 22F) is slightly shorter in specimens from Piauí. We tentatively assign all these specimens to one species.

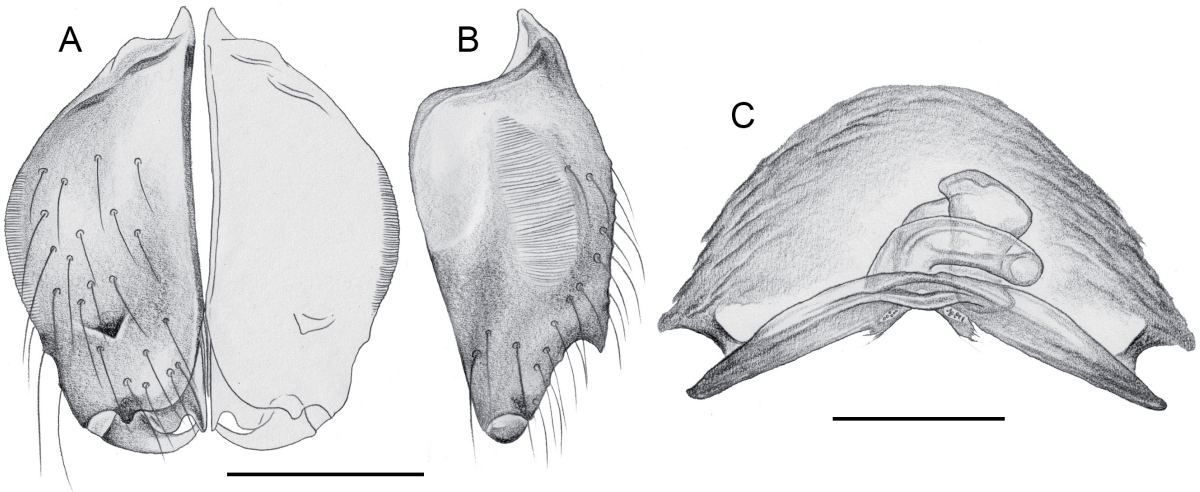

Fig. 23. *Kambiwa coribe* Huber sp. nov., paratypes, ♂♀, from Brazil, Bahia, E of São Felix do Coribe, ZFMK Ar 24720. **A**–**B**. Male chelicerae, frontal and lateral views. **C**. Cleared female genitalia, dorsal view. Scale lines = 0.1 mm.

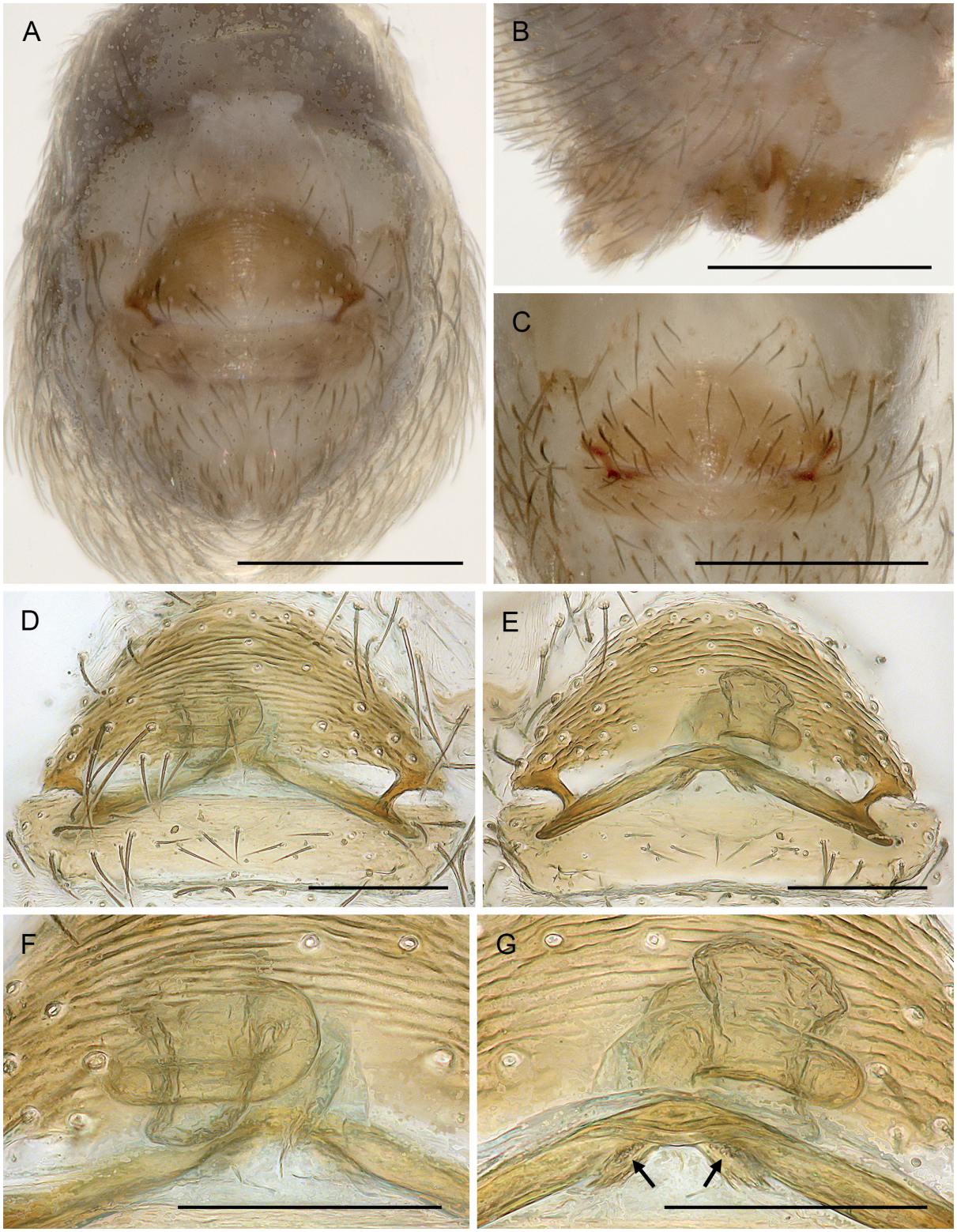

Fig. 24. *Kambiwa coribe* Huber sp. nov. **A–B, D–G**. Paratype, ♀, from Brazil, Bahia, E of São Felix do Coribe, ZFMK Ar 24720. **C**. ♀ from Piauí, Fazenda do Colégio Técnico de Floriano, CHNUFPI 5046. **A–B**. Abdomen, ventral and lateral views. **C**. Epigynum, ventral view. **D–E**. Cleared genitalia, ventral and dorsal views. **F–G**. Central element of internal genitalia, ventral and dorsal views; arrows point at putative pore plates. Scale lines: A–C = 0.3 mm; D–G = 0.1 mm.

Females

In general similar to males but chelicerae apparently without stridulatory files (not confirmed with SEM). Tibia 1 in 42 females: 0.48–0.66 (mean 0.54). Epigynum (Fig. 24A–C) anterior plate semicircular, weakly protruding, with pair of lateral posterior sclerites; posterior plate large but simple, roughly rectangular. Internal genitalia (Figs 23C, 24D–G, 25A–D) with curved transversal sclerite connected laterally to lateral posterior sclerites of anterior epigynal plate, medially with anterior rounded process from which membranous coiled tube originates; apparently with pair of small round pore plates (arrows in Figs 24G, 25D).

Barcoding

Two specimens were barcoded, from Brazil, Bahia and from Bolivia, Santa Cruz (geographic distance: 1900 km). The K2P distance was 14.1%. This relatively high distance reflects the morphological differences described above, and suggests that the specimens studied might represent more than one species.

Distribution

Known from several localities in Brazil (Bahia, Minas Gerais, Piauí, Maranhão), and from a single locality in Bolivia (Figs 13–14). The Bolivian record suggests that this species may be distributed across much of the Cerrado biome. Brazilian specimens were collected at an intermediate altitude (374 ± 273 m, n = 13) compared to congeners with broader distributions, being statistically higher than *K. neotropica* (145 ± 131 m, n = 14) and not differing significantly from *K. ibo* Huber sp. nov. (460 ± 120 m, n = 18; see Fig. 83). Specimens from further localities, deposited in CHNUFPI, MPEG, UFMG, and IBSP could

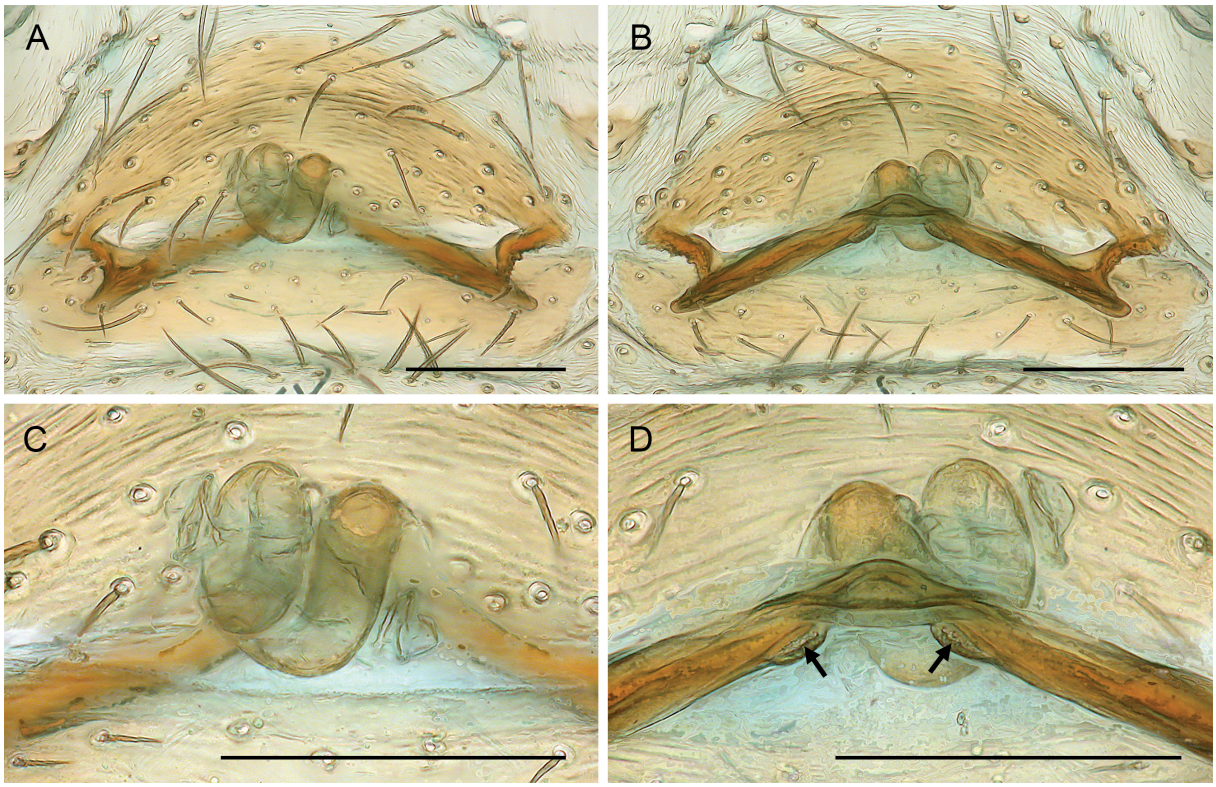

Fig. 25. *Kambiwa coribe* Huber sp. nov., ♀ from Brazil, Piauí, Fazenda do Colégio Técnico de Floriano, CHNUFPI 5046. **A**–**B**. Cleared genitalia, ventral and dorsal views. **C**–**D**. Central element of internal genitalia, ventral and dorsal views; arrows point at putative pore plates. Scale lines = 0.1 mm.

not be studied in detail (by BAH) or are represented by females only; available photos (L.S. Carvalho, unpubl. data) and distribution data suggest they are representatives of the present species. They originate from Minas Gerais, Manga, Parque Estadual da Mata Seca (14.849° S, 43.988–44.008° W); Minas Gerais, Prudente de Morais, Fazenda Sapé (19.4684° S, 44.2416° W); Minas Gerais, Lavras (21.2483° S, 45.0014° W); Piauí, José de Freitas, Fazenda Nazareth (4.7994° S, 42.6300° W); Piauí, Povoado Bela Vista (4.9224° S, 42.8633° W); Piauí, Povoado Boa Hora (4.9060° S, 42.8736° W); Piauí, Parque Nacional Serra da Capivara, 8,7672° S, 42.5600° W); and Maranhão, Reserva Ecológica Inhamum (4.8917° S, 43.4147° W).

Natural history

This species was mostly found in dry wood on the ground and in leaf litter, rather than under stones. At the type locality, it was abundant in dry wood in a secondary arboreous Caatinga on a granitic hillside (Fig. 11B). SW of São Felix do Coribe it was found in the leaf litter of arboreous Caatinga at the base of an outcrop, while the top of the hill was occupied by a different species (*Sertana sagarana* Huber gen. et sp. nov.). SE of Bom Jesus da Lapa it appeared restricted to the low forest (arboreous Caatinga), while two neighboring habitats (granite outcrop and degraded roadside) had different species (*Sertana igapora* Huber gen. et sp. nov. and *S. lapa* Huber gen. et sp. nov.). Near Correntina the spiders were collected in the leaf litter of degraded thorny shrubland (Cerrado) on clayish soil. NW of Itacarambi the single male was collected on a bare rocky field on clayish soil; this locality was dominated by another species of *Kambiwa* (*K. itacarambi* sp. nov.). Three egg sacs contained 4–5 eggs each and were flat (all eggs in a single layer); egg diameter was 0.44–0.48.

Kambiwa brumado Huber sp. nov.
urn:lsid:zoobank.org:act:E6D5228E-64A4-4346-B0FF-C8282CAD6DCC
Figs 2I–J, 3B, E, 4C, 5A–B, 6C, 7E, 9D, G, 26–29

Diagnosis

Males are easily distinguished from those of most known congeners (except *K. maracas* sp. nov. and *K. mucuge* sp. nov.) by very long retrolateral-dorsal process of genital bulb (Fig. 27D–F), and by shape of ventral bulbal apophysis (Fig. 27D–F; roughly rectangular flat element); from *K. maracas* and *K. mucuge* by course of retrolateral-dorsal process (compare Fig. 26 with Figs 30 and 34; directed back and upwards, passing palp on prolateral side); from *K. maracas* and *K. mucuge* also by short prolateral process on procursus (arrow in Fig. 27B; absent in *K. maracas*, longer in *K. mucuge*). Females appear externally indistinguishable from those of several congeners (*K. neotropica*; *K. coribe* sp. nov.; *K. maracas*; *K. mucuge*); they differ from *K. neotropica* internally by smaller median element and by convoluted membranous tube rather than simple sac (Fig. 28C); other similar species may be indistinguishable even internally (*K. coribe*; *K. maracas*; *K. mucuge*).

Etymology

The species name is derived from the type locality; noun in apposition.

Type material

Holotype

BRAZIL – **Bahia** • ♂; NE of Brumado; 14.1601° S, 41.5154° W; 470 m a.s.l.; 11 Nov. 2022; B.A. Huber and L.S. Carvalho leg.; CHNUFPI 9193.

Paratypes

BRAZIL – **Bahia** • 2 ♂♂, 2 ♀♀; same collection data as for holotype; CHNUFPI 9194 • 2 ♂♂, 2 ♀♀; same collection data as for holotype; CHNUFPI 9195 [deposited in ZFMK Ar 24725].

Other material examined

BRAZIL – **Bahia** • 1 ♂, 4 ♀♀, in pure ethanol; same collection data as for holotype; CHNUFPI 9196 [deposited in ZFMK Br22-155] • 5 ♂♂, 12 ♀♀; W of Marcolino Moura; 13.6028° S, 41.7166° W; 610 m a.s.l.; 19 Nov. 2022; B.A. Huber and L.S. Carvalho leg.; CHNUFPI 9197 • 2 ♂♂, 2 ♀♀; same collection data as for preceding; CHNUFPI 9198 [deposited in ZFMK Ar 24726] • 1 ♂, 1 ♀; same collection data as for preceding; CHNUFPI 9199 • 2 ♂♂, 13 ♀♀, in pure ethanol; same collection data as for preceding; CHNUFPI 9200 [deposited in ZFMK Br22-197] • 2 ♂♂, 1 ♀; NE of Marcolino Moura; 13.5883° S, 41.6635° W; 630 m a.s.l.; 19 Nov. 2022; B.A. Huber and L.S. Carvalho leg.; CHNUFPI 9201 • 1 ♂, 2 ♀♀, in pure ethanol; same collection data as for preceding; CHNUFPI 9202 [deposited in ZFMK Br22-199] • 1 ♂, 1 ♀; SE of Paramirim; 13.550° S, 42.202° W; 590–640 m a.s.l.; 18 Nov. 2022; B.A. Huber and L.S. Carvalho leg.; CHNUFPI 9203 [deposited in ZFMK Ar 24727] • 1 ♂, 1 ♀; same collection data as for preceding; CHNUFPI 9204 • 3 ♀♀, in pure ethanol; same collection data as for preceding; CHNUFPI 9205 [deposited in ZFMK Br22-196] • 1 ♂, 1 ♀; W of Mucugê, Parque Nacional da Chapada Diamantina; 13.0097° S, 41.4084° W; 1010 m a.s.l.; 19 Nov. 2022; B.A. Huber and L.S. Carvalho leg.; CHNUFPI 9206 • 9 ♂♂, 4 ♀♀; E of Milagres, Morro do São Cristóvão; 12.8711° S, 39.8548° W; 420 m a.s.l.; bare granite outcrop, in shrubland; 10 Nov. 2022; B.A. Huber and L.S. Carvalho leg.; CHNUFPI 9207 • 2 ♂♂, 8 ♀♀, in pure ethanol; same collection data as for preceding; CHNUFPI 9208 [deposited in ZFMK Br22-149] (1 ♂, 1 ♀ used for SEM).

Description

Male (holotype)

Measurements. Total body length 0.96, carapace width 0.49. Distance PME–PME 45 µm; diameter PME 50 µm; distance PME–ALE 15 µm; distance AME–AME 15 µm; diameter AME 20 µm. Leg 1: 2.42

Fig. 26. *Kambiwa brumado* Huber sp. nov., paratype, ♂, from Brazil, Bahia, NE of Brumado, ZFMK Ar 24725. Left palp, prolateral, dorsal, and retrolateral views. Scale line = 0.2 mm.

(0.66+0.18+0.62+0.62+0.34), tibia 2: 0.52, tibia 3: 0.49, tibia 4: 0.76; tibia 1 L/d: 10; diameters of leg femora 110 µm, of leg tibiae 65 µm.

Color (in ethanol). Prosoma and legs ochre-yellow, carapace and legs without darker marks or rings; abdomen monochromous ochre-gray.

Body. Habitus as in Fig. 2I. Ocular area not raised. Carapace without thoracic groove. Clypeus unmodified. Sternum slightly wider than long (0.35/0.32), with small but distinct anterior processes near coxae 1 (~30 µm high, 40 µm diameter at basis). Abdomen globular.

Chelicerae. As in Fig. 28A–B; with pair of small frontal apophyses; stridulatory files very fine and poorly visible in dissecting microscope.

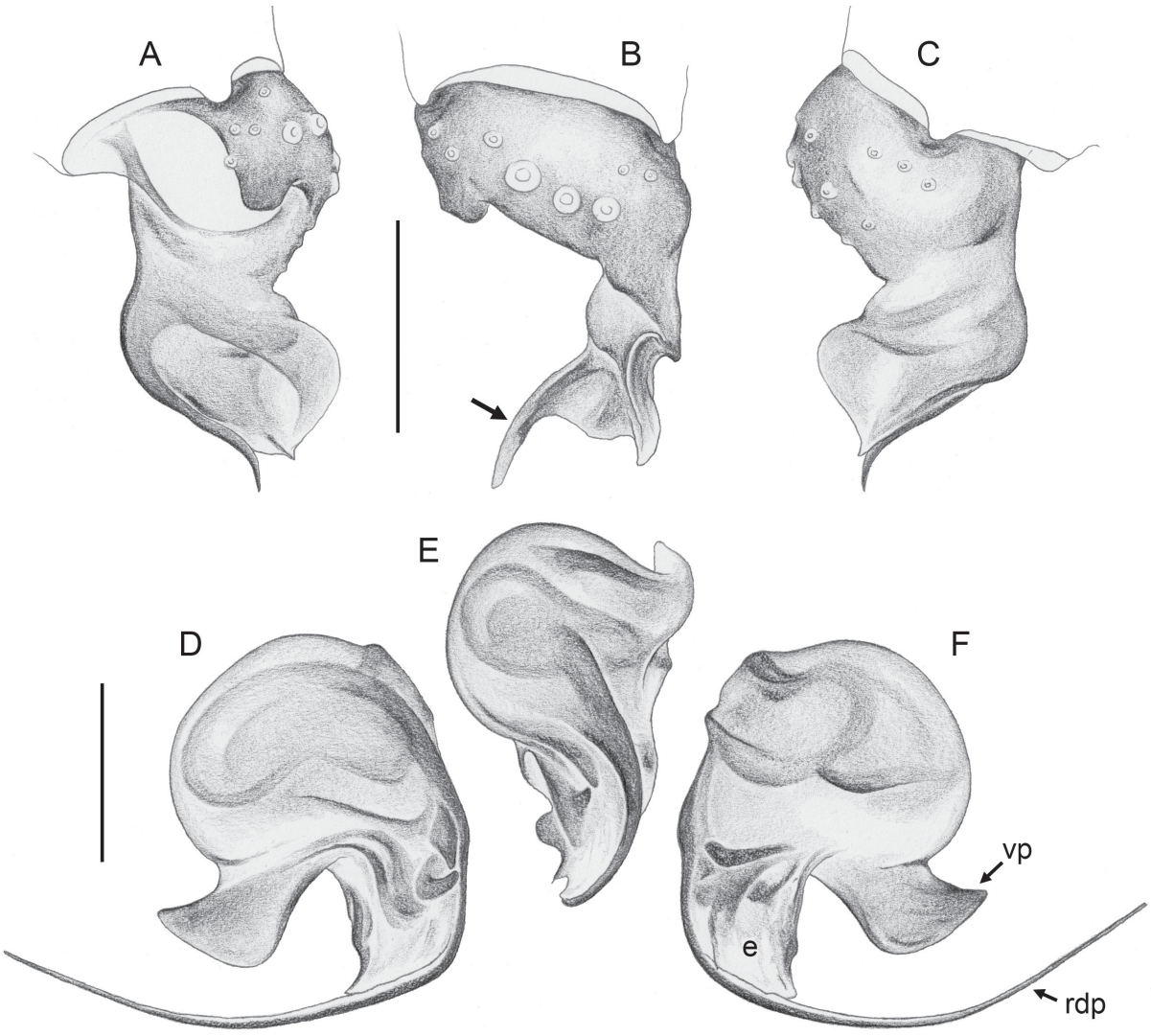

Fig. 27. *Kambiwa brumado* Huber sp. nov., paratype, ♂, from Brazil, Bahia, NE of Brumado, ZFMK Ar 24725. **A–C**. Left palpal tarsus and procursus, prolateral, dorsal, and retrolateral views; arrow in B points at distinctive prolateral process of procursus. **D–F**. Left genital bulb, prolateral, dorsal, and retrolateral views. Abbreviations: e = putative embolus; rdp = retrolateral-dorsal process; vp = ventral process. Scale lines = 0.1 mm.

Palps. As in Fig. 26; coxa unmodified; trochanter ventrally slightly protruding; femur proximally with ventral process, distally widened but otherwise unmodified; femur-patella condyles shifted toward prolateral side; tibia-tarsus condyles slightly shifted toward retrolateral side; tarsus with small prolateral sclerotized process; procursus (Fig. 27A–C) wide in lateral view, narrower in dorsal view, with transparent dorsal flap and distinctive distal sclerotized process directed towards distal and prolateral (arrow in Fig. 27B), poorly visible in undissected palp; genital bulb (Fig. 27D–F) with slightly sclerotized flat ventral process, short dorsal process (putative embolus) composed of membranous and sclerotized elements, and long retrolateral-dorsal process curved towards posterior, passing palp on prolateral side.

Legs. Without spines, without curved hairs; with short vertical hairs on tibiae 1 and 2; retrolateral trichobothrium of tibia 1 at 61%; prolateral trichobothrium absent on tibia 1; tarsus 1 with ~4–5 pseudosegments, fairly distinct.

Variation (males)

Tibia 1 in 25 males (incl. holotype): 0.54–0.66 (mean 0.61). In three males, the filiform process of the bulb of one side passed the palp on the retrolateral side; in all other palps (n = 47) it passed the palp on the prolateral side. Abdomen color variable, sometimes with indistinct internal marks.

Females

In general similar to males but sternum unmodified, chelicerae apparently without stridulatory files (not confirmed with SEM). Tibia 1 in 25 females: 0.54–0.62 (mean 0.57). Epigynum (Fig. 29A–B) anterior plate semicircular, weakly protruding, with pair of lateral posterior sclerites; posterior plate large but simple, roughly rectangular. Internal genitalia (Figs 28C, 29C–F) with curved transversal sclerite connected laterally to lateral posterior sclerites of anterior epigynal plate, medially with anterior rounded process from which membranous coiled tube originates; apparently with pair of small round pore plates (arrows in Fig. 29F).

Barcoding

Three specimens were barcoded, from NE of Brumado (type locality), from SE of Paramirim, and from E of Milagres (geographic distances: 100–265 km). K2P distances were surprisingly high considering the morphological uniformity, ranging from 8.2 to 11.2% (Table 2).

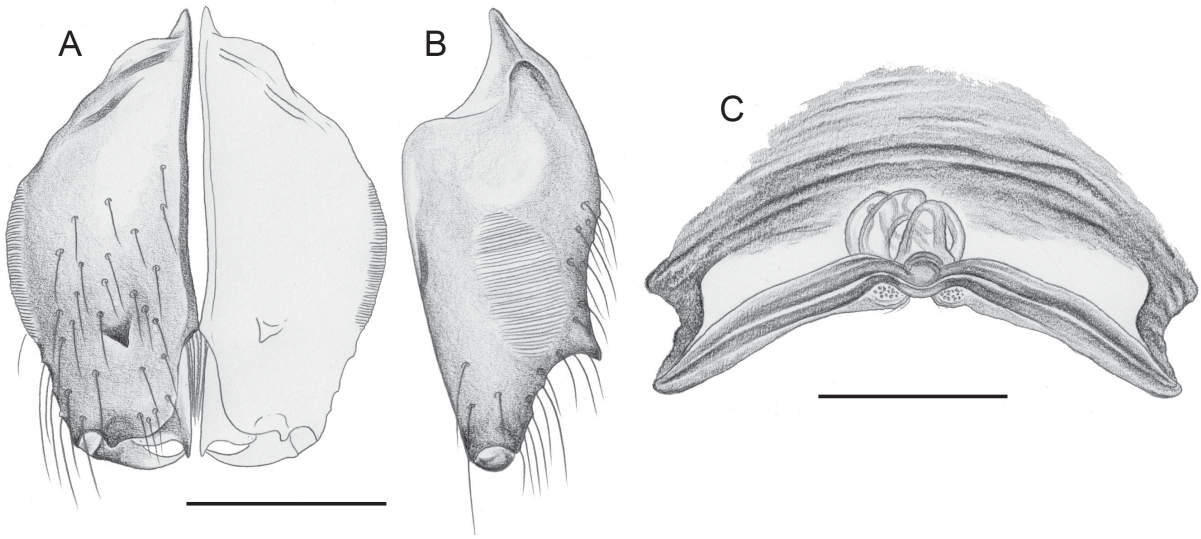

Fig. 28. *Kambiwa brumado* Huber sp. nov., paratypes, ♂♀, from Brazil, Bahia, NE of Brumado, ZFMK Ar 24725. **A**–**B**. Male chelicerae, frontal and lateral views. **C**. Cleared female genitalia, dorsal view. Scale lines = 0.1 mm.

Distribution

Known from several localities in southeastern Bahia, Brazil (Fig. 14).

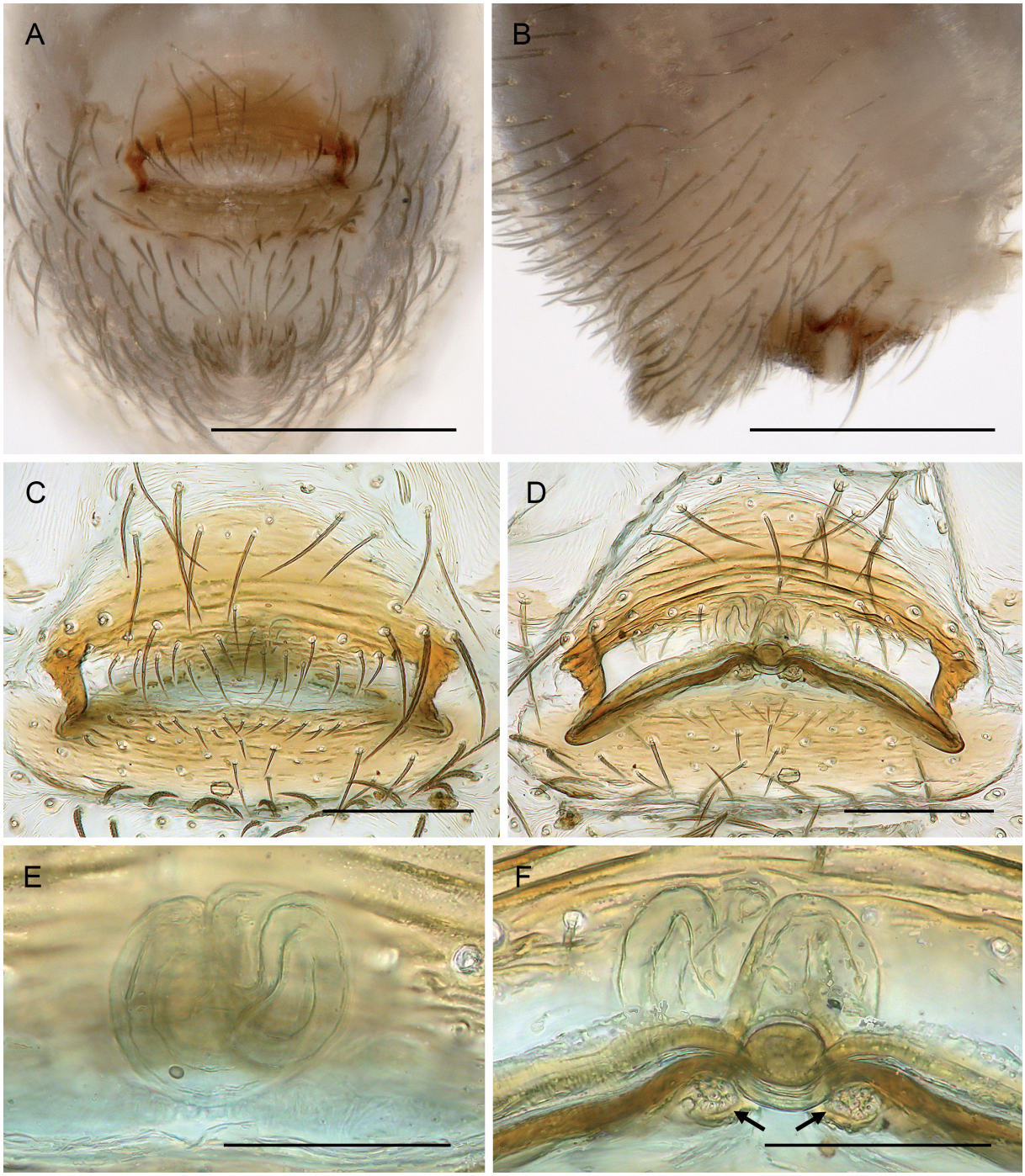

Fig. 29. *Kambiwa brumado* Huber sp. nov., paratype, ♀, from Brazil, Bahia, NE of Brumado, ZFMK Ar 24725. **A**–**B**. Abdomen, ventral and lateral views. **C**–**D**. Cleared genitalia, ventral and dorsal views. **E**–**F**. Central element of internal genitalia, ventral and dorsal views; arrows point at putative pore plates. Scale lines: A–B = 0.3 mm; C–D = 0.1 mm; E–F = 0.05 mm.

Natural history

At the type locality, the spiders were found under rocks in arboreous Caatinga on a marble outcrop (Fig. 11C). East of Milagres, they were collected at the basis of a large outcrop. They lived under rocks and small stones (the size of a hand). Upon disturbance, they ran until finding a depression in the stone to hide, or they dropped to the ground. Southeast of Paramirim they were found both under rocks on a hillside with bare granite and in dead wood and cacti in the neighboring thorny shrubland on clayish soil. West of Marcolino Moura they were collected in a flat thorny shrubland (Caatinga) on clayish soil, in dead wood on the ground, but not in the leaf litter. Northeast of Marcolino Moura they were found under rocks exposed to the sun, on a hillside with bare rock fields and thorny shrubs (Caatinga) on clayish soil. West of Mucugê, the spiders were collected under rocks in a shrubland at the base of a large granite outcrop. Eight egg sacs contained 5–10 eggs each (mean 6.9) and were flat (all eggs in a single layer); egg diameter was 0.44–0.45.

Kambiwa maracas Huber sp. nov.
urn:lsid:zoobank.org:act:BBF0DC5D-4BC9-4EDE-933F-FE91CE12C354
Figs 2G–H, 3D, F–G, 4D, 5E–F, 6A–B, 7B, F, 8A–D, 9F, 10B, D, 30–33

Diagnosis

Males are easily distinguished from those of most known congeners (except *K. brumado* sp. nov. and *K. mucuge* sp. nov.) by very long retrolateral-dorsal process of genital bulb (Fig. 31D–F), and by shape of ventral bulbal process (Fig. 31D–F; roughly rectangular flat element); from *K. brumado* and *K. mucuge* by absence of prolateral process on procursus (compare Fig. 31B with Figs 27B and 35B); from *K. brumado* also by course of retrolateral-dorsal process (compare Figs 27F and 31F; directed towards leg coxae, passing palp on retrolateral side). Females appear externally indistinguishable from those of several congeners (*K. neotropica*; *K. coribe* sp. nov.; *K. brumado*; *K. mucuge*); they differ from *K. neotropica* internally by smaller median element and by convoluted membranous tube rather than simple sac (Fig. 32C); other similar species may be indistinguishable even internally (*K. coribe*; *K. brumado*; *K. mucuge*).

Etymology

The species name is derived from the type locality; noun in apposition.

Type material

Holotype

BRAZIL – **Bahia** • ♂; SW of Maracas; 13.5858° S, 40.7226° W; 410 m a.s.l.; 11 Nov. 2022; B.A. Huber and L.S. Carvalho leg.; CHNUFPI 9185.

Paratypes

BRAZIL – **Bahia** • 2 ♂♂, 12 ♀♀; same collection data as for holotype; CHNUFPI 9186 • 3 ♂♂, 3 ♀♀; same collection data as for holotype; CHNUFPI 9187 [deposited in ZFMK Ar 24723].

Other material examined

BRAZIL – **Bahia** • 3 ♂♂, 8 ♀♀, 9 juvs, in pure ethanol; same collection data as for holotype; CHNUFPI 9188 [deposited in ZFMK Br22-150] (voucher of UH046; 1 ♂, 1 ♀ used for SEM) • 3 ♂♂, 5 ♀♀; NE of Contendas do Sincorá; 13.7474° S, 41.0227° W; 320 m a.s.l.; 11 Nov. 2022; B.A. Huber and L.S. Carvalho leg.; CHNUFPI 9189 • 1 ♂, 5 ♀♀, 7 juvs, in pure ethanol; same collection data as for preceding; CHNUFPI 9190 [deposited in ZFMK Br22-151] (voucher of UH481) • 1 ♂, 3 ♀♀; S of Contendas do Sincorá; 13.7826° S, 41.0507° W; 320 m a.s.l.; 11 Nov. 2022; B.A. Huber and L.S. Carvalho leg.; CHNUFPI 9191 [deposited in ZFMK Ar 24724] • 3 ♀♀, 3 juvs, in pure ethanol;

same collection data as for preceding; CHNUFPI 9192 [deposited in ZFMK Br22-152] • 1 ♂, assigned tentatively; Maracas, near Sede da Ferbasa; 13.4711° S, 40.4380° W; 945 m a.s.l.; 12 Mar. 2012; E.S Araujo and A.S Medeiros leg.; CHNUFPI 1127.

Description

Male (holotype)

Measurements. Total body length 1.00, carapace width 0.49. Distance PME–PME 50 µm; diameter PME 45 µm; distance PME–ALE 15 µm; distance AME–AME 15 µm; diameter AME 25 µm. Leg 1: 2.52 (0.70+0.16+0.64+0.64+0.38), tibia 2: 0.54, tibia 3: 0.50, tibia 4: 0.76; tibia 1 L/d: 10; diameters of leg femora 120 µm, of leg tibiae 65 µm.

Color (in ethanol). Prosoma and legs ochre-yellow, carapace and legs without darker marks or rings; abdomen monochromous ochre-gray.

Body. Habitus as in Fig. 2G. Ocular area not raised. Carapace without thoracic groove. Clypeus unmodified. Sternum slightly wider than long (0.35/0.32), with small but distinct anterior processes near coxae 1 (~30 µm high, 40 µm diameter at basis). Abdomen globular.

Chelicerae. As in Fig. 32A–B; with pair of small frontal apophyses; stridulatory files very fine and poorly visible in dissecting microscope.

Palps. As in Fig. 30; coxa unmodified; trochanter ventrally slightly protruding; femur proximally with small ventral process, distally widened but otherwise unmodified; femur-patella condyles shifted toward prolateral side; tibia-tarsus condyles slightly shifted toward retrolateral side; tarsus with small prolateral sclerotized process; procursus (Fig. 31A–C) wide in lateral view, narrower in dorsal view,

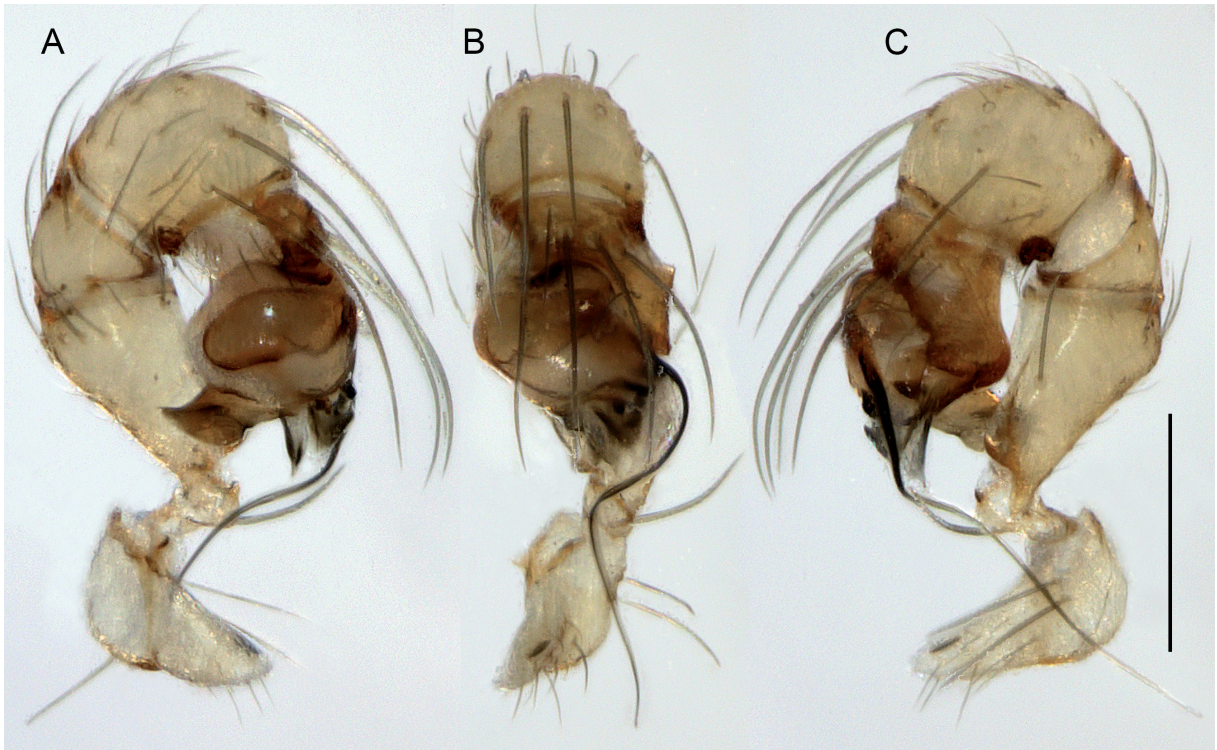

Fig. 30. *Kambiwa maracas* Huber sp. nov., paratype, ♂, from Brazil, Bahia, SW of Maracas, ZFMK Ar 24723. Left palp, prolateral, dorsal, and retrolateral views. Scale line = 0.2 mm.

with transparent dorsal flap, without distal sclerotized process; genital bulb (Fig. 31D–F) with slightly sclerotized flat ventral process, short dorsal process (putative embolus) composed of membranous and sclerotized elements, and filiform retrolateral-dorsal process reaching anterior side of leg coxa 2, passing palpal coxa on retrolateral side.

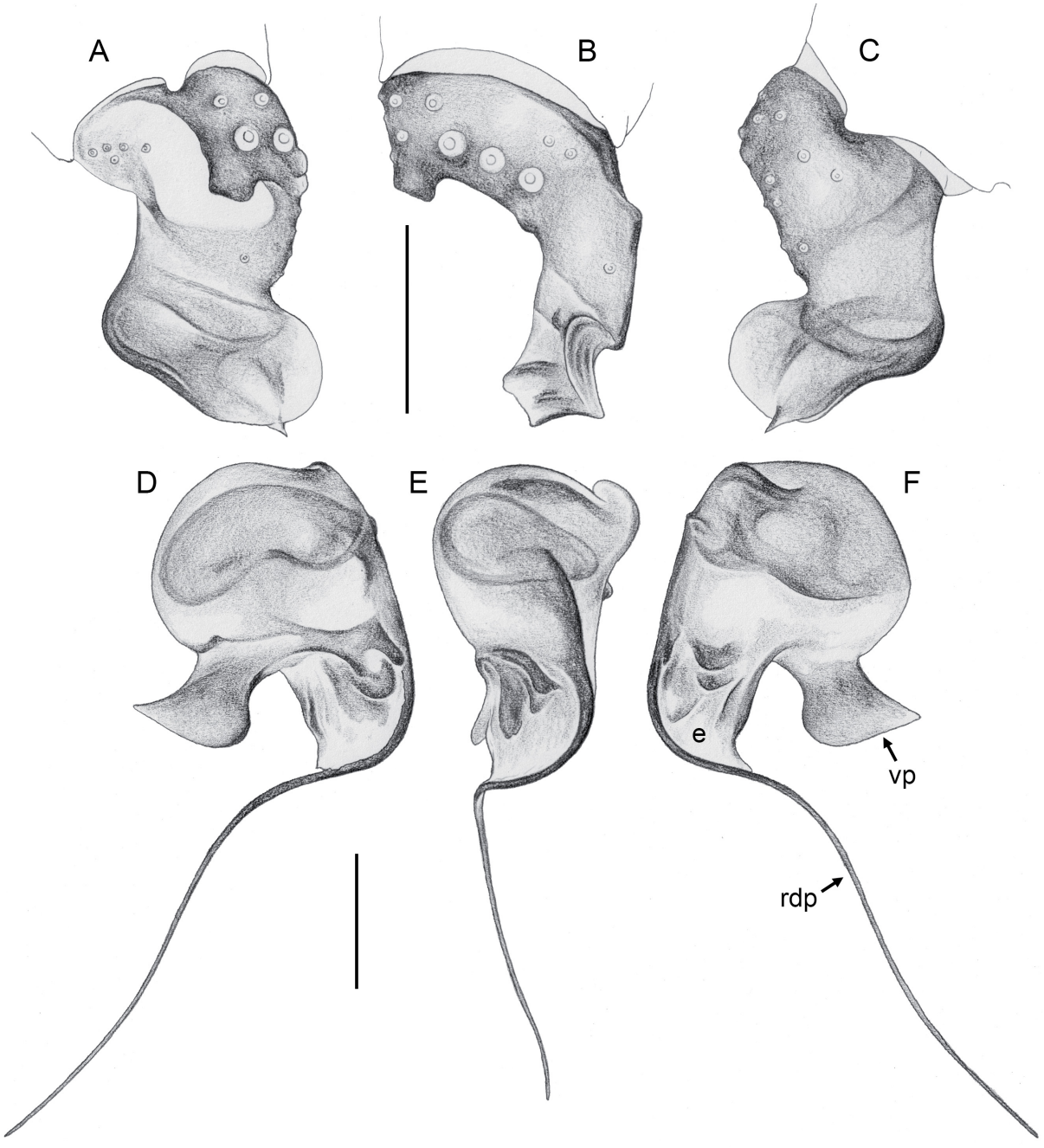

Fig. 31. *Kambiwa maracas* Huber sp. nov., paratype, ♂, from Brazil, Bahia, SW of Maracas, ZFMK Ar 24723. **A–C**. Left palpal tarsus and procursus, prolateral, dorsal, and retrolateral views. **D–F**. Left genital bulb, prolateral, dorsal, and retrolateral views. Abbreviations: e = putative embolus; rdp = retrolateral-dorsal process; vp = ventral process. Scale lines = 0.1 mm.

Legs. Without spines, without curved hairs; with short vertical hairs on tibiae 1 and 2; retrolateral trichobothrium of tibia 1 at 59%; prolateral trichobothrium absent on tibia 1; tarsus 1 with ~4–5 pseudosegments, fairly distinct.

Variation (males)

Tibia 1 in nine males (incl. holotype): 0.56–0.64 (mean 0.59). The male from near Sede da Ferbasa has shorter legs (tibia 1: 0.50) and also a slightly shorter retrolateral-dorsal bulbal process (similar to *K. mucuge* sp. nov.). It is tentatively assigned to this species because the procursus has no distal sclerotized process (in contrast to *K. mucuge*).

Females

In general similar to males but sternum unmodified, chelicerae without stridulatory files, legs without short vertical hairs. Tibia 1 in 23 females: 0.52–0.62 (mean 0.56). Epigynum (Fig. 33A–B) anterior plate semicircular, weakly protruding, with pair of lateral posterior sclerites; posterior plate large but simple, roughly rectangular. Internal genitalia (Figs 32C, 33C–F) with curved transversal sclerite connected laterally to lateral posterior sclerites of anterior epigynal plate, medially with anterior rounded process from which transparent coiled tube originates; apparently with pair of small round pore plates (arrows in Fig. 33F).

Barcoding

Two specimens were barcoded, from SW of Maracas (type locality) and from NE of Contendas do Sincorá (geographic distance: 37 km). The K2P distance was 1.8%.

Distribution

Known from four localities in Bahia, Brazil (Fig. 14).

Natural history

At the type locality, the spiders were beaten from dead wood on the ground in shrubby Caatinga woodland on clayish soil (Fig. 11D); in the dead branches, they apparently occupied the abandoned tunnels of termites. They were not found in the neighboring leaf litter. Northeast of Contendas do

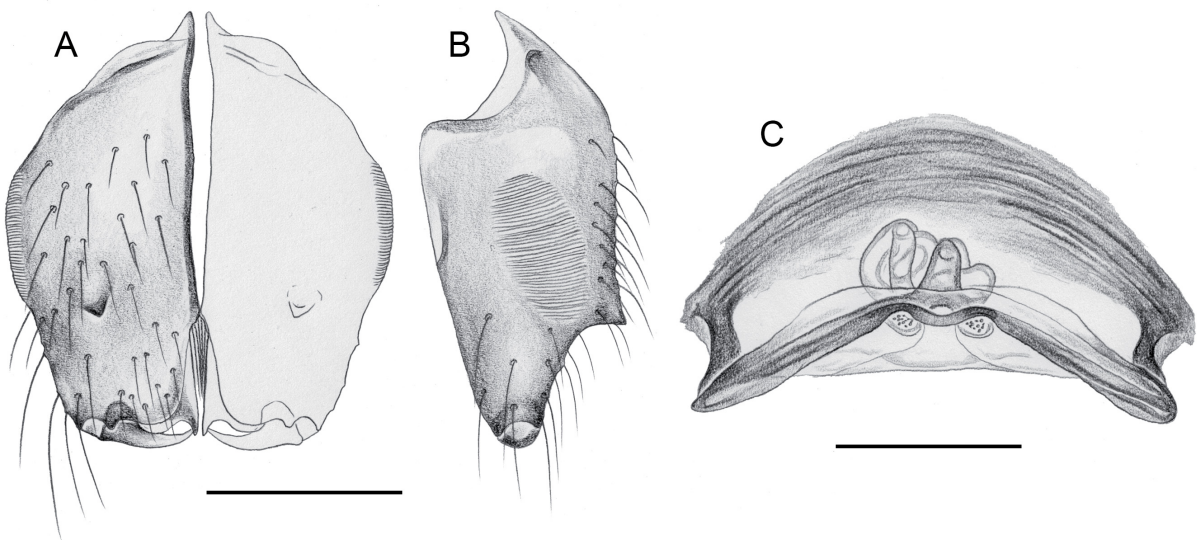

Fig. 32. *Kambiwa maracas* Huber sp. nov., paratypes, ♂♀, from Brazil, Bahia, SW of Maracas, ZFMK Ar 24723. **A**–**B**. Male chelicerae, frontal and lateral views. **C**. Cleared female genitalia, dorsal view. Scale lines = 0.1 mm.

Sincorá, they were found on the undersides of rocks in shrubby Caatinga woodland on a rocky hillside. South of Contendas do Sincorá, the spiders were collected on a hillside with shrubby Caatinga woodland on sandy soil; one specimen was beaten out of a dead cactus approximately 1 m above the ground. Four egg sacs contained 2–12 eggs each (mean 6.3) and were flat (all eggs in a single layer); egg diameter was 0.44–0.45.

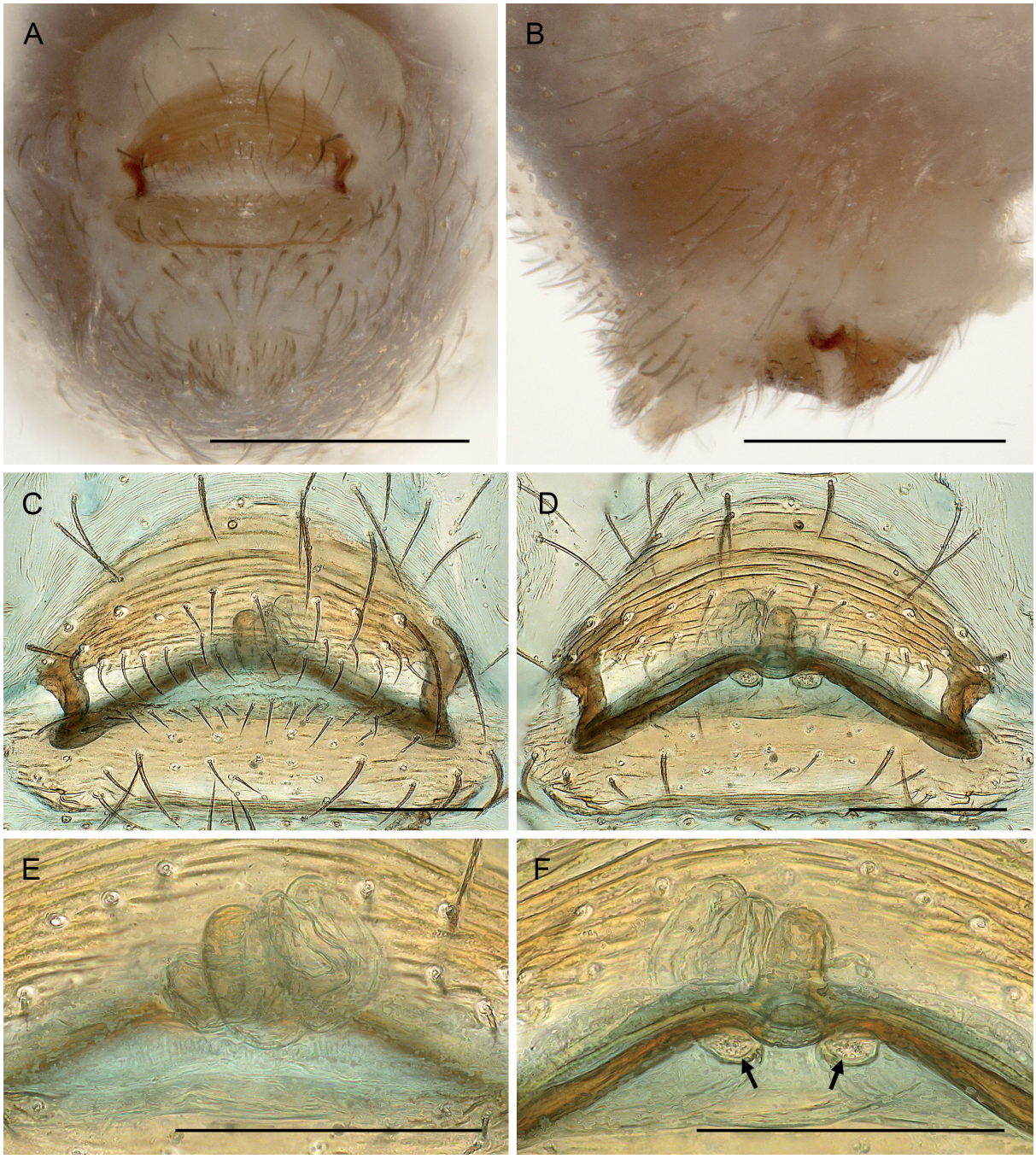

Fig. 33. *Kambiwa maracas* Huber sp. nov., paratype, ♀, from Brazil, Bahia, SW of Maracas, ZFMK Ar 24723. **A**–**B**. Abdomen, ventral and lateral views. **C**–**D**. Cleared genitalia, ventral and dorsal views. **E**–**F**. Central element of internal genitalia, ventral and dorsal views; arrows point at putative pore plates. Scale lines: A–B = 0.3 mm; C–F = 0.1 mm.

Kambiwa mucuge Huber sp. nov.
urn:lsid:zoobank.org:act:4AD6876B-D2F5-45C9-AAAD-24FA49C56078
Figs 2K–L, 34–37

Diagnosis

Males are easily distinguished from those of most known congeners (except *K. maracas* sp. nov. and *K. brumado* sp. nov.) by very long retrolateral-dorsal process of genital bulb (Fig. 35D–F), and by shape of ventral bulbal process (Fig. 35D–F; roughly rectangular flat element); from *K. maracas* by presence of prolateral process on procursus (compare Figs 31B and 35B); from *K. brumado* by course of retrolateral-dorsal process (compare Figs 27F and 35F; directed towards leg coxae, passing palp on retrolateral side). Females appear externally indistinguishable from those of several congeners (*K. neotropica*; *K. coribe* sp. nov.; *K. maracas*; *K. brumado*); they differ from *K. neotropica* internally by smaller median element and by convoluted membranous tube rather than simple sac (Fig. 36C); other similar species may be indistinguishable even internally (*K. coribe*; *K. maracas*; *K. brumado*).

Etymology

The species name is derived from the type locality; noun in apposition.

Type material

Holotype

BRAZIL – **Bahia** • ♂; NE of Mucugê, Parque "Sempre Viva"; 12.998° S, 41.363° W; 970–990 m a.s.l.; bare granite fields with shrubs on sandy soil; 20 Nov. 2022; B.A. Huber and L.S. Carvalho leg.; CHNUFPI 9209.

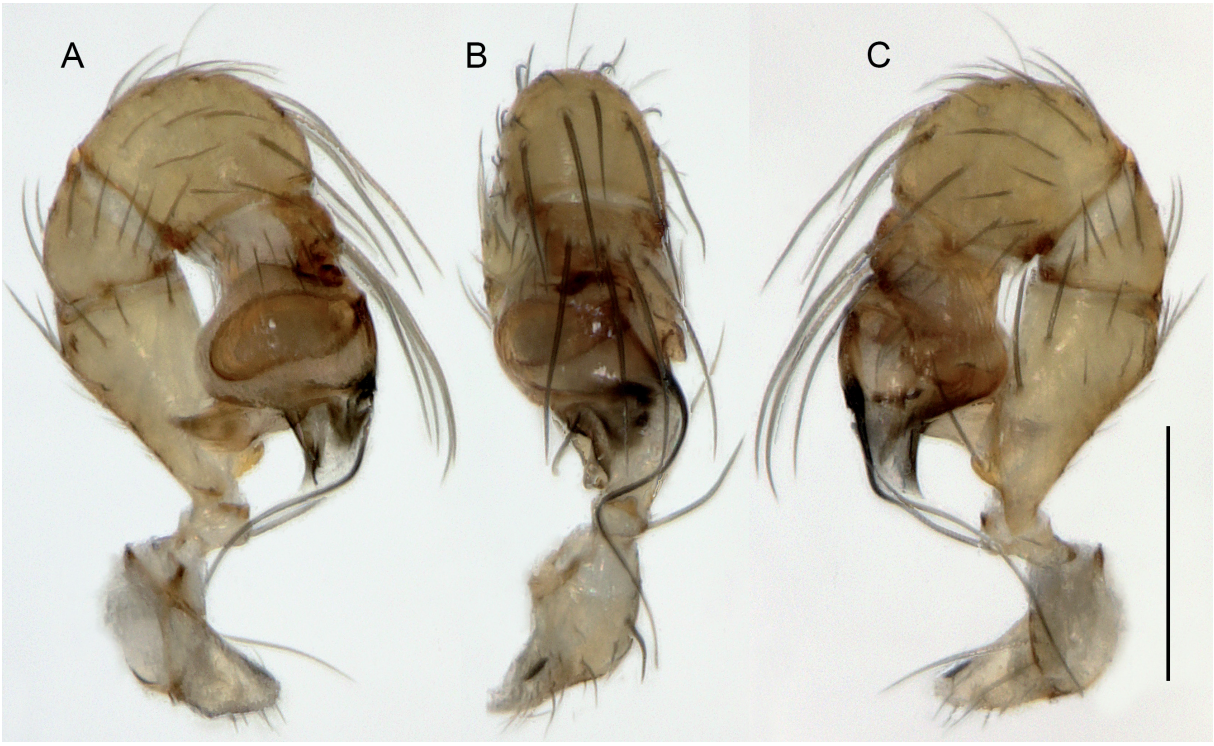

Fig. 34. *Kambiwa mucuge* Huber sp. nov., paratype, ♂, from Brazil, Bahia, NE of Mucugê, ZFMK Ar 24728. Left palp, prolateral, dorsal, and retrolateral views. Scale line = 0.2 mm.

Paratypes

BRAZIL – **Bahia** • 3 ♂♂, 2 ♀♀; same collection data as for holotype; CHNUFPI 9210 • 1 ♀; same collection data as for holotype; CHNUFPI 9211 • 2 ♂♂, 2 ♀♀; same collection data as for holotype; CHNUFPI 9212 [deposited in ZFMK Ar 24728].

Other material examined

BRAZIL – **Bahia** • 1 ♂, 5 ♀♀, 5 juvs, in pure ethanol; same collection data as for holotype; CHNUFPI 9213 [deposited in ZFMK Br22-201] • 1 ♀, 2 juvs, in pure ethanol; identity of female confirmed by

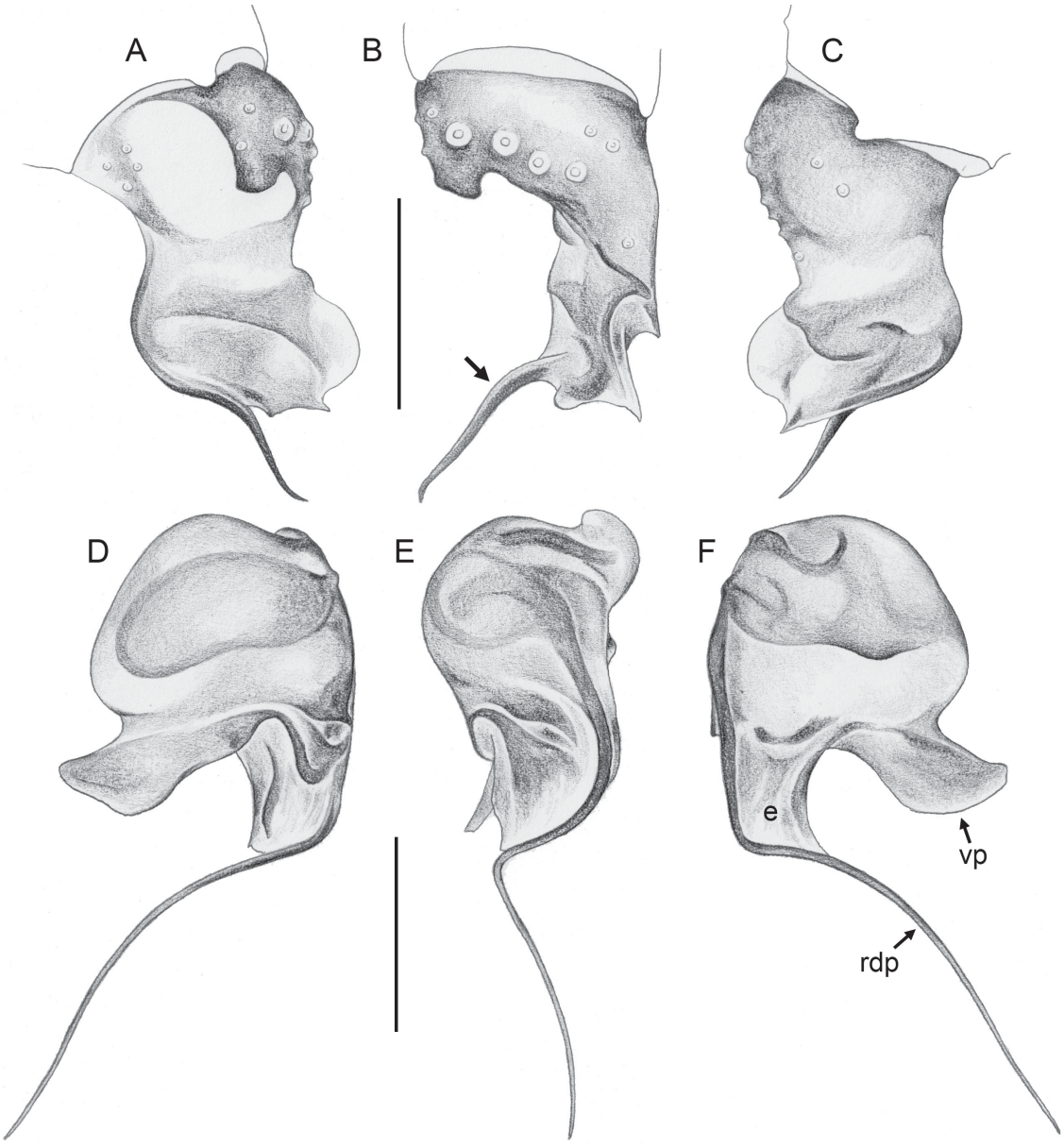

Fig. 35. *Kambiwa mucuge* Huber sp. nov., paratype, ♂, from Brazil, Bahia, NE of Mucugê, ZFMK Ar 24728. **A–C**. Left palpal tarsus and procursus, prolateral, dorsal, and retrolateral views; arrow points at distinctive prolateral process on procursus. **D–F**. Left genital bulb, prolateral, dorsal, and retrolateral views. Abbreviations: e = putative embolus; rdp = retrolateral-dorsal process; vp = ventral process. Scale lines = 0.1 mm.

CO1 barcode; W of Mucugê, Parque Nacional da Chapada Diamantina; 13.0097° S, 41.4084° W; 1010 m a.s.l.; 19 Nov. 2022; B.A. Huber and L.S. Carvalho leg.; CHNUFPI 9214 [deposited in ZFMK Br22-200] • 2 ♀♀, assigned tentatively, see below; same collection data as for preceding; CHNUFPI 9215 [deposited in ZFMK Ar 24729].

Description

Male (holotype)

Measurements. Total body length 1.14, carapace width 0.47. Distance PME–PME 50 µm; diameter PME 45 µm; distance PME–ALE 15 µm; distance AME–AME 15 µm; diameter AME 20 µm. Leg 1: 2.22 (0.62+0.16+0.56+0.54+0.34), tibia 2: 0.47, tibia 3: 0.44, tibia 4: 0.67; tibia 1 L/d: 9; diameters of leg femora 110 µm, of leg tibiae 65 µm.

Color (in ethanol). Prosoma and legs ochre-yellow, carapace and legs without darker marks or rings; abdomen ochre-gray, ventrally with slightly darker plate in front of gonopore.

Body. Habitus as Fig. 2K. Ocular area not raised. Carapace without thoracic groove. Clypeus unmodified. Sternum slightly wider than long (0.35/0.32), with small but distinct anterior processes near coxae 1 (~30 µm high, 40 µm diameter at basis). Abdomen globular.

Chelicerae. As in Fig. 36A–B; with pair of small frontal apophyses; stridulatory files very fine and poorly visible in dissecting microscope.

Palps. As in Fig. 34; coxa unmodified; trochanter ventrally slightly protruding; femur proximally with ventral process, distally widened but otherwise unmodified; femur-patella condyles shifted toward prolateral side; tibia-tarsus condyles slightly shifted toward retrolateral side; tarsus with small prolateral sclerotized process; procursus (Fig. 35A–C) wide in lateral view, narrower in dorsal view, with transparent dorsal flap and distinctive sclerotized process directed towards distal and prolateral, clearly visible in undissected palp; genital bulb (Fig. 35D–F) with slightly sclerotized ventral process, short dorsal process (putative embolus) composed of membranous and sclerotized elements, and filiform retrolateral-dorsal process reaching anterior side of leg coxa 1, passing palpal coxa on retrolateral side.

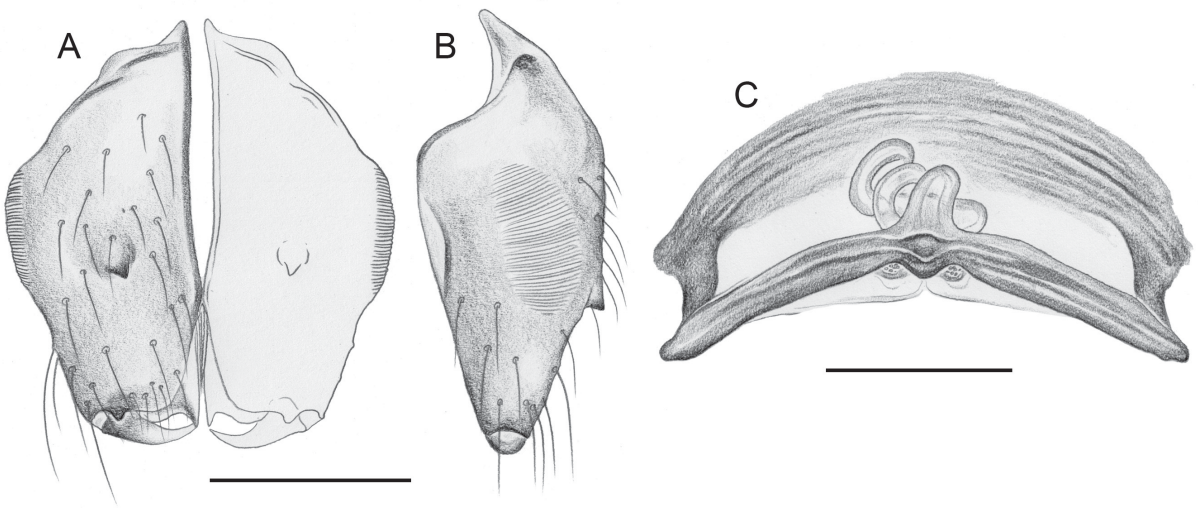

Fig. 36. *Kambiwa mucuge* Huber sp. nov., paratypes, ♂♀, from Brazil, Bahia, NE of Mucugê, ZFMK Ar 24728. **A**–**B**. Male chelicerae, frontal and lateral views. **C**. Cleared female genitalia, dorsal view. Scale lines = 0.1 mm.

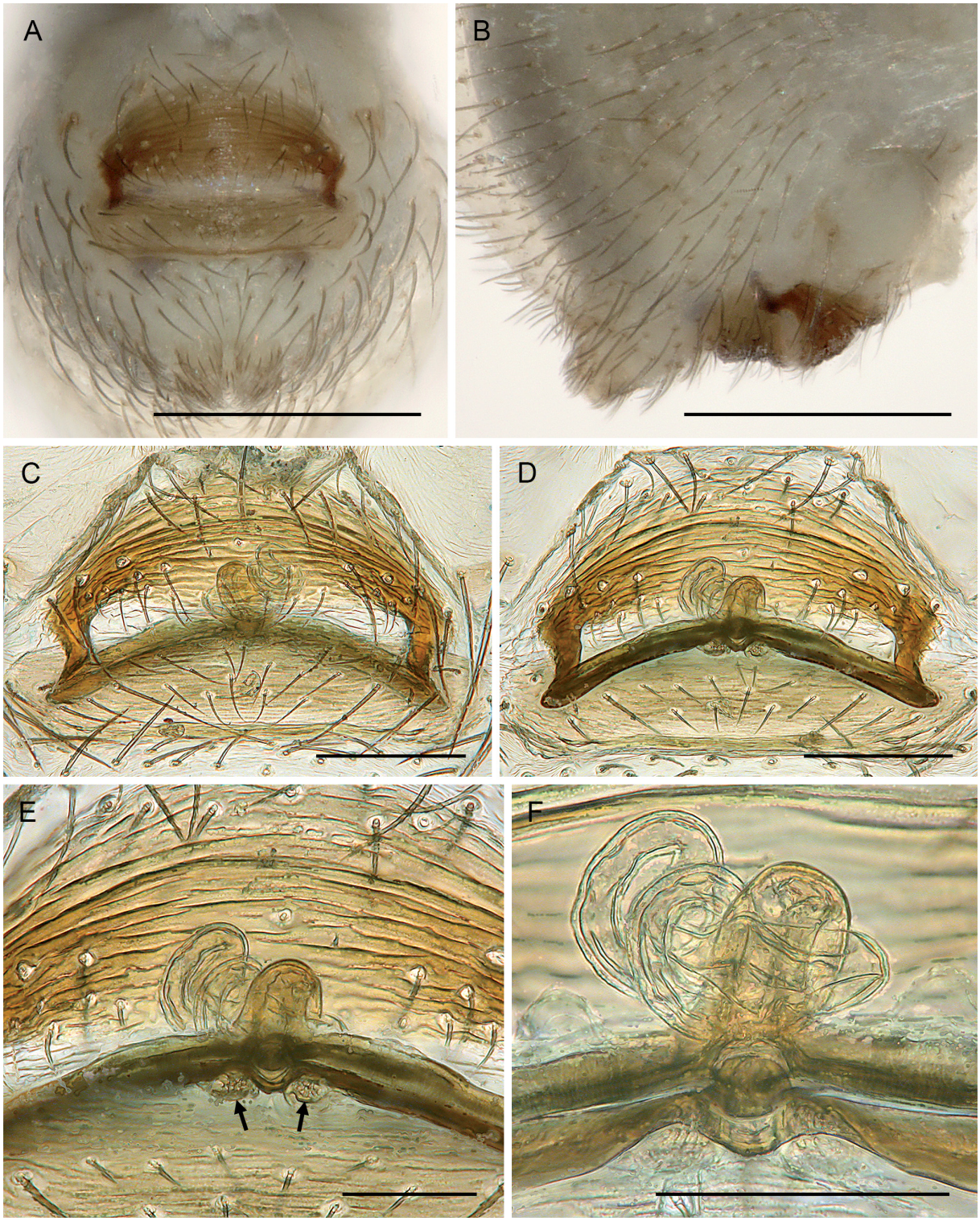

Fig. 37. *Kambiwa mucuge* Huber sp. nov., paratype, ♀, from Brazil, Bahia, NE of Mucugê, ZFMK Ar 24728. **A**–**B**. Abdomen, ventral and lateral views. **C**–**D**. Cleared genitalia, ventral and dorsal views. **E**–**F**. Central element of internal genitalia, dorsal views; arrows point at putative pore plates. Scale lines: A–B = 0.3 mm; C–D = 0.1 mm; E–F = 0.05 mm.

Legs. Without spines, without curved hairs; short vertical hairs not seen (not studied with SEM); retrolateral trichobothrium of tibia 1 at 59%; prolateral trichobothrium absent on tibia 1; tarsus 1 with ~4–5 pseudosegments, fairly distinct.

Variation (males)

Tibia 1 in six males from type locality (incl. holotype): 0.55–0.57 (mean 0.56). Abdomen color variable, sometimes with indistinct internal marks.

Females

In general similar to males but sternum unmodified, chelicerae apparently without stridulatory files (not confirmed with SEM). Tibia 1 in nine females from type locality: 0.48–0.53 (mean 0.50). The sequenced female from the neighboring locality W of Mucugê has minimally longer legs (tibia 1: 0.54); tibia 1 two further females from that locality: 0.46, 0.49. [The fourth female from W of Mucugê has much longer legs (tibia 1: 0.62); it is thus assigned to *K. brumado* sp. nov., together with the only male from this locality]. Epigynum (Fig. 37A–B) anterior plate semicircular, weakly protruding, with pair of lateral posterior sclerites; posterior plate large but simple, roughly rectangular. Internal genitalia (Figs 36C, 37C–F) with curved transversal sclerite connected laterally to lateral posterior sclerites of anterior epigynal plate, medially with anterior rounded process from which membranous coiled tube originates; apparently with pair of small round pore plates (arrows in Fig. 37E).

Barcoding

Two specimens were barcoded, from NE of Mucugê (type locality) and from W of Mucugê (geographic distance: 5 km). Haplotypes at both sites were identical.

Distribution

Known from two neighboring localities near Mucugê in Bahia, Brazil (Fig. 14).

Natural history

At both localities, the spiders were found under stones lying on large granitic rock plates with scattered shrubs on sandy soil (Fig. 11E). Two egg sacs contained 4 and 5 eggs, respectively, and were flat (all eggs in a single layer); egg diameter was 0.44–0.46.

Kambiwa itacarambi Huber sp. nov.
urn:lsid:zoobank.org:act:164FEB6B-6BFD-4D70-87E8-5935FB6CF0CC
Figs 2A–B, 3C, 4B, F, 5C, 6E–F, 8E–F, 9A, C, 10E–F, 38–41

Diagnosis

Easily distinguished from all known congeners by male chelicerae without frontal apophyses (Fig. 40A–B; only with pair of low ridges and distinctive whitish distal areas), by strong ventral bulbal process directed towards ventral and distally slightly hooked (Fig. 39D, F), and by arc-shaped anterior epigynal plate (Fig. 41A, C); also by tip of procursus (Fig. 39A–C; simple membranous flap, distally bent towards prolateral) and by female internal genitalia with very indistinct median modification (Fig. 40C; low anterior protrusion).

Etymology

The species name is derived from the type locality; noun in apposition.

Type material

Holotype

BRAZIL – **Minas Gerais** • ♂; NW of Itacarambi, 'site 1', near radio/TV towers; 15.0500° S, 44.1820° W; 780 m a.s.l.; 13 Nov. 2022; B.A. Huber, L.S. Carvalho and R.A. Torres leg.; CHNUFPI 9120.

Paratypes

BRAZIL – **Minas Gerais** • 8 ♂♂, 6 ♀♀; same collection data as for holotype; CHNUFPI 9121 • 1 ♂, 1 ♀; same collection data as for holotype; CHNUFPI 9122 • 3 ♂♂, 3 ♀♀; same collection data as for holotype; CHNUFPI 9123 [deposited in ZFMK Ar 24711].

Other material examined

BRAZIL – **Minas Gerais** • 2 ♂♂, 6 ♀♀, 4 juvs, in pure ethanol; same collection data as for holotype; CHNUFPI 9124 [deposited in ZFMK Br22-159] • 1 ♂; same locality as for holotype; 3 Mar. 2020; A.J. Santos leg.; CHNUFPI 3502 • 1 ♀; same collection data as for preceding; CHNUFPI 3504 ("Carv56"; voucher of E072) • 2 ♀♀; same collection data as for preceding; CHNUFPI 3501, 3503 • 13 ♂♂, 19 ♀♀; SW of Manga, Parque Estadual da Mata Seca; 14.8438° S, 44.0592° W; 500 m a.s.l.; 15 Nov. 2022; B.A. Huber and L.S. Carvalho leg.; CHNUFPI 9125–9126 • 3 ♂♂, 8 ♀♀, 8 juvs, in pure ethanol; same collection data as for preceding; CHNUFPI 9127 [deposited in ZFMK Br22-170] (voucher of G50; 1 ♂, 1 ♀ used for SEM).

Description

Male (holotype)

Measurements. Total body length 1.07, carapace width 0.51. Distance PME–PME 45 µm; diameter PME 55 µm; distance PME–ALE 15 µm; distance AME–AME 15 µm; diameter AME 30 µm. Leg 1: 2.54 (0.62+0.19+0.67+0.68+0.38), tibia 2: 0.54, tibia 3: 0.50, tibia 4: 0.81; tibia 1 L/d: 10; diameters of leg femora 110–120 µm, of leg tibiae 65 µm.

Fig. 38. *Kambiwa itacarambi* Huber sp. nov., paratype, ♂, from Brazil, Minas Gerais, NW of Itacarambi, ZFMK Ar 24711. Left palp, prolateral, dorsal, and retrolateral views. Scale line = 0.2 mm.

Color (in ethanol). Prosoma and legs ochre-yellow, carapace and legs without darker marks or rings; abdomen ochre-gray with very indistinct internal marks, with slightly darker ochre plate in front of gonopore.

Body. Habitus as in Fig. 2A. Ocular area not raised. Carapace with very shallow thoracic groove. Clypeus unmodified. Sternum slightly wider than long (0.37/0.33), with pair of anterior humps near coxae 1 (~30 µm high, 60 µm diameter at basis). Abdomen globular.

Chelicerae. As in Fig. 40A–B; without frontal apophyses, with pair of low sclerotized ridges followed distally by whitish area; with very fine stridulatory files (Fig. 6E), not visible in dissecting microscope.

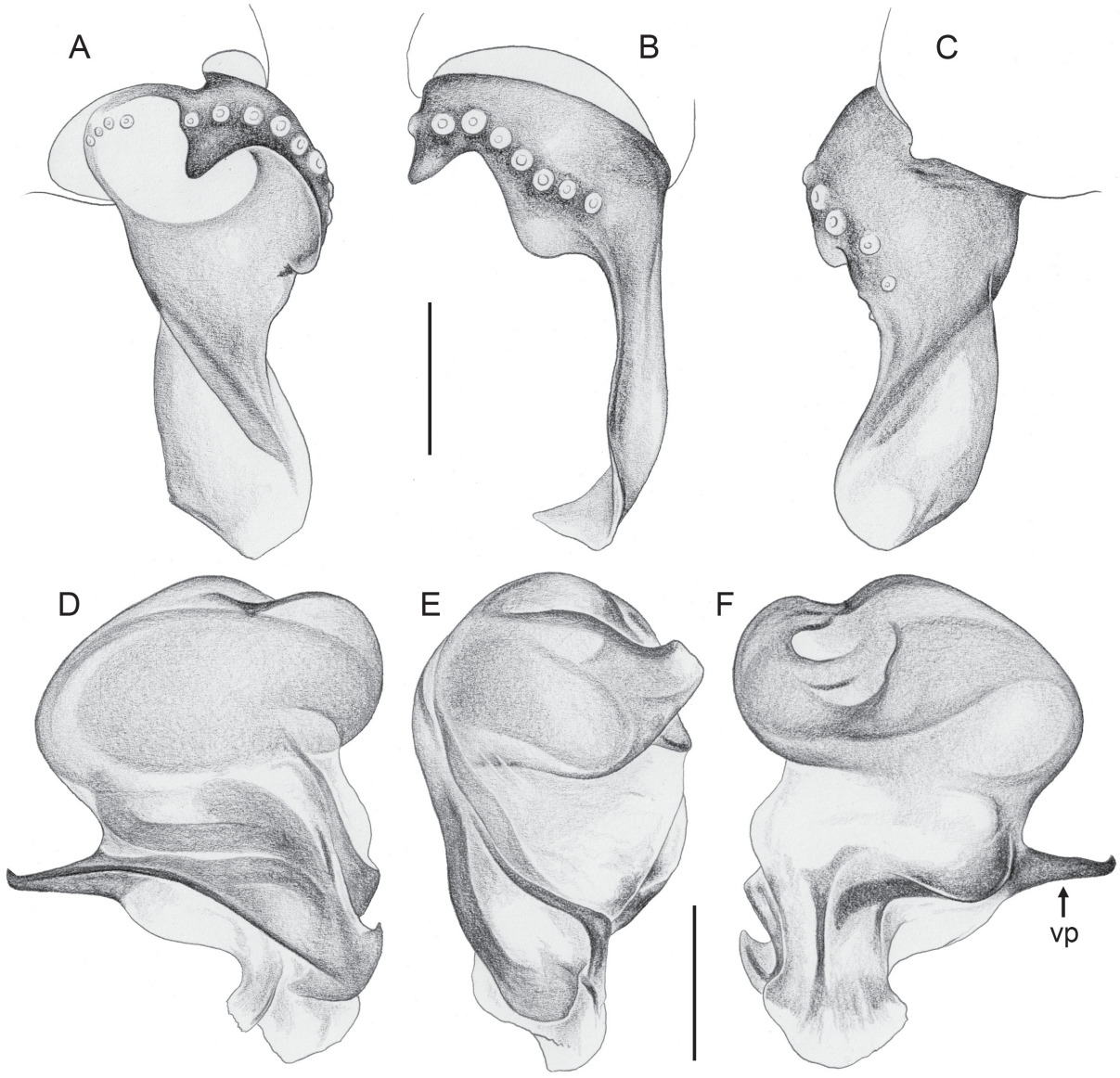

Fig. 39. *Kambiwa itacarambi* Huber sp. nov., paratype, ♂, from Brazil, Minas Gerais, NW of Itacarambi, ZFMK Ar 24711. **A–C**. Left palpal tarsus and procursus, prolateral, dorsal, and retrolateral views. **D–F**. Left genital bulb, prolateral, dorsal, and retrolateral views. Abbreviation: vp = ventral process. Scale lines = 0.1 mm.

Palps. As in Fig. 38; coxa unmodified; trochanter ventrally slightly protruding; femur proximally with small ventral process, distally widened but otherwise unmodified; femur-patella condyles slightly shifted towards prolateral side; tibia-tarsus condyles slightly shifted towards retrolateral side; tarsus with strong prolateral process; procursus (Fig. 39A–C) wide in lateral view, narrower in dorsal view, with semi-transparent distal flap distally directed towards prolateral; genital bulb (Fig. 39D–F) with complex distal process composed of membranous and sclerotized elements, with strong and distally hooked ventral process, without recognizable retrolateral-dorsal process.

Legs. Without spines, without curved hairs; with short vertical hairs on tibiae 1 and 2; retrolateral trichobothrium of tibia 1 at 56%; prolateral trichobothrium absent on tibia 1; tarsus 1 with four fairly distinct pseudosegments.

Variation (males)

Tibia 1 in 27 males: 0.62–0.71 (mean 0.67). Some males with distinct dark internal marks on abdomen.

Females

In general similar to males (including color variation), but sternum without anterior humps and tibiae without vertical hairs; chelicerae without stridulatory files. Tibia 1 in 29 females: 0.60–0.69 (mean 0.65). Epigynum (Fig. 41A–C) anterior plate reduced to narrow ark around whitish central area, weakly protruding, variably spread away from posterior plate; posterior plate much larger than anterior plate, roughly rectangular. Internal genitalia (Figs 40C, 41D–G) with curved transversal sclerite connected laterally to lateral corners of anterior epigynal plate, medially with small anterior bulge but without membranous sac; posteriorly with pair of small weakly sclerotized processes but apparently without pore plates.

Barcoding

Two specimens were barcoded, from NW of Itacarambi (type locality) and from SW of Manga (geographic distance: 26 km). The K2P distance was 11.5%. Considering the small geographic distance and the absence of morphological differences, we suspect that the large molecular distance (and the long terminal branch leading to E072 in Fig. 1) results from an artifact.

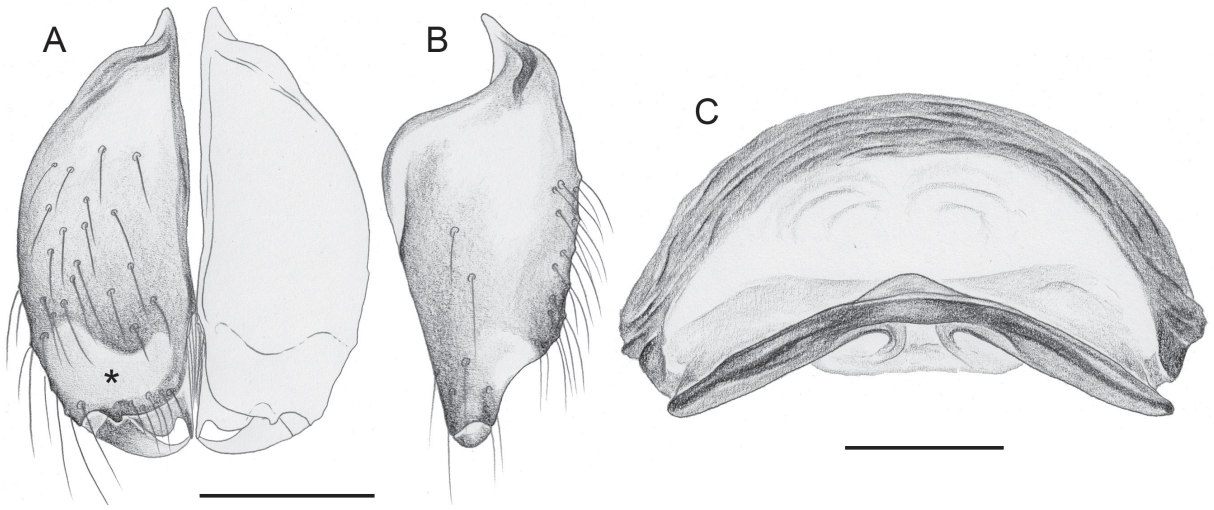

Fig. 40. *Kambiwa itacarambi* Huber sp. nov., paratypes, ♂♀, from Brazil, Minas Gerais, NW of Itacarambi, ZFMK Ar 24711. **A**–**B**. Male chelicerae, frontal and lateral views; asterisk marks distinctive whitish area. **C**. Cleared female genitalia, dorsal view. Scale lines = 0.1 mm.

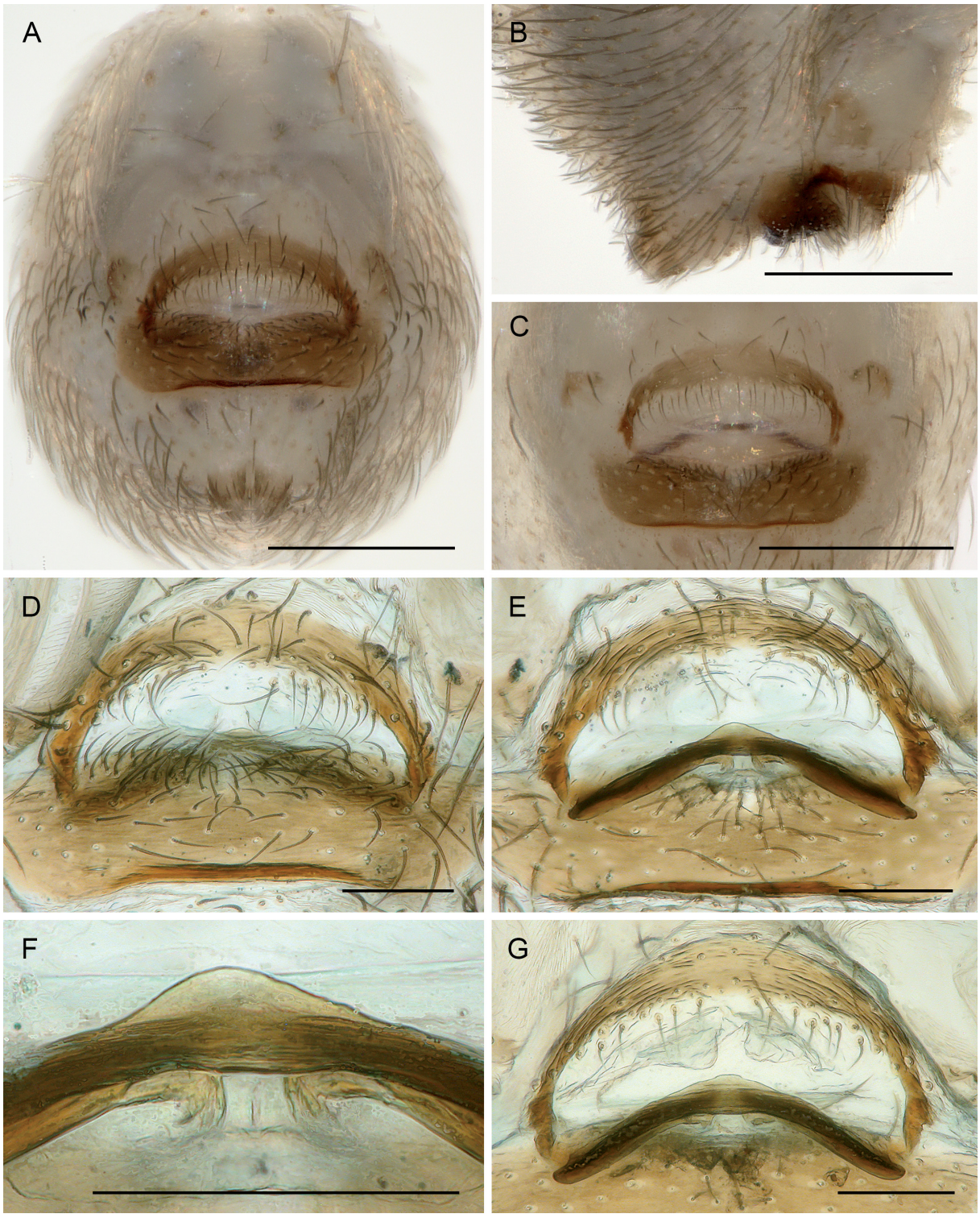

Fig. 41. *Kambiwa itacarambi* Huber sp. nov. **A–B, D–F**. Paratype, ♀, from Brazil, Minas Gerais, NW of Itacarambi, ZFMK Ar 24711. **C, G**. ♀, from Minas Gerais, SW of Manga, CHNUFPI 9126. **A–B**. Abdomen, ventral and lateral views. **C**. Epigynum, ventral view. **D–E**. Cleared genitalia, ventral and dorsal views. **F**. Detail of previous figure. **G**. Cleared genitalia, dorsal view. Scale lines: A–C = 0.3 mm; D–G = 0.1 mm.

Distribution

Known from two localities in northern Minas Gerais, Brazil (Fig. 14).

Natural history

At the type locality, the spiders were extremely abundant on a bare degraded hill-top with numerous small stones on clayish soil fully exposed to the sun (Fig. 11F). At Parque Estadual da Mata Seca they occupied a very different habitat, the leaf litter among bushes and low trees on flat terrain, in a thorny shrubland (Caatinga) on sandy soil. Upon moving the leave litter, the spiders started to run. A semi-quantitative collecting effort covering 1 m^2 resulted in 19 adult specimens within 45 min. Eleven egg sacs contained 4–10 eggs each (mean 7.5) and were flat (all eggs in a single layer); egg diameter was 0.44–0.48.

Kambiwa ibo Huber sp. nov.
urn:lsid:zoobank.org:act:E1412702-D173-4244-834A-2CF75643B212
Figs 2C–D, 4E, 5D, 6D, 7C–D, 9B, E, 10A, 42–45

Diagnosis

Males are distinguished from those of most known congeners (except *K. sapo*) by shape of ventral bulbal process (Fig. 43D, F; short and pointed, slightly twisted), by tip of procursus (Fig. 43A–C; mostly membranous, set with numerous tiny spikes), and by male cheliceral apophyses relatively far apart (Fig. 44A); from *K. sapo* by simple rounded tip of procursus (rather than bifid), by distinct separation between distal membranous part of procursus from proximal sclerotized part, and by genital bulb slightly more rounded rather than elongate and with slightly different sclerotized elements (compare Figs 43D–F with 46D–F). Females are externally very similar to those of several congeners (e.g., *K. neotropica*; *K. coribe* sp. nov.; *K. maracas* sp. nov.; *K. brumado* sp. nov.; *K. mucuge* sp. nov.; *K. sapo*); they differ by internal genitalia with indistinct median element leading into small membranous sac (Fig. 44C).

Etymology

The species name is derived from the type locality; noun in apposition.

Type material

Holotype

BRAZIL – **Bahia** • ♂; S of Ibó; 8.6906° S, 39.2682° W; 340 m a.s.l.; 2 Dec. 2022; B.A. Huber and A.S. Michelotto leg.; CHNUFPI 9128.

Paratypes

BRAZIL – **Bahia** • 3 ♂♂, 9 ♀♀; same collection data as for holotype; CHNUFPI 9129 • 3 ♂♂, 3 ♀♀; same collection data as for holotype; CHNUFPI 9130 [deposited in ZFMK Ar 24712].

Other material examined

BRAZIL – **Bahia** • 1 ♂, 6 ♀♀, in pure ethanol; same collection data as for holotype; CHNUFPI 9131 [deposited in ZFMK Br22-255] (voucher of UH510) • 2 ♀♀; between Ibó and Curaçá, Serra do Furtuoso; 8.6420° S, 39.5266° W; 390 m a.s.l.; 2 Dec. 2022; B.A. Huber and A.S. Michelotto leg.; CHNUFPI 9132 • 1 ♀, in pure ethanol; same collection data as for preceding; CHNUFPI 9133 [deposited in ZFMK Br22-256a] (voucher of UH511) • 6 ♂♂, 12 ♀♀; S of Curaçá; 9.2571° S, 39.8163° W; 390 m a.s.l.; 3 Dec. 2022; B.A. Huber and A.S. Michelotto leg.; CHNUFPI 9134 • 1 ♂, 7 ♀♀, in pure ethanol; same collection data as for preceding; CHNUFPI 9135 [deposited in ZFMK Br22-258] (voucher of UH513, G64) • 7 ♂♂, 19 ♀♀; N of Poço de Fora; 9.588° S, 39.787° W; 450–490 m a.s.l.; 3 Dec. 2022; B.A. Huber and A.S. Michelotto leg.; CHNUFPI 9136–9137 • 2 ♂♂, 2 ♀♀; same collection data as for preceding; CHNUFPI 9138 [deposited in ZFMK Ar 24713] • 2 ♂♂, 11 ♀♀, in pure ethanol;

same collection data as for preceding; CHNUFPI 9139 [deposited in ZFMK Br22-260] (voucher of UH110) • 1 ♂, 1 ♀; SE of Juazeiro; 9.5512° S, 40.4408° W; 400 m a.s.l.; 29 Nov. 2022; B.A. Huber and A.S. Michelotto leg.; CHNUFPI 9140 • 2 ♀♀, in pure ethanol; same collection data as for preceding; CHNUFPI 9141 [deposited in ZFMK Br22-242] • 9 ♂♂, 4 ♀♀; N of Senhor do Bonfim; 10.1515° S, 40.2297° W; 630 m a.s.l.; 29 Nov. 2022; B.A. Huber and A.S. Michelotto leg.; CHNUFPI 9142 • 1 ♂, 5 ♀♀, in pure ethanol; same collection data as for preceding; CHNUFPI 9143 [deposited in ZFMK Br22-241] (voucher of UH503) • 7 ♂♂, 8 ♀♀ (3 males used for karyotype analysis); 9 km W of Andorinha; 10.3650° S, 39.9114° W; 440 m a.s.l.; 28 Nov. 2022; B.A. Huber and A.S. Michelotto leg.; CHNUFPI 9144 • 2 ♂♂, 2 ♀♀; same collection data as for preceding; CHNUFPI 9145 [deposited in ZFMK Ar 24714] • 2 ♂♂, 7 ♀♀, in pure ethanol; same collection data as for preceding; CHNUFPI 9146 [deposited in ZFMK Br22-240] (voucher of UH502). – **Ceará** • 1 ♂, 1 ♀; SE of Nova Olinda; 7.1457° S, 39.6331° W; 770 m a.s.l.; 1 Dec. 2022; B.A. Huber and A.S. Michelotto leg.; CHNUFPI 9156 [deposited in ZFMK Ar 24717]. – **Pernambuco** • 8 ♂♂, 28 ♀♀; W of Orocó; 8.6157° S, 39.6316° W; 370 m a.s.l.; 30 Nov. 2022; B.A. Huber and A.S. Michelotto leg.; CHNUFPI 9147 • 4 ♂♂, 5 ♀♀, in pure ethanol; same collection data as for preceding; CHNUFPI 9148 [deposited in ZFMK Br22-249; 1 ♂, 1 ♀ used for SEM] • 6 ♂♂, 6 ♀♀; NE of Cabrobó; 8.420° S, 39.176° W; 450 m a.s.l.; 2 Dec. 2022; B.A. Huber and A.S. Michelotto leg.; CHNUFPI 9149 • 2 ♂♂, 2 ♀♀; same collection data as for preceding; CHNUFPI 9150 [deposited in ZFMK Ar 24715] • 1 ♂, 4 ♀♀, 1 juv., in pure ethanol; same collection data as for preceding; CHNUFPI 9151 [deposited in ZFMK Br22-254] (voucher of UH509) • 6 ♂♂, 11 ♀♀; NE of Lagoa Grande; 8.9117° S, 40.0547° W; 450 m a.s.l.; 30 Nov. 2022; B.A. Huber and A.S. Michelotto leg.; CHNUFPI 9152 • 1 ♂, 4 ♀♀, in pure ethanol; same collection data as for preceding; CHNUFPI 9153 [deposited in ZFMK Br22-247] • 6 ♂♂, 7 ♀♀; NE of Petrolina; 9.1957° S, 40.3832° W; 440 m a.s.l.; 30 Nov. 2022; B.A. Huber and A.S. Michelotto leg.; CHNUFPI 9154 [deposited in ZFMK Ar 24716] • 2 ♂♂, 8 ♀♀, in pure ethanol; same collection data as for preceding; CHNUFPI 9155 [deposited in ZFMK Br22-244] (voucher of UH103) • 1 ♂; Itacuruba, near Riacho Itacuruba; 8.7874° S, 38.6983° W; 310 m a.s.l.; 2014; S.C. Sousa leg.; CHNUFPI 4189.

Fig. 42. *Kambiwa ibo* Huber sp. nov., paratype, ♂, from Brazil, Bahia, S of Ibó, ZFMK Ar 24712. Left palp, prolateral, dorsal, and retrolateral views. Scale line = 0.2 mm.

Material assigned tentatively (see Variation and Barcoding sections below)

BRAZIL – **Bahia** • 5 ♂♂, 8 ♀♀; NW of Ibipeba; 11.540° S, 42.170° W; 590–640 m a.s.l.; 22 Nov. 2022; B.A. Huber and A.S. Michelotto leg.; CHNUFPI 9157 • 1 ♂, 7 ♀♀, in pure ethanol; same collection data as for preceding; CHNUFPI 9158 [deposited in ZFMK Br22-207] (voucher of UH496) • 5 ♂♂, 8 ♀♀; S of Xique-Xique, 'loc. 1'; 11.1196° S, 42.7376° W; 420 m a.s.l.; 23 Nov. 2022; B.A. Huber and A.S. Michelotto leg.; CHNUFPI 9159 [deposited in ZFMK Ar 24718] • 1 ♂, 7 ♀♀, 2 juvs, in pure ethanol; same collection data as for preceding; CHNUFPI 9160 [deposited in ZFMK Br22-217] (voucher of UH087) • 2 ♂♂; S of Xique-Xique, 'loc. 2'; 11.0870° S, 42.7313° W; 410 m a.s.l.; 24 Nov. 2022; B.A. Huber and A.S. Michelotto leg.; CHNUFPI 9161 • 1 ♀, in pure ethanol; same collection data as for preceding; CHNUFPI 9162 [deposited in ZFMK Br22-218] • 2 ♂♂, 7 ♀♀; S of Xique-Xique, 'loc. 3'; 11.0398° S, 42.7311° W; 430 m a.s.l.; 24 Nov. 2022; B.A. Huber and A.S. Michelotto leg.; CHNUFPI 9163 • 10 ♀♀, in pure ethanol; same collection data as for preceding; CHNUFPI 9164 [deposited in ZFMK Br22-219] • 1 ♂; NW of Gameleira do Assuruá; 11.1942° S, 42.7165° W; 640 m a.s.l.; 23 Nov.

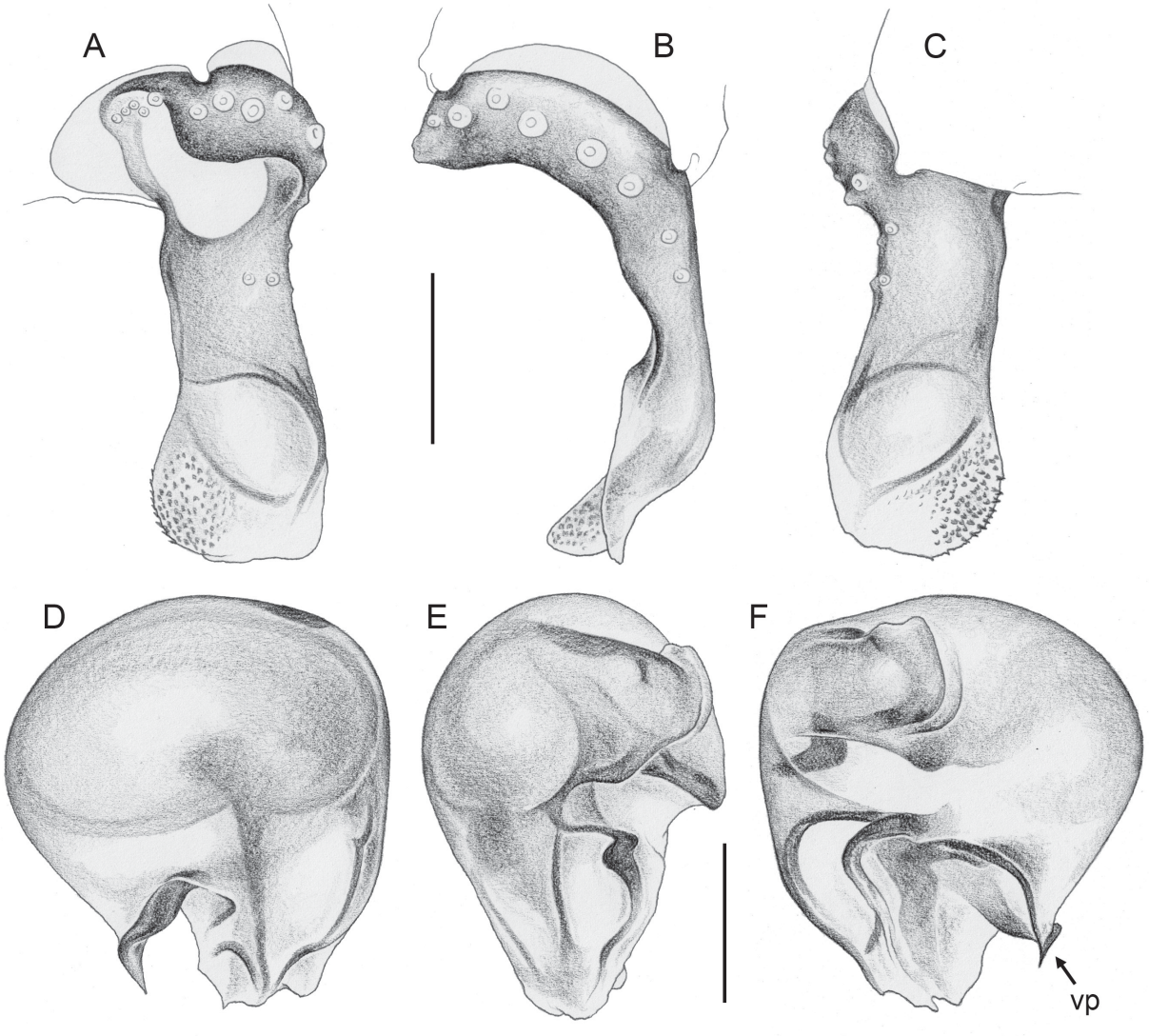

Fig. 43. *Kambiwa ibo* Huber sp. nov., paratype, ♂, from Brazil, Bahia, S of Ibó, ZFMK Ar 24712. **A–C**. Left palpal tarsus and procursus, prolateral, dorsal, and retrolateral views. **D–F**. Left genital bulb, prolateral, dorsal, and retrolateral views. Abbreviation: vp = ventral process. Scale lines = 0.1 mm.

2022; B.A. Huber and A.S. Michelotto leg.; CHNUFPI 9165 [deposited in ZFMK Ar 24719] • 2 ♀♀, in pure ethanol; same collection data as for preceding; CHNUFPI 9166 [deposited in ZFMK Br22-214].

Description

Male (holotype)

Measurements. Total body length 1.30, carapace width 0.53. Distance PME–PME 40 µm; diameter PME 50 µm; distance PME–ALE 25 µm; distance AME–AME 15 µm; diameter AME 30 µm. Leg 1: 2.61 (0.70+0.20+0.66+0.70+0.35), tibia 2: 0.54, tibia 3: 0.52, tibia 4: 0.83; tibia 1 L/d: 9; diameters of leg femora 120 µm, of leg tibiae 70 µm.

Color (in ethanol). Prosoma and legs ochre-yellow to light brown, carapace and legs without darker marks or rings; abdomen ochre-gray with very indistinct internal marks, with light ochre-brown plate in front of gonopore.

Body. Habitus as in Fig. 2C. Ocular area not raised. Carapace without thoracic groove. Clypeus unmodified. Sternum slightly wider than long (0.38/0.35), with small but distinct anterior humps near coxae 1 (~30 µm high, 50 µm diameter at basis). Abdomen globular.

Chelicerae. As in Fig. 44A–B; with pair of small frontal apophyses; stridulatory files very fine and poorly visible in dissecting microscope.

Palps. As in Fig. 42; coxa unmodified; trochanter ventrally slightly protruding; femur proximally with small ventral process, distally widened but otherwise unmodified; femur-patella condyles and tibia-tarsus condyles not shifted toward one side; tarsus with strong prolateral rim slightly protruding; procursus (Fig. 43A–C) wide in lateral view, narrower in dorsal view, with large transparent distal flap bent towards prolateral and set with numerous tiny spikes; genital bulb (Fig. 43D–F) with very short but complex distal process composed of membranous and sclerotized elements, with short and pointed, slightly twisted ventral process, with barely recognizable retrolateral-dorsal process.

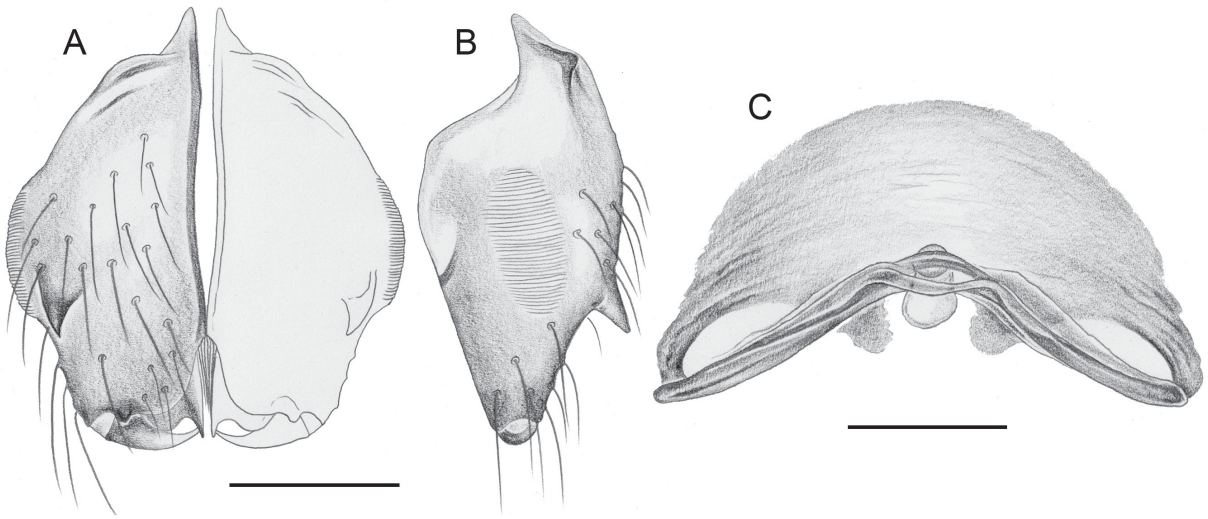

Fig. 44. *Kambiwa ibo* Huber sp. nov., paratypes, ♂♀, from Brazil, Bahia, S of Ibó, ZFMK Ar 24712. **A**–**B**. Male chelicerae, frontal and lateral views. **C**. Cleared female genitalia, dorsal view. Scale lines = 0.1 mm.

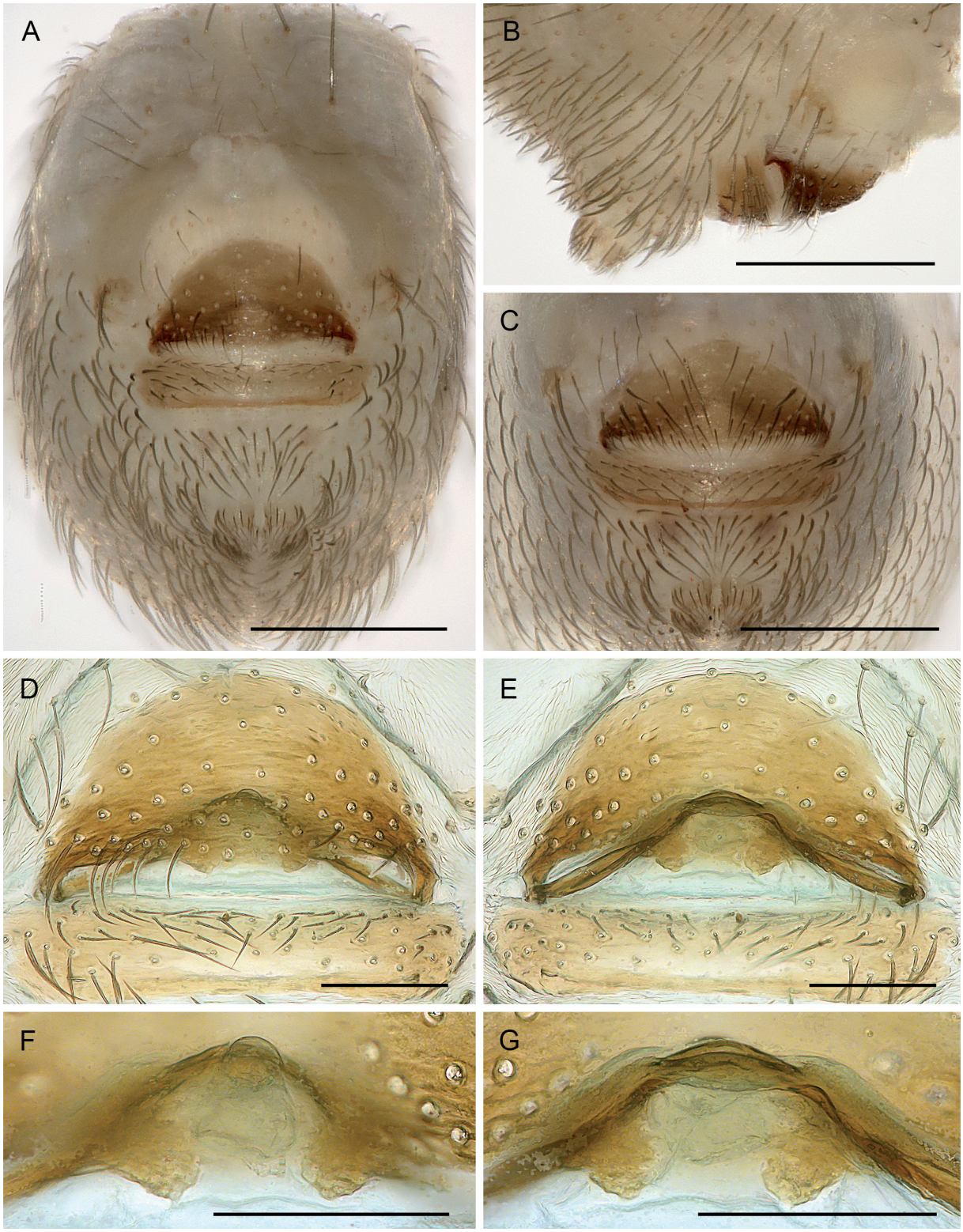

Fig. 45. *Kambiwa ibo* Huber sp. nov. **A–B, D–G**. Paratype, ♀, from Brazil, Bahia, S of Ibó, ZFMK Ar 24712. **C**. ♀, from Bahia, N of Senhor do Bonfim, CHNUFPI 9142. **A–B**. Abdomen, ventral and lateral views. **C**. Epigynum, ventral view. **D–E**. Cleared genitalia, ventral and dorsal views. **F–G**. Central element of internal genitalia, ventral and dorsal views. Scale lines: A–C = 0.3 mm; D–G = 0.1 mm.

Legs. Without spines, without curved hairs; with short vertical hairs on tibia 1; retrolateral trichobothrium of tibia 1 at 62%; prolateral trichobothrium absent on tibia 1; tarsus 1 with ~4–5 pseudosegments, distally fairly distinct.

Variation (males)

Tibia 1 in 83 males: 0.56–0.72 (mean 0.650). Males from southwestern localities (near Ibipeba, Xique-Xique, and Gameleira do Assuruá) tend to be minimally smaller than males from all other localities (mean tibia 1 length: 0.625 vs 0.655) but otherwise they appear morphologically indistinguishable. See Barcoding section below.

Females

In general similar to males (Fig. 2D) but sternum without anterior humps and tibia 1 without vertical hairs; chelicerae apparently without stridulatory files (not confirmed with SEM). Tibia 1 in 137 females: 0.56–0.72 (mean 0.639). Females from southwestern localities (near Ibipeba, Xique-Xique, and Gameleira do Assuruá) tend to be minimally smaller than females from all other localities (mean tibia 1 length: 0.616 vs 0.643) but otherwise they appear morphologically indistinguishable. Epigynum (Fig. 45A–C) anterior plate semicircular, weakly protruding, with pair of lateral posterior sclerites; internal transversal sclerite often visible in uncleared specimens; posterior plate large but simple, roughly rectangular. Internal genitalia (Figs 44C, 45D–G) with curved transversal sclerite connected laterally to lateral posterior sclerites of anterior epigynal plate, medially with small membranous sac; posteriorly with pair of sclerotized plates connected to transversal sclerotized element, apparently without pore plates.

Barcoding

Ten specimens were barcoded: eight from northeastern localities (including the type locality), and two from southwestern localities (Fig. 14). Among northeastern localities (maximal geographic distance: 225 km), K2P distances mostly ranged from 0.0% to 0.6% (Table 2); only the specimen from west of Andorinha had a higher distance to other northeastern specimens: 5.3–5.6%. The two southwestern specimens (geographic distances to northeastern specimens: 260–500 km) had much higher genetic distances to northeastern specimens: 10.0–12.9%. Even between the two southwestern specimens (geographic distance: 78 km), the K2P distance was high: 9.6%.

Distribution

Known from numerous localities in Bahia, Pernambuco and Ceará, Brazil (Fig. 14). Specimens were collected at a higher mean altitude (460 ± 120 m, n = 18; see Fig. 83) compared to congeners with broader distributions, being significantly higher than that of *K. neotropica* (145 ± 131 m, n = 14), and not differing statistically from *K. coribe* Huber sp. nov. (374 ± 273 m, n = 13).

Natural history

This species was found in a range of microhabitats (Fig. 12). At the type locality, a degraded thorny roadside shrubland dominated by bushes and grasses (Fig. 12A), most specimens were beaten out of pieces of dead wood. They ran rapidly but stopped suddenly as soon as they encountered a small piece of 'dirt' for hiding. Between Ibó and Curaçá, the spiders were collected under stones on a rocky hillside with thorny shrubs. West of Andorinha, they were found under stones lying on a large flat rock plate (Fig. 12B); several specimens sometimes shared one stone. North of Senhor do Bonfim, they were collected on a dry hillside at the margin of a cactus plantation, under small stones in the plain sun; upon moving the stones, they started to run rapidly. Northeast of Petrolina, they were found under stones on a rock outcrop (Fig. 12C) and in the neighboring thorny woodland; upon turning the stones, the spiders usually stayed on the ground (rather than on the stone) and often did not move, making them barely visible. Northeast of Lagoa Grande, they were found in a highly degraded thorny shrubland (Caatinga) (Fig. 12D) with cattle; they were very abundant under stones and small rocks. West of Orocó, they were found in a well-preserved thorny shrubland (Caatinga), in very high abundance (often three or four

specimens on one stone). Northeast of Cabrobó, they were found on a rock outcrop with scattered shrubs, under stones on bare rock, together with *Ibotyporanga sertao* Huber, 2024. South of Curaçá they were found under stones in a degraded roadside shrubland. North of Poço de Fora, they were abundant under stones and in dead wood on a hill with shrubs and scattered trees. Southeast of Juazeiro they were found under small stones in the plain sun in a degraded roadside shrubland. Specimens assigned tentatively occupied a similar range of habitats. Northwest of Ibipeba, they were found on a semiarid hillside with scattered trees and thorny shrubs, mostly in leaf litter, but also on the underside of rocks. South of Xique-Xique 'site 1', they were found in a flat area dominated by rocks on white sand (Fig. 12E); they lived in the thin layer of organic material between stone and sand; upon disturbance, they ran extremely fast but then stopped abruptly and became almost invisible. South of Xique-Xique 'site 2' they were found

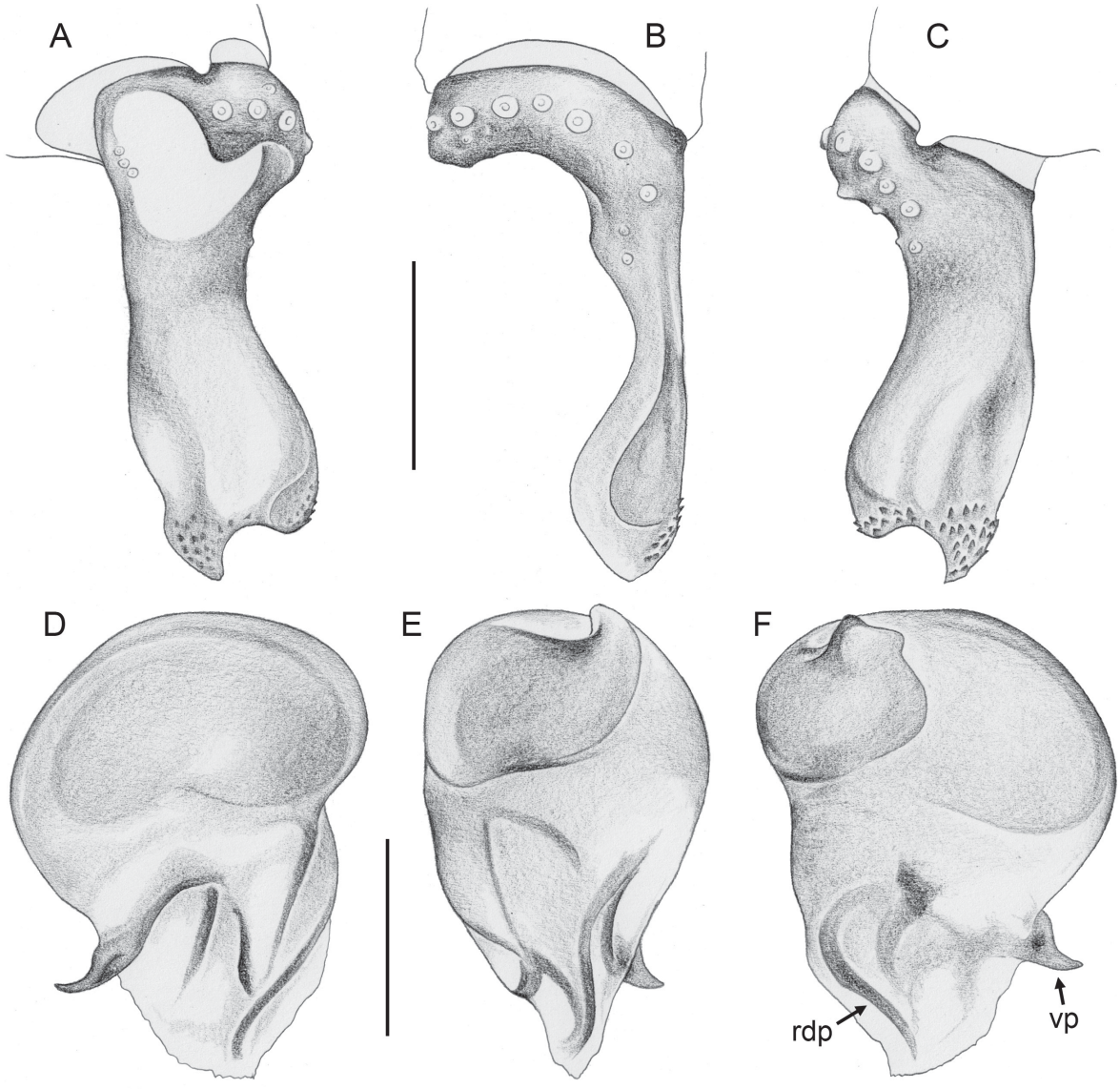

Fig. 46. *Kambiwa sapo* (Huber, 2019) comb. nov., ♂, from Venezuela, Bolívar, Canaima, ZFMK Ar 20621. **A–C**. Left palpal tarsus and procursus, prolateral, dorsal, and retrolateral views. **D–F**. Left genital bulb, prolateral, dorsal, and retrolateral views. Abbreviations: rdp = retrolateral-dorsal process; vp = ventral process. Scale lines = 0.1 mm.

under small stone pebbles lying on the soil in the plain sun in thorny shrubland. South of Xique-Xique 'site 3' they were found under stones lying on a large rock plate in the plain sun, near thorny shrubs and scattered trees (Fig. 12F). Northwest of Gameleira do Assuruá, the spiders were found on a rock outcrop with thorny shrubs and trees. 26 egg sacs contained 6–14 eggs each (mean 9.6) and were flat (all eggs in a single layer); egg diameter was 0.44–0.49.

Kambiwa sapo (Huber, 2019) comb. nov.
Figs 46–47

Pemona sapo Huber in Huber & Carvalho, 2019: 34, figs 114–122.

Gen.n. Ven01 – Eberle *et al.* 2018 (molecular data). — Huber *et al.* 2018: fig. 2.

Diagnosis

Males are distinguished from those of most known congeners (except *K. ibo* sp. nov.) by shape of ventral bulbal process (Fig. 46D, F; short and pointed, slightly twisted), by tip of procursus (Fig. 46A–C; mostly membranous, set with numerous tiny spikes), and by male cheliceral apophyses relatively far apart (cf. Fig. 44A; see also Huber & Carvalho 2019: fig. 119); from *K. ibo* by bifid tip of procursus (rather than simple rounded), by absence of distinct separation between distal membranous part of procursus and proximal sclerotized part, by genital bulb slightly more elongate rather than rounded and with slightly different sclerotized elements (compare Figs 43D–F and 46D–F), and by smaller palp (tibia length/width: 180/140 µm, vs 230/180 µm in *K. ibo*; femur length: 190 µm, vs 250 µm in *K. ibo*). Females are externally very similar to those of several congeners (e.g., *K. neotropica*; *K. coribe* sp. nov.; *K. maracas* sp. nov.; *K. brumado* sp. nov.; *K. mucuge* sp. nov.; *K. ibo*); they differ by internal genitalia without distinct median modification (Fig. 47; see also Huber & Carvalho 2019: figs 121–122).

Type material

Holotype

VENEZUELA – **Bolívar** • ♂; Canaima, forest near Salto El Sapo; 6.254° N, 62.848° W; 400 m a.s.l.; 9 Dec. 2002; B.A. Huber leg.; ZFMK Ar 20620.

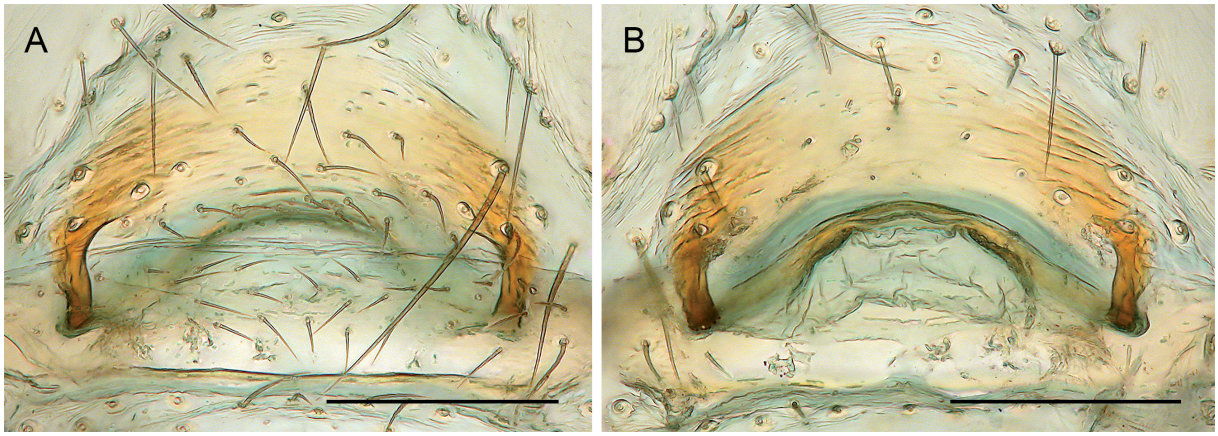

Fig. 47. *Kambiwa sapo* (Huber, 2019) comb. nov.; ♀, from Venezuela, Bolívar, Canaima, ZFMK Ar 20621. **A**–**B**. Cleared genitalia, ventral and dorsal views. Scale lines = 0.1 mm.

Remarks

A reanalysis of topotypical material (ZFMK Ar 20621) shows that the retrolateral-dorsal process on the genital bulb distinctive for *Kambiwa* is also present in *K. sapo* even though indistinct (Fig. 46F). The female genitalia are in several respects very similar to other species of *Kambiwa* (semicircular epigynal plate with strong lateral sclerites extending posteriorly; lateral sclerites connected to internal transversal element). However, a median internal process or sac seems to be absent (Fig. 47B).

The coordinates published in Huber & Carvalho (2019) are slightly wrong. The collecting site was 1.4 km further north, at 6.254° N, 62.848° W.

Genus ***Sertana*** Huber gen. nov.
urn:lsid:zoobank.org:act:8D1E1801-AD95-48B2-9783-E031B60D08FA

Type species

Sertana igapora Huber gen. et sp. nov.

Diagnosis

Small short-legged pholcids with eight eyes and globular abdomen (Fig. 48), similar in size and body shape to closely related South American Ninetinae (*Guaranita*, *Galapa*, *Kambiwa*). Males are distinguished from these by pair of distinctive ventral processes on genital bulb, one rather pointed, the other rather rounded (e.g., Figs 59E, 63E, 67E; *Kambiwa* with single ventral process; *Galapa spiniphila* also with pair of small pointed ventral processes), and by absence of processes on sternum; from *Galapa* also distinguished by unmodified cheliceral fangs, presence of pair of apophyses on main cheliceral segments (e.g., Figs 60A, 64A), and absence of sclerotized retrolateral process on procursus; from *Galapa* and *Guaranita* also by absence of dorsal flap on procursus (present only in *S. bumba* Huber gen. et sp. nov.; some species with retrolateral membrane that might also be homologous to dorsal flap of *Galapa* and *Guaranita*); from *Guaranita* also by absence of ventral membrane on procursus; from *Kambiwa* also distinguished by much longer male cheliceral apophyses (compare Figs 17B, 23B, 36B with 60B, 64B, 68B), and by main branch of procursus slender and sclerotized in lateral view (wide and partly membranous in *Kambiwa*). Females are morphologically barely distinguishable from females of *Guaranita*, *Galapa*, and *Kambiwa*, but anterior epigynal plate without or with weak lateral posterior sclerites (e.g., Figs 60C, 64C; *Guaranita* and *Kambiwa* with strong lateral posterior sclerites).

Etymology

The genus name is derived from "sertão", the Brazilian backlands, home of the known species. Due to regular draughts, this region is economically poor, yet particularly rich in history and folklore. Gender feminine.

Description

Males

Measurements. Total body length 0.9–1.4; carapace width 0.4–0.7. PME diameter 40–60 μm; AME diameter 20–35 μm. Leg 1 length 2.1–3.3; tibia 1 length 0.5–0.9; metatarsus 1 approximately same length as tibia 1 (metatarsus 1 / tibia 1 length: 0.93–1.10); tibia 4 longer than tibia 1 (tibia 4 / tibia 1 length: 1.2–1.4); leg femora diameters 85–145 μm; leg tibiae diameters 50–75 μm. Tibia 1 L/d 9–12.

Color. In ethanol mostly ochre-yellow to light brown, carapace without darker marks or with indistinct darker lateral borders, legs without dark rings; abdomen usually pale gray with darker internal marks dorsally and laterally; ventrally with light ochre to brown plate in front of gonopore. Live specimens sometimes with slightly reddish prosoma and shiny brown or black abdomen (Fig. 48).

Body. Habitus as in Fig. 48. Ocular area not or slightly raised. Carapace without thoracic groove (Fig. 49A–B). Clypeus unmodified. Sternum barely wider than long, without pair of anterior processes near coxae 1. Abdomen globular. Gonopore either with four epiandrous spigots (Fig. 49C–D) or without spigots (Fig. 49E). General arrangement of spinnerets as usual in Pholcidae (Fig. 50A, C); ALS with seven spigots each (Fig. 50): one strongly widened spigot, one long and slender spigot, and five cylindrical spigots (of which one is much wider than the others); PMS with two short conical spigots; PLS with strong hairs but without spigots.

Chelicerae. With pair of relatively long frontal apophyses (e.g., Figs 60B, 64B; longer than in *Kambiwa*). Stridulatory files mostly fine but distinct (Fig. 51C), very indistinct in *S. igapora* gen. et sp. nov. (Fig. 51A; not visible in dissecting microscope), with ~25–30 ridges, distances between ridges (in three species studied with SEM) 2.3–2.7 µm, distances between ridges homogeneous throughout file.

Palps. Coxa unmodified; trochanter with indistinct ventral protrusion; femur proximally without or with indistinct retrolateral protrusion, distally slightly widened but otherwise unmodified; femur-patella condyles not or slightly shifted toward prolateral side; tibia almost globular, with two trichobothria; tibia-tarsus condyles not or slightly shifted toward retrolateral side; palpal tarsal organ capsulate with small opening (Fig. 52C–E), strongly elevated (approximately twice as high as diameter), outer diameter 5–8 µm, opening diameter 0.7–0.9 µm; procursus relatively small and simple, sclerotized main branch bent towards dorsal, in some species covered retrolaterally by large membranous flap (Figs 51E–F, 59C, 63C), in *S. bumba* gen. et sp. nov. with small dorsal transparent flap (Figs 52A, 72C); genital bulb with proximal sclerite connecting to tarsus; bulbous part of genital bulb with two distinctive ventral processes,

Fig. 48. *Sertana* Huber gen. nov., live specimens from Brazil; all at same scale. **A**–**B**. *S. igapora* Huber gen. et sp. nov., ♂, from SE of Bom Jesus and ♀ with egg sac from W of Bom Jesus. **C**–**D**. *S. sagarana* Huber gen. et sp. nov., ♂♀ with egg sac from SW of São Felix do Coribe. **E**–**F**. *S. lapa* Huber gen. et sp. nov., ♂♀ with egg sac from SE of Bom Jesus.

one rather pointed and variably long, the other rather rounded and mostly short (e.g., Figs 59E, 63E, 67E); dorsal bulbal process with sclerotized and membranous elements, presumably carrying sperm duct opening hidden between membranous folds (cf. Fig. 52B).

Legs. Without spines; without curved hairs. Usually with sexually dimorphic short vertical hairs on tibia 1 or tibia 1+tibia 2 (Fig. 53D–G), only in *S. sagarana* gen. et sp. nov. apparently without such hairs (not studied with SEM); base diameter 5.0–6.5 µm, length 15–20 µm, diameter at half-length 0.7–1.1 µm. Distal leg segments (tarsi and metatarsi) with putative chemoreceptors (Fig. 54E–H), in light microscope

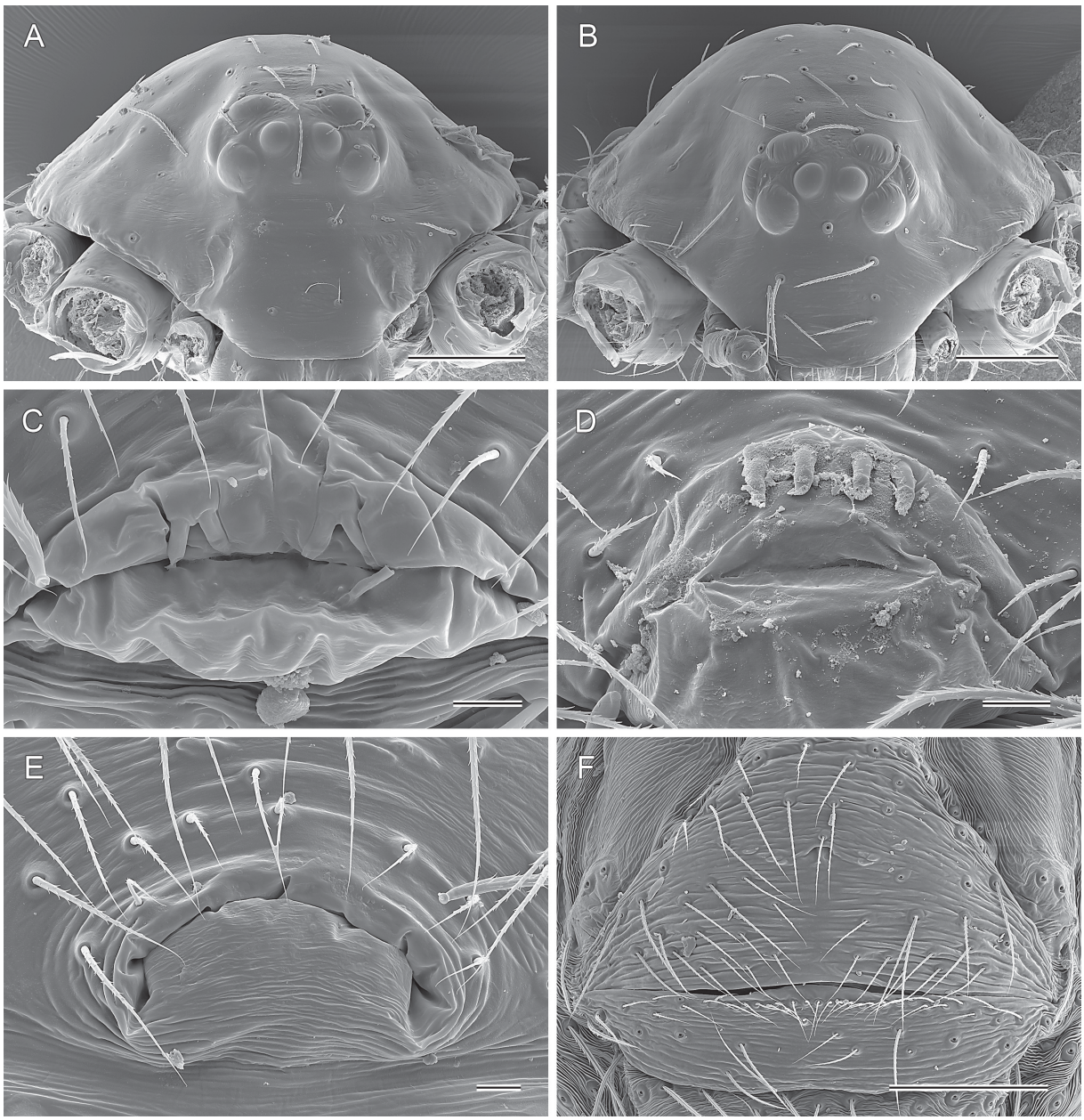

Fig. 49. Species of *Sertana* Huber gen. nov., prosoma, male gonopore, and epigynum. **A**–**B**. *S. igapora* Huber gen. et sp. nov., male and female prosomata, frontal views. **C**. *S. igapora*, male gonopore. **D**. *S. bumba* Huber gen. et sp. nov., male gonopore. **E**. *S. lapa* Huber gen. et sp. nov., male gonopore. **F**. *S. igapora*, epigynum, ventral view. Scale lines: A–B, F = 100 µm; C–E = 10 µm.

similar to sexually dimorphic short 'vertical' hairs but with one or two distal side branches, with one or two oblique furrows, and flattened distally (i.e., with oval diameter); base diameter 4.0–4.5 µm, length 15–20 µm, diameter proximally 1.5–1.8 µm. Rimmed pores (Fig. 54A–B) at regular intervals especially dorsally on tibiae, metatarsi, and tarsi; outer diameter 2.8–3.2 µm; opening diameter: 0.2–0.5 µm. Femora, tibiae, metatarsi, and tarsi with round or oval cuticular plates (Fig. 54C–D) at regular intervals, diameter ~4.5–6.0 µm. Base of trichobothria round or with pair of indistinct lateral humps (Fig. 53A–C);

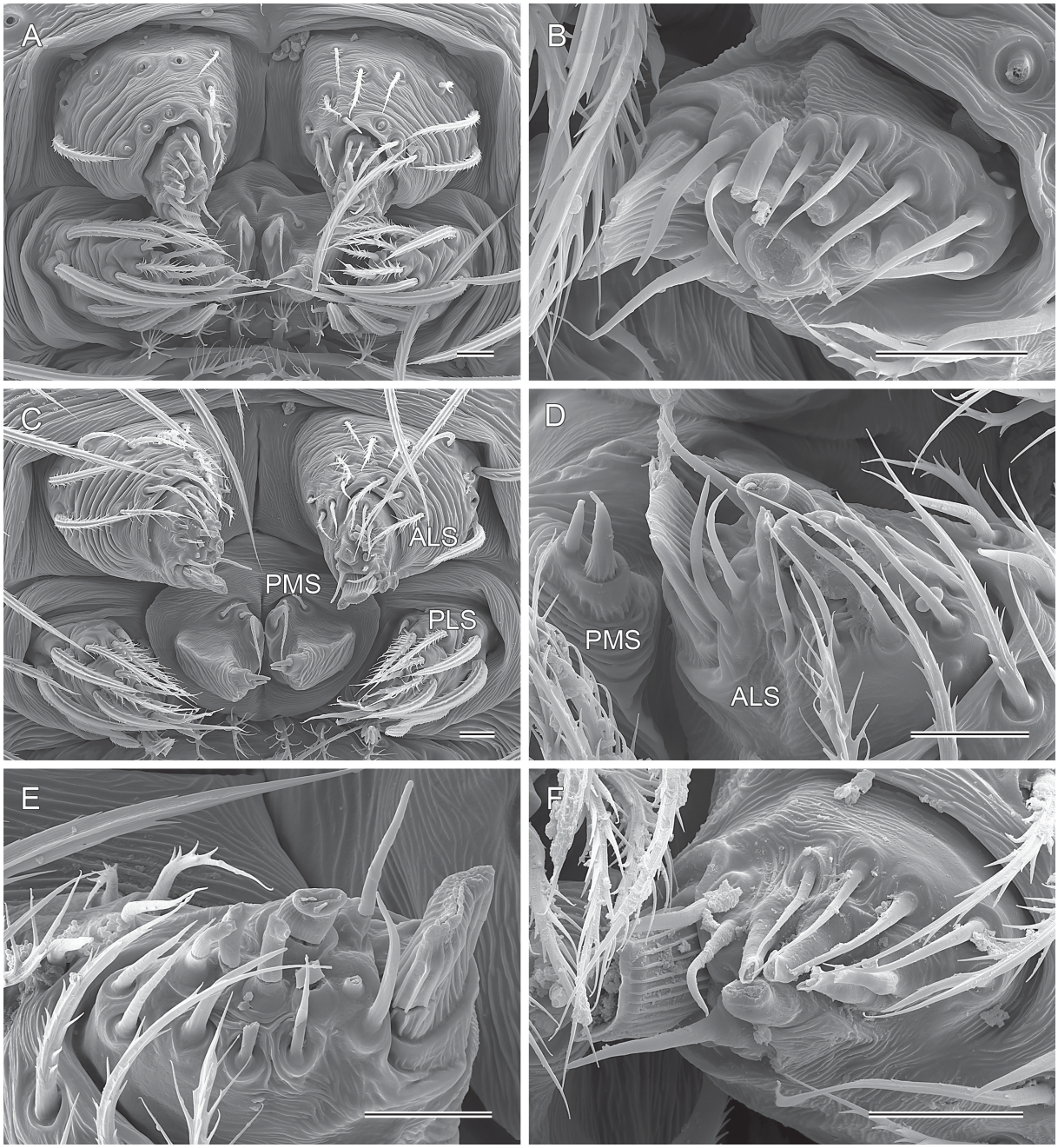

Fig. 50. Species of *Sertana* Huber gen. nov., spinnerets. **A**–**B**. *S. igapora* Huber gen. et sp. nov., female spinnerets and female ALS. **C**. *S. lapa* Huber gen. et sp. nov., male spinnerets. **D**. *S. lapa*, female ALS and PMS. **E**. *S. lapa*, male ALS. **F**. *S. bumba* Huber gen. et sp. nov., male ALS. Scale lines = 10 µm.

outer diameter of base: 10–14 µm; proximal diameter of seta: 0.8–1.1 µm; retrolateral trichobothrium on tibia 1 at 55–62% of tibia length; prolateral trichobothrium absent on tibia 1. Without slender metatarsal hairs (as described in Huber *et al.* 2023c, 2024d). Tarsi with 3–5 pseudosegments, variably distinct. Leg tarsal organs capsulate with small opening (Fig. 55A–F), outer diameter 3.5–6.0 µm, opening diameter 0.8–1.0 µm. Tarsus 4 with two comb hairs distally on prolateral side. Tarsal claws as usual for family (Fig. 55G–H); main claws with 9–11 teeth; teeth on tarsus 4 slightly different (shorter and directed more towards distal).

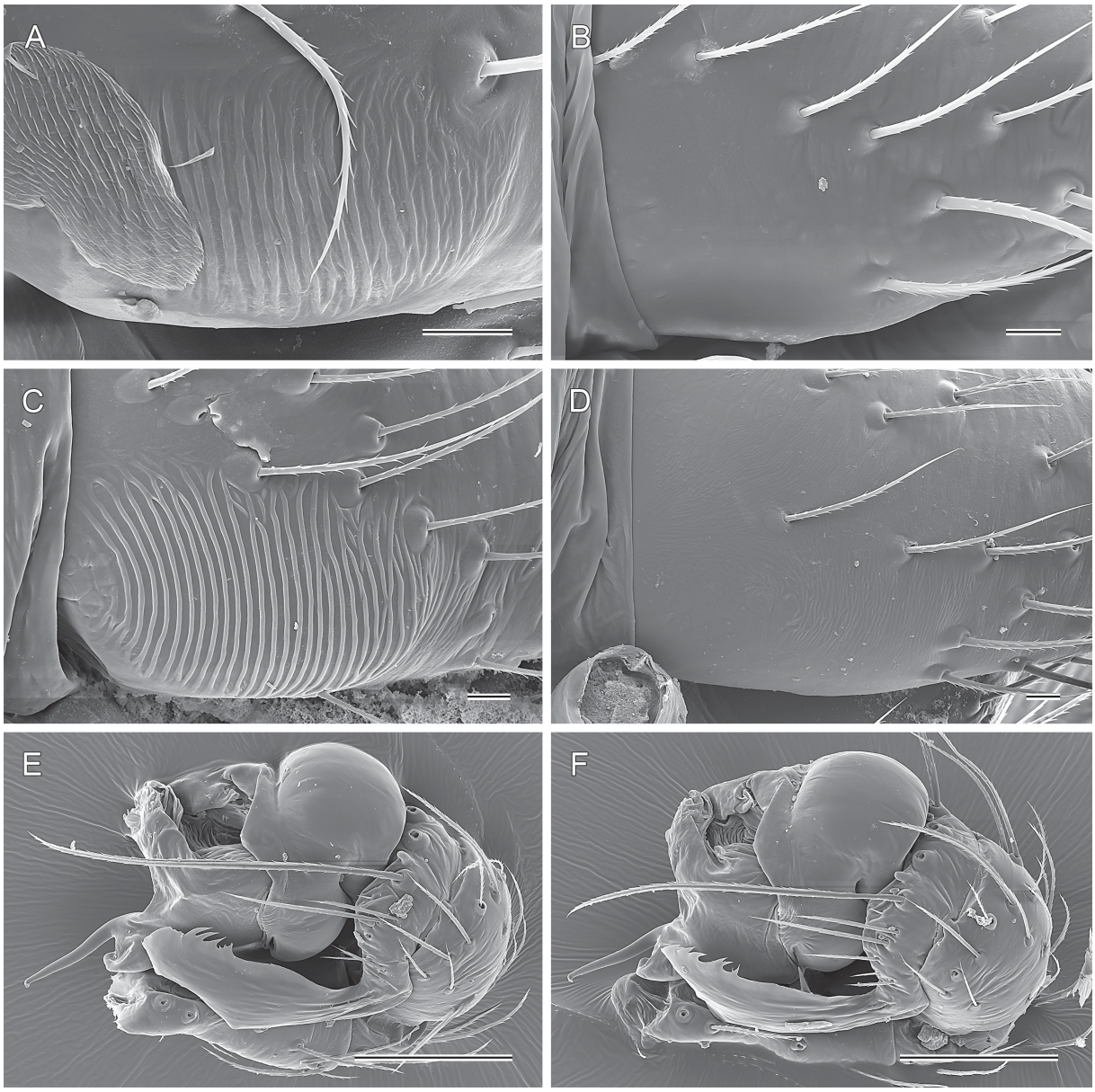

Fig. 51. Species of *Sertana* Huber gen. nov., chelicerae and male palp. **A**–**B**. *S. igapora* Huber gen. et sp. nov., male and female right chelicerae, lateral views. **C**–**D**. *S. lapa* Huber gen. et sp. nov., male and female right chelicerae, lateral views. **E**–**F**. *S. igapora*, male palp, retrolateral and retrolateral-dorsal views. Scale lines: A–D = 10 µm; E–F = 100 µm.

Females

In general, similar to males (Fig. 48), but legs on average slightly shorter than in males (male / female tibia 1 length: 1.0–1.2); chelicerae without stridulatory files (Fig. 51B, D); without sexually dimorphic short vertical hairs on tibiae; coloration sometimes lighter and abdomen less shiny (Fig. 48). Palpal tarsal organ as in males (Fig. 52F), but less elevated, outer diameter 5–6 μm, opening diameter 0.9–1.0 μm. Other sensory organs and comb hairs on tarsus 4 as in males. Spinnerets and spigots as in males (Fig. 50). Tip of palp with simple pointed process (Fig. 52F). Epigynum anterior plate trapezoidal to semicircular,

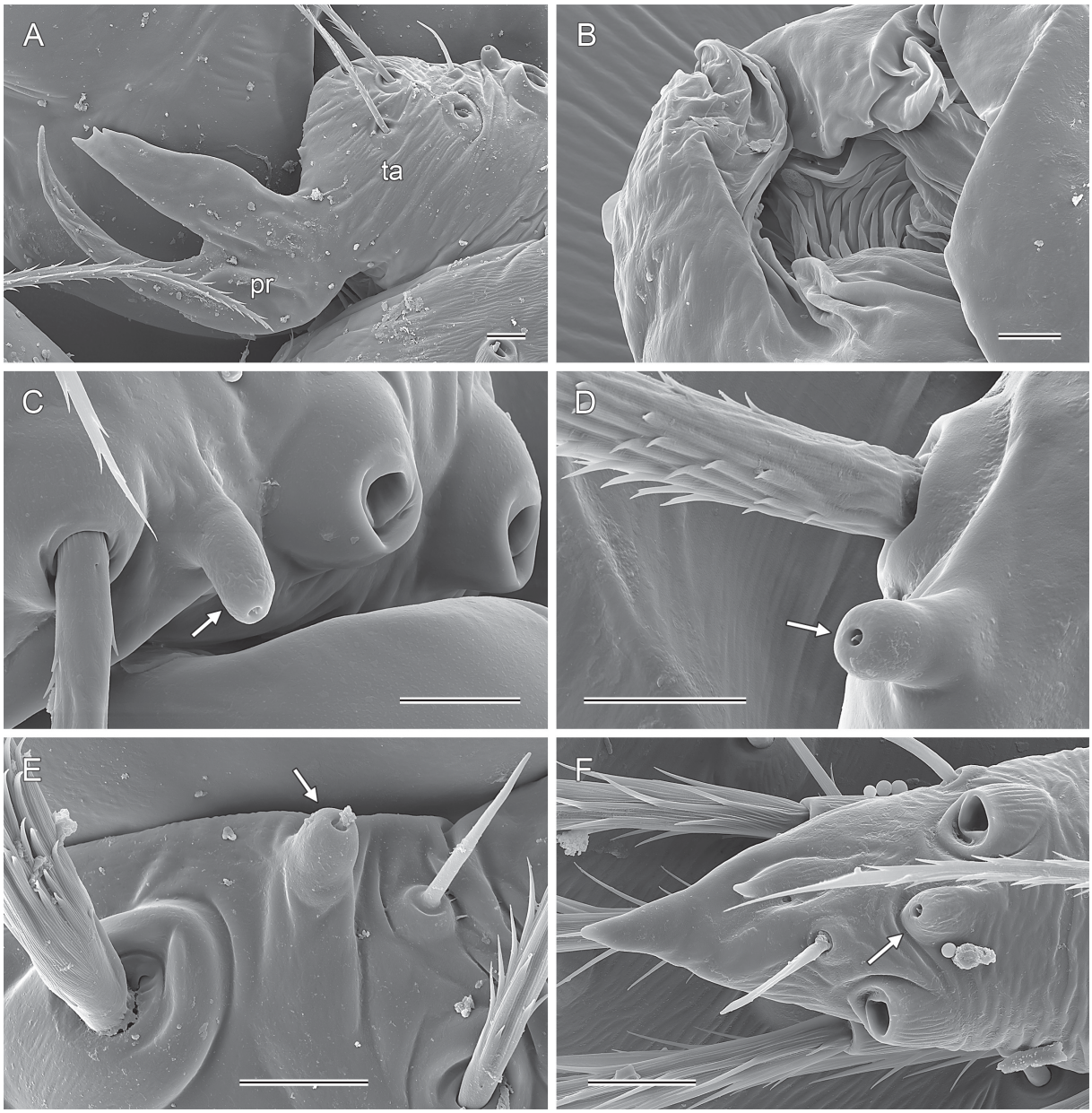

Fig. 52. Species of *Sertana* Huber gen. nov., male and female palps; arrows point at tarsal organs. **A**. *S. bumba* Huber gen. et sp. nov., left male tarsus and procursus, retrolateral view. **B**. *S. igapora* Huber gen. et sp. nov., left male genital bulb, distal part, dorsal view. **C**. *S. igapora*, male palpal tarsal organ. **D**. *S. lapa* Huber gen. et sp. nov., male palpal tarsal organ. **E**. *S. bumba*, male palpal tarsal organ. **F**. *S. lapa*, left female palp tip, dorsal view. Abbreviations: pr = procursus; ta = tarsus. Scale lines = 10 μm.

without pockets or processes (Fig. 49F). Posterior epigynal plate simple, unmodified. Internal genitalia usually with transversal sclerite that is medially complex in some species (Figs 61G, 65E–F, 70G–H), but medially reduced in *S. capivara* Huber gen. et sp. nov. (Fig. 78C, E); some species with membranous anterior sac (e.g., Figs 61D–E, 65D); without or with very small and indistinct pore plates (arrows in Figs 70G, 78C).

Relationships

The latest molecular phylogeny of Pholcidae (Meng *et al.* 2025) includes one representative of *Sertana* gen. nov. (under the name "E074_Ninetinae-Gen?_L21-272_Carv64"; now *S. capivara* gen. et sp. nov.). This species is resolved as sister to *Galapa*, and both together are sister to *Kambiwa* (inset in Fig. 1).

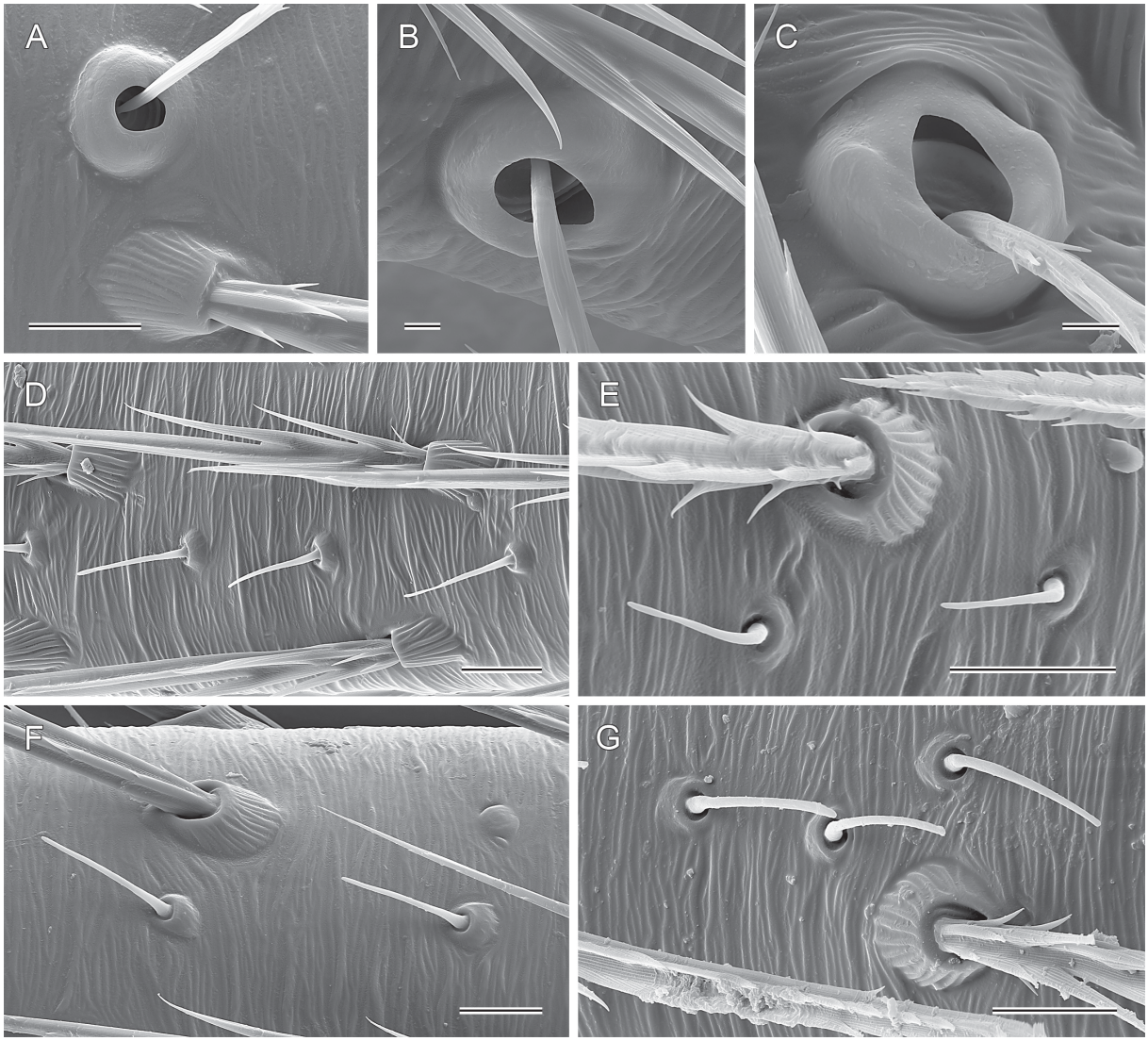

Fig. 53. Species of *Sertana* Huber gen. nov., trichobothria and sexually dimorphic short vertical hairs. **A**. *S. lapa* Huber gen. et sp. nov., left tibia 3, retrolateral trichobothrium. **B**. *S. lapa*, left female metatarsus 1. **C**. *S. igapora* Huber gen. et sp. nov., right male metatarsus 3. **D**–**E**. *S. igapora*, right male tibia 2, prolateral view, and right male tibia 1, prolateral view. **F**. *S. lapa*, left male tibia 1, retrolateral view. **G**. *S. bumba* Huber gen. et sp. nov., left male tibia 1, retrolateral view. Scale lines: A, D–G = 10 μm; B–C = 2 μm.

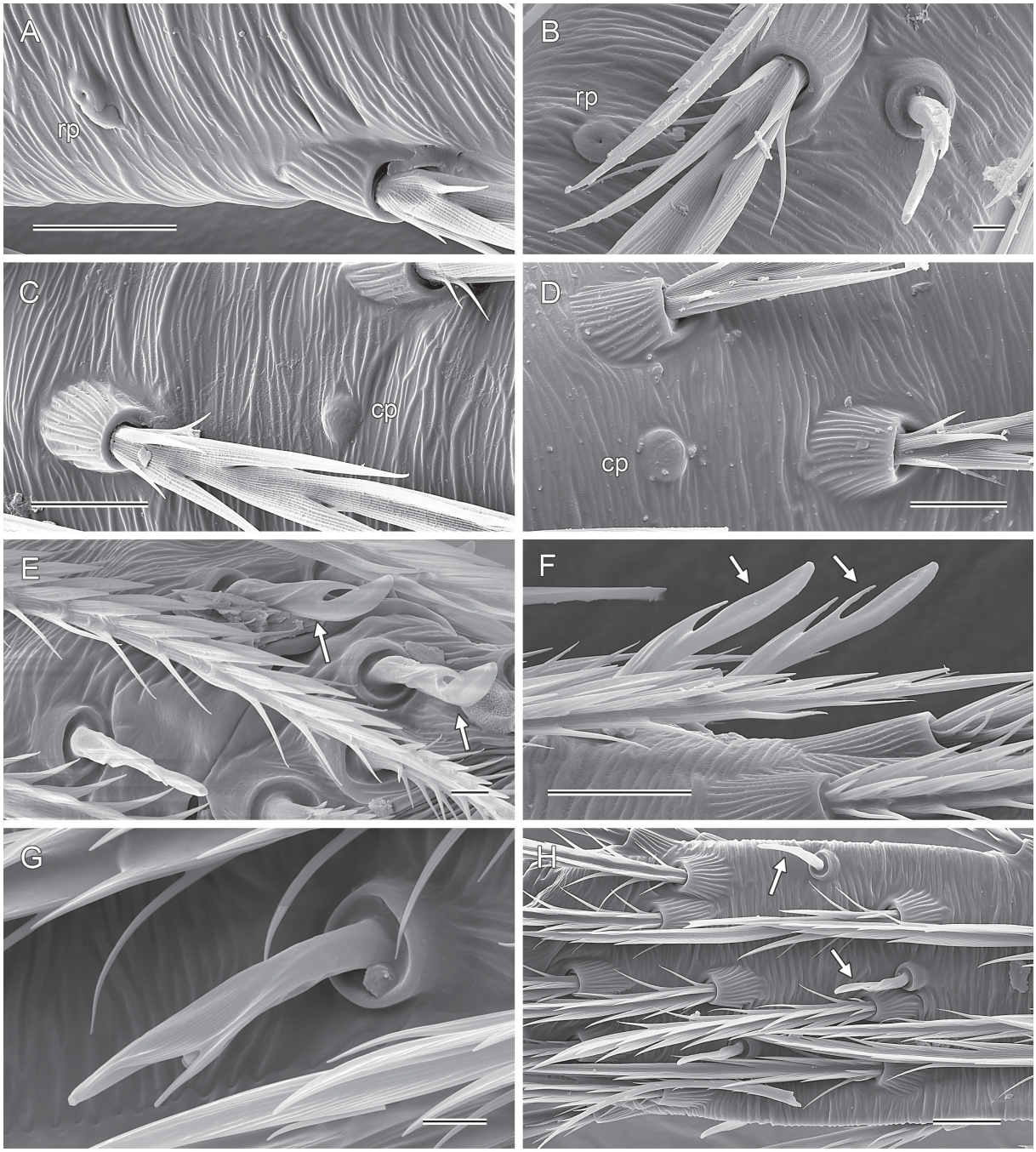

Fig. 54. Species of *Sertana* Huber gen. nov., rimmed pores, cuticular plates, and chemoreceptors (arrows). **A**. *S. igapora* Huber gen. et sp. nov., rimmed pore on left male tibia 3. **B**. *S. bumba* Huber gen. et sp. nov., rimmed pore on right male metatarsus 3. **C**. *S. igapora*, cuticular plate on left male tibia 3. **D**. *S. bumba* Huber gen. et sp. nov., cuticular plate on left male tibia 4. **E**. *S. igapora*, chemoreceptors on right female tarsus 1. **F**. *S. lapa* Huber gen. et sp. nov., chemoreceptors on left male tarsus 1. **G**. *S. igapora*, chemoreceptor on right female tarsus 2. **H**. *S. igapora*, chemoreceptors distally on right female metatarsus 3. Abbreviations: cp = cuticular plate; rp = rimmed pore. Scale lines: A, C–D, F, H = 10 μm; B, E, G = 2 μm.

This topology is confirmed in an upcoming, larger dataset that combines the UCA data of Meng *et al.* (2025) with results from low coverage genome sequencing (G. Meng, L. Podsiadlowski, B.A. Huber, unpubl. data). This dataset includes four species of *Sertana* gen. nov. (*S. igapora* gen. et sp. nov.; *S. lapa* Huber gen. et sp. nov.; *S. sagarana* gen. et sp. nov.; *S. capivara*) and results in maximum support for the monophyly of *Sertana* and for the sister group relationship with *Galapa*.

Natural history

Sertana gen. nov. spiders were found in very similar semiarid habitats as *Kambiwa*, also ranging from flat areas with bushes and grasses to rock outcrops (Fig. 56). They occupied the same ground-level

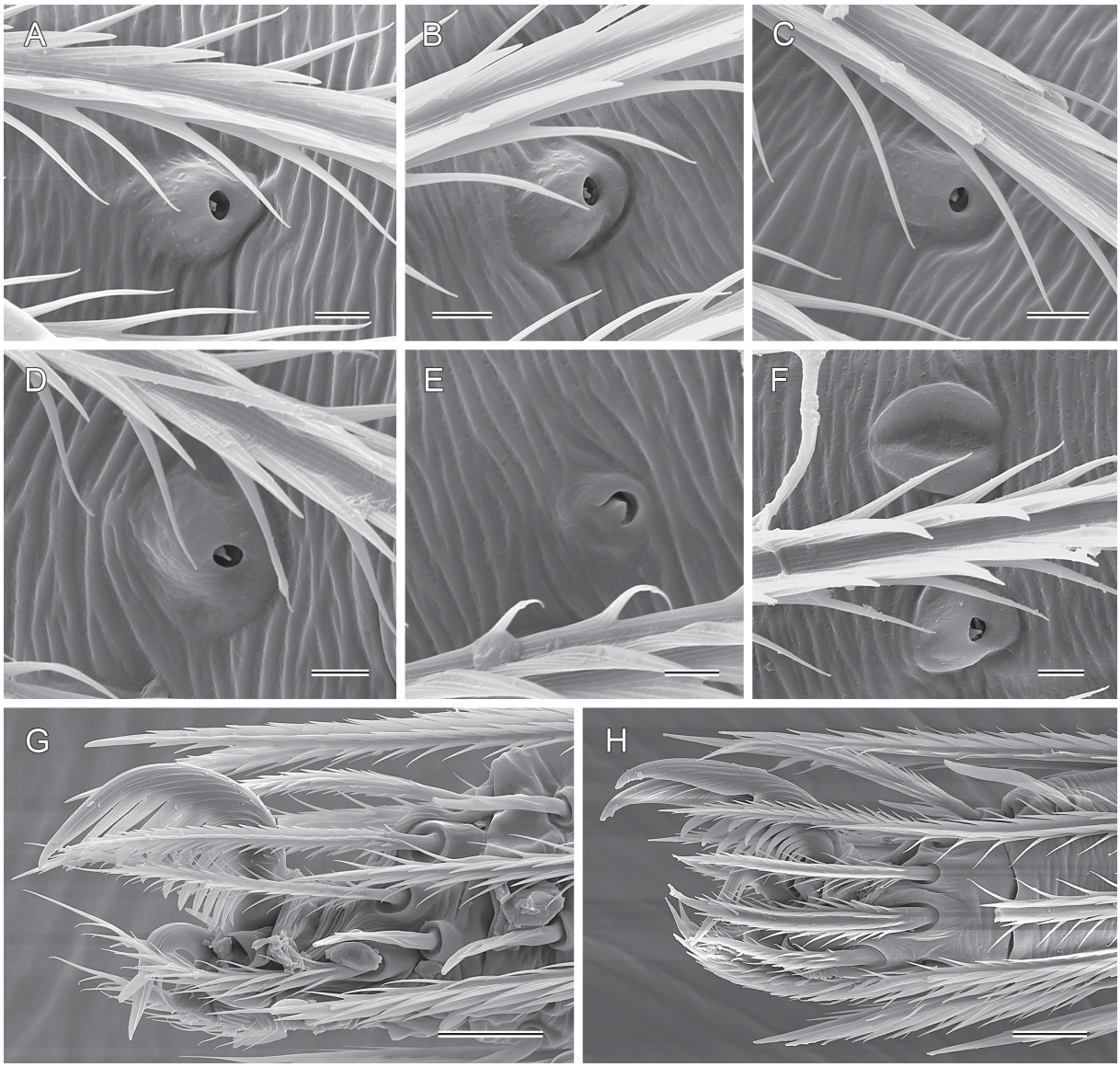

Fig. 55. Species of *Sertana* Huber gen. nov., leg tarsal organs and tips of leg tarsi. **A–C**. *S. igapora* Huber gen. et sp. nov., tarsal organs on female tarsi 1, 2, and 3. **D–E**. *S. lapa* Huber gen. et sp. nov., tarsal organs on female tarsi 2 and 4. **F**. *S. bumba* Huber gen. et sp. nov., tarsal organ (and slit sensillum) on male tarsus 2. **G**. *S. igapora*, right female tarsus 1, prolateral view. **H**. *S. lapa*, left male tarsus 4, retrolateral view. Scale lines: A–F = 2 µm; G–H = 10 µm.

microhabitats as *Kambiwa*, such as undersides of stones, leaf litter, and dead wood, both shaded and fully exposed to the sun. At least one species (*S. igapora* gen. et sp. nov.) occurs in a range of very different microhabitats, similar to *Kambiwa ibo* sp. nov. (cf. Fig. 12). Abundances were often high, and the reaction to disturbance was as in *Kambiwa*, i.e., fast running until a suitable spot for hiding was found. We rarely found more than one species of *Sertana* gen. nov. at one locality (*S. igapora* and *S. lapa* gen. et sp. nov., SE of Bom Jesus da Lapa), but localities were sometimes shared with a representative of *Ibotyporanga* or *Kambiwa*. These other Ninetinae were usually found in slightly different microhabitats. Egg sacs were carried under the prosoma (Fig. 48), and consisted of 5–8 eggs that were arranged in a single flat layer; eggs were covered with a few barely visible lines of silk. For further details, see individual natural history sections below.

Distribution

Sertana gen. nov. is apparently restricted to the Cerrado and Caatinga biomes of northeastern Brazil (Fig. 57). Similar to *Kambiwa* above, we suspect that the large Cerrado region SW of Maranhão/Piauí/Bahia that has currently no record of *Sertana* may in fact be occupied by the genus.

Fig. 56. *Sertana* Huber gen. nov. spp., typical habitats; all localities are in Brazil, Bahia. **A**. SE of Igaporã; type locality of *S. igapora* Huber gen. et sp. nov. **B**. W of Bom Jesus da Lapa; *S. igapora*. **C**. SW of São Felix do Coribe; type locality of *S. sagarana* Huber gen. et sp. nov. **D**. SE of Bom Jesus da Lapa; type locality of *S. lapa* Huber gen. et sp. nov.

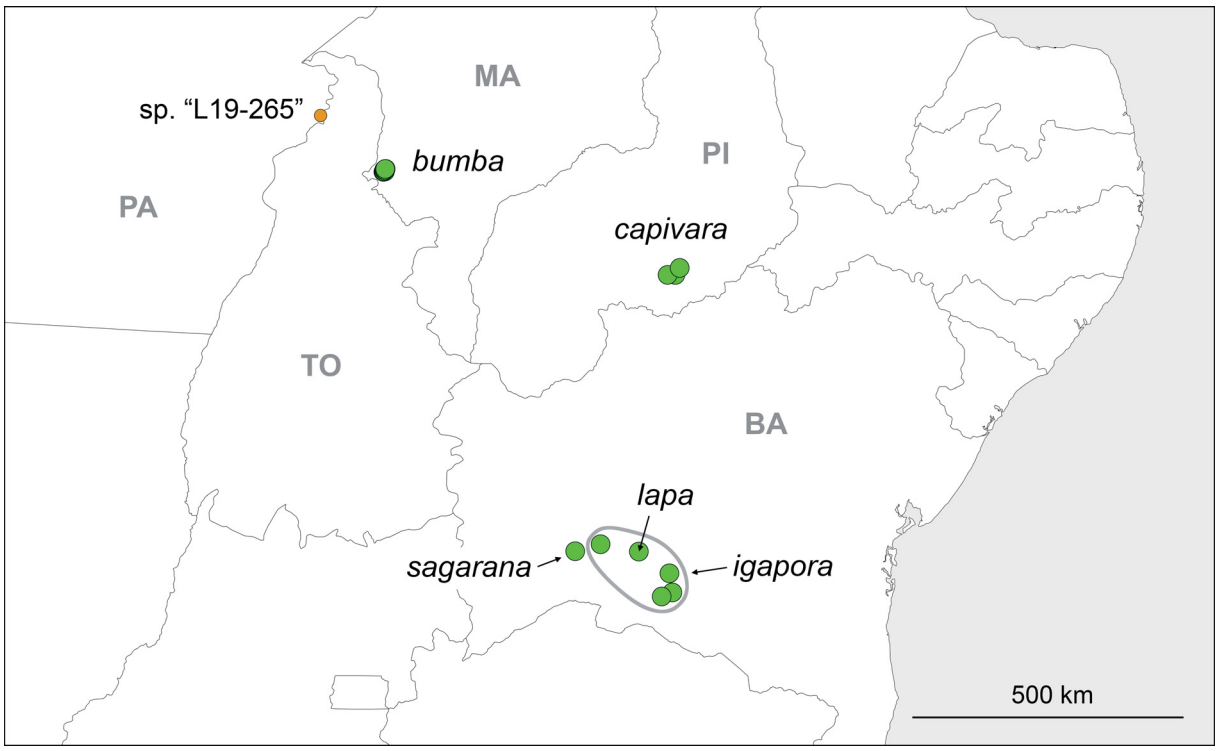

Fig. 57. Known distribution of *Sertana* Huber gen. nov. The small orange dot denotes a probable further species that we do not describe. Abbreviations: BA = Bahia; MA = Maranhão; PA = Pará; PI = Piauí; TO = Tocantins.

Composition and species limits

The genus includes five nominal species, all of them newly described below. The IBSP has specimens of an additional probable species that we could not study in detail; these specimens originate from Pará, Santa Isabel, Cave SI-15 (6.2247° S, 48.4317° W) (shown as "L19-265" in Fig. 57).

Identification key (males only)

1. One distal process of genital bulb (vp2 in Fig. 63E) very long, reaching palpal coxa (Figs 62C, 63D–F) ..... ***S. sagarana*** Huber gen. et sp. nov.
– Processes of genital bulb shorter, not reaching palpal coxa (Figs 58, 66, 71) 2

2. Procursus with large membranous flap hiding main sclerotized branch of procursus in retrolateral view (Fig. 59C) ..... ***S. igapora*** Huber gen. et sp. nov.
– Procursus without membranous flap (Figs 67C, 76C) or with small dorsal flap not hiding main sclerotized branch of procursus in retrolateral view (Fig. 72C) 3

3. Procursus consists of slender main branch and small transparent dorsal flap .... ***S. bumba*** Huber gen. et sp. nov.
– Procursus consists of strong apophysis curved dorsally, without transparent dorsal flap 4

4. Cheliceral apophyses short, at half-length of chelicerae, and directed distally (Fig. 68A–B); tip of procursus short, wide, and strongly curved (Fig. 67C) ..... ***S. lapa*** Huber gen. et sp. nov.
– Cheliceral apophyses longer, in more proximal position, and directed frontally (Fig. 77A–B); tip of procursus longer, slenderer, and less strongly curved ..... ***S. capivara*** Huber gen. et sp. nov.

Sertana igapora Huber gen. et sp. nov.
urn:lsid:zoobank.org:act:E4097297-6257-4353-A405-E91C775BD0C1
Figs 48A–B, 49A–C, F, 50A–B, 51A–B, E–F, 52B–C, 53C–E, 54A, C, E, G–H, 55A–C, G, 58–61

Diagnosis

Males are easily distinguished from those of most known congeners (except *S. sagarana* gen. et sp. nov.) by presence of large retrolateral membranous flap of procursus with serrated distal margin (Fig. 59C); from *S. sagarana* by much shorter retrolateral-ventral apophysis on genital bulb (compare Figs 59E and 63E) and by shorter main branch of procursus largely hidden by retrolateral membranous flap (compare Figs 59C and 63C). Females externally very similar to those of known congeners; internally distinguished by complex median modifications (similar to *S. sagarana* and *S. lapa* gen. et sp. nov.) and large semicircular membranous pouch (Fig. 60C; larger than in *S. sagarana* and *S. lapa*).

Etymology

The species name is derived from the type locality; noun in apposition.

Type material

Holotype

BRAZIL – **Bahia** • ♂; SE of Igaporã; 13.7977° S, 42.6578° W; 1000 m a.s.l.; 18 Nov. 2022; B.A. Huber and L.S. Carvalho leg.; CHNUFPI 9216.

Paratypes

BRAZIL – **Bahia** • 8 ♂♂, 10 ♀♀; same collection data as for holotype; CHNUFPI 9217 • 1 ♀; same collection data as for holotype; CHNUFPI 9218 • 4 ♂♂, 4 ♀♀; same collection data as for holotype; CHNUFPI 9219 [deposited in ZFMK Ar 25074].

Fig. 58. *Sertana igapora* Huber gen. et sp. nov., paratype, ♂, from Brazil, Bahia, SE of Igaporã, ZFMK Ar 25074. Left palp, prolateral, dorsal, and retrolateral views. Scale line = 0.2 mm.

Other material examined

BRAZIL – **Bahia** • 2 ♂♂, 4 ♀♀, in pure ethanol; same collection data as for holotype; CHNUFPI 9220 [deposited in ZFMK Br22-194] (voucher of UH070; 1 ♂, 1 ♀ used for SEM) • 5 ♂♂, 2 ♀♀; SW of Caetité, Caetité Wind Farm; 14.1155° S, 42.6087° W; 1000 m a.s.l.; 12 Nov. 2022; B.A. Huber and L.S. Carvalho leg.; CHNUFPI 9221 • 1 ♂, 4 ♀♀, 4 juvs, in pure ethanol; same collection data as for preceding; CHNUFPI 9222 [deposited in ZFMK Br22-156] (voucher of UH050) • 2 ♀♀; N of Guanambi; 14.1797° S, 42.7812° W; 560 m a.s.l.; 12 Nov. 2022; B.A. Huber, L.S. Carvalho and R.A. Torres leg.; CHNUFPI 9223 • 4 ♀♀, in pure ethanol; same collection data as for preceding;

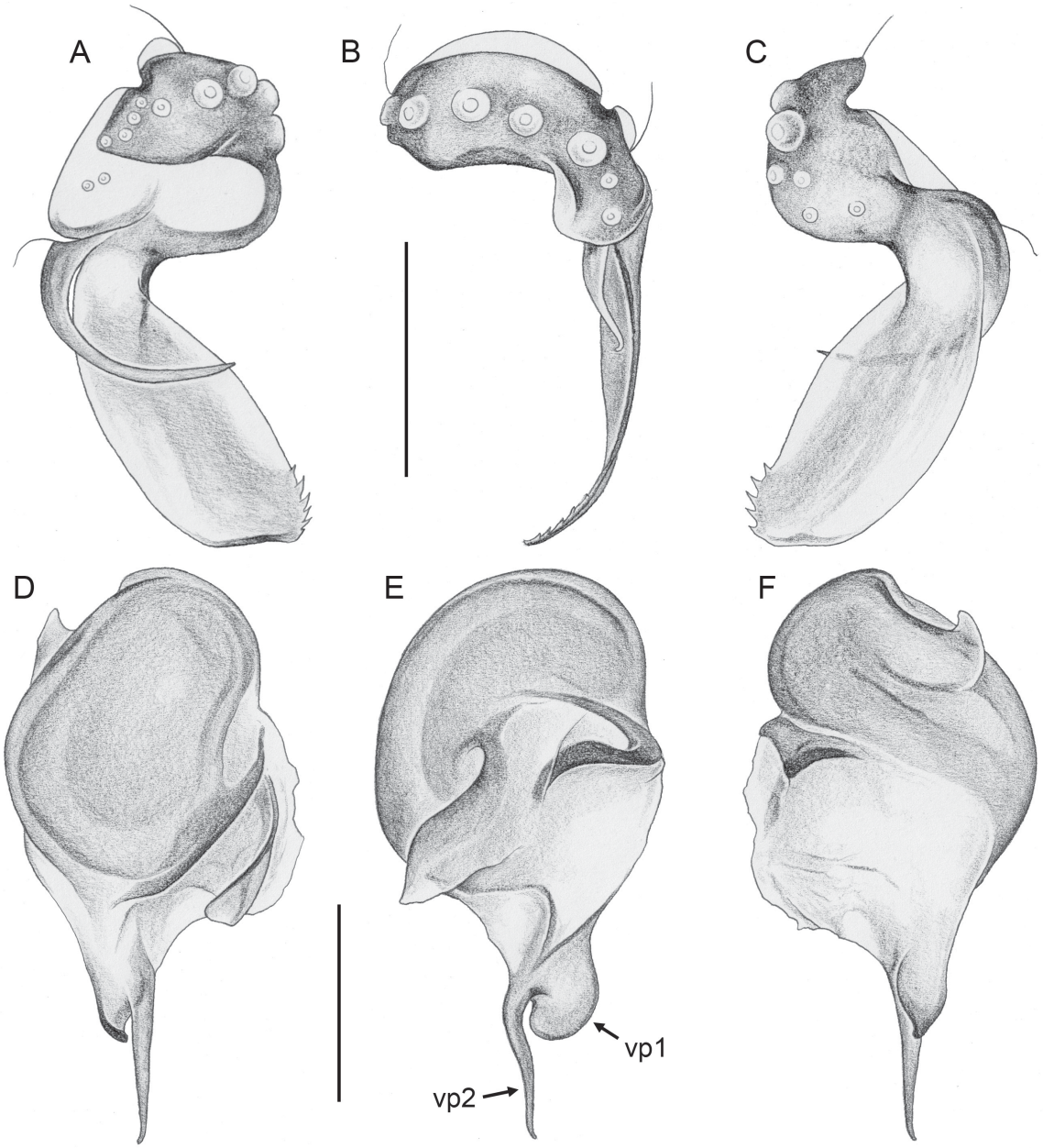

Fig. 59. *Sertana igapora* Huber gen. et sp. nov., paratype, ♂, from Brazil, Bahia, SE of Igaporã, ZFMK Ar 25074. **A–C**. Left palpal tarsus and procursus, prolateral, dorsal, and retrolateral views. **D–F**. Left genital bulb, prolateral, dorsal, and retrolateral views. Abbreviations: vp1/vp2 = ventral processes. Scale lines = 0.1 mm.

CHNUFPI 9224 [deposited in ZFMK Br22-157] • 5 ♂♂, 11 ♀♀; SE of Bom Jesus da Lapa, 'site 2'; 13.4383° S, 43.1645° W; 480 m a.s.l.; 18 Nov. 2022; B.A. Huber and L.S. Carvalho leg.; CHNUFPI 9225 • 2 ♂♂, 2 ♀♀; same collection data as for preceding; CHNUFPI 9226 [deposited in ZFMK Ar 25075] • 1 ♀; probably same collection data as for preceding (see Natural history section of *S. lapa* gen. et sp. nov.); CHNUFPI 9227 • 2 ♂♂, 4 ♀♀, in pure ethanol; same collection data as for preceding; CHNUFPI 9228 [deposited in ZFMK Br22-190] (voucher of UH492, G54) • 3 ♂♂, 1 ♀; W of Bom Jesus da Lapa, Fazenda Pedra Branca; 13.315° S, 43.795° W; 470 m a.s.l.; 17 Nov. 2022; B.A. Huber and L.S. Carvalho leg.; CHNUFPI 9229 • 5 ♂♂, 4 ♀♀; same collection data as for preceding; CHNUFPI 9230 [deposited in ZFMK Ar 24730] • 1 ♂, 5 ♀♀, in pure ethanol; same collection data as for preceding; CHNUFPI 9231 [deposited in ZFMK Br22-184] • 2 ♂♂, 1 ♀, in pure ethanol; same collection data as for preceding; CHNUFPI 9232 [deposited in ZFMK Br22-186].

Description

Male (holotype)

Measurements. Total body length 1.04, carapace width 0.46. Distance PME–PME 40 µm; diameter PME 50 µm; distance PME–ALE 20 µm; distance AME–AME 10 µm; diameter AME 25 µm. Leg 1: 2.32 (0.64+0.14+0.58+0.62+0.34), tibia 2: 0.51, tibia 3: 0.48, tibia 4: 0.79; tibia 1 L/d: 10; diameters of leg femora 95–100 µm, of leg tibiae 60 µm.

Color (in ethanol). Prosoma and legs ochre-yellow, carapace and legs without darker marks or rings; abdomen ochre-gray, with very indistinct internal marks, ventrally with slightly darker ochre plate in front of gonopore.

Body. Habitus as in Fig. 48A. Ocular area not raised. Carapace without thoracic groove. Clypeus unmodified. Sternum barely wider than long (0.33/0.32), without anterior processes. Abdomen globular.

Chelicerae. As in Fig. 60A–B; with pair of frontal apophyses; with very indistinct stridulatory files (Fig. 51A) not visible in dissecting microscope.

Palps. As in Fig. 58; coxa unmodified; trochanter ventrally slightly protruding; femur proximally with very indistinct retrolateral protrusion, distally slightly widened but otherwise unmodified; femur-patella condyles shifted toward prolateral side; tibia-tarsus condyles not shifted toward one side; tarsus with strong dorsal hairs, without prolateral process; procursus (Fig. 59A–C) consisting of large

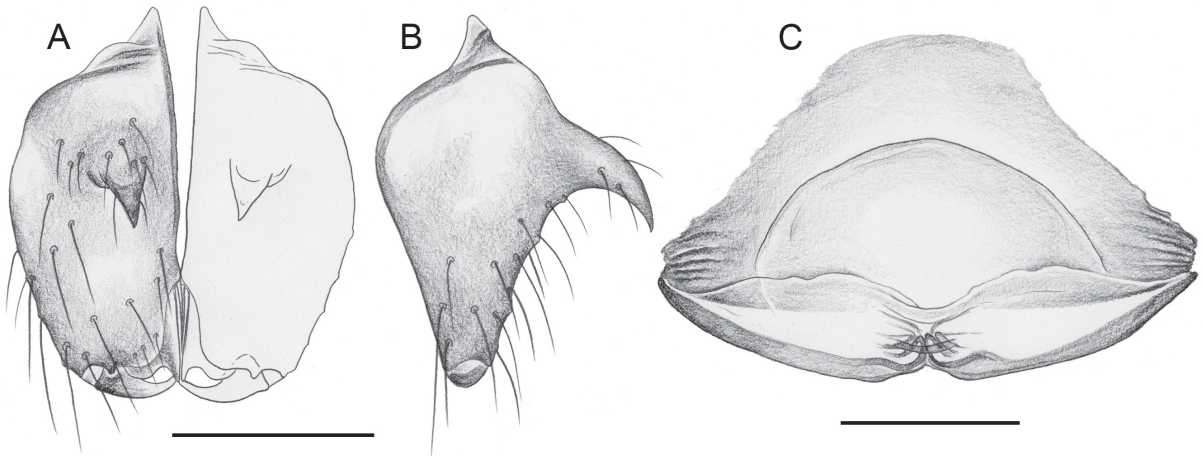

Fig. 60. *Sertana igapora* Huber gen. et sp. nov., paratypes, ♂♀, from Brazil, Bahia, SE of Igaporã, ZFMK Ar 25074. **A**–**B**. Male chelicerae, frontal and lateral views. **C**. Cleared female genitalia, dorsal view. Scale lines = 0.1 mm.

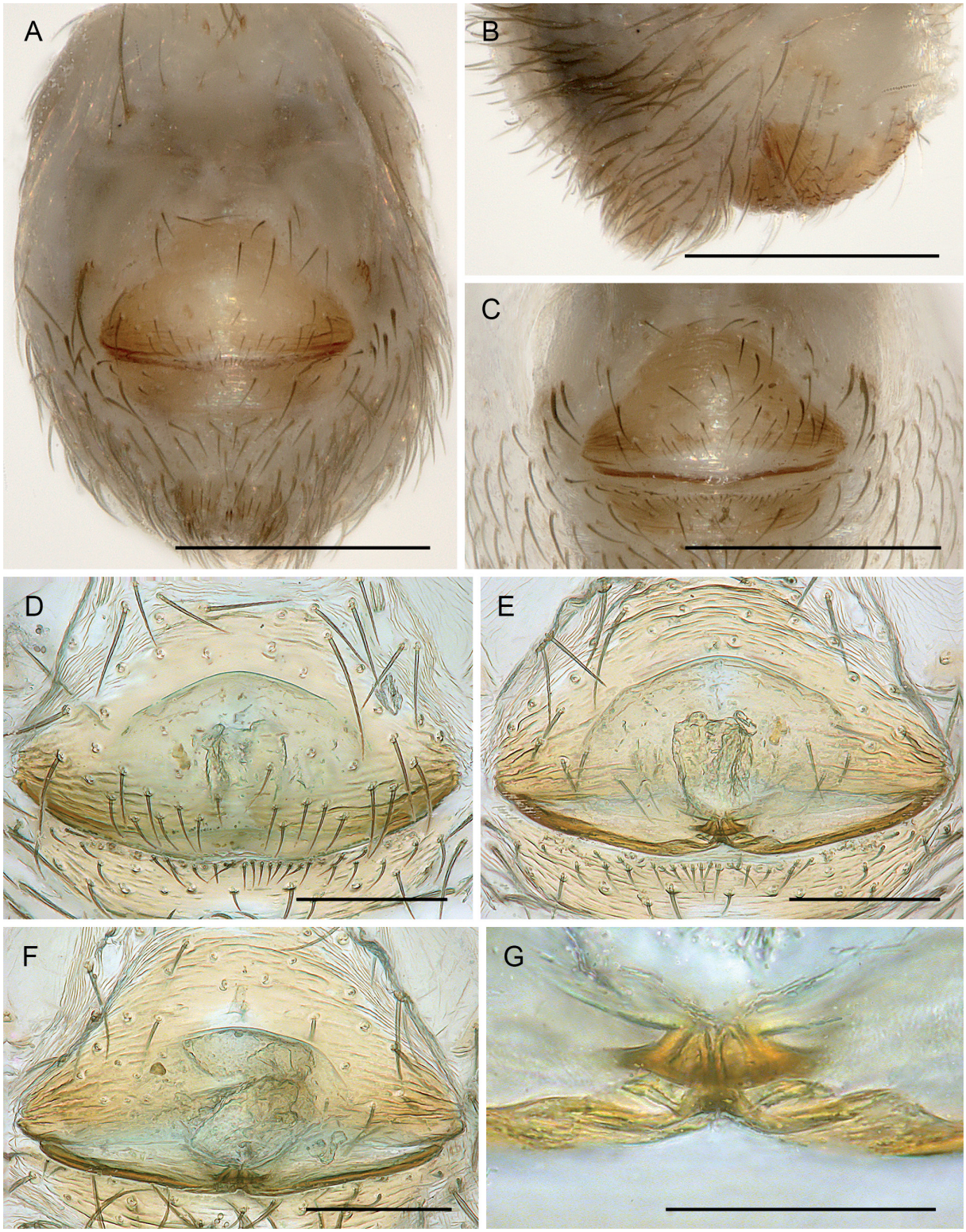

Fig. 61. *Sertana igapora* Huber gen. et sp. nov., paratypes, ♀♀, from Brazil, Bahia, SE of Igaporã, ZFMK Ar 25074. **A–B, D–E, G**. ♀ 1, **C, F**. ♀ 2. **A–B**. Abdomen, ventral and lateral views. **C**. Epigynum, ventral view. **D–E**. Cleared genitalia, ventral and dorsal views. **F**. Cleared genitalia, dorsal view. **G**. Detail of E. Scale lines: A–C = 0.3 mm; D–F = 0.1 mm; G = 0.05 mm.

semitransparent flap and strongly curved process originating proximally on ventral side and curving towards dorsal, hidden in retrolateral view by large flap; flap distally serrated; genital bulb (Fig. 59D–F) with prolateral-dorsal oblique flat process and distinctive pair of ventral processes distally: slender prolateral process and spoon-shaped retrolateral process.

Legs. Without spines, without curved hairs; with short vertical hairs on tibiae 1 and 2, barely visible in dissecting microscope; retrolateral trichobothrium of tibia 1 at 62%; prolateral trichobothrium absent on tibia 1; tarsus 1 with 4 pseudosegments, fairly distinct.

Variation (males)

Tibia 1 in 33 males: 0.50–0.62 (mean 0.58). Abdomen color variable, ranging from monochromous pale gray to dark gray with black internal marks.

Females

In general similar to males but usually lighter and abdomen less shiny (Fig. 48B); chelicerae without stridulatory files (Fig. 51B). Tibia 1 in 38 females: 0.52–0.62 (mean 0.57). Epigynum (Fig. 61A–C) anterior plate trapezoidal, weakly protruding, medially often lighter; posterior plate simple, sometimes indistinct (especially medially). Internal genitalia (Figs 60C, 61D–G) with curved transversal sclerite connected laterally to posterior lateral corners of anterior epigynal plate, medially with small but complex sclerotized elements and large anterior membranous sac; apparently without pore plates.

Barcoding

Three specimens were barcoded, from SE of Igaporã (type locality), from SW of Caetité, and from SE of Bom Jesus da Lapa (geographic distances: 36–95 km). K2P distances ranged from 0.5% to 0.8%.

Distribution

Known from several localities in southern Bahia, Brazil (Fig. 57).

Natural history

At the type locality, the spiders were collected on an arenite outcrop, in thorny shrubland on clayish soil (Fig. 56A); they were found in high abundance among the pebbles in the shade of the bushes. Southeast of Bom Jesus da Lapa, they were very abundant in the leaf litter of degraded roadside vegetation with shrubs and grasses; two neighboring habitats had different species of Ninetinae (*Kambiwa coribe* sp. nov., *Sertana lapa* gen. et sp. nov.). At the other localities (shrubland with scattered trees on clayish soil), they occupied different microhabitats, i.e., the leaf litter (Fig. 56B) and dead wood on the ground. Eight egg sacs contained 5–8 eggs each (mean 6.1), and were flat (all eggs in a single layer); egg diameter was usually 0.42–0.46, in one egg sac 0.48.

Sertana sagarana Huber gen. et sp. nov.
urn:lsid:zoobank.org:act:A021CB38-C4B3-489B-984E-FA7DAD0E7AC8
Figs 48C–D, 62–65

Diagnosis

Males are easily distinguished from those of known congeners by very long prolateral-ventral process on genital bulb (Fig. 63D–F; reaching palpal coxa); from most congeners (except *S. igapora* gen. et sp. nov.) also by presence of large retrolateral membranous flap of procursus with serrated distal margin (Fig. 63A–C); from *S. igapora* also distinguished by longer main branch of procursus distally not hidden by retrolateral flap (compare Figs 59C and 63C). Females externally very similar to those of known congeners; internally distinguished by complex median modifications (Fig. 65E–F; similar to *S. igapora* and *S. lapa* gen. et sp. nov.) and large globular membranous pouch (Fig. 64C; smaller than in *S. igapora*, larger than in *S. lapa*).

Etymology

The species name is a noun in apposition, derived from *Sagarana*, a collection of nine short stories published in 1946 by João Guimarães Rosa (1908–1967). All of them have their setting in the sertão.

Type material

Holotype

BRAZIL – **Bahia** • ♂; SW of São Felix do Coribe, 'site 2'; 13.4329° S, 44.2168° W; 480 m a.s.l.; 17 Nov. 2022; B.A. Huber and L.S. Carvalho leg.; CHNUFPI 9233.

Paratypes

BRAZIL – **Bahia** • 2 ♂♂, 1 ♀; same collection data as for holotype; CHNUFPI 9234 • 2 ♂♂; same collection data as for holotype; CHNUFPI 9235 [deposited in ZFMK Ar 24731].

Other material examined

BRAZIL – **Bahia** • 1 ♂, 3 ♀♀, in pure ethanol (one female prosoma used for molecular work; abdomen cleared and transferred to ZFMK Ar 24731); same collection data as for holotype; CHNUFPI 9236 [deposited in ZFMK Br22-179] (voucher of G52).

Description

Male (holotype)

Measurements. Total body length 0.88, carapace width 0.43. Distance PME–PME 40 µm; diameter PME 40 µm; distance PME–ALE 15 µm; distance AME–AME 10 µm; diameter AME 25 µm. Leg 1: 2.50 (0.70+0.14+0.62+0.68+0.36), tibia 2: 0.54, tibia 3: 0.50, tibia 4: 0.73; tibia 1 L/d: 12; diameters of leg femora 90 µm, of leg tibiae 50 µm.

Fig. 62. *Sertana sagarana* Huber gen. et sp. nov., paratype, ♂, from Brazil, Bahia, SW of São Felix do Coribe, ZFMK Ar 24731. Left palp, prolateral, dorsal, and retrolateral views. Scale line = 0.2 mm.

Color (in ethanol). Prosoma and legs pale ochre-yellow, carapace and legs without darker marks or rings; abdomen ochre-gray, with very indistinct internal marks, ventrally with slightly darker ochre plate in front of gonopore.

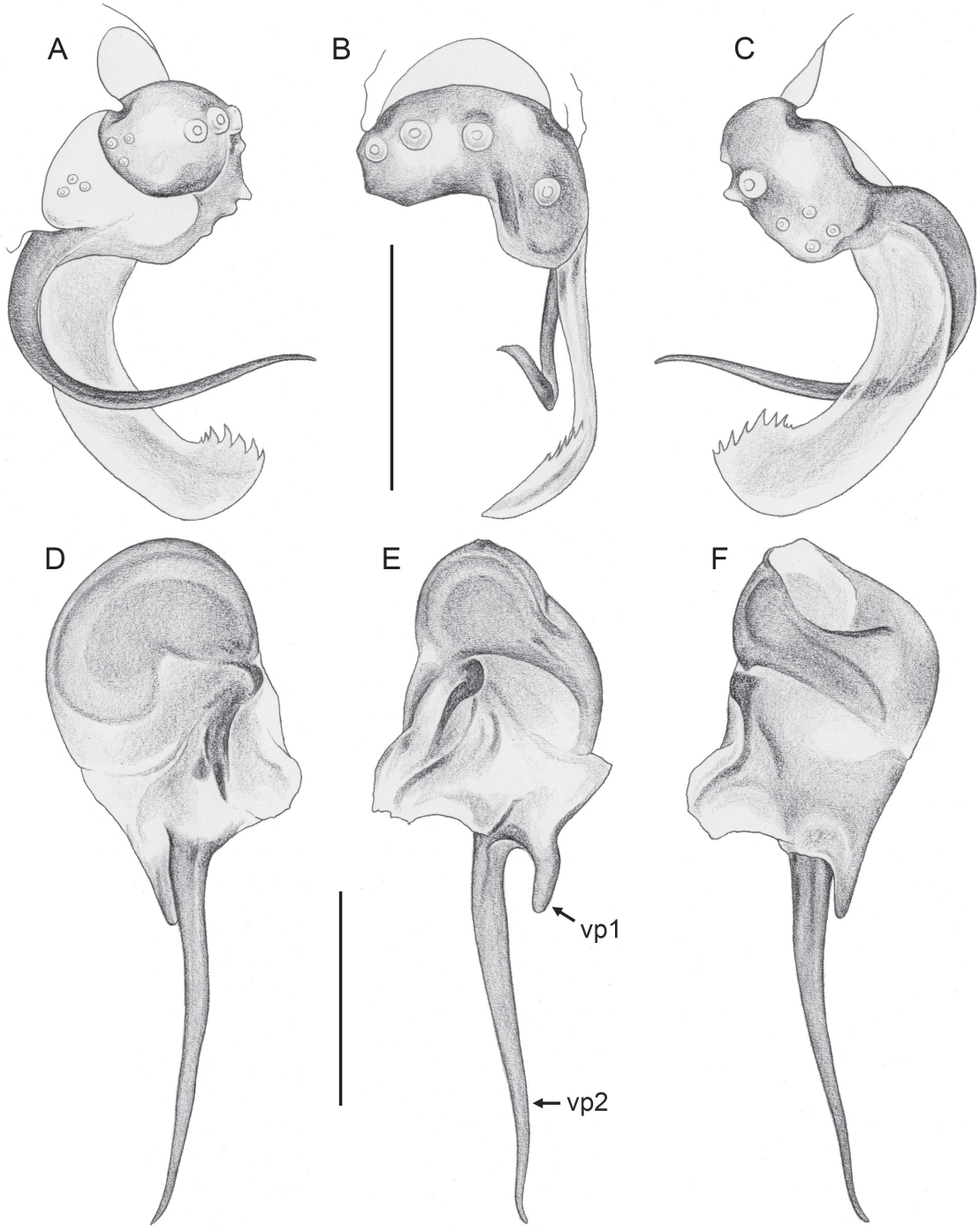

Fig. 63. *Sertana sagarana* Huber gen. et sp. nov., paratype, ♂, from Brazil, Bahia, SW of São Felix do Coribe, ZFMK Ar 24731. **A–C**. Left palpal tarsus and procursus, prolateral, dorsal, and retrolateral views. **D–F**. Left genital bulb, prolateral, dorsal, and retrolateral views. Abbreviations: vp1/vp2 = ventral processes. Scale lines = 0.1 mm.

Body. Habitus as in Fig. 48C. Ocular area not raised. Carapace without thoracic groove. Clypeus unmodified. Sternum barely wider than long (0.29/0.28), without anterior processes. Abdomen globular.

Chelicerae. As in Fig. 64A–B; with pair of frontal apophyses; with stridulatory files (barely visible in dissecting microscope).

Palps. As in Fig. 62; coxa unmodified; trochanter ventrally slightly protruding; femur proximally with small retrolateral protrusion, distally slightly widened but otherwise unmodified; femur-patella condyles shifted toward prolateral side; tibia-tarsus condyles not shifted toward one side; tarsus with strong dorsal hairs, without prolateral process; procursus (Fig. 63A–C) consisting of large semitransparent flap and strongly curved process on prolateral side of large flap, originating proximally on ventral side and curving towards dorsal; membranous flap distally serrated; genital bulb (Fig. 63D–F) with prolateral-dorsal process consisting of membranous and sclerotized elements, and distinctive pair of ventral distal elements: long and slender prolateral process and short retrolateral process.

Legs. Without spines, without curved hairs; apparently without short vertical hairs; retrolateral trichobothrium of tibia 1 at 55%; prolateral trichobothrium absent on tibia 1; tarsus 1 with 3–4 indistinct pseudosegments.

Variation (males)

Tibia 1 in six males (incl. holotype): 0.60–0.66 (mean 0.63).

Females

In general, similar to males; chelicerae apparently without stridulatory files (not confirmed with SEM). Tibia 1 in three females: 0.60, 0.61, 0.62. Epigynum (Fig. 65A–B) anterior plate trapezoidal, weakly protruding, medially lighter; posterior plate simple, indistinct. Internal genitalia (Figs 64C, 65C–F) with transversal sclerite connected laterally to posterior lateral corners of anterior epigynal plate, medially with small but complex sclerotized elements and large anterior membranous sac; apparently without pore plates.

Distribution

Known from type locality only, in southern Bahia, Brazil (Fig. 57).

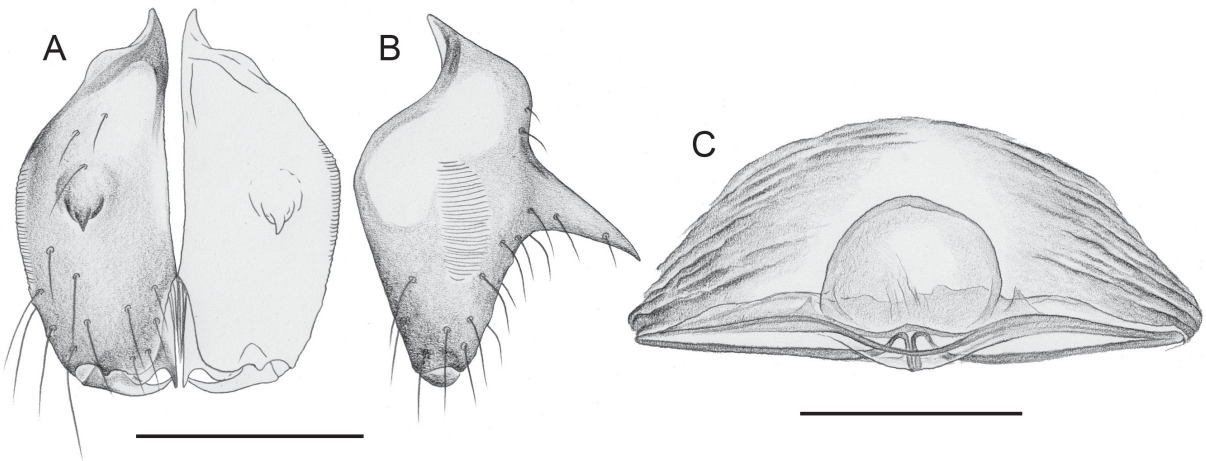

Fig. 64. *Sertana sagarana* Huber gen. et sp. nov., paratypes, ♂♀, from Brazil, Bahia, SW of São Felix do Coribe, ZFMK Ar 24731. **A**–**B**. Male chelicerae, frontal and lateral views. **C**. Cleared female genitalia, dorsal view. Scale lines = 0.1 mm.

Natural history

The spiders were collected on the top of a rocky outcrop, under stones among cacti and thorny shrubs (Fig. 56C). Another species of Ninetinae was found at the bottom of the outcrop (*Kambiwa coribe* sp. nov.). Two egg sacs contained five and six eggs, respectively, and were flat (all eggs in a single layer); egg diameter was 0.42–0.44.

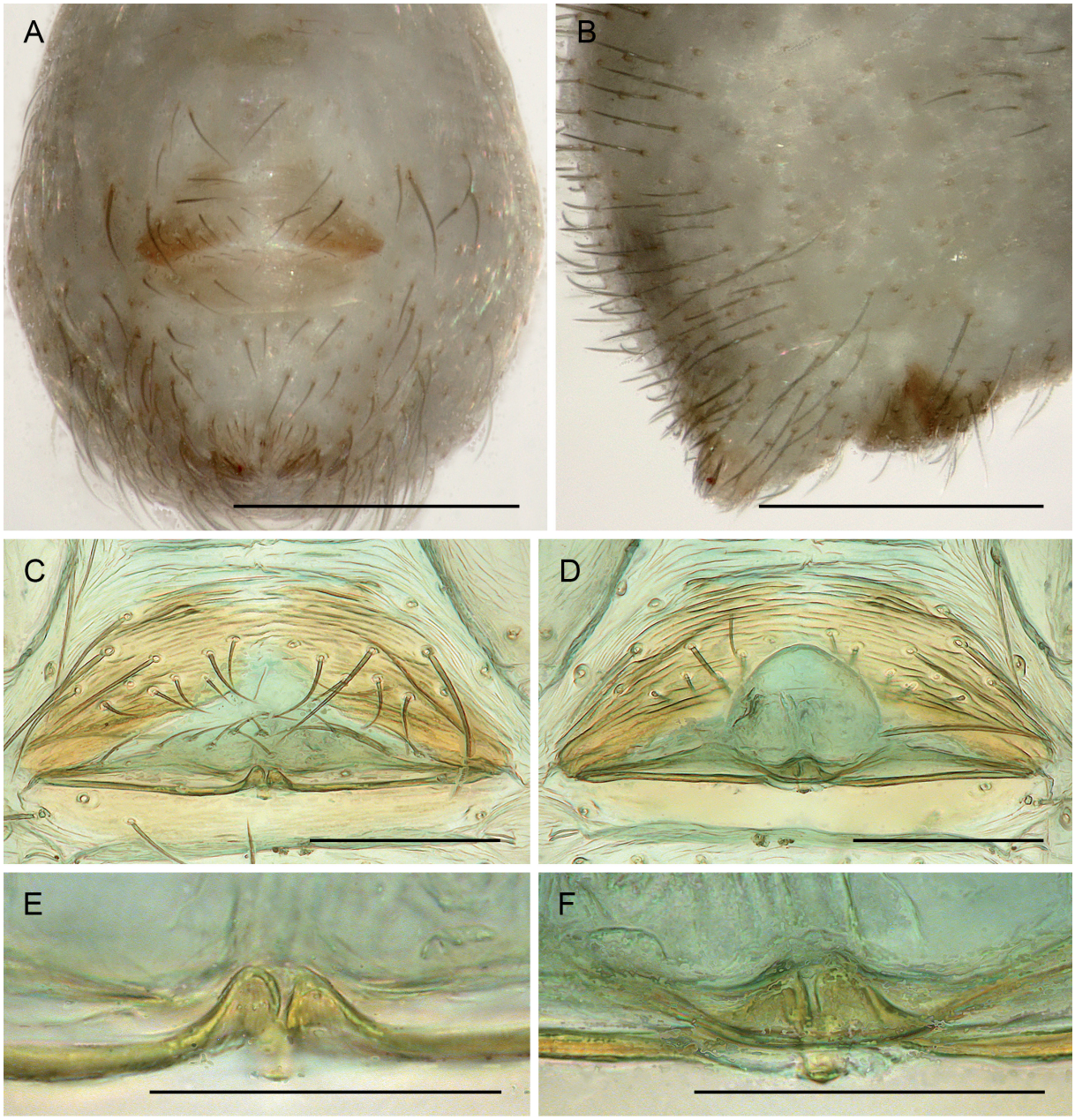

Fig. 65. *Sertana sagarana* Huber gen. et sp. nov., ♀, from Brazil, Bahia, SW of São Felix do Coribe, ZFMK Ar 24731. **A**–**B**. Abdomen, ventral and lateral views. **C**–**D**. Cleared genitalia, ventral and dorsal views. **E**–**F**. Central element of internal genitalia, ventral and dorsal views. Scale lines: A–B = 0.3 mm; C–D = 0.1 mm; E–F = 0.05 mm.

Sertana lapa Huber gen. et sp. nov.
urn:lsid:zoobank.org:act:964B82CD-5748-48F5-A7E2-6510F71CFA5B
Figs 48E–F, 49E, 50C–E, 51C–D, 52D, F, 53A–B, F, 54F, 55D–E, H, 66–70

Diagnosis

Males are easily distinguished from those of known congeners by shape of procursus (Fig. 67A–C; proximally wide, distally tapering and strongly curved towards dorsal, with prolateral subdistal side branch), by shapes of bulbal processes (Fig. 67D–F; dorsal processes complex, partly almost as long as ventral processes), and by male cheliceral apophyses strongly pointing downward (Fig. 68B); from *S. igapora* gen. et sp. nov. and *S. sagarana* gen. et sp. nov. also by absence of retrolateral membranous flap on procursus. Females very similar to those of known congeners but posterior margin of anterior epigynal plate medially light (Fig. 69A, C); internally with complex median modifications similar to *S. igapora* and *S. sagarana* but with smaller membranous pouch (Fig. 70G–H).

Etymology

The species name is derived from the type locality; noun in apposition.

Type material

Holotype

BRAZIL – **Bahia** • ♂; SE of Bom Jesus da Lapa, 'site 1'; 13.4398° S, 43.1643° W; 520 m a.s.l.; 18 Nov. 2022; B.A. Huber and L.S. Carvalho leg.; CHNUFPI 9237.

Paratypes

BRAZIL – **Bahia** • 6 ♂♂, 1 ♀; same collection data as for holotype; CHNUFPI 9238 • 1 ♂; same collection data as for holotype; CHNUFPI 9239 • 2 ♂♂, 1 ♀; same collection data as for holotype; CHNUFPI 9240 [deposited in ZFMK Ar 24732].

Fig. 66. *Sertana lapa* Huber gen. et sp. nov., paratype, ♂, from Brazil, Bahia, SE of Bom Jesus da Lapa, ZFMK Ar 24732. Left palp, prolateral, dorsal, and retrolateral views. Scale line = 0.2 mm.

Other material examined

BRAZIL – **Bahia** • 2 ♂♂, 4 ♀♀, in pure ethanol (1 female prosoma used for molecular work; abdomen cleared and transferred to ZFMK Ar 24732); same collection data as for holotype; CHNUFPI 9241 [deposited in ZFMK Br22-187] (voucher of UH490, G53; 1 ♂, 1 ♀ used for SEM) • 2 ♀♀, in pure ethanol (1 female abdomen cleared and transferred to ZFMK Ar 24732); same collection data as for holotype; CHNUFPI 9242 [deposited in ZFMK Br22-188] (voucher of UH066) • 1 ♀, in pure ethanol; probably same collection data as for holotype (see Natural history section below); CHNUFPI 9243 [deposited in ZFMK Br22-191] (voucher of UH067).

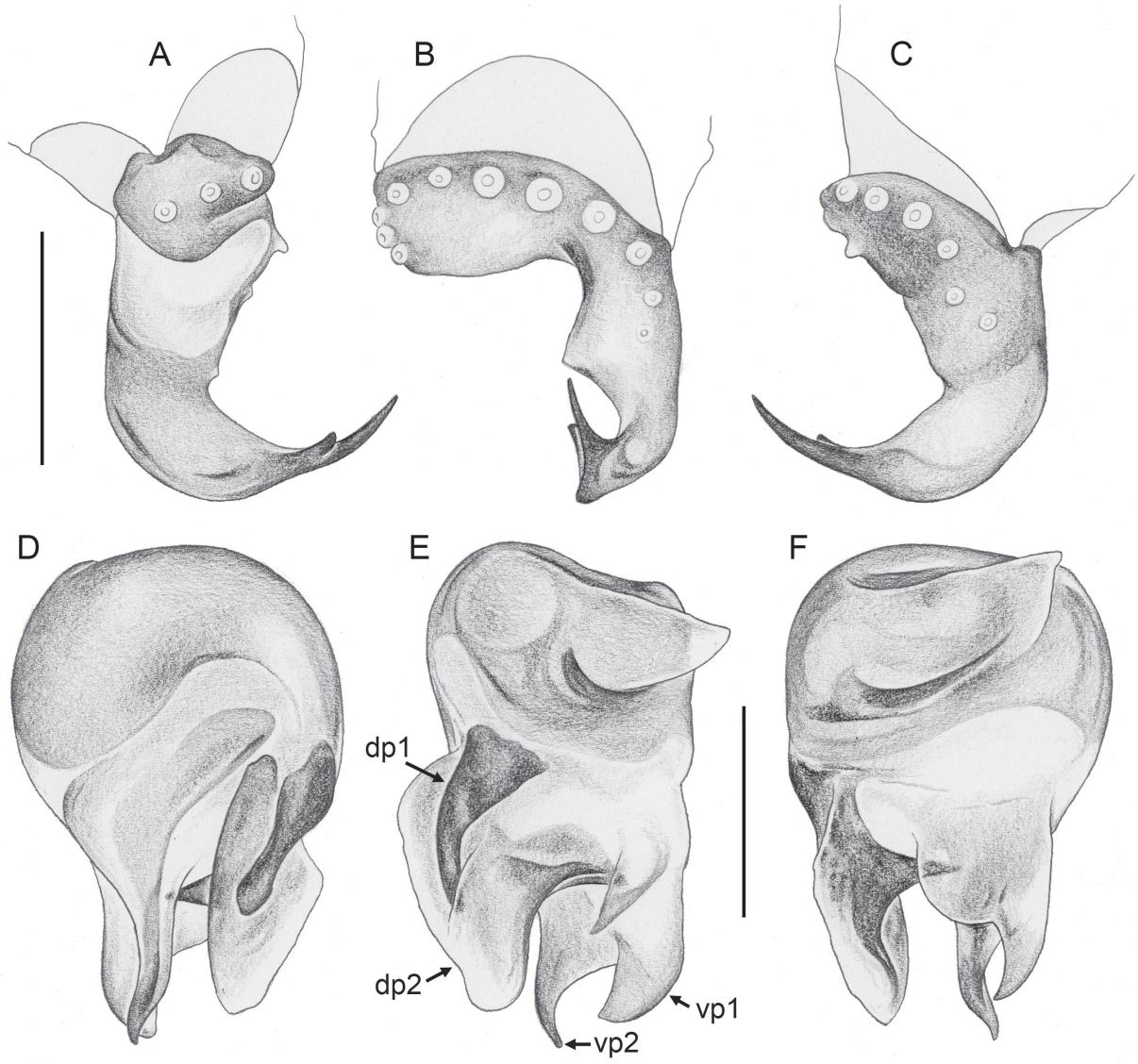

Fig. 67. *Sertana lapa* Huber gen. et sp. nov., paratype, ♂, from Brazil, Bahia, SE of Bom Jesus da Lapa, ZFMK Ar 24732. **A–C**. Left palpal tarsus and procursus, prolateral, dorsal, and retrolateral views. **D–F**. Left genital bulb, prolateral, dorsal, and retrolateral views. Abbreviations: dp1/dp2 = dorsal processes; vp1/vp2 = ventral processes. Scale lines = 0.1 mm.

Description

Male (holotype)

Measurements. Total body length 1.38, carapace width 0.66. Distance PME–PME 50 µm; diameter PME 60 µm; distance PME–ALE 20 µm; distance AME–AME 15 µm; diameter AME 35 µm. Leg 1: 3.32 (0.96+0.22+0.86+0.90+0.38), tibia 2: 0.78, tibia 3: 0.76, tibia 4: 1.04; tibia 1 L/d: 11; diameters of leg femora 140–145 µm, of leg tibiae 75 µm.

Color (in ethanol). Prosoma and legs ochre to light brown, carapace and legs without darker marks or rings; abdomen gray, with indistinct internal marks, ventrally with slightly darker ochre plate in front of gonopore.

Body. Habitus as in Fig. 48E. Ocular area barely raised. Carapace without thoracic groove. Clypeus unmodified. Sternum slightly wider than long (0.44/0.40), without anterior processes. Abdomen globular.

Chelicerae. As in Fig. 68A–B; with pair of frontal apophyses; with stridulatory files (Fig. 51C; poorly visible in dissecting microscope).

Palps. As in Fig. 66; coxa unmodified; trochanter ventrally barely protruding; femur proximally with small retrolateral protrusion, distally slightly widened but otherwise unmodified; femur-patella condyles and tibia-tarsus condyles not shifted to one side; tarsus with strong dorsal hairs, without prolateral process; procursus (Fig. 67A–C) very simple, strongly curved towards dorsal, with small subdistal side branch, without semitransparent flap; genital bulb (Fig. 67D–F) distally complex, with two ventral processes (vp1 and vp2 in Fig. 67E) and two dorsal processes (dp1 and dp2 in Fig. 67E); location of sperm duct opening unclear.

Legs. Without spines, without curved hairs; with short vertical hairs on tibia 1; retrolateral trichobothrium of tibia 1 at 56%; prolateral trichobothrium absent on tibia 1; tarsus 1 with 3–4 pseudosegments, distally fairly distinct.

Variation (males)

Tibia 1 in 12 males (incl. holotype): 0.76–0.90 (mean 0.82). Some males darker brown, with distinct brown plate in front of gonopore and indistinct plate in front of spinnerets.

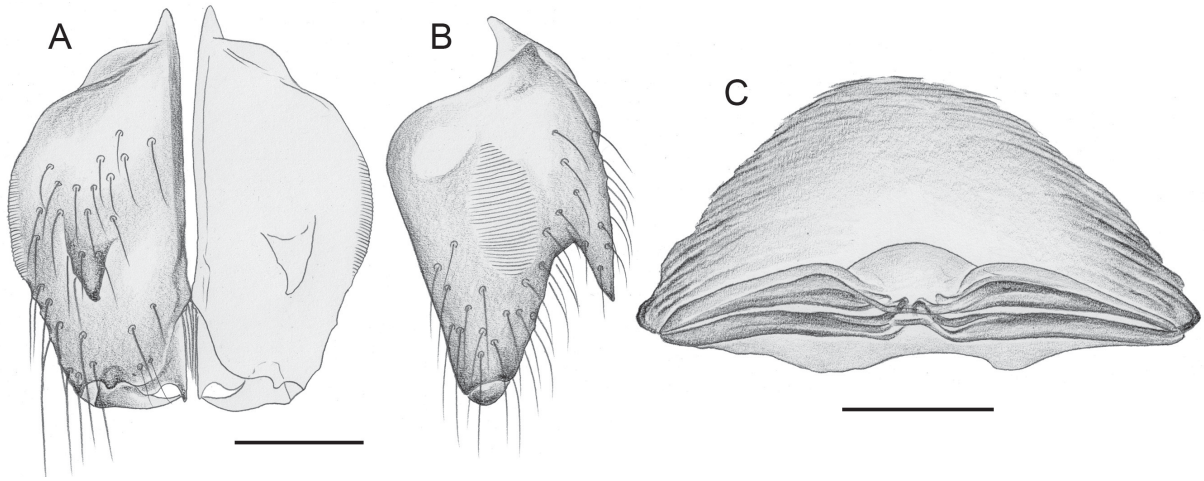

Fig. 68. *Sertana lapa* Huber gen. et sp. nov.; paratype, ♂, and non-type, ♀, from Brazil, Bahia, SE of Bom Jesus da Lapa, ZFMK Ar 24732. **A**–**B**. Male chelicerae, frontal and lateral views. **C**. Cleared female genitalia, dorsal view. Scale lines = 0.1 mm.

Females

In general, similar to males (Fig. 48F); chelicerae without stridulatory files; tibia 1 without short vertical hairs. Tibia 1 in seven females: 0.58–0.78 (mean 0.70). Epigynum slightly variable in size, shape, and color (Fig. 69), anterior plate semicircular, weakly protruding, medially at posterior margin whitish, lateral posterior margins usually darker brown to black; posterior plate large but simple. Internal genitalia (Figs 68C, 70) with transversal sclerite connected laterally to posterior lateral corners of anterior epigynal plate, medially with small but complex sclerotized elements and anterior membranous sac; possibly with pair of pore plates (arrows in Fig. 70G).

Barcoding

Three female specimens from the type locality were barcoded to check the significance of the minor variations seen in the epigynum. K2P distances ranged from 0.0% to 0.2% (Table 2).

Distribution

Known from type locality only, in southern Bahia, Brazil (Fig. 57).

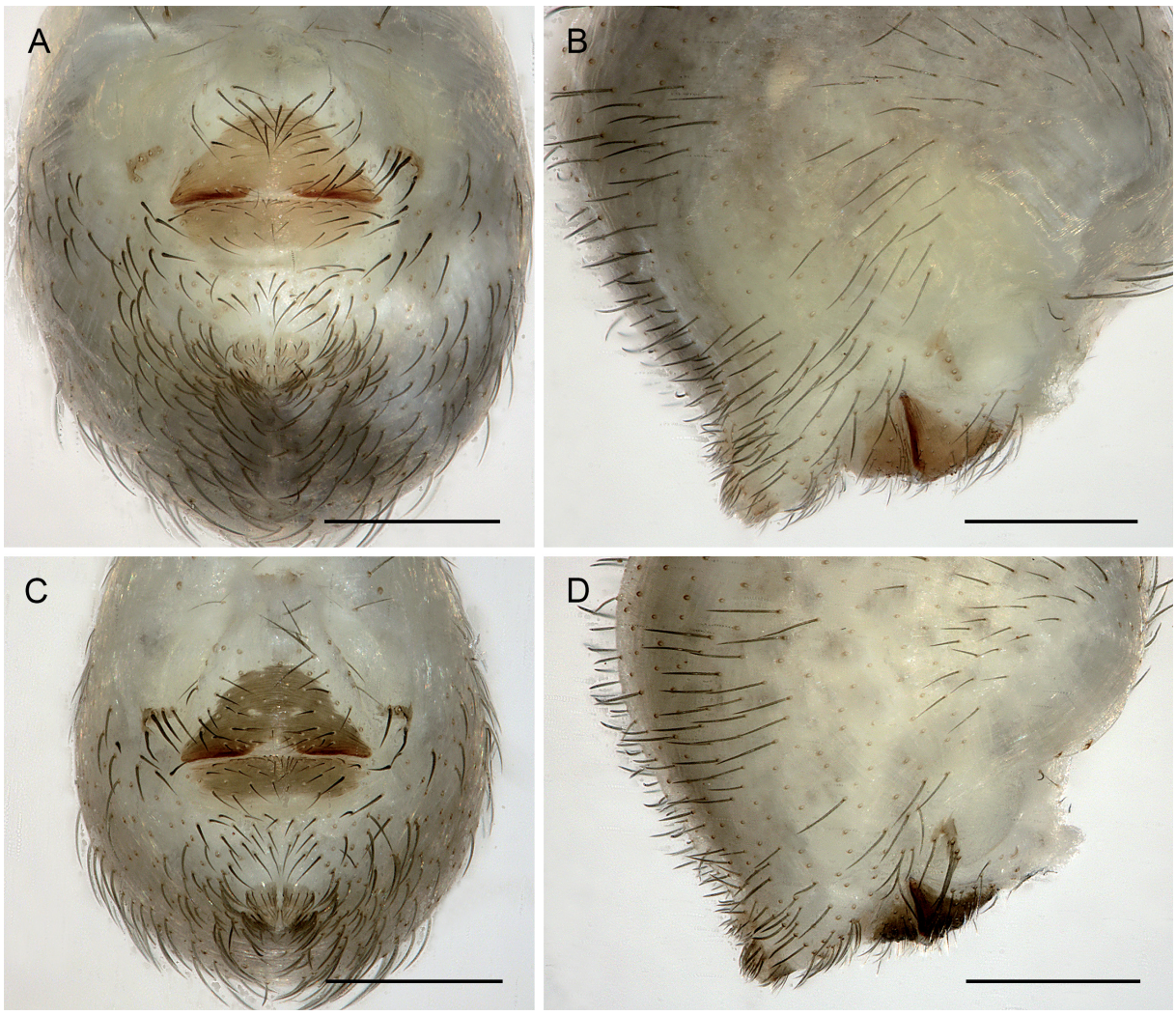

Fig. 69. *Sertana lapa* Huber gen. et sp. nov., paratypes, ♀♀, from Brazil, Bahia, SE of Bom Jesus da Lapa, ZFMK Ar 24732. **A–B**. ♀ 1. **C–D**. ♀ 2. **A, C**. Abdomens, ventral views. **B, D**. Abdomens, lateral views. Scale lines = 0.3 mm.

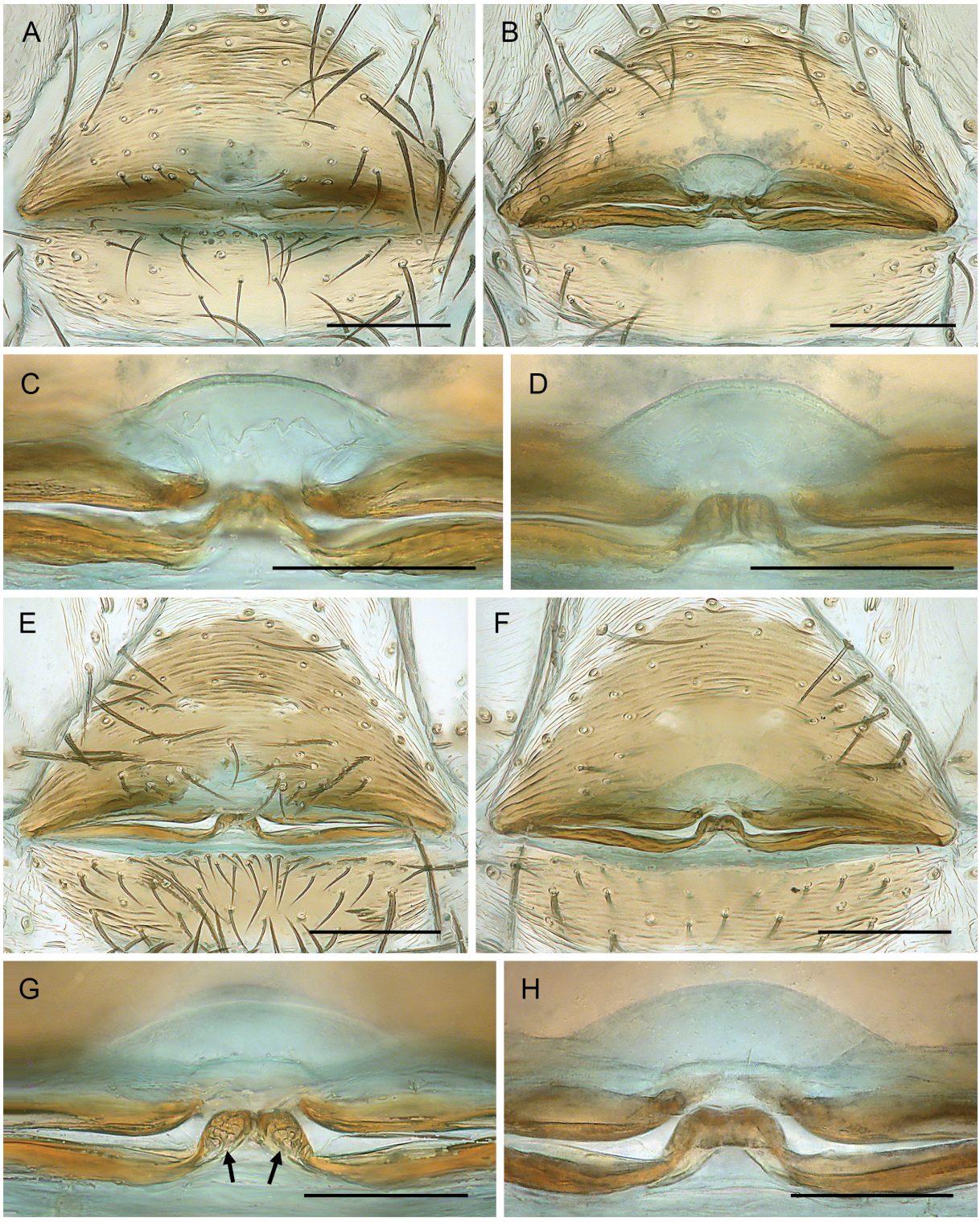

Fig. 70. *Sertana lapa* Huber gen. et sp. nov., paratypes, ♀♀, from Brazil, Bahia, SE of Bom Jesus da Lapa, ZFMK Ar 24732. **A–D**. ♀ 1. **E–H**. ♀ 2. **A–B, E–F**. Cleared genitalia, ventral and dorsal views. **C–D, G–H**. Central elements of internal genitalia, ventral and dorsal views; arrows point at putative pore plates. Scale lines: A–B, E–F = 0.1 mm; C–D, G–H = 0.05 mm.

Natural history

At the type locality, southeast of Bom Jesus da Lapa, we collected in three different habitats: on a granite outcrop with bare rock fields; in the neighboring arboreous Caatinga; and in leaf litter at the roadside. Except for two dubious specimens, all specimens from the granite outcrop were *S. lapa* gen. et sp. nov. (n = 20), and all specimens from the roadside litter were *S. igapora* gen. et sp. nov. (n = 26). We thus suspect that the two dubious specimens were mixed up and mislabeled and that the two species are restricted to different neighboring habitats (170 m distance). One egg sac contained seven eggs; egg diameter was 0.50–0.52.

Sertana bumba Huber gen. et sp. nov.
urn:lsid:zoobank.org:act:2E405CD8-8A8F-4997-8531-FE90F64241C3
Figs 49D, 50F, 52A, E, 53G, 54B, D, 55F, 71–74

Ninetinae L23-284 – Carvalho *et al.* 2026. — de Paula *et al.* 2026.

Diagnosis

Males are distinguished from those of known congeners by shape of procursus (Fig. 72A–C; short and slender main branch, small transparent dorsal flap without serrated margin), by shapes of bulbal processes (Fig. 72D–F; two complex dorsal processes, two ventral processes similar to *S. igapora* gen. et sp. nov.), and by male cheliceral apophyses proximally directed towards lateral (Fig. 73A). Females very similar to those of known congeners; internally with simple median modifications (Figs 73C, 74F; complex in *S. igapora*; *S. sagarana* gen. et sp. nov.; *S. lapa* gen. et sp. nov.), with large but very indistinct transparent sac.

Etymology

The species name is derived from Bumba-meu-boi (Bumba-boi, Boi-bumbá, etc.), a popular and comic-dramatic dance widespread in Brazil but particularly famous in Maranhão; noun in apposition.

Type material

Holotype

BRAZIL – **Maranhão** • ♂; Parque Nacional da Chapada das Mesas, 'site 1'; 7.155° S, 47.392° W; 300–320 m a.s.l.; 16 Dec. 2022; L.S. Carvalho *et al*. leg.; CHNUFPI 9244.

Paratypes

BRAZIL – **Maranhão** • 7 ♂♂, 1 ♀; same collection data as for holotype; CHNUFPI 5164 • 5 ♂♂, 1 ♀; same collection data as for preceding; CHNUFPI 5148 • 4 ♂♂; same collection data as for preceding; CHNUFPI 5095 • 3 ♂♂; same collection data as for preceding; CHNUFPI 5231 • 8 ♂♂, 1 ♀; same collection data as for preceding; CHNUFPI 5103 • 2 ♂♂; same collection data as for preceding; CHNUFPI 5102 • 1 ♂, 1 ♀; same collection data as for preceding; CHNUFPI 5128 • 1 ♂, 1 ♀; same collection data as for preceding; CHNUFPI 5117 • 2 ♂♂; same collection data as for preceding; CHNUFPI 5120 • 4 ♂♂; same collection data as for preceding; CHNUFPI 5113 • 5 ♂♂; same collection data as for preceding; CHNUFPI 5228, 5177, 5181, 5156, 5169 • 3 ♂♂; Parque Nacional da Chapada das Mesas, 'site 2'; 7.150° S, 47.366° W; 300–310 m a.s.l.; 17 Dec. 2022; L.S. Carvalho *et al*. leg.; CHNUFPI 5101 • 3 ♂♂; same collection data as for preceding; CHNUFPI 5122 • 3 ♂♂; same collection data as for preceding; CHNUFPI 5166 • 2 ♂♂; same collection data as for preceding; CHNUFPI 5125 • 5 ♂♂; same collection data as for preceding; CHNUFPI 5153, 5150, 5152, 5225, 5112 • 1 ♀; same collection data as for preceding; CHNUFPI 5178 • 1 ♂, 1 ♀; Parque Nacional da Chapada das Mesas, 'site 3'; 7.146° S, 47.380° W; 320–330 m a.s.l.; 16 Dec. 2022; L.S. Carvalho *et al*. leg.; CHNUFPI 5158 • 2 ♂♂, 1 ♀; same collection data as for preceding; CHNUFPI 5088 • 3 ♂♂, 1 ♀; same collection data

as for preceding; CHNUFPI 5155 • 3 ♂♂; same collection data as for preceding; CHNUFPI 5123 • 4 ♂♂, 1 ♀; same collection data as for preceding; CHNUFPI 5159 • 1 ♂, 1 ♀; same collection data as for preceding; CHNUFPI 5147 • 4 ♂♂; same collection data as for preceding; CHNUFPI 5162 • 5 ♂♂, 1 ♀; same collection data as for preceding; CHNUFPI 5107 (2 ♂ used for SEM) • 5 ♂♂; same collection data as for preceding; CHNUFPI 5172 • 2 ♂♂; same collection data as for preceding; CHNUFPI 5179 • 1 ♂, 1 ♀; same collection data as for preceding; CHNUFPI 5118 • 2 ♂♂; same collection data as for preceding; CHNUFPI 5161 • 6 ♂♂; same collection data as for preceding; CHNUFPI 5096, 5129, 5184, 5140, 5133, 5180 • 4 ♂♂; Parque Nacional da Chapada das Mesas, 'site 4'; 7.128° S, 47.375° W; 290–300 m a.s.l.; 23 Aug. 2022; L.S. Carvalho and L.S. Carvalho leg.; CHNUFPI 5227 • 2 ♂♂; same collection data as for preceding; CHNUFPI 5145 • 2 ♂♂; same collection data as for preceding; CHNUFPI 5151 • 2 ♂♂; same collection data as for preceding; CHNUFPI 5142 • 2 ♂♂, 1 ♀; same collection data as for preceding; CHNUFPI 5154 • 16 ♂♂; same collection data as for preceding; CHNUFPI 5135, 5126, 5105, 5146, 5092, 5108, 5170, 5144, 5100, 5124, 5149, 5106, 5119, 5134, 5174, 5176 • 1 ♂, 1 ♀; Parque Nacional da Chapada das Mesas, 'site 5'; 7.125° S, 47.364° W; 280–290 m a.s.l.; 23 Aug. 2022; L.S. Carvalho and L.S. Carvalho leg.; CHNUFPI 5091 • 9 ♂♂; same collection data as for preceding; CHNUFPI 5094, 5104, 5115, 5173, 5097, 5109, 5099, 5127, 5165 • 3 ♂♂; Parque Nacional da Chapada das Mesas, 'site 6'; 7.109° S, 47.355° W; 270–280 m a.s.l.; 24 Aug. 2022; L.S. Carvalho and L.S. Carvalho leg.; CHNUFPI 5139 • 3 ♂♂, 3 ♀♀; same collection data as for preceding; CHNUFPI 5137 • 5 ♂♂; same collection data as for preceding; CHNUFPI 5183 • 3 ♂♂; same collection data as for preceding; CHNUFPI 5090 • 2 ♂♂; same collection data as for preceding; CHNUFPI 5093 • 2 ♂♂; same collection data as for preceding; CHNUFPI 5141 • 2 ♂♂; same collection data as for preceding; CHNUFPI 5168 • 8 ♂♂, 1 ♀; same collection data as for preceding; CHNUFPI 5175 • 5 ♂♂; same collection data as for preceding; CHNUFPI 5131 • 6 ♂♂; same collection data as

Fig. 71. *Sertana bumba* Huber gen. et sp. nov., paratype, ♂, from Brazil, Maranhão, Parque Nacional da Chapada das Mesas, CHNUFPI 5164. Left palp, prolateral, dorsal, and retrolateral views. Scale line = 0.2 mm.

for preceding; CHNUFPI 5132 • 4 ♂♂; same collection data as for preceding; CHNUFPI 5121 • 1 ♂, 2 ♀♀; same collection data as for preceding; CHNUFPI 5143 • 4 ♂♂, 1 ♀; same collection data as for preceding; CHNUFPI 5167 • 2 ♂♂; same collection data as for preceding; CHNUFPI 5136 • 4 ♂♂; same collection data as for preceding; CHNUFPI 5130 • 3 ♂♂; same collection data as for preceding; CHNUFPI 5229 • 2 ♂♂; same collection data as for preceding; CHNUFPI 5226 • 4 ♂♂; same collection data as for preceding; CHNUFPI 5089 • 3 ♂♂, 1 ♀; same collection data as for preceding; CHNUFPI 5098 • 2 ♂♂; same collection data as for preceding; CHNUFPI 5138 • 4 ♂♂; same collection data as for preceding; CHNUFPI 5160 • 9 ♂♂; same collection data as for preceding; CHNUFPI 5182, 5157, 5116, 5163, 5110, 5232, 5114, 5171, 5230.

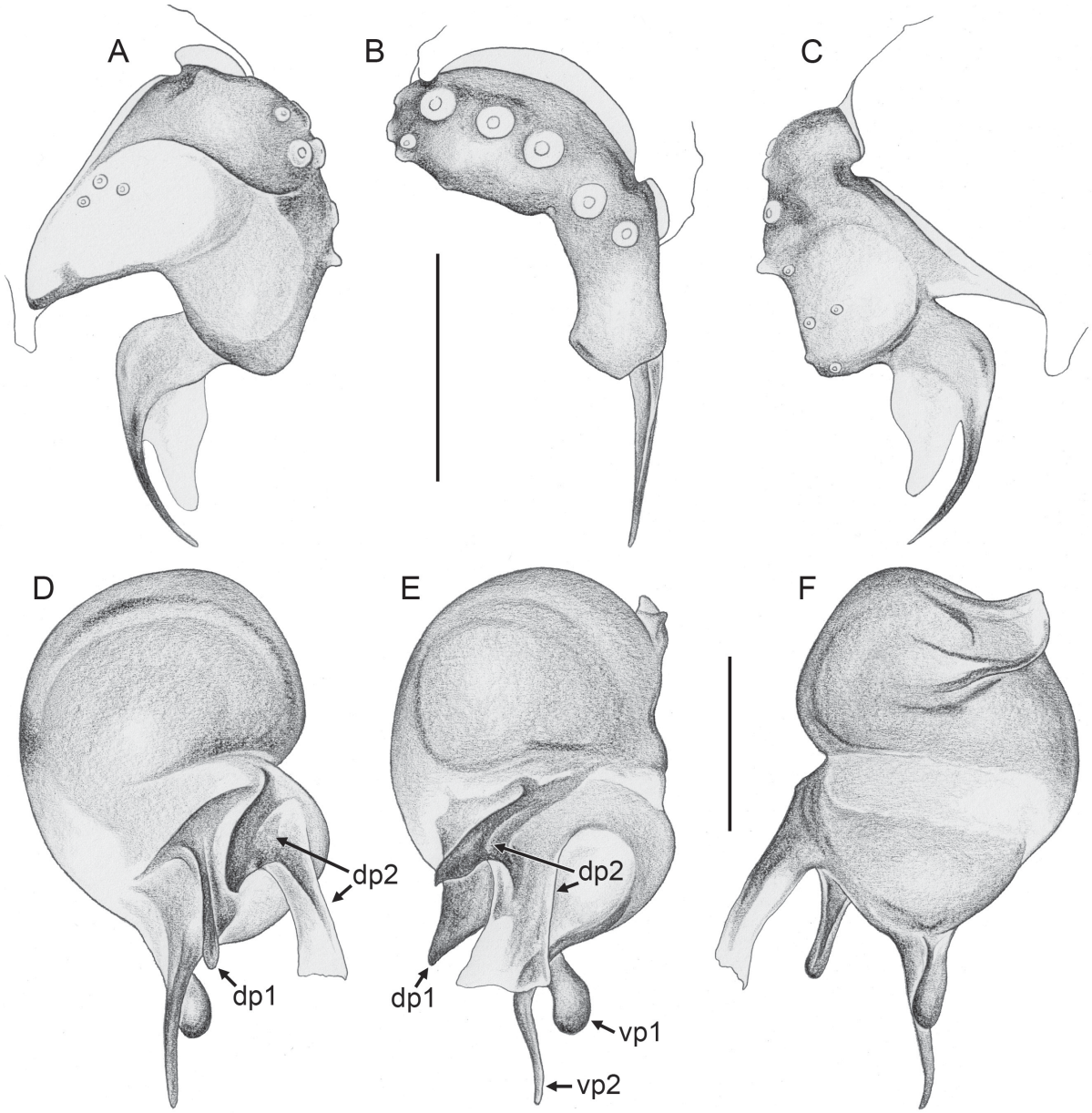

Fig. 72. *Sertana bumba* Huber gen. et sp. nov., paratype, ♂, from Brazil, Maranhão, Parque Nacional da Chapada das Mesas, CHNUFPI 5164. **A–C**. Left palpal tarsus and procursus, prolateral, dorsal, and retrolateral views. **D–F**. Left genital bulb, prolateral, dorsal, and retrolateral views. Abbreviations: dp1/dp2 = dorsal processes; vp1/vp2 = ventral processes. Scale lines = 0.1 mm.

Description

Male (holotype)

Measurements. Total body length 1.24, carapace width 0.50. Distance PME–PME 50 µm; diameter PME 40 µm; distance PME–ALE 20 µm; distance AME–AME 15 µm; diameter AME 35 µm. Leg 1: 2.65 (0.71+0.18+0.69+0.71+0.36), tibia 2: 0.64, tibia 3: 0.64, tibia 4: 0.98; tibia 1 L/d: 12; diameters of leg femora 100–110 µm, of leg tibiae 60 µm.

Color (in ethanol). Prosoma and legs pale ochre-yellow, carapace and legs without darker marks or rings; abdomen gray, with darker gray internal marks, ventrally with dark ochre plate in front of gonopore.

Body. Habitus similar to congeners (cf. Fig. 48). Ocular area barely raised. Carapace without thoracic groove. Clypeus unmodified. Sternum slightly wider than long (0.38/0.32), without anterior processes. Abdomen globular.

Chelicerae. As in Fig. 73A–B; with pair of long frontal apophyses in proximal position, distance between tips 115 µm; with stridulatory files (poorly visible in dissecting microscope).

Palps. As in Fig. 71; coxa unmodified; trochanter ventrally barely protruding; femur without proximal protrusion or process, distally slightly widened but otherwise unmodified; femur-patella condyles slightly shifted toward prolateral side; tibia-tarsus condyles slightly shifted toward retrolateral side; tarsus with strong dorsal hairs, without prolateral process; procursus (Fig. 72A–C) very simple, proximally light and with transparent dorsal flap, distally thin and sclerotized (dark); genital bulb (Fig. 72D–F) distally complex, with two ventral processes (vp1 and vp2 in Fig. 72E) and two dorsal processes (dp1 and dp2 in Fig. 72D–E); location of sperm duct opening presumably on membranous element of 'dp2'.

Legs. Without spines, without curved hairs; with short vertical hairs on tibia 1; retrolateral trichobothrium of tibia 1 at 59%; prolateral trichobothrium absent on tibia 1; tarsus 1 with 4–5 pseudosegments, distally fairly distinct.

Variation (males)

Tibia 1 in 66 males: 0.61–0.73 (mean 0.67).

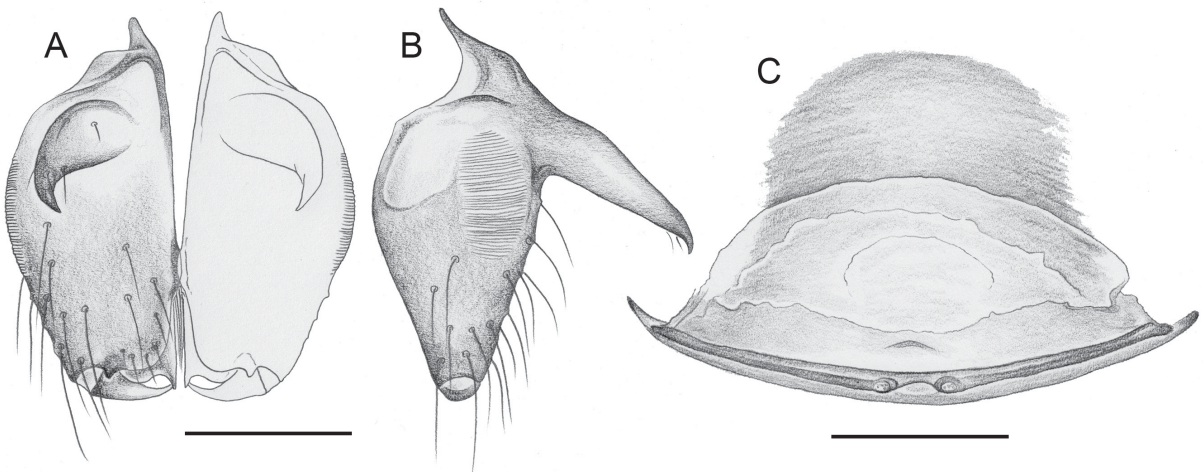

Fig. 73. *Sertana bumba* Huber gen. et sp. nov. **A–B**. Paratype, ♂, from Brazil, Maranhão, Parque Nacional da Chapada das Mesas, CHNUFPI 5164. **C**. Paratype, ♀, from Brazil, Maranhão, Parque Nacional da Chapada das Mesas, CHNUFPI 5137. **A–B**. Male chelicerae, frontal and lateral views. **C**. Cleared female genitalia, dorsal view. Scale lines = 0.1 mm.

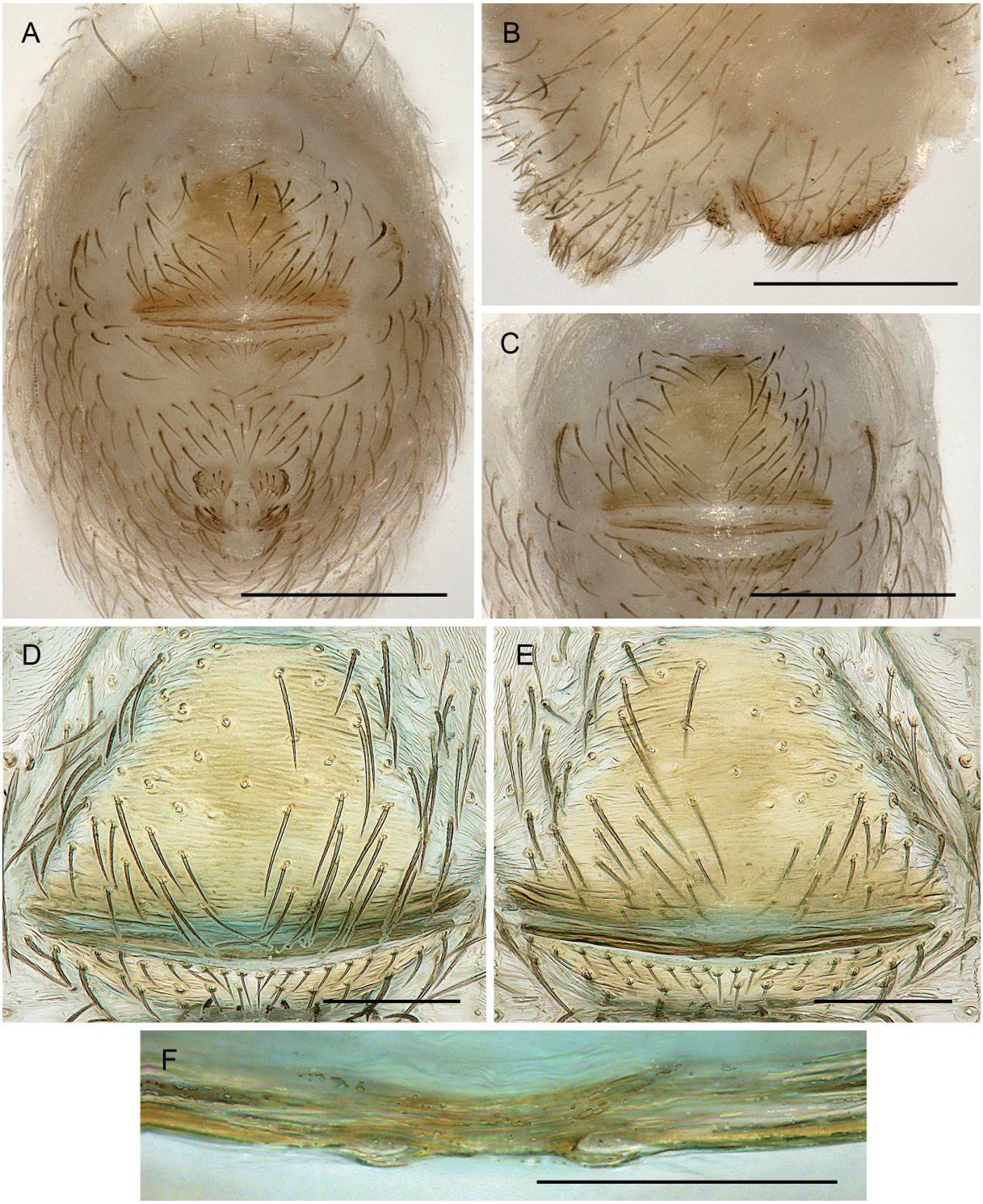

Fig. 74. *Sertana bumba* Huber gen. et sp. nov., paratypes, ♀♀, from Brazil, Maranhão, Parque Nacional da Chapada das Mesas. **A–B**. Female 1, CHNUFPI 5137. **C–F**. Female 2, CHNUFPI 5107. **A–B**. Abdomen, ventral and lateral views. **C**. Epigynum, ventral view. **D–E**. Cleared genitalia, ventral and dorsal views. **F**. Central element of internal genitalia, dorsal view. Scale lines: A–C = 0.3 mm; D–E = 0.1 mm; F = 0.05 mm.

Females

In general, similar to males; chelicerae apparently without stridulatory files (not confirmed with SEM); tibia 1 without short vertical hairs. Tibia 1 in 20 females: 0.62–0.70 (mean 0.67). Epigynum (Fig. 74A–C) anterior plate semicircular, weakly protruding, medially often slightly darker than laterally; posterior plate wide but short, simple; internal transversal sclerite often visible in uncleared females between anterior and posterior epigynal plates. Internal genitalia (Figs 73C, 74D–F) with transversal sclerite mostly very simple except medially; with large but very indistinct anterior membranous sac; apparently without pore plates.

Distribution

Known from a few neighboring localities (within 7 km) in western Maranhão, Brazil (Fig. 57).

Natural history

A total of 435 specimens were collected at the type locality, including 384 males (88%) and 51 females (12%). Sampling was conducted using pitfall traps placed in Cerrado s. str. vegetation on sandy soils. The strong male bias is likely a result of the sampling method, as pitfall traps tend to be more efficient for capturing the more mobile males that actively search for females (Uetz & Unzicker 1976; Churchill 1993; Álvares *et al.* 2004). In contrast, hand-collecting Ninetinae generally yields a female bias (e.g., ~60–70% females in the five species treated herein that were exclusively collected by hand and represented by more than 50 specimens each: *K. maracas* sp. nov.; *K. brumado* sp. nov.; *K. itacarambi* sp. nov.; *K. ibo* sp. nov.; *S. igapora* gen. et sp. nov.). Pitfall traps were arranged in 4 × 4 grids with three inter-trap spacings –1 m, 10 m, and 20 m– with nine replicates for each spacing (L.S. Carvalho *et al.* 2026). Nearly half of the specimens (n = 217; mean per replicate = 24.1 ± 19.5) were collected in the widest-spaced grids (20 m), while 26% (n = 115; mean = 12.8 ± 13.5) and 24% (n = 103; mean = 11.4 ± 8.25) were captured in the 1 m and 10 m grids, respectively. A generalized linear model with a negative binomial error distribution detected no significant effect of trap spacing on total specimen abundance when compared to a null model (likelihood-ratio test: $\chi^2 = 3.51$, df = 2, p = 0.173). Additionally, sampling conducted at twelve gallery forest sites yielded only one specimen of this species out of 1474 specimens collected using pitfall traps, suggesting an association with open environments (de Paula *et al*. 2026).

Sertana capivara Huber gen. et sp. nov.
urn:lsid:zoobank.org:act:8969CEBD-4AFE-424E-95D6-5387FEE4E119
Figs 75–78

Diagnosis

Males are distinguished from those of known congeners by shape of procursus (Fig. 76A–C; long and slender, proximally bent towards dorsal, distal part straight, without side branch, without transparent flap), by shapes of bulbal processes (Fig. 76D–G; dorsally with pointed prolateral process, dorsal elements large and hiding ventral processes in dorsal view), and by male cheliceral apophyses in proximal position and directed towards frontal (Fig. 77A–B). Females very similar to those of known congeners; internally distinguished from all congeners by medially interrupted transversal sclerite (Figs 77C, 78C, E).

Etymology

The species name is derived from the type locality; noun in apposition.

Type material

Holotype

BRAZIL – **Piauí** • ♂; Coronel José Dias, Parque Nacional da Serra da Capivara, around Toca de Cima dos Pilões; 8.8635° S, 42.5571° W; 415 m a.s.l.; 15 Jul. 2023; L.S. Carvalho and E.G. Noetzold leg.; CHNUFPI 5010.

Paratype

BRAZIL – **Piauí** • 1 ♀; together with holotype and eight juveniles; CHNUFPI 5010.

Other material examined

BRAZIL – **Piauí** • 1 ♂; Coronel José Dias, Parque Nacional da Serra da Capivara, near Boqueirão do Ferreira; 8.7476° S, 42.4870° W; 585 m a.s.l.; 9 Dec. 2019; L.S. Carvalho leg.; CHNUFPI 4047 ("Carv64"; voucher of E074) • 1 ♀; São Raimundo Nonato, Parque Nacional da Serra da Capivara, Baixão das Andorinhas; 8.8625° S, 42.6873° W; 485 m a.s.l.; 15 Jul. 2023; L.S. Carvalho and E.G. Noetzold leg.; CHNUFPI 5013 • 1 ♀, 12 juvs; same collection data as for preceding; CHNUFPI 5014 • 1 ♂, 1 ♀; same collection data as for preceding; CHNUFPI 5022.

Description

Male (holotype)

Measurements. Total body length 0.96, carapace width 0.47. Distance PME–PME 45 µm; diameter PME 45 µm; distance PME–ALE 20 µm; distance AME–AME 15 µm; diameter AME 20 µm. Leg 1: 2.15 (0.62+0.15+0.56+0.52+0.30), tibia 2: 0.49, tibia 3: 0.46, tibia 4: 0.66; tibia 1 L/d: 9; diameters of leg femora 80–90 µm, of leg tibiae 60 µm.

Color (in ethanol). Prosoma and legs pale ochre-yellow, carapace and legs without darker marks or rings; abdomen mostly pale orange, ventrally ochre-gray with dark ochre plate in front of gonopore.

Body. Habitus similar to congeners (cf. Fig. 48). Ocular area barely raised. Carapace without thoracic groove. Clypeus unmodified. Sternum barely wider than long (0.31/0.28), without anterior processes. Abdomen globular.

Chelicerae. As in Fig. 77A–B; with pair of long frontal apophyses in proximal position, distance between tips 65 µm; with distinct stridulatory files.

Fig. 75. *Sertana capivara* Huber gen. et sp. nov., ♂, from Brazil, Piauí, Parque Nacional da Serra da Capivara, near Boqueirão do Ferreira, CHNUFPI 4047. Left palp, prolateral, dorsal, and retrolateral views. Scale line = 0.2 mm.

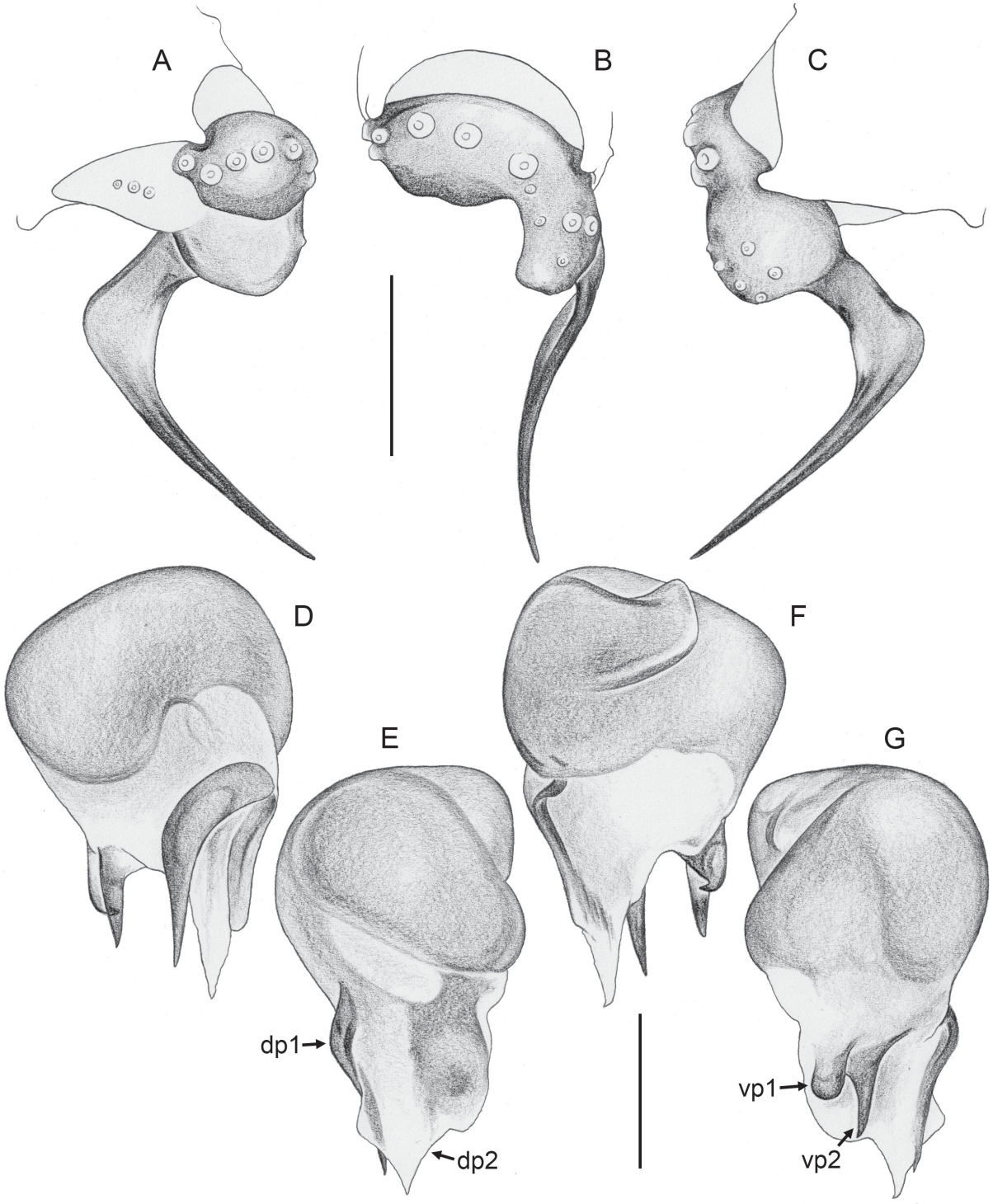

Fig. 76. *Sertana capivara* Huber gen. et sp. nov., ♂, from Brazil, Piauí, Parque Nacional da Serra da Capivara, near Boqueirão do Ferreira, CHNUFPI 4047. **A–C**. Left palpal tarsus and procursus, prolateral, dorsal, and retrolateral views. **D–G**. Left genital bulb, prolateral, dorsal, retrolateral, and ventral views. Abbreviations: dp1/dp2 = dorsal processes; vp1/vp2 = ventral processes. Scale lines = 0.1 mm.

Palps. As in Fig. 75; coxa unmodified; trochanter ventrally barely protruding; femur with very indistinct retrolateral proximal protrusion, distally slightly widened but otherwise unmodified; femur-patella condyles shifted toward prolateral side; tibia-tarsus condyles slightly shifted toward retrolateral side; tarsus with strong dorsal hairs, without prolateral process; procursus (Fig. 76A–C) very simple, proximally light, without membranous flap, distally thin and sclerotized, directed towards dorsal; genital bulb (Fig. 76D–G) distally complex, with two ventral processes (vp1 and vp2 in Fig. 76G) and two dorsal processes (dp1 and dp2 in Fig. 76E); location of sperm duct opening presumably at element 'dp2'.

Legs. Without spines, without curved hairs; with short vertical hairs on tibiae 1 and 2; retrolateral trichobothrium of tibia 1 at 62%; prolateral trichobothrium absent on tibia 1; tarsus 1 with 4–5 pseudosegments, distally fairly distinct.

Variation (males)

Tibia 1 in other male: 0.58 (missing in third male). Abdomen in other specimens ochre-gray.

Females

In general, similar to males; chelicerae apparently without stridulatory files (not confirmed with SEM); tibia 1 without short vertical hairs. Tibia 1 in four females: 0.53, 0.56, 0.56, 0.59. Epigynum (Fig. 78A–B) anterior plate semicircular, weakly protruding; posterior plate wide but short, simple; internal transversal sclerite not visible in uncleared females. Internal genitalia (Figs 77C, 78C–E) with indistinct transversal sclerite only laterally, i.e., medially absent or unsclerotized, without complex median elements but possibly with tiny pore plates limited to a few pores (arrows in Fig. 78C); with indistinct anterior membranous sac.

Distribution

Known from three neighboring localities in the Serra da Capivara, southern Piauí, Brazil (Fig. 57).

Natural history

This species is known solely from Parque Nacional da Serra da Capivara, a protected area in Brazil's semiarid Caatinga biome. All individuals were collected beneath stones, fallen logs, or among ground

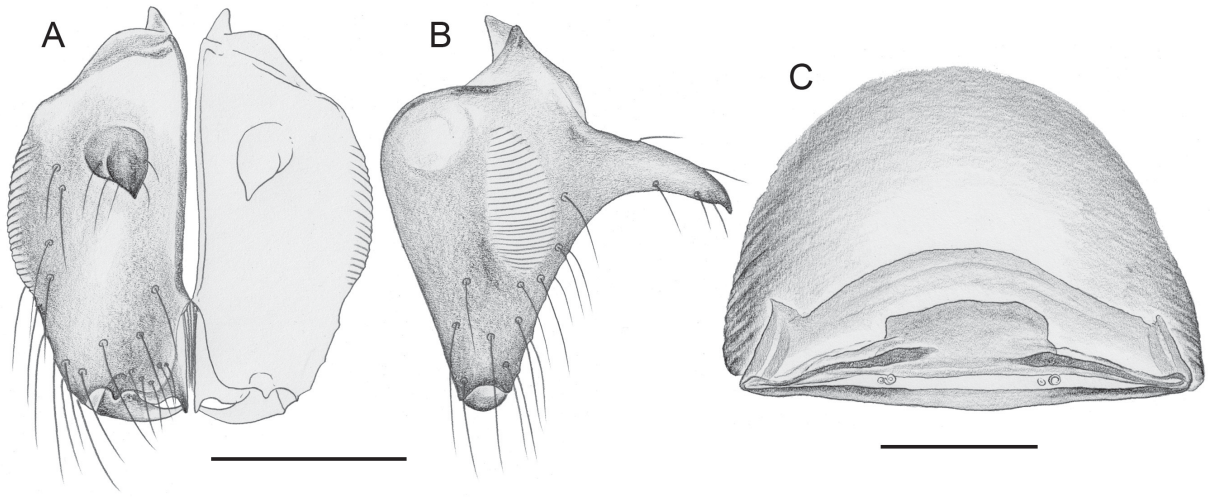

Fig. 77. *Sertana capivara* Huber gen. et sp. nov. **A–B**. ♂, from Brazil, Piauí, Parque Nacional da Serra da Capivara, near Boqueirão do Ferreira, CHNUFPI 4047. **C**. Paratype, ♀, from Parque Nacional da Serra da Capivara, around Toca de Cima dos Pilões, CHNUFPI 5010. **A–B**. Male chelicerae, frontal and lateral views. **C**. Cleared female genitalia, dorsal view. Scale lines = 0.1 mm.

pebbles. When disturbed, the spiders ran swiftly, and no webs were observed during any collection event. Some specimens were found on sun-exposed sandstone outcrops, among loose pebbles where no shade was available. A sampling carried out in a nearby limestone karst site did not reveal any specimens, neither in epigean nor in hypogean environments. One egg sac had six eggs arranged in a single layer; egg diameter was 0.44.

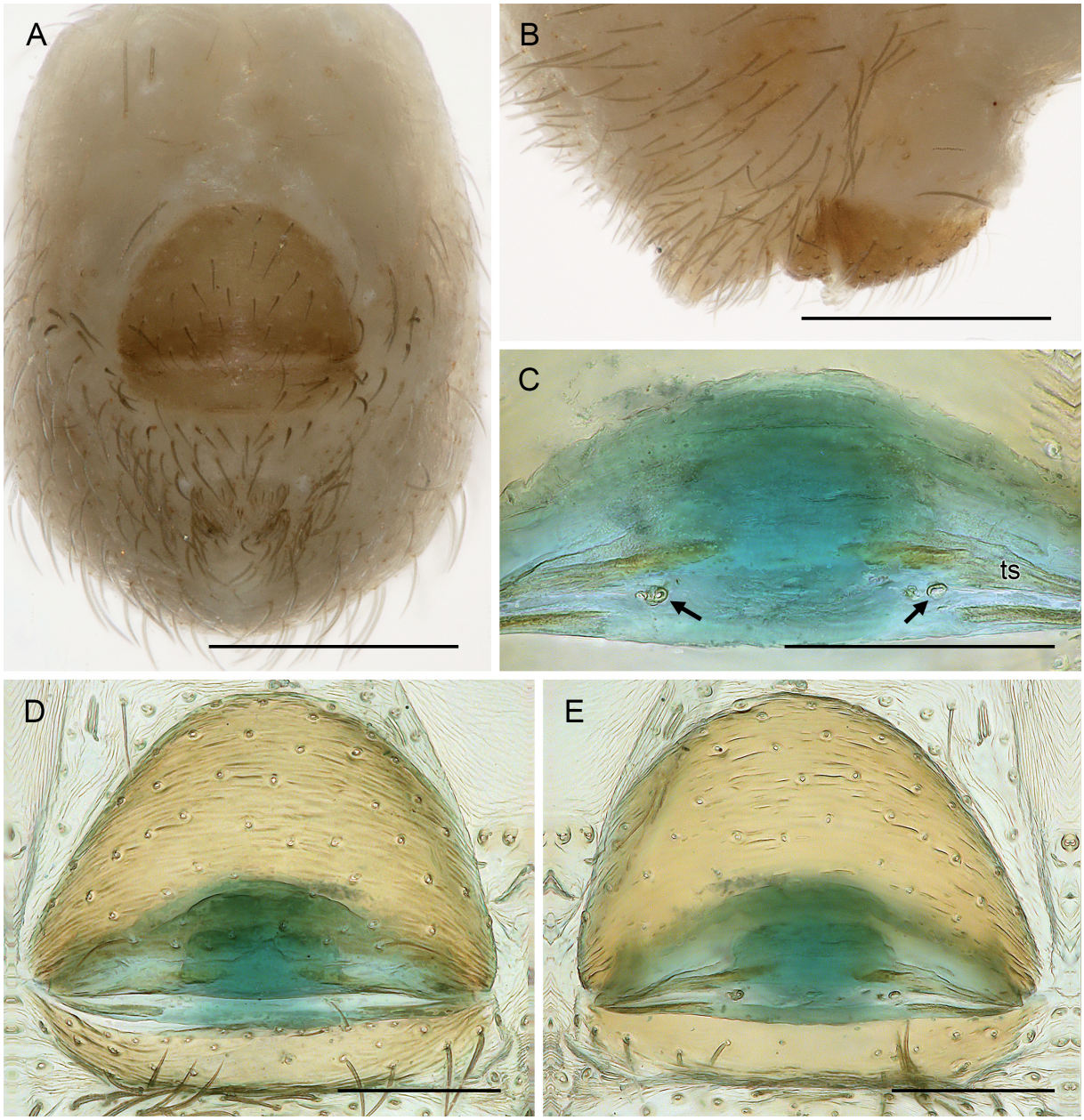

Fig. 78. *Sertana capivara* Huber gen. et sp. nov., paratype, ♀, from Parque Nacional da Serra da Capivara, around Toca de Cima dos Pilões, CHNUFPI 5010. **A**–**B**. Abdomen, ventral and lateral views. **C**. Central element of internal genitalia, dorsal view; arrows point at putative pore plates. **D**–**E**. Cleared genitalia, ventral and dorsal views. Scale lines: A–B = 0.3 mm; C–E = 0.1 mm.

Environmental niche modeling

Kambiwa neotropica (Kraus, 1957)

Environmental niche modeling revealed high relative habitat suitability (RHS) under current conditions in the region extending from eastern Maranhão to western Rio Grande do Norte, encompassing areas of Cerrado (between Maranhão and Piauí), and Caatinga (between Piauí, Ceará, and Rio Grande do Norte) biomes (Fig. 79). The southernmost and easternmost records of *K. neotropica* were not recovered in areas of high RHS. Additionally, isolated regions of median RHS were observed in the eastern boundaries of the Caatinga biome (Fig. 79; Supp. file 2). The total area with relatively high habitat suitability for this species in the current climate is estimated at approximately 90 000 km², with only 1363 km² (1.5% of the total area) located within strict protection conservation units (Table 3). Under global warming scenarios, habitat suitability for this species is projected to increase significantly (Fig. 82A–B; Table 3). For the closest (2041–2060) and less aggressive global warming scenario (i.e., ssp245), this increase results in an area 1.6 times greater than the current suitable area. Under the longer-term (2081–2100) and more severe (i.e., ssp585) scenarios, the increase is even higher (Fig. 82A–B; Table 3). The expansion of suitable area is projected to occur in the westernmost and easternmost regions with median-to-high environmental suitability in the present time (Fig. 79B–E).

Kambiwa coribe sp. nov.

Environmental niche modeling revealed high relative habitat suitability (RHS) under current conditions in the ecotonal region between the Cerrado and Caatinga biomes in central Brazil (Fig. 80). Additionally, isolated regions of high RHS were observed within the Caatinga biome in the state of Ceará and within the Cerrado biome in the state of Mato Grosso (Fig. 80). The total area with relatively high habitat suitability for this species in the current climate is estimated at approximately 75 000 km², with only 5520 km² (7.4% of the total area) situated within strict protection conservation units (Table 3). Under global warming scenarios, habitat suitability for this species is projected to increase significantly (Fig. 82C–D; Table 3). For the nearest-term (2041–2060) and less aggressive global warming scenario (i.e., ssp245), this increase is nearly six-fold compared to the current suitable area. Under longer-term (2081–2100) and more severe scenarios (i.e., ssp585), it is even greater (up to 20 times; Fig. 82C–D; Table 3). The expansion of suitable area is projected to occur throughout the Cerrado biome, particularly southward and southwestward, as well as extending into the core region of the Caatinga biome (Fig. 80).

Kambiwa ibo sp. nov.

Environmental niche modeling revealed high relative habitat suitability (RHS) under current conditions across nearly the entire Caatinga biome (Fig. 81). The total area with relatively high habitat suitability for this species in the present climate is estimated at approximately 47 000 km², with only 3773 km² (8.0% of the total area) situated within strict protection conservation units (Table 3). Under global warming scenarios, habitat suitability for this species is mostly projected to decrease (Fig. 82E–F; Table 3). Under the nearest-term (2041–2060) and less aggressive global warming scenario (i.e., ssp245), the area of high relative suitability remains almost identical to that of the current period (Table 3). However, this apparent stability results from a contraction in the northern portion and a southwestward expansion of areas with environmental suitability (Fig. 81B). When considering longer time scales (2081–2100) and/or more severe global warming scenarios (i.e., ssp585), the area of high relative suitability is expected to retain up to as little as 7.7% of its present extent (Fig. 81C, E; Table 3).

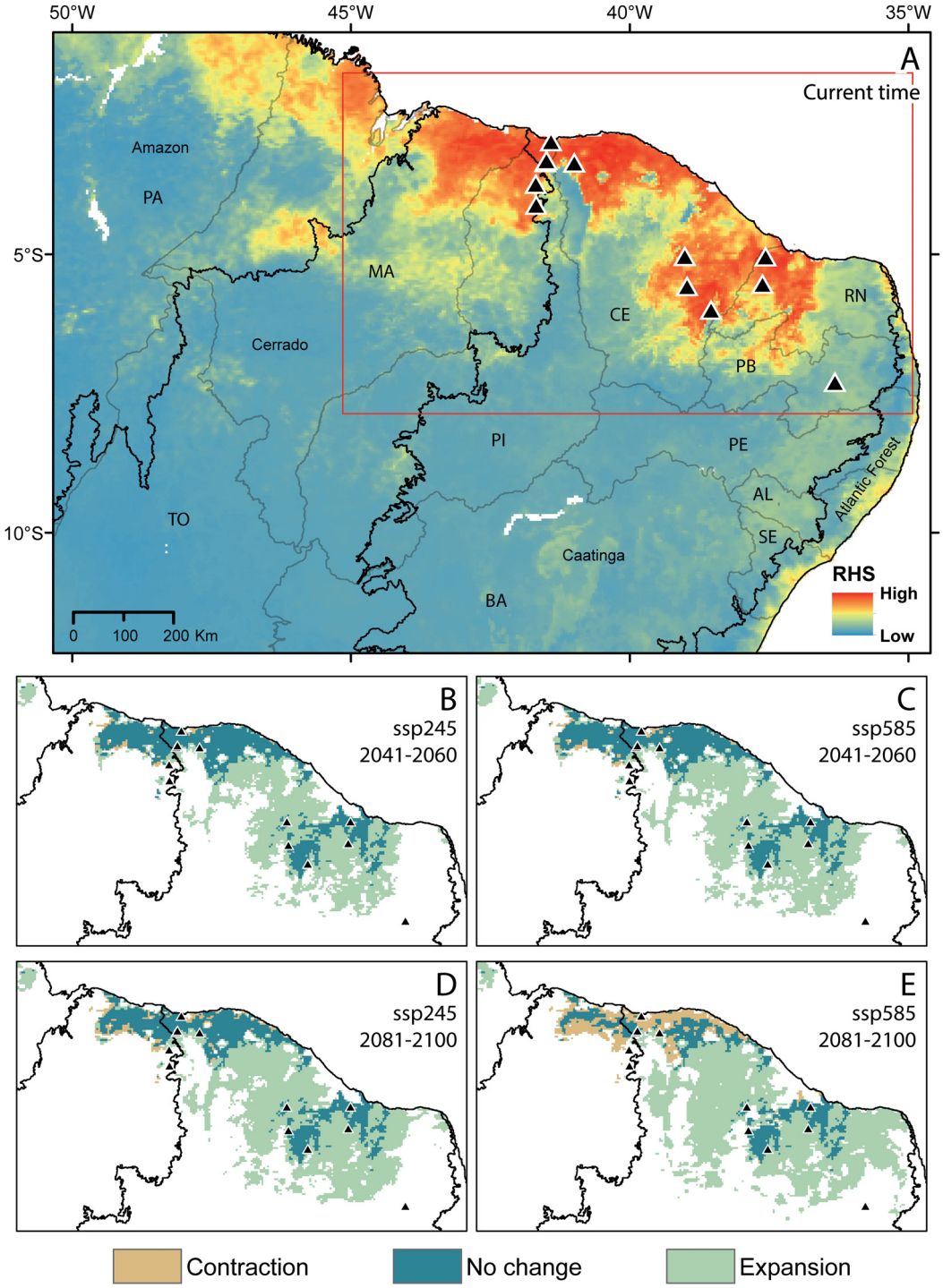

Fig. 79. Environmental niche modeling under current (A) and future (B–E) climatic and edaphic conditions for *Kambiwa neotropica* (Kraus, 1957), considering two time periods (B–C: 2041–2060; D–E: 2081–2100) and two carbon emission scenarios (B, D: ssp245; C, E: ssp585). Different colors in the future scenarios (B–E) represent changes compared to the current scenario: orange indicates contraction, light green denotes expansion, and dark green indicates stability. Abbreviation: RHS = relative habitat suitability. Brazilian states: AL = Alagoas; BA = Bahia; CE = Ceará; MA = Maranhão; PA = Pará; PB = Paraíba; PE = Pernambuco; PI = Piauí; RN = Rio Grande do Norte; SE = Sergipe; TO = Tocantins. Red rectangle in A represents the region depicted in Figs B–E.

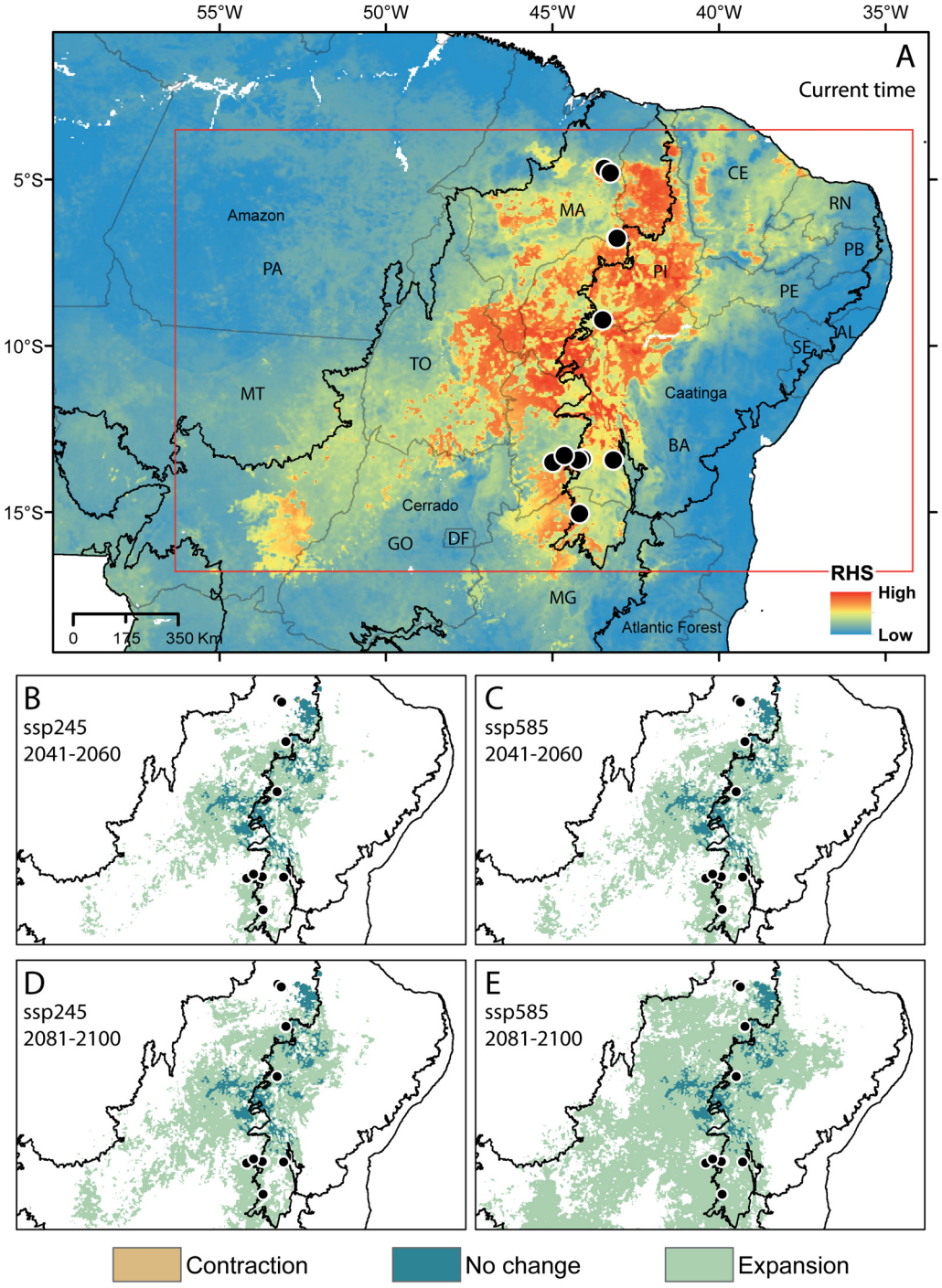

Fig. 80. Environmental niche modeling under current (A) and future (B–E) climatic and edaphic conditions for *Kambiwa coribe* Huber sp. nov., considering two time periods (B–C: 2041–2060; D–E: 2081–2100) and two carbon emission scenarios (B, D: ssp245; C, E: ssp585). Different colors in the future scenarios (B–E) represent changes compared to the current scenario: orange indicates contraction, light green denotes expansion, and dark green indicates stability. Abbreviation: RHS = relative habitat suitability. Brazilian states: AL = Alagoas; BA = Bahia; CE = Ceará; DF = Distrito Federal; GO = Goiás; MA = Maranhão; MG = Minas Gerais; MT = Mato Grosso; PA = Pará; PB = Paraíba; PE = Pernambuco; PI = Piauí; RN = Rio Grande do Norte; SE = Sergipe; TO = Tocantins. Red rectangle in A represents the region depicted in Figs B–E.

Table 3. Current and future projected suitable habitat for three species of *Kambiwa* Huber, 2000. Summary of total and protected suitable habitat (in km²), along with the percentage of protected area, for three species of *Kambiwa* under different climate scenarios and time periods. Values in parentheses indicate the ratio between the projected scenario mean and the mean value for the current period.

Species	Scenario	Total area (km²)	Protected area (km²)	Protected area (%)
Kambiwa neotropica	Current	89 619	1363	1.5
	ssp245 | 2041–2060	146 311 ± 4399 (163%)	2546 ± 181 (187%)	1.7 ± 0.1 (114%)
	ssp245 | 2081–2100	166 354 ± 4305 (186%)	3377 ± 191 (248%)	2.0 ± 0.2 (134%)
	ssp585 | 2041–2060	156 948 ± 6179 (175%)	3011 ± 288 (221%)	1.9 ± 0.2 (126%)
	ssp585 | 2081–2100	173 343 ± 19529 (193%)	4534 ± 257 (333%)	2.6 ± 0.3 (173%)
Kambiwa coribe	Current	74 852	5519	7.4
	ssp245 | 2041–2060	439 174 ± 76 282 (587%)	35 124 ± 4148 (636%)	8.1 ± 0.5 (109%)
	ssp245 | 2081–2100	663 065 ± 132 852 (886%)	44 207 ± 5136 (801%)	6.8 ± 0.5 (92%)
	ssp585 | 2041–2060	528 921 ± 58 353 (707%)	38 711 ± 3706 (701%)	7.3 ± 0.3 (99%)
	ssp585 | 2081–2100	1 434 895 ± 316 322 (1917%)	79 745 ± 14 999 (1445%)	5.659 ± 0.3 (76%)
Kambiwa ibo	Current	47 470	3773	8.0
	ssp245 | 2041–2060	47 556 ± 7844 (100%)	3272 ± 580 (87%)	6.9 ± 0.3 (87%)
	ssp245 | 2081–2100	27 690 ± 11 737 (58%)	1915 ± 865 (51%)	6.8 ± 0.8 (86%)
	ssp585 | 2041–2060	42 546 ± 9892 (90%)	2882 ± 685 (76%)	6.8 ± 0.6 (85%)
	ssp585 | 2081–2100	3659 ± 4289 (7.7%)	256 ± 275 (6.8%)	7.2 ± 4.1 (90%)

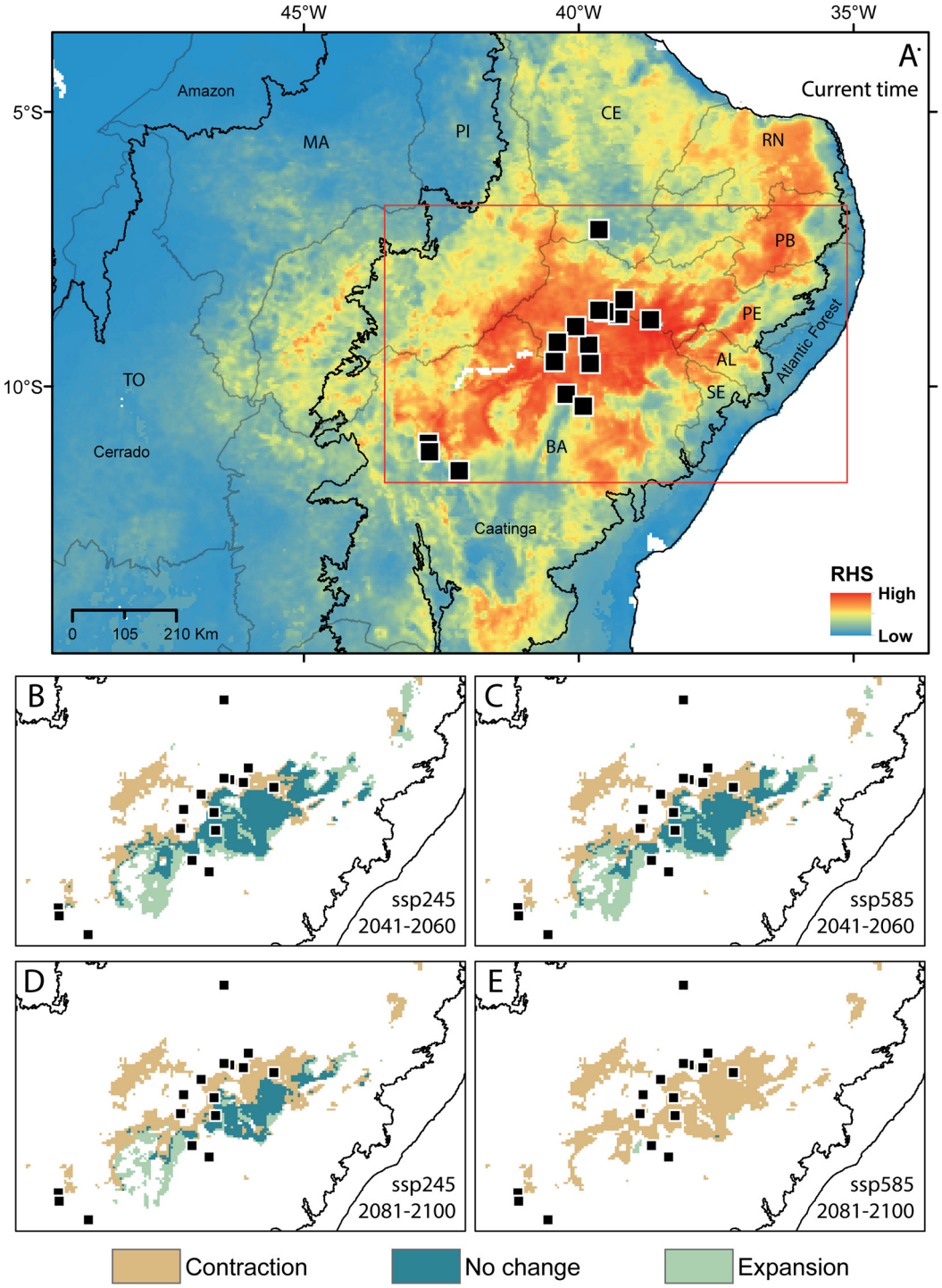

Fig. 81. Environmental niche modeling under current (A) and future (B–E) climatic and edaphic conditions for *Kambiwa ibo* Huber sp. nov., considering two time periods (B–C: 2041–2060; D–E: 2081–2100) and two carbon emission scenarios (B, D: ssp245; C, E: ssp585). Different colors in the future scenarios (B–E) represent changes compared to the current scenario: orange indicates contraction, light green denotes expansion, and dark green indicates stability. Abbreviation: RHS = relative habitat suitability. Brazilian states: AL = Alagoas; BA = Bahia; CE = Ceará; MA = Maranhão; PB = Paraíba; PE = Pernambuco; PI = Piauí; RN = Rio Grande do Norte; SE = Sergipe; and TO = Tocantins. Red rectangle in A represents the region depicted in Figs B–E.

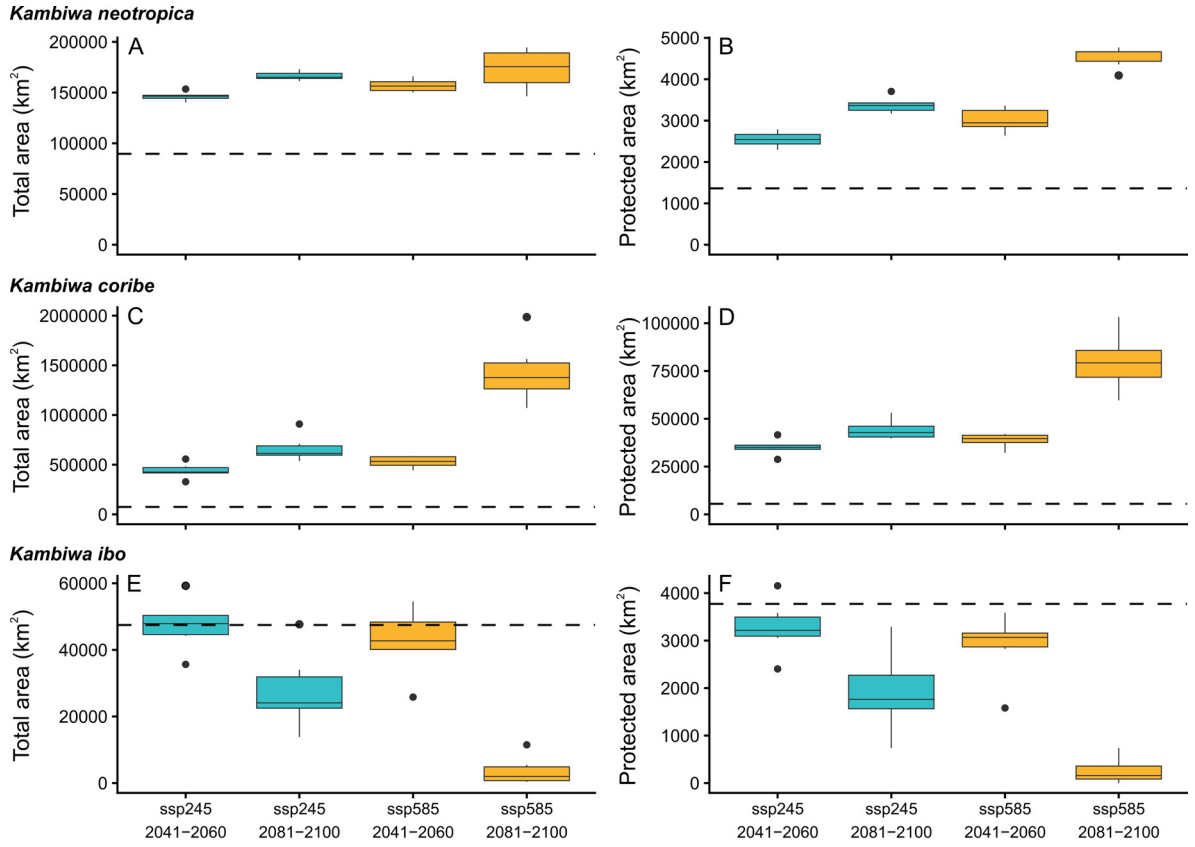

Fig. 82. Summary of total and protected suitable habitat (in km²), and the percentage protected, for three species of *Kambiwa* Huber, 2000 under different climate scenarios (turquoise: ssp245; orange: ssp585) and time periods (2041–2060 and 2081–2100). The dotted line reflects the mean estimated value for the current period.

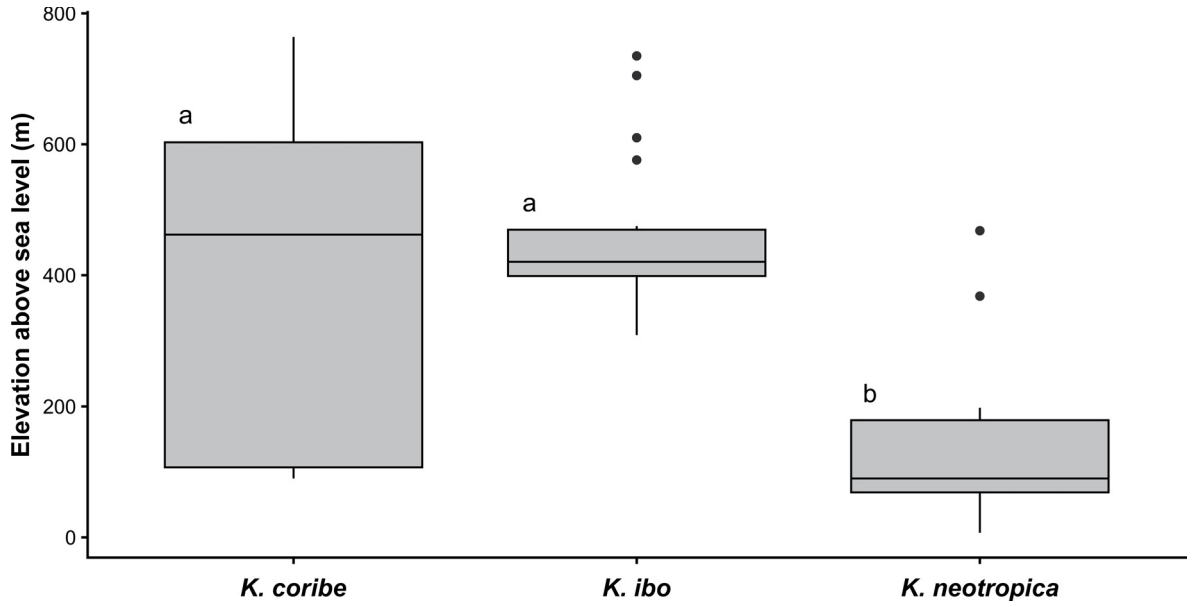

Fig. 83. Known altitudinal variation for records of *Kambiwa coribe* Huber sp. nov., *K. ibo* Huber sp. nov. and *K. neotropica* (Kraus, 1957). Letters above boxes indicate significantly different groups.

Karyology

The male diploid karyotype of *Kambiwa ibo* sp. nov. comprises 28 chromosomes including a $X_1X_2X_3Y$ system (Figs 84, 85G). The chromosomes are biarmed except for the tiny Y chromosome (Fig. 84), which has a transient morphology between submetacentric and subtelocentric (Figs 84B, 85I). The biarmed chromosomes are metacentric, except for a large submetacentric chromosome (no. 3) in the karyotype containing X chromosomes (Fig. 84A) and the chromosomes of a small submetacentric pair. The large submetacentric chromosome is only present in the karyotype with X chromosomes, suggesting that it is one of these chromosomes. As for the chromosome of the small submetacentric pair, it is in the ninth position in a haploid karyotype containing a Y chromosome (Fig. 84B) but in the twelfth position in a haploid karyotype containing three X chromosomes (Fig. 84A). Although chromosomes X_1, X_2, and X_3 cannot be unequivocally distinguished from other chromosomes in the karyotype containing X chromosomes, they are larger than the chromosome of the small metacentric pair. Consequently, the chromosome of this pair is located in the karyotype with X chromosomes at the twelfth position, not at the ninth position as in the karyotype with Y chromosomes. The length of chromosome pairs ranged from 9.48 to 6.04% of the TCL of the haploid karyotype including the Y chromosome (each pair was represented by one chromosome at this karyotype); the relative length of the Y chromosome at this set was 1.21% only. The absolute length of the Y chromosome depended on the phase of division, and ranged from 1.19 μm (mitotic metaphase) to 2.83 μm (metaphase II) and 3.27 μm (prophase II). Chromosomes of the $X_1X_2X_3Y$ system did not differ by their behavior or pycnosis from the other chromosomes at the spermatogonial mitotic metaphase (Fig. 85A). In contrast, they exhibited positive heteropycnosis (i.e., they were stained more intensively than chromosome pairs) during premeiotic interphase, some periods

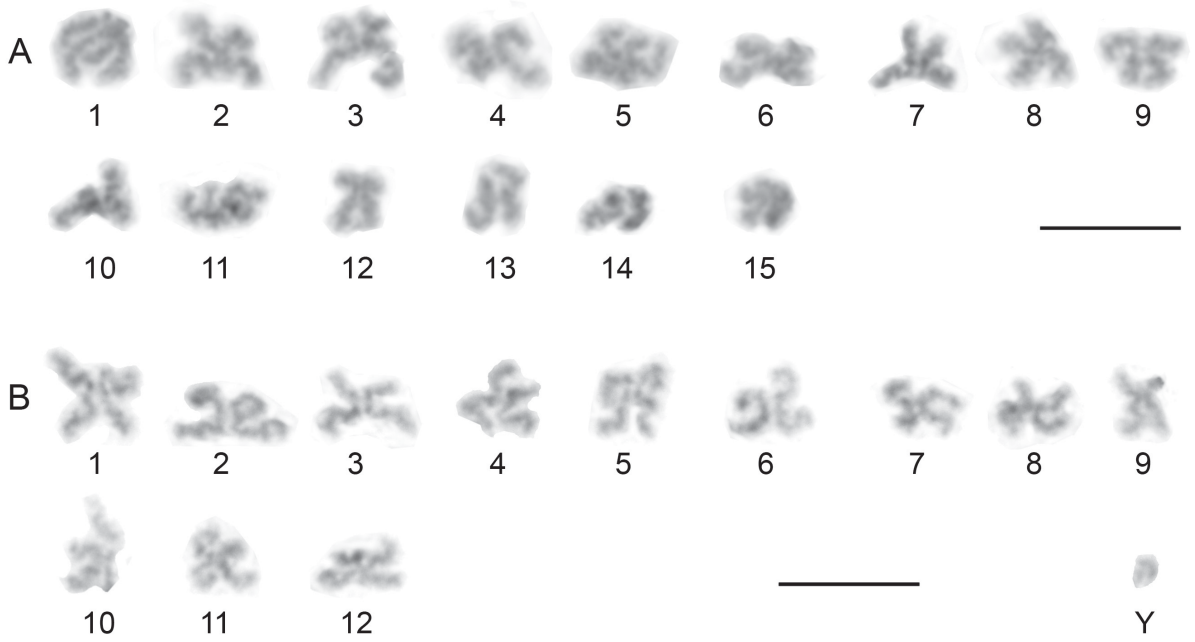

Fig. 84. Male haploid karyotypes of *Kambiwa ibo* Huber sp. nov. **A**. Karyotype comprising 15 chromosomes. Each chromosome pair is represented by one chromosome. The karyotype also includes three X chromosomes, which cannot be distinguished from other chromosomes. All chromosomes are metacentric except for the third and twelfth chromosomes, which are submetacentric. **B**. Karyotype consisting of 13 chromosomes including tiny Y chromosome. All chromosomes are metacentric except for the ninth chromosome, which is submetacentric, and the Y chromosome, which has a transient submetacentric/subtelocentric morphology. Scale lines = 10 μm.

of prophase I, as well as throughout prophase II (Fig. 85B–F, H–I). During the premeiotic interphase, the sex chromosomes formed a highly condensed body on the periphery of the nucleus (Fig. 85B). During pachytene, the sex chromosomes were positively heteropycnotic and associated at the periphery of the plate (Fig. 85C–D); their mode of pairing could not be determined. Following the pachytene, the nuclei entered the so-called diffuse stage. Bivalents became considerably decondensed. In contrast to this, sex chromosomes formed a compact, highly condensed body (Fig. 85E). During early diplotene, the sex chromosome body persisted and bivalents recondensed. Remarkably, bivalents had a similar

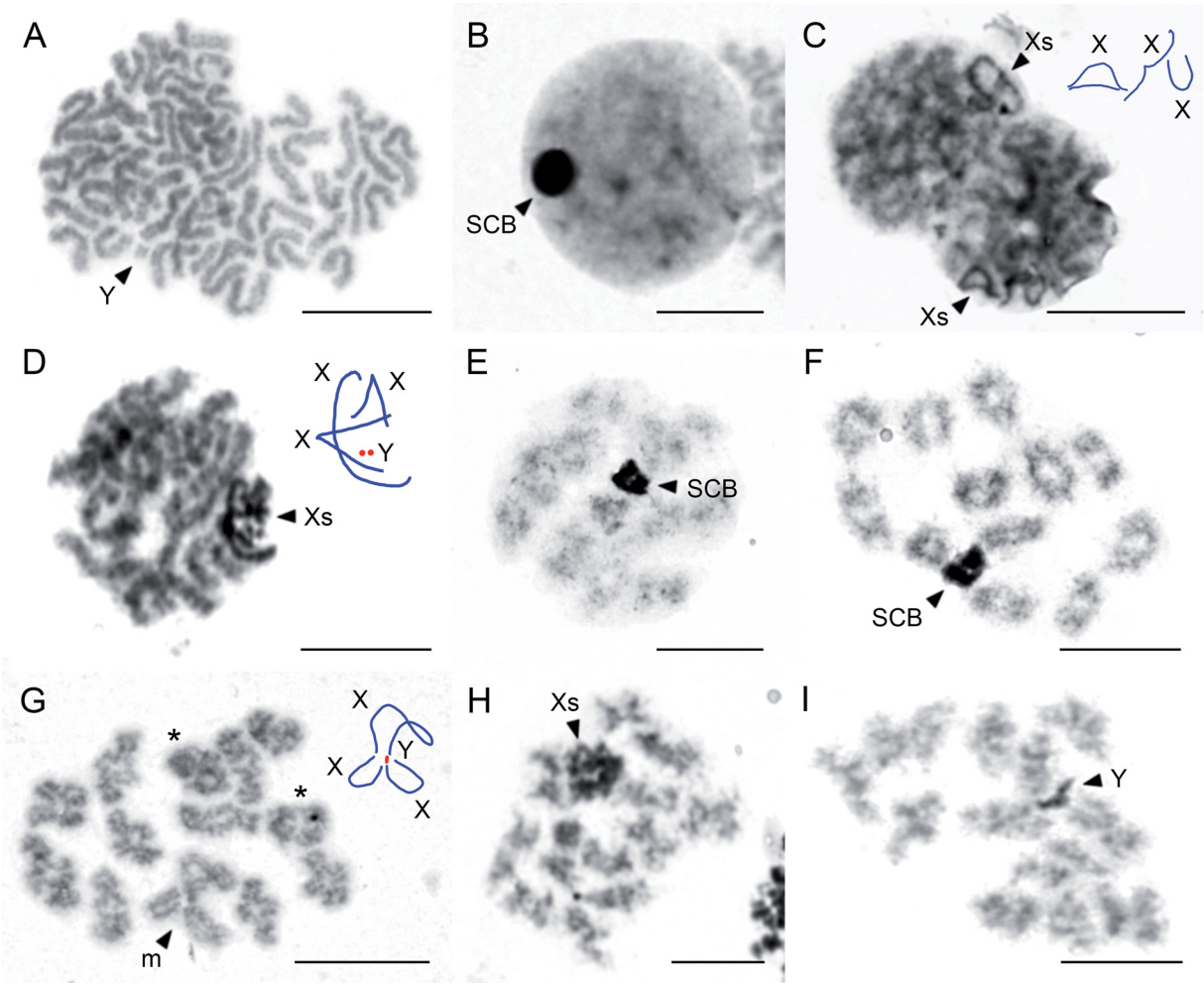

Fig. 85. Male germline and chromosome plates of *Kambiwa ibo* Huber sp. nov. **A**. Two spermatogonial mitotic metaphases, partially fused. Note tiny Y chromosome. **B**. Premeiotic interphase. Note highly condensed sex chromosome body at periphery of nucleus. **C–D**. Pachytene, sex chromosomes are positively heteropycnotic and associated at periphery of nucleus. Note schemes of sex chromosome association (blue: X chromosomes; red: Y chromosome). **E**. Diffuse stage. Bivalents are considerably decondensed; sex chromosomes form highly condensed body. **F**. Early diplotene consisting of 12 bivalents and highly condensed sex chromosome body. **G**. Late diplotene comprising 12 bivalents and sex chromosome tetravalent. Note scheme of sex chromosome pairing (blue: X chromosomes; red: Y chromosome). Asterisks denote bivalents with two chiasmata. **H**. Prophase II containing positively heteropycnotic cluster of X chromosomes. **I**. Prophase II containing positively heteropycnotic Y chromosome. Abbreviations: m = sex chromosome multivalent (tetravalent); SCB = sex chromosome body; Xs = X chromosomes; Y = Y chromosome. Scale lines = 10 µm.

morphology as in diakinesis during this period (their chiasmata looked as if they were terminalized). This was probably due to a relatively high condensation of bivalents during this period (Fig. 85F). During late diplotene and diakinesis, bivalents and sex chromosomes did not differ in the degree of condensation. Chiasmata were not terminalized during late diplotene. The sex chromosomes formed a tetravalent during these periods. Each X chromosome formed a loop, pairing by both ends with the tiny Y chromosome, which was placed in the middle of the tetravalent. Bivalents contained a low number of chiasmata; most bivalents had a single chiasma only (Fig. 85G). The number of chromosome plates was, however, too low to determine the frequency of chiasmata. Sex chromosomes were more condensed than the other chromosomes during prophase II (Fig. 85H–I). Moreover, X chromosomes were associated during this period (Fig. 85H).

Discussion

Habitat suitability

The genera *Kambiwa* and *Sertana* gen. nov. are typical ninetine spiders with respect to the environmental niche they occupy. In Brazil, Ninetinae appear largely restricted to the diagonal of open formations (sensu Werneck 2011), including the Cerrado in central Brazil and the Caatinga in northeastern Brazil (e.g., Figs 13, 57; Huber *et al.* 2024b). These biomes are expected to face significant climate change, including an increase in mean temperatures, reduction in rainfall, and increased desertification (Torres *et al.* 2017; Hofmann *et al.* 2021). Previous studies carried out with plants (Velazco *et al.* 2019; Moura *et al.* 2023a), scorpions (Lira *et al.* 2020), psammophilous squamates (Oliveira *et al.* 2024), mammals (Moura *et al.* 2023b; Costa-Pinto *et al.* 2024) and birds (Gonçalves *et al.* 2023) from these biomes have provided evidence of species richness impoverishment and a decrease in habitat suitability for most taxa.

Following these predictions, we expected that ninetine spiders would face similar challenges. However, the three modeled species of *Kambiwa* revealed contrasting responses to possible future climate changes. While Ninetinae in general are recognized for their niche conservatism (Huber *et al.* 2023b), significant shifts in the location of areas of high habitat suitability were observed for all species and scenarios (Figs 79–81). *Kambiwa neotropica* (a lowland species) and *K. coribe* sp. nov. (a species with a large altitudinal range, encompassing lowlands) exhibited significant niche expansions (Figs 79–80). Interestingly, the expansion projected for the environmental niche of *K. coribe* is consistent with models carried out for plants, where climatically stable areas have been recovered in the southern and southwestern parts of the Cerrado biome (Velazco *et al.* 2019).

An opposite pattern was observed for *K. ibo* sp. nov., a species occurring at a higher mean altitude, which is projected to lose up to most of its suitable habitat under future scenarios (Fig. 81). Elevation has been recognized as an important factor modulating species-specific responses to future climate warming for plants, with lowland species being able to find more suitable environments at higher elevations (Silva *et al.* 2024). The scenarios presented here suggest that the highland species *K. ibo* is a candidate for red listing. This species is expected to undergo a reduction that may be drastic in areas of high habitat suitability; moreover, it is currently known mostly from outside of strictly protected areas.

Ninetinae karyology

Karyology in Pholcidae has been summarized in Ávila Herrera *et al.* (2021), with additional data on Ninetinae in Huber *et al.* (2023a, 2023b, 2023c, 2024b, 2024c). So far, thirteen ninetines belonging to nine genera have been karyotyped. Although Ninetinae exhibit a relatively low species diversity, they show a considerable range of diploid numbers, sex chromosome systems, and NOR patterns. The lowest diploid numbers found in ninetines (Huber *et al.* 2023b, 2023c) are among the lowest known in araneomorph spiders with standard chromosome structure; the highest are close to the assumed ancestral pholcid diploid number (Ávila Herrera *et al.* 2021; Huber *et al.* 2024b, 2024c, present study). During

the evolution of pholcids (Ávila Herrera *et al.* 2021) including ninetines (Huber *et al.* 2023a, 2023b, 2023c) as well as most of the other araneomorph spiders (e.g., Suzuki 1954; Kořínková & Král 2013), the number of chromosome pairs has been reduced independently in various clades by fusions.

The morphology of chromosome pairs of ninetines is quite uniform; all pairs are biarmed (i.e., metacentric and submetacentric). However, in some species it was not possible to determine the morphology of all pairs (Ávila Herrera *et al.* 2021; Huber *et al.* 2023a, 2023b, 2023c, 2024b, 2024c). Karyotypes of almost all pholcids karyotyped so far are predominated by metacentric chromosomes (Ávila Herrera *et al.* 2021; Král *et al.* 2022; Huber *et al.* 2023a, 2023b, 2024b, present study).

Four sex chromosome systems have been found in ninetines, namely X0, X_1X_2Y, $X_1X_2X_3Y$, and $X_1X_2X_3X_4Y$. The most common is the $X_1X_2X_3Y$ system, which has been described in the two major ninetine evolutionary lineages (clades 1 and 2 in Fig. 86) (Huber *et al.* 2023a, 2024b, 2024c, present study). This system has not been found in any other synspermiate spider so far. The $X_1X_2X_3Y$ system probably arose from the X_1X_2Y system, which is ancestral to araneomorph spiders (Paula-Neto *et al.* 2017) including pholcids (Ávila Herrera *et al.* 2021). The original X chromosomes of these systems were large biarmed elements, while the Y chromosome was a microchromosome (Ávila Herrera *et al.* 2021; Huber *et al.* 2023a). While X chromosomes of ninetine X_1X_2Y and $X_1X_2X_3Y$ systems retain a biarmed morphology (Huber *et al.* 2023a, 2023b, 2024b, present study), the size and morphology of their Y chromosome is more variable. The length of this element has increased in many ninetine lineages (Huber *et al.* 2023a, 2023b, 2024b, 2024c), which has also been observed in some other synspermiate lineages (Král *et al.* 2006, 2019, 2022; Ávila Herrera *et al.* 2021). In general, an enlargement of the Y chromosome is not common during sex chromosome evolution. The Y chromosome degenerates during evolution, which is usually accompanied by reduction of this element (Bachtrog 2013). An increase of the Y chromosome may be the result of heterochromatin expansion (Kejnovsky *et al.* 2009) and/or addition of autosome material (Schartl *et al.* 2016). Sex chromosomes of ninetines pair achiasmatically in male meiosis (Ávila Herrera *et al.* 2021; Král *et al.* 2022; Huber *et al.* 2023a, 2023b, 2024b, 2024c, present study) like in other Synspermiata (Ávila Herrera *et al.* 2021).

The number of NOR loci in ninetines ranges from one to four; in some species, one of these loci is undoubtedly sex chromosome-linked (Ávila Herrera *et al.* 2021; Huber *et al.* 2023a, 2023b). Sex chromosome linked NORs are common in synspermiate spiders; NORs have spread to sex chromosomes repeatedly during the evolution of these spiders (Král *et al.* 2006; Ávila Herrera *et al.* 2021).

So far, only two species of *Kambiwa*, *K. ibo* sp.nov. (present study) and *K. neotropica* (Ávila Herrera *et al.* 2021) have been karyotyped. They differ in the sex chromosome system. While *K. ibo* exhibits a $X_1X_2X_3Y$ system, *K. neotropica* has a $X_1X_2X_3X_4Y$ system. Among synspermiate spiders, the $X_1X_2X_3X_4Y$ system has so far been found only in *K. neotropica*. According to the original hypothesis (Ávila Herrera *et al.* 2021), the sex chromosome system of this species arose from the X_1X_2Y system by the integration of an autosome pair among the sex chromosomes, through a rearrangement between one original X chromosome and an autosome. The occurrence of the $X_1X_2X_3Y$ system in *K. ibo*, an early-diverging species of *Kambiwa* (present study), supports an alternative hypothesis stating that the $X_1X_2X_3X_4Y$ system arose from the $X_1X_2X_3Y$ system by nondisjunction of the X chromosome or by chromosome fission of one original biarmed X chromosome into two monoarmed chromosomes (Huber *et al.* 2023a). The latter hypothesis is supported by the monoarmed morphology of the X_3 and X_4 chromosomes of *K. neotropica*.

Ninetinae biology: a summary

This paper concludes a series of recent papers that revised most known ninetine genera (Huber *et al.* 2023a, 2023b, 2023c, 2024a, 2024b, 2024c; Huber & Meng 2025). We take this opportunity to summarize

current knowledge about this previously most enigmatic subfamily of Pholcidae. Figure 86 gives an overview of the genera included in the subfamily, their relationships, and their distribution. However, here we focus on some contrasting aspects united in this subfamily. In some respects, Ninetinae is a very homogeneous group, for example regarding ecology and general morphology. In other respects, Ninetinae exhibit substantial variation, as for example in sexual morphology and sperm morphology (and karyology, see above).

Most Ninetinae occupy very similar ecoregions, ranging from xeric shrubland to dry forests. They are rarely found in more humid environments such as the Southern Andean Yungas, and they are conspicuously absent from moist forests, which are otherwise the ecoregions with the highest species richness in Pholcidae (Huber & Rheims 2011; Castanheira *et al.* 2016). Ninetinae also occupy a very limited number of different microhabitats. The most promising methods to find Ninetinae are turning

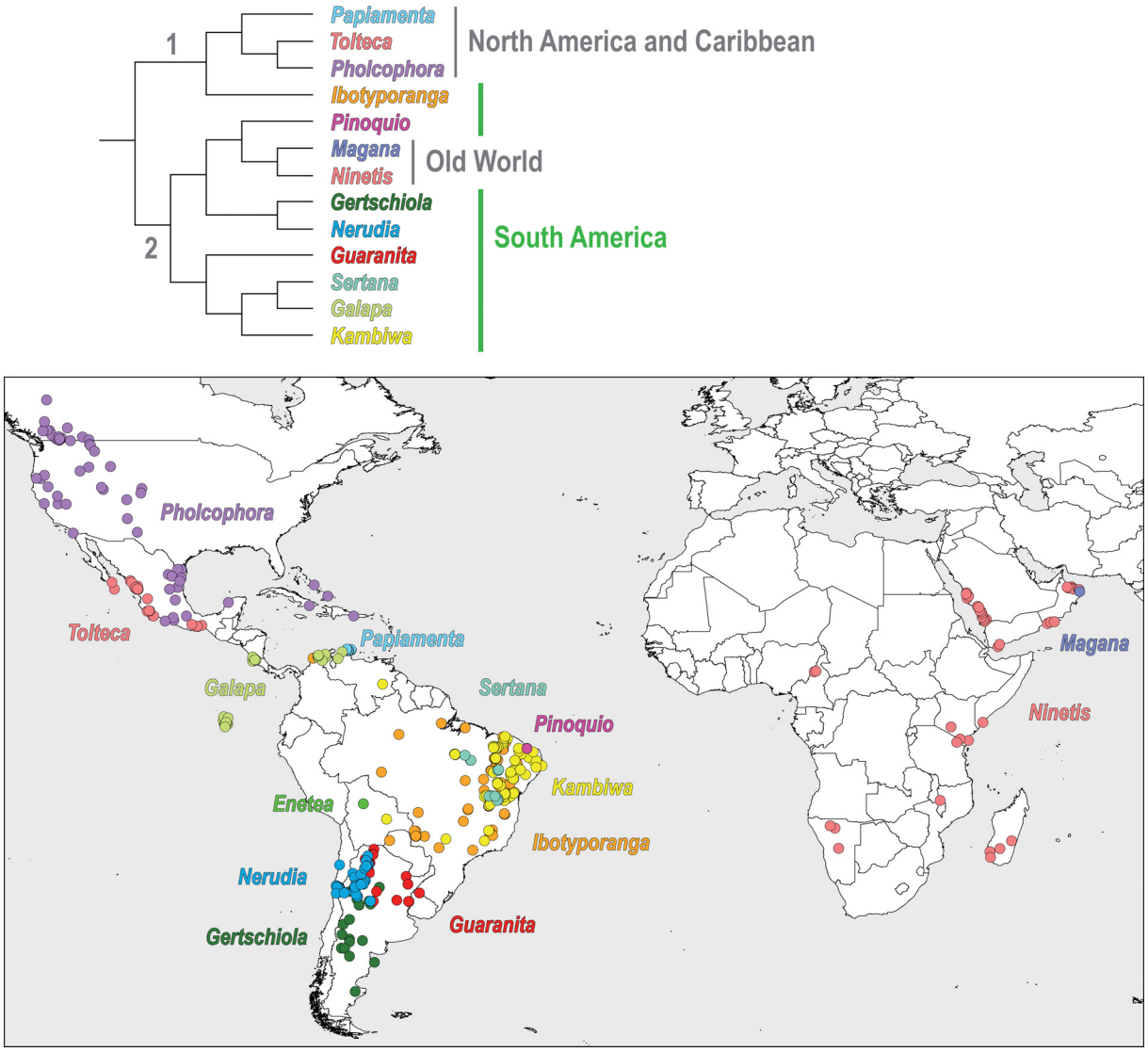

Fig. 86. Ninetinae Simon, 1890 phylogeny (excluding the genus *Enetea* Huber, 2000; simplified from Meng *et al.* 2025) and distribution. Numbers in the cladogram denote the two major clades mentioned in the text.

stones and rocks, beating dead branches and cacti lying on the ground, and sifting dry leaf litter. Upon disturbance, the spiders usually run quickly; the vibrating, bouncing, or whirling that is so typical of long-legged relatives (e.g., Jackson *et al.* 1990, 1992, 1993) is precluded by their short legs. Webs have never been observed in the field, but representatives of several genera have been observed to build and to rest on small sheets of silk in collecting vials; except for their size, these webs look fundamentally very similar to the typical Pholcidae domed sheet web supported by some scaffolding lines (cf. Eberhard 1992).

Related to this ecological homogeneity is a conservative general morphology. Ninetinae are usually small spiders (body length mostly 1–2 mm) with short legs, domed carapace without or with a very shallow thoracic groove, and globular abdomen. The short leg length probably affects a range of other characters that are characteristic for Ninetinae, such as (1) the very distal position of the retrolateral trichobothrium on the leg tibia (usually at ~50–70% of tibia length; in most other pholcids at 1–40%); (2) the flattened rather than round egg-sac (many Ninetinae would not be able to run carrying an egg sac under the prosoma that is higher than one egg diameter); and (3) the low number of comb hairs on the prolateral side of tarsus 4 (only one or two). Beyond absolute leg-length, also leg proportions are unusual for Pholcidae but similar among Ninetinae: the fourth leg is usually longer than the first leg; the metatarsus is barely longer or even shorter than the tibia; the first leg is barely longer than the second leg; and 'leg slenderness' (measured as tibia 1 length / diameter) is usually at ~7–15 (in other pholcids mostly ~20–120). Ninetinae occasionally enter caves as is generally true for many species of Pholcidae (reviewed in Huber 2018b), but no troglomorphisms are known in the subfamily. Thus, pigmentation is also homogeneous within the subfamily, with little color except for shades of ochre and brown, and with very little color pattern. Finally, as expected from the similar ecology and webs, tarsal tip morphology (claws and setae) is also very homogeneous among Ninetinae.

This morphological conservatism extends to traits that are not easily explained by ecology alone. (1) All Ninetinae share a very similar eye pattern: the AME that have repeatedly been lost in other subfamilies are always present and relatively big. (2) The spinneret and spigot morphology is almost identical across the entire subfamily: except for *Ibotyporanga*, all Ninetinae have the identical set of ALS spigots, even with remarkably consistent shapes and relative sizes of the individual spigots. (3) All Ninetinae except for *Tolteca* Huber, 2000 have retained male cheliceral stridulation, which has repeatedly been lost in other subfamilies. Ninetinae females, on the other hand, have apparently never developed any kind of stridulation; such female stridulation (prosoma-abdomen) has evolved at least ten times in other subfamilies (Huber 2021). (4) All Ninetinae have very short hairs ("short vertical hairs") on the anterior (or rarely all) leg tibiae that are sexually dimorphic (males only, see below). (5) All Ninetinae share capsulate tarsal organs with a very small opening (~1–2 μm); exposed tarsal organs have repeatedly evolved in other subfamilies but not in Ninetinae.

In contrast to this, considerable variation occurs in morphological characters related to sexual biology, far beyond the ubiquitous phenomenon of species-specific genitalia. (1) The male chelicerae are usually set with a pair of apophyses; in *Ibotyporanga*, these apophyses are fused to a single median process; in *Galapa* and in certain species of *Nerudia* Huber, 2000, *Ninetis* Simon, 1890, and *Kambiwa*, they are lost. (2) The male cheliceral fangs are usually unmodified, but in *Galapa* they carry a pair of processes. (3) The male clypeus is unmodified in most Ninetinae, but provided with a median process in *Pinoquio barauna* (Huber & Carvalho, 2019) and *Guaranita dobby* Torres *et al.*, 2016, with a notch in *Ibotyporanga*, and with modified hairs in *Galapa murphyi* Huber, 2024. (4) Male sternum humps are present in some genera but absent in others, with no apparent phylogenetic pattern. (5) The male gonopore of most Ninetinae is provided with four epiandrous spigots, usually arranged in two pairs; however, several genera seem to contain both species with and without epiandrous spigots (*Tolteca*, *Ninetis*, *Sertana*, *Galapa*, *Kambiwa*). This suggests multiple convergent losses, similar to other Pholcidae subfamilies. (6) The epigynal plate

is usually simple, with little sculpture, but in *Ibotyporanga* and some species of *Ninetis*, it is provided with a median pocket, presumably with different functions in the two genera. (7) Females of *Tolteca* are provided with a unique knob between the epigynum and the pedicel; its function is unknown. (8) Glandular pore plates in the female internal genitalia are present in *Ibotyporanga*, similar to most other Pholcidae, but strongly reduced or absent in all other Ninetinae. (9) Further details of the female internal genitalia are poorly explored, but long tubes have apparently evolved repeatedly in *Ibotyporanga*, *Gertschiola* Brignoli, 1981, and *Kambiwa*. In all three cases, this seems correlated with an elongation of certain male palpal sclerites (Izquierdo *et al.* 2023; Huber *et al.* 2024c, present paper).

Sperm ultrastructure in Pholcidae has been summarized in Dederichs *et al.* (2022), with additional data on the ninetine genus *Papiamenta* Huber, 2000 in Huber *et al.* (2024b). The most intriguing variation among Ninetinae concerns the sperm transfer form (cleistospermia vs synspermia). This finding is difficult to interpret in evolutionary terms. If the synspermia of Ninetinae (confirmed in *Gertschiola*, *Nerudia*, *Guaranita*, *Galapa*, *Kambiwa*) are retained from the ancestral Synspermiata, then the cleistospermia in other Pholcidae must have evolved at least five times independently (Pholcinae + Smeringopinae; Caipirinae; Arteminae; Modisiminae; *Papiamenta* + *Tolteca* + *Pholcophora*) (based on the cladogram in Meng *et al*. 2026). Alternatively, the synspermia in Ninetinae might represent a reversal to the original mode of Synspermiata sperm transfer; this scenario requires only two evolutionary steps within Synspermiata.

Sexual dimorphisms have evolved many times independently in Pholcidae, also within Ninetinae (reviewed in Huber 2021; updated for Ninetinae in Huber *et al.* 2023c). According to our current understanding of Ninetinae phylogeny, sexual dimorphisms have evolved approximately nine times in this subfamily: (#1) Modified male cheliceral fangs originated in the ancestor of *Galapa*. (#2) All Ninetinae except *Tolteca* have sexually dimorphic cheliceral stridulation: present in males, absent in females. However, it is not clear if this is plesiomorphic or derived. (#3–6) Clypeus modifications have evolved at least four times in Ninetinae: in *Pinoquio barauna*, *Guaranita dobby*, *Galapa murphyi*, and in the ancestor of *Ibotyporanga*. Subtle dimorphisms (male clypeus slightly more protruding and with sclerotized rim) occur in additional taxa and may represent one or more further origins. (#7) A pair of anterior humps on the male sternum occur in several ninetine genera, but it is unclear if this is the result of multiple origins or losses. Such humps are absent in the sister group of Ninetinae, suggesting at least one origin (in the ancestor of Ninetinae). (#8) Very short hairs (~15–20 μm) that remind of chemoreceptors but are unbranched and restricted to (or occur in much higher densities on) male legs (the so-called "vertical hairs") seem to occur in all Ninetinae, but not in the sister group of Ninetinae. (#9) Raised male palpal tarsal organs may have evolved in the ancestor of Ninetinae. However, they also occur in *Priscula* and might thus not represent an independent origin for Ninetinae.

Open questions and further research

Naturally, there are many more open than answered questions. Here we focus on a few details that we consider both relevant and relatively easy to address. (1) Regarding taxonomy, some genera are probably much more species rich than presently known. This is especially true for the genera occurring in the Brazilian Cerrado (*Ibotyporanga*, *Kambiwa*, *Sertana*), where large areas remain virtually unexplored (e.g., Tocantins, Goiás, Mato Grosso do Sul). The same is true for *Ninetis* in Africa. At genus level, the identity of Caribbean representatives of *Pholcophora* remains dubious. The taxonomically most enigmatic ninetine genus is *Enetea*, based on a single male specimen from Bolivia. The only other ninetine genus that has not been revised recently is *Gertschiola* (Argentina), but for this genus, we do not expect a substantial number of undiscovered species. (2) Regarding distribution, many gaps remain in addition to those in Brazil, Bolivia, and Africa mentioned above (e.g., northern Chile, northern Colombia), but of particular interest is the distribution of Old World Ninetinae. *Ninetis* has spread over much of Subsahara Africa, the Arabian Peninsula, and it even reached Madagascar. It can thus be expected to have crossed

the Arabian Gulf (Persian Gulf and Gulf of Oman) into Iran. (3) Our knowledge of Ninetinae natural history is fragmentary at best and mostly limited to anecdotal data from field collecting. A notable exception is the study of Izquierdo *et al.* (2023) on the sexual biology of *Gertschiola neuquena* Huber, 2000. Similar studies on other ninetine genera are likely to uncover a wealth of information and answer a number of open questions. For example, do all Ninetinae share insertion of a single palp at a time, in contrast to all other studied Pholcidae? Has sperm storage in sac- or tube-like containers repeatedly replaced the ancestral mode of sperm storage in Pholcidae, i.e., in secretions discharged into the uterus externus through a pair of glandular pore plates? (4) Given the karyotype diversity of ninetines, and the apparent discordance between karyological similarities and molecular phylogeny reconstructions, a much denser sample of species should be examined to reconstruct the karyotype evolution in this clade. This is especially true for the evolution of NORs. (5) Finally, an intriguing question refers to the number of synspermia transferred during copulation and to the number of synspermia required by females for their entire life span. In *Galapa bella* (Gertsch & Peck, 1992), a single synsperm contains 64 spermatozoa (Dederichs *et al.* 2022). Egg-sacs in *Galapa* contain up to six eggs (Huber *et al.* 2024a). In theory, a single synsperm could thus fertilize ten egg sacs, which is close to the maximum number of fertilized egg-sacs ever reported for Pholcidae (nine; Huber 1998).

Acknowledgements

For the loan of specimens, we thank Jana Grüger, Cristian Grismado, and Martín Ramírez. For help with field work in Brazil, we are grateful to Richard A. Torres Contreras, Alexandre S. Michelotto, Eloá Noetzold, and Luana Silva Carvalho. For help with molecular lab work, we thank Jana Thormann (LIB, Bonn). We thank M. Rix and two anonymous referees for valuable comments on the manuscript. This publication is registered in compliance with Brazilian regulations at the Sistema Nacional de Gestão do Patrimônio Genético e do Conhecimento Tradicional Associado (SISGen; AOB7188). Brazilian specimens were collected under sampling permits issued by the Instituto Chico Mendes de Conservação da Biodiversidade through the Sistema de Autorização e Informação em Biodiversidade (SISBio; #48611, #55229, #59280, #67654, #81301, #73013). Field expeditions in Brazil were supported by Fundação de Amparo à Pesquisa do Estado de Minas Gerais (Chamada 07/2018 – FAPEMIG-VALE, #RDP-00098-18 to Adalberto J. Santos), Conselho Nacional de Desenvolvimento Científico e Tecnológico (#407288/2013-9 to Adalberto J. Santos; #441545/2020-3 to LSC), Fundação de Amparo à Pesquisa do Estado do Piauí (FAPEPI/CNPq/PROTAX, Termo de Aceitação e Outorga Nº 001/2022 to LSC), and the German Research Foundation (DFG, project HU980/12-1 to BAH). The DFG is also acknowledged for funding the PhD position of GM (project HU980/12-1). The cytogenetic part was supported by two projects of the Ministry of Education, Youth, and Sports of the Czech Republic (LTAUSA 19142, IMAH, JK; SVV 260807, IMAH, JK) and by the Agencia Nacional de Investigación y Desarrollo, Chile (IMAH).

Author contributions

BAH: initiation of project, collecting, taxonomy, writing.
GM: curation and analysis of molecular data, writing.
JK, IMAH: preparation of chromosome slides, evaluation of karyological data, writing.
LSC: permits, collecting, biogeography, writing.

References

Aharon S., Huber B.A. & Gavish-Regev E. 2017. Daddy-long-leg giants: revision of the spider genus *Artema* Walckenaer, 1837 (Araneae, Pholcidae). *European Journal of Taxonomy* 376: 1–57. https://doi.org/10.5852/ejt.2017.376

Álvares E.S.S., Machado E.O., Azevedo C.S. & De-Maria M. 2004. Composition of the spider assemblage in an urban forest reserve in southeastern Brazil and evaluation of two sampling method

protocols of species richness estimates. *Revista Ibérica de Aracnología* 10: 185–194. Available from https://dialnet.unirioja.es/servlet/articulo?codigo=1088718 [accessed 22 Oct. 2025].

Araujo H.F.P., Canassa N.F., Machado C.C.C. & Tabarelli M. 2023. Human disturbance is the major driver of vegetation changes in the Caatinga dry forest region. *Scientific Reports* 13: 18440. https://doi.org/10.1038/s41598-023-45571-9

Astrin J.J., Huber B.A., Misof B. & Kluetsch C.F.C. 2006. Molecular taxonomy in pholcid spiders (Pholcidae, Araneae): evaluation of species identification methods using CO1 and 16S rRNA. *Zoologica Scripta* 35: 441–457. https://doi.org/10.1111/j.1463-6409.2006.00239.x

Ávila Herrera I.M., Král J., Pastuchová M., Forman M., Musilová J., Kořínková T., Šťáhlavský F., Zrzavá M., Nguyen P., Just P., Haddad C.R., Hiřman M., Koubová M., Sadílek D. & Huber B.A. 2021. Evolutionary pattern of karyotypes and meiosis in pholcid spiders (Araneae: Pholcidae): implications for reconstructing chromosome evolution of araneomorph spiders. *BMC Ecology and Evolution* 21: 75. https://doi.org/10.1186/s12862-021-01750-8

Bachtrog D. 2013. Y-chromosome evolution: emerging insights into processes of Y-chromosome degeneration. *Nature Reviews Genetics* 14: 113–124. https://doi.org/10.1038/nrg3366

Barbet-Massin M., Jiguet F., Albert C.H. & Thuiller W. 2012. Selecting pseudo-absences for species distribution models: how, where and how many? *Methods in Ecology and Evolution* 3: 327–338. https://doi.org/10.1111/j.2041-210X.2011.00172.x

Bengtson P. 1988. Open nomenclature. *Palaeontology* 31: 223–227.

Beuchle R., Grecchi R.C., Shimabukuro Y.E., Seliger R., Eva H.D., Sano E. & Achard F. 2015. Land cover changes in the Brazilian Cerrado and Caatinga biomes from 1990 to 2010 based on a systematic remote sensing sampling approach. *Applied Geography* 58: 116–127. https://doi.org/10.1016/j.apgeog.2015.01.017.

Boyce M.S., Vernier P.R., Nielsen S.E. & Schmiegelow F.K.A. 2002. Evaluating resource selection functions. *Ecological Modelling* 157: 281–300. https://doi.org/10.1016/S0304-3800(02)00200-4

Brown B.V. 1993. A further chemical alternative to critical-point-drying for preparing small (or large) flies. *Fly Times* 11: 10.

Carvalho L.S. & Avelino M.T.L. 2010. Composição e diversidade da fauna de aranhas (Arachnida, Araneae) da Fazenda Nazareth, Município de José de Freitas, Piauí, Brasil. *Biota Neotropica* 10: 21–31. https://doi.org/10.1590/S1676-06032010000300001

Carvalho L.S., Sanches Ruiz G.R., Saturnino R. & Carvalho L.S. 2026. Optimizing sampling protocols: spider assemblages are robust to pitfall trap spacing in Neotropical savannas. *Community Ecology* 27: 149–160. https://doi.org/10.1007/s42974-025-00287-w

Castanheira P., Pérez-González A. & Baptista R.L.C. 2016. Spider diversity (Arachnida: Araneae) in Atlantic Forest areas at Pedra Branca State Park, Rio de Janeiro, Brazil. *Biodiversity Data Journal* 4: e7055. https://doi.org/10.3897/BDJ.4.e7055

Churchill T.B. 1993. Effects of sampling method on composition of a Tasmanian coastal heathland spider assemblage. *Memoirs of the Queensland Museum* 33: 475–481.

Colli G.R., Vieira C.R. & Dianese J.C. 2020. Biodiversity and conservation of the Cerrado: recent advances and old challenges. *Biodiversity and Conservation* 29: 1465–1475. https://doi.org/10.1007/s10531-020-01967-x

Costa-Pinto A.L. da, Bovendorp R.S., Heming N.M., Malhado A.C. & Ladle R.J. 2024. Where could they go? Potential distribution of small mammals in the Caatinga under climate change scenarios. *Journal of Arid Environments* 221: 105133. https://doi.org/10.1016/j.jaridenv.2024.105133

Dantas L.G., dos Santos C.A.C., Santos C.A.G., Martins E.S.P.R. & Alves L.M. 2022. Future changes in temperature and precipitation over northeastern Brazil by CMIP6 Model. *Water* 14: 4118. https://doi.org/10.3390/w14244118

de Paula Y.R.A.A., Bustamante A.A., Saturnino R. & Carvalho L.S. 2026. Influence of habitat complexity on the ground spider community in gallery forests of the Cerrado biome. *Acta Oecologica* 131: 104165. https://doi.org/10.1016/j.actao.2026.104165

Dederichs T.M., Huber B.A. & Michalik P. 2022. Evolutionary morphology of sperm in pholcid spiders (Pholcidae, Synspermiata). *BMC Zoology* 7: 52. https://doi.org/10.1186/s40850-022-00148-3

Dolejš P., Kořínková T., Musilová J., Opatová V., Kubcová L., Buchar J. & Král J. 2011. Karyotypes of central European spiders of the genera *Arctosa*, *Tricca* and *Xerolycosa* (Araneae: Lycosidae). *European Journal of Entomology* 108: 1–16. https://doi.org/10.14411/eje.2011.001

Eberhard W.G. 1992. Web construction by *Modisimus* sp. (Araneae, Pholcidae). *Journal of Arachnology* 20: 25–34.

Eberle J., Dimitrov D., Valdez-Mondragón A. & Huber B.A. 2018. Microhabitat change drives diversification in pholcid spiders. *BMC Evolutionary Biology* 18: 141. https://doi.org/10.1186/s12862-018-1244-8

Eyring V., Bony S., Meehl G.A., Senior C., Stevens B., Stouffer R.J. & Taylor K.E. 2015. Overview of the Coupled Model Intercomparison Project Phase 6 (CMIP6) experimental design and organisation. *Geoscientific Model Development* 9: 1937–1958. https://doi.org/10.5194/gmd-9-1937-2016

Fick S.E. & Hijmans R.J. 2017. WorldClim 2: new 1-km spatial resolution climate surfaces for global land areas. *International Journal of Climatology* 37: 4302–4315. https://doi.org/10.1002/joc.5086

Fielding A.H. & Bell J.F. 1997. A review of methods for the assessment of prediction errors in conservation presence/absence models. *Environmental Conservation* 24: 38–49. https://doi.org/10.1017/S0376892997000088

Firpo M.Â.F., Guimarães B. dos S., Dantas L.G., Silva M.G.B. da, Alves L.M., Chadwick R., Llopart M.P. & Oliveira G.S. de. 2022. Assessment of CMIP6 models' performance in simulating present-day climate in Brazil. *Frontiers in Climate* 4: 948499. https://doi.org/10.3389/fclim.2022.948499

Forman M., Nguyen P., Hula P. & Král J. 2013. Sex chromosome pairing and extensive NOR polymorphism in *Wadicosa fidelis* (Araneae: Lycosidae). *Cytogenetic and Genome Research* 141: 43–49. https://doi.org/10.1159/000351041

Gonçalves G.S.R., Cerqueira P.V., Silva D.P., Gomes L.B., Leão C.F., Andrade A.F.A. de & Santos M.P.D. 2023. Multi-temporal ecological niche modeling for bird conservation in the face of climate change scenarios in Caatinga, Brazil. *PeerJ* 11: e14882. https://doi.org/10.7717/peerj.14882

Guindon S., Dufayard J.-F., Lefort V., Anisimova M., Hordijk W. & Gascuel O. 2010. New algorithms and methods to estimate maximum-likelihood phylogenies: assessing the performance of PhyML 3.0. *Systematic Biology* 59: 307–321. https://doi.org/10.1093/sysbio/syq010

Hijmans R.J. 2023a. raster: Geographic Data Analysis and Modeling. Available from https://cran.r-project.org/web/packages/raster/raster.pdf [accessed 22 Oct. 2025].

Hijmans R.J. 2023b. terra: Spatial Data Analysis. CRAN: Contributed Packages. Available from https://cran.r-project.org/web/packages/terra/index.html [accessed 22 Oct. 2025].

Hoang D.T., Chernomor O., von Haeseler A., Minh B.Q. & Vinh L.S. 2018. UFBoot2: improving the ultrafast bootstrap approximation. *Molecular Biology and Evolution* 35: 518–522. https://doi.org/10.1093/molbev/msx281

Hofmann G.S., Cardoso M.F., Alves R.J.V., Weber E.J., Barbosa A.A., de Toledo P.M., Pontual F.B., Salles L. de O., Hasenack H., Cordeiro J.L.P., Aquino F.E. & de Oliveira L.F.B. 2021. The Brazilian Cerrado is becoming hotter and drier. *Global Change Biology* 27: 4060–4073. https://doi.org/10.1111/gcb.15712

Horton T., Marsh L., Bett B.J., Gates A.R., Jones D.O.B., Benoist N.M.A., Pfeifer S., Simon-Lledó E., Durden J.M., Vandepitte L. & Appeltans W. 2021. Recommendations for the standardisation of open taxonomic nomenclature for image-based identifications. *Frontiers in Marine Science* 8: 620702. https://doi.org/10.3389/fmars.2021.620702

Huber B.A. 1998. Genital mechanics in some neotropical pholcid spiders (Araneae: Pholcidae), with implications for systematics. *Journal of Zoology* 244: 587–599. https://doi.org/10.1111/j.1469-7998.1998.tb00063.x

Huber B.A. 2000. New World pholcid spiders (Araneae: Pholcidae): a revision at generic level. *Bulletin of the American Museum of Natural History* 254: 1–348. https://doi.org/10.1206/0003-0090(2000)254<0001:NWPSAP>2.0.CO;2

Huber B.A. 2001. The pholcids of Australia (Araneae; Pholcidae): taxonomy, biogeography, and relationships. *Bulletin of the American Museum of Natural History* 260: 1–144. https://doi.org/10.1206/0003-0090(2001)260%3C0001:TPOAAP%3E2.0.CO;2

Huber B.A. 2004. The significance of copulatory structures in spider systematics. *In*: Schult J. (ed.) *Studien zur Theorie der Biologie, Band 5, Biosemiotik - Praktische Anwendung und Konsequenzen für die Einzeldisziplinen*: 89–100. VWB-Verlag für Wissenschaft und Bildung, Berlin.

Huber B.A. 2012. Revision and cladistic analysis of the Afrotropical endemic genus *Smeringopus* Simon, 1890 (Araneae: Pholcidae). *Zootaxa* 3461: 1–138. https://doi.org/10.11646/zootaxa.3461.1.1

Huber B.A. 2018a. The South American spider genera *Mesabolivar* and *Carapoia* (Araneae, Pholcidae): new species and a framework for redrawing generic limits. *Zootaxa* 4395: 1–178. https://doi.org/10.11646/zootaxa.4395.1.1

Huber B.A. 2018b. Cave-dwelling pholcid spiders (Araneae, Pholcidae): a review. *Subterranean Biology* 26: 1–18. https://doi.org/10.3897/subtbiol.26.26430

Huber B.A. 2021. Beyond size: sexual dimorphisms in pholcid spiders. *Arachnology* 18: 656–677. https://doi.org/10.13156/arac.2020.18.7.656

Huber B.A. 2022. Revisions of *Holocnemus* and *Crossopriza*: the spotted-leg clade of Smeringopinae (Araneae, Pholcidae). *European Journal of Taxonomy* 795: 1–241. https://doi.org/10.5852/ejt.2022.795.1663

Huber B.A. & Carvalho L.S. 2019. Filling the gaps: descriptions of unnamed species included in the latest molecular phylogeny of Pholcidae (Araneae). *Zootaxa* 4546: 1–96. https://doi.org/10.11646/zootaxa.4546.1.1

Huber B.A. & Meng G. 2024. Old World *Micropholcus* spiders, with first records of acrocerid parasitoids in Pholcidae (Araneae). *ZooKeys* 1213: 95–182. https://doi.org/10.3897/zookeys.1213.133178

Huber B.A. & Meng G. 2025. Like grains of sand: *Ninetis* spiders on the Arabian Peninsula (Araneae: Pholcidae). *Zootaxa* 5563: 290–335. https://doi.org/10.11646/zootaxa.5563.1.19

Huber B.A. & Rheims C.A. 2011. Diversity and endemism of pholcid spiders in Brazil's Atlantic Forest, with descriptions of four new species of the Atlantic Forest endemic genus *Tupigea* (Araneae: Pholcidae). *Journal of Natural History* 45: 275–301. https://doi.org/10.1080/00222933.2010.524319

Huber B.A., Nuñeza O.M. & Leh Moi Ung C. 2015. Revision, phylogeny, and microhabitat shifts in the Southeast Asian spider genus *Aetana* (Araneae, Pholcidae). *European Journal of Taxonomy* 162: 1–78. https://doi.org/10.5852/ejt.2015.162

Huber B.A., Eberle J. & Dimitrov D. 2018. The phylogeny of pholcid spiders: a critical evaluation of relationships suggested by molecular data (Araneae, Pholcidae). *ZooKeys* 789: 51–101. https://doi.org/10.3897/zookeys.789.22781

Huber B.A., Caspar K. & Eberle J. 2019. New species reveal unexpected interspecific microhabitat diversity in the genus *Uthina* Simon, 1893 (Araneae: Pholcidae). *Invertebrate Systematics* 33: 181–207. https://doi.org/10.1071/IS18002

Huber B.A., Meng G., Král J., Ávila Herrera I.M., Izquierdo M.A. & Carvalho L.S. 2023a. High and dry: integrative taxonomy of the Andean spider genus *Nerudia* (Araneae: Pholcidae). *Zoological Journal of the Linnean Society* 198: 534–591. https://doi.org/10.1093/zoolinnean/zlac100

Huber B.A., Meng G., Valdez-Mondragón A., Král J., Ávila Herrera I.M. & Carvalho L.S. 2023b. Short-legged daddy-long-leg spiders in North America: the genera *Pholcophora* and *Tolteca* (Araneae, Pholcidae). *European Journal of Taxonomy* 880: 1–89. https://doi.org/10.5852/ejt.2023.880.2173

Huber B.A., Meng G., Král J., Ávila Herrera I.M. & Izquierdo M.A. 2023c. Revision of the South American Ninetinae genus *Guaranita* (Araneae, Pholcidae). *European Journal of Taxonomy* 900: 32–80. https://doi.org/10.5852/ejt.2023.900.2301

Huber B.A., Meng G., Cabra García J. & Carvalho L.S. 2024a. Thriving in dry conditions: on the Neotropical spider genus *Galapa* (Araneae: Pholcidae). *Zootaxa* 5419: 301–347. https://doi.org/10.11646/zootaxa.5419.3.1

Huber B.A., Meng G., Dederichs T.M., Michalik P., Forman M. & Král J. 2024b. Castaways: the Leeward Antilles endemic spider genus *Papiamenta* (Araneae: Pholcidae). *Invertebrate Systematics* 38: IS23052. https://doi.org/10.1071/IS23052

Huber B.A., Meng G., Král J., Ávila Herrera I.M. & Carvalho L.S. 2024c. Diamonds in the rough: *Ibotyporanga* (Araneae, Pholcidae) spiders in semi-arid Neotropical environments. *European Journal of Taxonomy* 963: 1–169. https://doi.org/10.5852/ejt.2024.963.2687

Huber B.A., Meng G. & Valdez-Mondragón A. 2024d. Notes on *Chisosa* (Araneae, Pholcidae), with the description of a new species from Mexico. *Zootaxa* 5419: 217–244. https://doi.org/10.11646/zootaxa.5419.2.3

Huber B.A., Szymański H. & Bennett-West A. 2024e. Progress or burden? Formal description of every apparently new species available in collections is neither necessary nor useful. *ZooKeys* 1214: 77–90. https://doi.org/10.3897/zookeys.1214.130592

Izquierdo M.A., Dederichs T.M., Cargnelutti F. & Michalik P. 2023. Copulatory behaviour and genital mechanics suggest sperm allocation by a non-intromittent sclerite in a pholcid spider. *Royal Society Open Science* 10: 230263. https://doi.org/10.1098/rsos.230263

Jackson D.A. 1993. Stopping rules in principal components analysis: A comparison of heuristical and statistical approaches. *Ecology* 74: 2204–2214. https://doi.org/10.2307/1939574

Jackson R.R., Brassington R.J. & Rowe R.J. 1990. Anti-predator defences of *Pholcus phalangioides* (Araneae, Pholcidae), a web-building and web-invading spider. *Journal of Zoology* 220: 543–552. https://doi.org/10.1111/j.1469-7998.1990.tb04733.x

Jackson R.R., Rowe R.J. & Campbell G.E. 1992. Anti-predator defences of *Psilochorus sphaeroides* and *Smeringopus pallidus* (Araneae, Pholcidae), tropical web-building spiders. *Journal of Zoology* 228: 227–232. https://doi.org/10.1111/j.1469-7998.1992.tb04604.x

Jackson R.R., Jakob E.M., Willey M.B. & Campbell G.E. 1993. Anti-predator defences of a web-building spider, *Holocnemus pluchei* (Araneae, Pholcidae). *Journal of Zoology* 229: 347–352. https://doi.org/10.1111/j.1469-7998.1993.tb02641.x

Kalyaanamoorthy S., Minh B.Q., Wong T.K.F., von Haeseler A. & Jermiin L.S. 2017. ModelFinder: fast model selection for accurate phylogenetic estimates. *Nature Methods* 14: 587–589. https://doi.org/10.1038/nmeth.4285

Katoh K. & Standley D.M. 2013. MAFFT multiple sequence alignment software version 7: improvements in performance and usability. *Molecular Biology and Evolution* 30: 772–780. https://doi.org/10.1093/molbev/mst010

Kejnovsky E., Hobza R., Cermak T., Kubat Z. & Vyskot B. 2009. The role of repetitive DNA in structure and evolution of sex chromosomes in plants. *Heredity* 102: 533–541. https://doi.org/10.1038/hdy.2009.17

Kimura M. 1980. A simple method for estimating evolutionary rates of base substitutions through comparative studies of nucleotide sequences. *Journal of Molecular Evolution* 16: 111–120. https://doi.org/10.1007/BF01731581

Kořínková T. & Král J. 2013. Karyotypes, sex chromosomes, and meiotic division in spiders. *In*: Nentwig W. (ed.) *Spider Ecophysiology*: 159–171. Springer, Berlin. https://doi.org/10.1007/978-3-642-33989-9_12

Král J. 2007. Evolution of multiple sex chromosomes in the spider genus *Malthonica* (Araneae: Agelenidae) indicates unique structure of the spider sex chromosome systems. *Chromosome Research* 15: 863–879. https://doi.org/10.1007/s10577-007-1169-3

Král J., Musilová J., Šťáhlavský F., Řezáč M., Akan Z., Edwards R.L., Coyle F.A. & Ribera Almerje C. 2006. Evolution of the karyotype and sex chromosome systems in basal clades of araneomorph spiders (Araneae: Araneomorphae). *Chromosome Research* 14: 859–880. https://doi.org/10.1007/s10577-006-1095-9

Král J., Kořínková T., Forman M. & Krkavcová L. 2011. Insights into the meiotic behavior and evolution of multiple sex chromosome systems in spiders. *Cytogenetic and Genome Research* 133 (1): 43–66. https://doi.org/10.1159/000323497

Král J., Forman M., Kořínková T., Reyes Lerma A.C., Haddad C.R., Musilová J., Řezáč M., Ávila Herrera I.M., Thakur S., Dippenaar-Schoeman A.S., Marec F., Horová L. & Bureš P. 2019. Insights into the karyotype and genome evolution of haplogyne spiders indicate a polyploid origin of lineage with holokinetic chromosomes. *Scientific Reports* 9: 3001. https://doi.org/10.1038/s41598-019-39034-3

Král J., Ávila Herrera I.M., Šťáhlavský F., Sadílek D., Pavelka J., Chatzaki M. & Huber B.A. 2022. Karyotype differentiation and male meiosis in European clades of the spider genus *Pholcus* (Araneae, Pholcidae). *Comparative Cytogenetics* 16 (4): 185–209. https://doi.org/10.3897/compcytogen.v16i4.85059

Kraus O. 1957. Araneenstudien 1. Pholcidae (Smeringopodinae, Ninetinae). *Senckenbergiana Biologica* 38: 217–243.

Levan A.K., Fredga K. & Sandberg A.A. 1964. Nomenclature for centromeric position on chromosomes. *Hereditas* 52: 201–220. https://doi.org/10.1111/j.1601-5223.1964.tb01953.x

Lira A.F. de A., Badillo-Montaño R., Lira-Noriega A. & de Albuquerque C.M.R. 2020. Potential distribution patterns of scorpions in north-eastern Brazil under scenarios of future climate change. *Austral Ecology* 45: 215–228. https://doi.org/10.1111/aec.12849

Mello-Leitão C.F. de 1918. Scytodidas e pholcidas do Brasil. *Revista do Museu Paulista* 10: 83–144.

Mello-Leitão C.F. de 1946. Notas sobre os Filistatidae e Pholcidae. *Anais da Academia Brasileira de Ciências* 18: 39–83.

Meng G., Podsiadlowski L., Dimitrov D. & Huber B.A. 2025. The complex interplay between evolutionary flexibility and diversification in a family of spiders. *Systematic Biology*: syaf070. https://doi.org/10.1093/sysbio/syaf070

Meng G., Carvalho L.S., Podsiadlowski L. & Huber B.A. 2026. Low coverage whole genome sequencing reveals a new subfamily of daddy long-legs spiders from Brazilian Caatinga (Araneae: Pholcidae). *Arthropod Systematics and Phylogeny* 84: 95–121. https://doi.org/10.3897/asp.84.e174748

Minelli A. 2019. The galaxy of the non-Linnaean nomenclature. *History and Philosophy of the Life Sciences* 41: 31. https://doi.org/10.1007/s40656-019-0271-0

Minh B.Q., Nguyen M.A.T. & Haeseler A. 2013. Ultrafast approximation for phylogenetic bootstrap. *Molecular Biology and Evolution* 30: 1188–1195. https://doi.org/10.1093/molbev/mst024

Minh B.Q., Schmidt H.A., Chernomor O., Schrempf D., Woodhams M.D., von Haeseler A. & Lanfear R. 2020. IQ-TREE 2: new models and efficient methods for phylogenetic inference in the genomic era. *Molecular Biology and Evolution* 37: 1530–1534. https://doi.org/10.1093/molbev/msaa015

Monteverde C., De Sales F. & Jones C. 2022. Evaluation of the CMIP6 performance in simulating precipitation in the Amazon river basin. *Climate* 10: 122. https://doi.org/10.3390/cli10080122

Moura M.R., do Nascimento F.A.O., Paolucci L.N., Silva D.P. & Santos B.A. 2023a. Pervasive impacts of climate change on the woodiness and ecological generalism of dry forest plant assemblages. *Journal of Ecology* 111: 1762–1776. https://doi.org/10.1111/1365-2745.14139

Moura M.R., Oliveira G.A., Paglia A.P., Pires M.M. & Santos B.A. 2023b. Climate change should drive mammal defaunation in tropical dry forests. *Global Change Biology* 29: 6931–6944. https://doi.org/10.1111/gcb.16979

Myers N., Mittermeier R.A., Mittermeier C.G., da Fonseca G.A.B. & Kent J. 2000. Biodiversity hotspots for conservation priorities. *Nature* 403 (6772): 853–858. https://doi.org/10.1038/35002501

Neves M.O., Broennimann O., Mod H.K., Bolochio B.E., Santana D.J., Guisan A. & Moura M.R. 2025. Climate change threatens amphibians and species representation within protected areas in tropical wetlands. *Journal of Applied Ecology* 62: 290–302. https://doi.org/10.1111/1365-2664.14846

Oliveira J.S., Santana D.J., Pantoja D.L., Ceron K. & Guedes T.B. 2024. Climate change in open environments: revisiting the current distribution to understand and safeguard the future of psammophilous squamates of the Diagonal of Open Formations of South America. *Journal of Arid Environments* 220: 105117. https://doi.org/10.1016/j.jaridenv.2023.105117

Oliveira U., Paglia A.P., Brescovit A.D., de Carvalho C.J.B., Silva D.P., Rezende D.T., Leite F.S.F., Batista J.A.N., Barbosa J.P.P.P., Stehmann J.R., Ascher J.S., de Vasconcelos M.F., de Marco P., Löwenberg-Neto P., Dias P.G., Ferro V.G. & Santos A.J. 2016. The strong influence of collection bias on biodiversity knowledge shortfalls of Brazilian terrestrial biodiversity. *Diversity and Distributions* 22 (12): 1232–1244. https://doi.org/10.1111/ddi.12489

Oliveira U., Brescovit A.D. & Santos A.J. 2017. Sampling effort and species richness assessment: a case study on Brazilian spiders. *Biodiversity and Conservation* 26 (6): 1481–1493. https://doi.org/10.1007/s10531-017-1312-1

Paula-Neto E., Cella D.M., Araujo D., Brescovit A.D. & Schneider M.C. 2017. Comparative cytogenetic analysis among filistatid spiders (Araneomorphae: Haplogynae). *Journal of Arachnology* 45: 123–128. https://doi.org/10.1636/M14-69.1

Pebesma E. 2018. Simple features for R: standardized support for spatial vector data. *The R Journal* 10: 439–446. https://doi.org/10.32614/RJ-2018-009

Poggio L., de Sousa L.M., Batjes N.H., Heuvelink G.B.M., Kempen B., Ribeiro E. & Rossiter D. 2021. SoilGrids 2.0: producing soil information for the globe with quantified spatial uncertainty. *SOIL* 7: 217–240. https://doi.org/10.5194/soil-7-217-2021

R Core Team 2023. R: A language and environment for statistical computing, version 4.3.0. R Foundation for Statistical Computing, Vienna. Available from https://www.R-project.org/ [accessed 22 Oct. 2025].

Reis Júnior R., Oliveira M.L. de & Borges G.R.A. 2015. RT4Bio – R Tools for Biologists. https://doi.org/10.13140/RG.2.1.4532.2966

Schartl M., Schmid M. & Nanda I. 2016. Dynamics of vertebrate sex chromosome evolution: from equal size to giants and dwarfs. *Chromosoma* 125: 553–571. https://doi.org/10.1007/s00412-015-0569-y

Sember A., Pappová M., Forman M., Nguyen P., Marec F., Dalíková M., Divišová K., Doležálková-Kaštánková M., Zrzavá M., Sadílek D., Hrubá B. & Král J. 2020. Patterns of sex chromosome differentiation in spiders: insights from comparative genomic hybridisation. *Genes* 11: 849. https://doi.org/10.3390/genes11080849

Sigovini M., Keppel E. & Tagliapietra D. 2016. Open nomenclature in the biodiversity era. *Methods in Ecology and Evolution* 7: 1217–1225. https://doi.org/10.1111/2041-210X.12594

Silva M.C., Rowland L., Oliveira R.S., Pennington R.T. & Moonlight P. 2024. Elevation modulates the impacts of climate change on the Brazilian Cerrado flora. *Diversity and Distributions* 30 (5): e13832. https://doi.org/10.1111/ddi.13832

Strassburg B.B.N., Brooks T., Feltran-Barbieri R., Iribarrem A., Crouzeilles R., Loyola R., Latawiek A.E., Oliveira Filho F.J.B., Scaramuzza C.A. de M., Scarano F.R., Soares-Filho B. & Balmford A. 2017. Moment of truth for the Cerrado hotspot. *Nature Ecology & Evolution* 1: 0099. https://doi.org/10.1038/s41559-017-0099

Suyama M., Torrents D. & Bork P. 2006. PAL2NAL: robust conversion of protein sequence alignments into the corresponding codon alignments. *Nucleic Acids Research* 34: W609–W612. https://doi.org/10.1093/nar/gkl315

Suzuki S. 1954. Cytological studies in spiders. III. Studies on the chromosomes of fifty-seven species of spiders belonging to seventeen families, with general considerations on chromosomal evolution. *Journal of Science of Hiroshima University, Series B* 2: 23–136.

Tamura K., Stecher G. & Kumar S. 2021. MEGA11: Molecular Evolutionary Genetics Analysis Version 11. *Molecular Biology and Evolution* 38: 3022–3027. https://doi.org/10.1093/molbev/msab120

Thuiller W., Georges D., Gueguen M., Engler R., Breiner F., Lafourcade B., Patin R. & Blancheteau H. 2025. biomod2: ensemble platform for species distribution modeling. Available from https://cran.r-project.org/web/packages/biomod2/index.html [accessed 22 Oct. 2025].

Torres R.R., Lapola D.M. & Gamarra N.L.R. 2017. Future climate change in the Caatinga. *In*: Silva J.M.C., Leal I.R. & Tabarelli M. (eds) *Caatinga*: 383–410. Springer, Cham. https://doi.org/10.1007/978-3-319-68339-3_15

Uetz G.E. & Unzicker J.D. 1976. Pitfall trapping in ecological studies of wandering spiders. *Journal of Arachnology* 3: 101–111.

Velazco S.J.E., Villalobos F., Galvão F. & De Marco P. Jr 2019. A dark scenario for Cerrado plant species: effects of future climate, land use and protected areas ineffectiveness. *Diversity and Distributions* 25: 660–673. https://doi.org/10.1111/ddi.12886

Velazco S.J.E., Rose M.B., de Andrade A.F.A., Minoli I. & Franklin J. 2022. flexsdm: an R package for supporting a comprehensive and flexible species distribution modelling workflow. *Methods in Ecology and Evolution* 13: 1661–1669. https://doi.org/10.1111/2041-210X.13874

Venables W.N. & Ripley B.D. 2002. *Modern Applied Statistics with S*. New York, Springer.

Werneck F.P. 2011. The diversification of eastern South American open vegetation biomes: historical biogeography and perspectives. *Quaternary Science Reviews* 30: 1630–1648. https://doi.org/10.1016/j.quascirev.2011.03.009

World Spider Catalog 2025. World Spider Catalog. Version 26. Natural History Museum Bern. Available from http://wsc.nmbe.ch [accessed 22 Oct. 2025]. https://doi.org/10.24436/2

Zizka A., Silvestro D., Andermann T., Azevedo J., Duarte Ritter C., Edler D., Farooq H., Herdean A., Ariza M., Scharn R., Svantesson S., Wengström N., Zizka V. & Antonelli A. 2019. CoordinateCleaner: standardized cleaning of occurrence records from biological collection databases. *Methods in Ecology and Evolution* 10: 744–751. https://doi.org/10.1111/2041-210X.13152

Printed versions of all papers are deposited in the libraries of two of the institutes that are members of the *EJT* consortium: Muséum national d'Histoire naturelle, Paris, France and Royal Museum for Central Africa, Tervuren, Belgium. The other members of the consortium are: Royal Belgian Institute of Natural Sciences, Brussels, Belgium; Meise Botanic Garden, Meise, Belgium; Natural History Museum of Denmark, Copenhagen, Denmark; Naturalis Biodiversity Center, Leiden, the Netherlands; Museo Nacional de Ciencias Naturales-CSIC, Madrid, Spain; Leibniz Institute for the Analysis of Biodiversity Change, Bonn – Hamburg, Germany; National Museum of the Czech Republic, Prague, Czech Republic; The Steinhardt Museum of Natural History, Tel Aviv, Israël.

Supplementary files

Supp. file 1. Summary of the carried out models, with their respective evaluation metrics. All models used for projecting and assembling the data are listed as "true" in the corresponding column. Other models were discarded. https://doi.org/10.5852/ejt.2026.1054.3276.14460

Supp. file 2. Binary and continuous ensemble raster for each carbon emission scenario (i.e., ssp245 and ssp585), global circulation models (i.e., CMCC-ESM2, MRI-ESM2-0, IPSL-CM6A-LR, EC-Earth3-Veg, and MIROC6), time (i.e., current, 2041–2060 and 2081–2100) and species (i.e., *Kambiwa coribe* Huber sp, nov., *K. ibo* Huber sp, nov. and *K. neotropica* (Kraus, 1957)).
https://doi.org/10.5852/ejt.2026.1054.3276.14461